JSCSEN 77(1)1–129(2012)

Journal of the Serbian Chemical Society

Electronic Version

Society 115th Anniversary 1897 - 2012

VOLUME 77

No 1

BELGRADE 2012

Available on line at

www.shd.org.rs/JSCS/

The full search of JSCS is available through

DOAJ DIRECTORY OF OPEN ACCESS JOURNALS

www.doaj.org

The **Journal of the Serbian Chemical Society** (formerly Glasnik Hemijskog društva Beograd) publishes articles from the fields of fundamental and applied chemistry. The Journal is financially supported by the Ministry of Science and Technological Development of the Republic of Serbia.

Articles published in this Journal are indexed in the Institute for **Scientific Information®** products: **SciSearch®**, also known as the **Science Citation Index - Expanded™** (2011 announced **Impact Factor 0.725**), **Research Alert®**, and **Chemistry Citation Index - Extended®**. Also, articles appearing in this Journal are abstracted by: *Chemical Abstracts*, *Referativnii Zhurnal*, *Analytical Abstracts*, *Mass Spectrometry Bulletin*, *Corrosion Abstracts*, *Aluminium Industry Abstracts*, *the Alerts Series*, *Engineering Materials Abstracts*, *Mineralogical Abstracts and Metal Finishing Abstracts.*

Copies of the articles appearing in this *Journal* can be ordered from **ISI Document Solution®** document delivery service of the *Institute for Scientific Information* (ISI), 3501 Market Street, Philadelphia, PA 19104, USA, or from the UnCover Company, 3801 E. Florida, Suite 200, Denver, CO 80210, USA.

Publisher: Serbian Chemical Society (SCS), Karnegijeva 4, 11120 Belgrade, Serbia
Tel/fax: ++381–11–3370–467, E-mails: Society – shd@shd.org.rs, Journal – jscs-info@shd.org.rs
Internet Home Page: Society – http://www.shd.org.rs/; Journal - http://www.shd.org.rs/JSCS/

Internet Service: Contents, Abstracts and full papers of issues (from Vol 64, No. 5-6, 1999) are available in the electronic form at the Web Site of the Journal (http://www.shd.org.rs/JSCS/).

Former Editors of the Journal: Nikola A. Pušin (1930–1947), Aleksandar M. Leko (1948–1954), Panta S. Tutundžić (1955–1961), Miloš K. Mladenović (1962–1964), Đorđe M. Dimitrijević (1965–1969), Aleksandar R. Despić (1969–1975), Slobodan V. Ribnikar (1975–1985), Dragutin Dražić (1986–2006).

Editor-in-Chief: BRANISLAV **NIKOLIĆ**, Serbian Chemical Society
Deputy Editor: DUŠAN **SLADIĆ**, Faculty of Chemistry, University of Belgrade
Co Editor: DANKA **JOVANOVIĆ**, Serbian Chemical Society
Sub editors:
Organic Chemistry RADE **MARKOVIĆ**, Faculty of Chemistry, University of Belgrade and DEJAN **OPSENICA**, Institute of Chemistry, Technology and Metallurgy, University of Belgrade
Biochemistry and Biotechnology OLGICA **NEDIĆ**, INEP – Institute for the Application of Nuclear Energy, Zemun
Inorganic Chemistry MILOŠ **ĐURAN**, Faculty of Science, University of Kragujevac
Theoretical Chemistry IVAN **GUTMAN**, Faculty of Science, University of Kragujevac
Physical Chemistry VERA **DONDUR**, Faculty of Physical Chemistry, University of Belgrade
Electrochemistry SNEŽANA **GOJKOVIĆ**, Faculty of Technology and Metallurgy, University of Belgrade
Analytical Chemistry SLAVICA **RAŽIĆ**, Faculty of Pharmacy, University of Belgrade
Polymers JASNA **ĐONLAGIĆ**, Faculty of Technology and Metallurgy, University of Belgrade
Thermodynamics- SLOBODAN **ŠERBANOVIĆ**, Faculty of Technology and Metallurgy, University of Belgrade
Chemical Engineering MENKA **PETKOVSKA**, Faculty of Technology and Metallurgy, University of Belgrade
Materials VELIMIR **RADMILOVIĆ**, Faculty of Technology and Metallurgy, University of Belgrade
Environmental BOJAN **RADAK**, Vinča Institute of Nuclear Science, Belgrade
English Language Editor: LYNNE **KATSIKAS**, Faculty of Technology and Metallurgy, University of Belgrade
Technical Editors: VLADIMIR **PANIĆ**, ALEKSANDAR **DEKANSKI**, Institute of Chemistry, Technology and Metallurgy, University of Belgrade
Web Master: ALEKSANDAR **DEKANSKI,** Institute of Chemistry, Technology and Metallurgy, Univ. of Belgrade
Office: VERA **STUPLJANIN**, SCS, Karnegijeva 4/III, 11120 Belgrade, Serbia (E-mail: JSCS-info@shd.org.rs)

Editorial Board:

From abroad: R. Adžić, Brookhaven National Laboratory (USA), J .O. M. Bockris, Texas A&M University (USA), D. Douglas, University of British Columbia (Canada), A. R. Katritzky, FRS, University of Florida (USA), Ya. I. Korenman, Voronezh Academy of Technology (Russian Federation) M. D. Lechner, University of Osnabruck (Germany), M. Spiteller, INFU- Technical University Dortmund (Germany).

From Serbia: B. Abramović, T. Ast, Ž. Čeković, A. Dekanski, V. Dondur, J. Đongalić, B. Đorđević, M. Đuran, F. Gaál, M. J. Gašić, S. Gojković, I. Gutman, B. Jovančićević, D. Jovanović, M. Jovanović, V. Leovac, R. Marković, S. Milonjić. U. Mioč, J. Nedeljković, O. Nedić, B. Nikolić, D. Opsenica, V. Panić, V. Pavlović, M. Petkovska, I. Popović, P. Premović, B. Radak, V. Radmilović, S. Ražić, D. Sladić, S. Sovilj, M. Spasić, S. Šerbanović, B. Šolaja, D. Vitorović, G. Vučković.

Subscription: The annual (12 issues) subscription rate is **150.00 €** including postage (surface mail) and handling. For Society members from abroad rate is **50.00 €**. For the proforma invoice with the instruction for bank payment contact the Society Office (E-mail: shd@shd.org.rs) or see JSCS Web Site http://www.shd.org.rs/JSCS/, option Subscription.

Godišnja pretplata: Za članove Srpskog hemijskog društva godišnja pretplata iznosi **2.500,00 RSD**, za penzionere i studente **1000,00 RSD**, a za ostale **3.500,00 RSD**. Za organizacije i ustanove godišnja pretplata iznosi **16.000,00 RSD**. Uplate se mogu vršiti na tekući račun Društva: **205-13815-62**, poziv na broj **320**, sa naznakom "pretplata za JSCS".

Nota: Odlukom Odbora za hemiju Republičkog fonda za nauku Srbije, br. 66788/1 od 22. 11. 1990. godine, koja je kasnije potvrđena odlukom Saveta Fonda, časopis je uvršten u kategoriju međunarodnih časopisa (**M-23**). Takođe, aktom Ministarstva za nauku i tehnologiju Republike Srbije, 413-00-247/2000-01 od 15. 06. 2000. godine, ovaj časopis je proglašen za publikaciju od posebnog interesa za nauku. Prema SCI-Expanded™ **Impact Factor** časopisa objavljen 2011. godine iznosi **0,725**. Radovi čiji su svi autori aktivni članovi Društva prioriteno se publikuju.

J. Serb. Chem. Soc. Vol. 77, No. 1 (2012)

ISSN 0352-5139

CONTENTS

Published by the Serbian Chemical Society
Karnegijeva 4/III, 11000 Belgrade, Serbia
Printed by the Faculty of Technology and Metallurgy
Karnegijeva 4, P.O. Box 35-03, 11120 Belgrade, Serbia

Journal of the Serbian Chemical Society
JSCS-info@shd.org.rs • www.shd.org.rs/JSCS
J. Serb. Chem. Soc. *77* (1) 1–8 (2012)
JSCS–4243
UDC 547.497.1+547.792+542.913:57–188
Original scientific paper

Synthesis of 1,6-hexanediyl-bis(semicarbazides) and 1,6-hexanediyl-bis(1,2,4-triazol-5-ones) and their antiproliferative and antimicrobial activity

MONIKA PITUCHA[1]*, JOLANTA RZYMOWSKA[2], ALINA OLENDER[3] and LUDMIŁA GRZYBOWSKA-SZATKOWSKA[4]

[1]Department of Organic Chemistry, Medical University, 20-081 Lublin, Poland, [2]Department of Biology and Genetics, Medical University, 20-081 Lublin, Poland, [3]Chair and Department of Medical Microbiology, Medical University, 20-093 Lublin, Poland and [4]Department of Oncology, Medical University, 20-090 Lublin, Poland

(Received 12 February, revised 14 August 2011)

Abstract. A series of 1,6-bis(3-substituted 1,5-dihydro-5-oxo-4*H*-1,2,4-triazol-4-yl)hexanes **3a**–**g** were synthesized by the cyclization reaction of 1,6-bis{[(2-substituted hydrazinyl)carbonyl]amino}hexanes **2a**–**g** in alkaline medium. The new derivatives **3a**–**c** were screened *in vitro* for their antiproliferative and anticancer activity in human tumor cell lines derived from breast and lung carcinoma cells. Compounds **3a** (at a concentration of 0.18 mM), **3b** (at concentrations of 0.12 and 0.02 mM) and **3c** (at concentrations of 0.23 and 0.11 mM) were found to be the most effective against the lung cell line. Compound **3a** had the greatest antiproliferative effect on the breast carcinoma cell line. Representative compounds were established and evaluated as antimicrobial agents. All the tested derivatives showed minimum inhibitory concentrations (*MIC*) in the range 1.87–7.5 μg mL^{-1}. Compound **3b** was the most effective against *Candida albicans* (*MIC* 1.87 μg mL^{-1}).

Keywords: synthesis; semicarbazide; 1,2,4–triazole; biological activity.

INTRODUCTION

The synthesis of compounds containing a 1,2,4–triazole ring in their structure has attracted widespread attention, mainly in connection with their wide range of pharmacological properties. A variety of biological activities, such as antidepressant,[1,2] anticonvulsant,[3] antitumor[4] and antimicrobial[5,6] have been reported for mono-substituted 1,2,4–triazole systems. A great number of these derivatives display interesting anticancer activity.[7,8] It was reported that compounds having triazole moieties, such as vorozole, anastrozole and letrozole, appear to be very effective aromatase inhibitors and are very useful for preventing breast cancer.[9]

* Corresponding author. E-mail: monika.pitucha@umlub.pl
doi: 10.2298/JSC110212157P

Moreover, several compounds involving the triazole moiety and having diverse antibacterial and antifungal activities were reported.[10–12] 1,2,4-Triazol-3-ones have been prepared by different methods. One of the most common routes leading to the preparation of these compounds involves cyclodehydration of 1-acetylsemicarbazide with a variety of reagents, such as tris(formylamino)methane,[13] sodium hydroxide[14,15] and formic acid.[16] 4,5-Disubstituted and 2,4,5-trisubstituted 1,2,4-triazol-3-ones have been obtained in the reaction of amidrazones salts with isocyanate or urea performed in the melt.[17] Some bis(3,4-disubstituted 5-oxo-1,2,4-triazol-5-4-yl)alkanes were synthesized using esters of ethoxalkylidene)hydrazinecarboxylic acids and diamines.[18]

On the other hand, it is known that semicarbazides, the key intermediates used in the synthesis of 1,2,4-triazol-3-one derivatives, are compounds with various pharmacological activities: antitubercular,[19] anticonvulsant[20] and antinociceptive.[21] It was found that some compounds possess antibacterial activity against Gram-positive bacteria, including staphylococci (coagulase-positive *Staphylococcus aureus* and coagulase-negative *Staphylococcus epidermidis*).[22] Semicarbazides possessing a heterocyclic ring show anticancer activity against human gastric carcinoma cell line.[23]

In view of the above-mentioned findings and in continuation of our research in the domain of heterocyclic compounds of the 1,2,4-triazole class with expected biological activity,[24,25] herein, the synthesis of some new bis-semicarbazides and their cyclization derivatives from the bis-1,2,4-triazole class with potential biological activity are described.

The newly obtained compounds were screened *in vitro* for their anticancer and antimicrobial activity.

RESULTS AND DISCUSSION

Synthesis

The carboxylic acid hydrazides **1a**–**g**, the key intermediates used for the synthesis of the 1,6-bis{[(2-substituted hydrazinyl)carbonyl]amino}hexanes **2a**–**g**, were synthesized according to a literature method.[26,27] New semicarbazide derivatives were obtained by the reaction of corresponding carboxylic acid hydrazide **1** with 1,6-hexamethylene diisocyanate (HDI). The reaction medium was diethyl ether and the process was realized at room temperature. Next, the obtained semicarbazides were subjected to cyclization in a 2 % solution of sodium hydroxide obtaining the corresponding 1,6-bis(3-substituted 1,5-dihydro-5-oxo-4*H*-1,2,4-triazol-4-yl)hexanes **3a**–**g**. The synthetic pathway followed for the preparation of the title compounds is presented in Scheme 1.

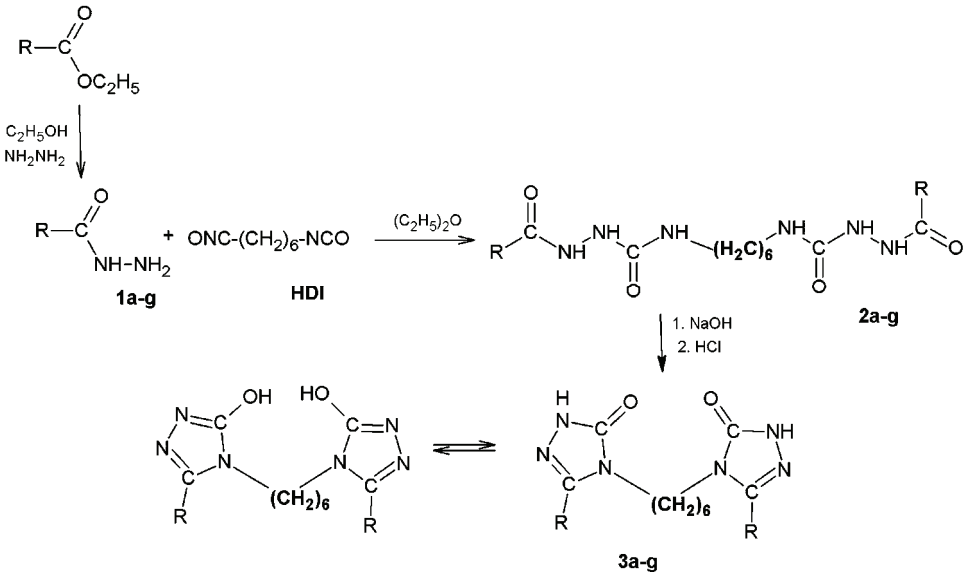

Comp.	R
a	CH_3
b	C_6H_5
c	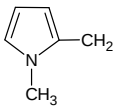
d	H
e	
f	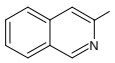
g	

Scheme 1. Synthesis of the 1,6-bis[(hydrazinylcarbonyl)amino)hexanes **2a**–**g** and of the 1,6-bis(5-oxo-1,2,4-triazol-4-yl)hexanes **3a**–**g**.

Characterization

The structures of the sy nthesized compounds were elucidated by ^{1}H-NMR, ^{13}C-NMR, MS and IR spectroscopy . Analytical and spectral data of the synthesized compounds are given in the Supplementary material.

The reaction products m ay exist in two different tautomeric forms (Schem e 1). The IR and ^{1}H-NMR data indicated that the obtained cy clization products exist in the keto form both in the solution and in the solid. In the IR spectra of the cyclic compounds containing the 1,2,4-triazole system, absorption bands of the

C=O group at 1683–1651 cm^{-1} were observed. ^{1}H-NMR spectra showed protons signals for the –N–C(O)–NH– group in the δ range 8.00–10.46 ppm.

Preliminary anticancer screening

The bis-1,2,4-triazol-3-one derivatives **3a–c** were evaluated for their antiproliferative and anticancer activity in two human cell lines derived from lung and breast carcinoma cells. One normal cell line was included in the cytotoxicity study – primary cell line of human skin fibroblasts (HSF). The results for each tested compound are reported as the growth inhibition percentage of the tested cells in comparison with the untreated cells. According to the data listed in Table I, compounds **3a–c** were found to be the most effective against human lung carcinoma cells *in vitro*. In the case of the human breast cancer cell line, a slight inhibition for compounds **3a** and **3b** was observed. A non-cytotoxic or stimulation effect of compound **3a** referring to normal cell line HSF and several-fold higher effect on the two observed carcinoma cell lines were ascertained. The investigated compounds exhibited dose-dependent effects. The most evident action was observed for all the examined compounds at a 50 μg mL^{-1} dose.

TABLE I. *In vitro* inhibition of the growth of normal and cancer cells by compounds **3a–c**; the examined concentration of compounds: I – a concentration of 100 μg mL^{-1}, which corresponds to a concentration of 0.35 (**3a**), 0.25 (**3b**) and 0.23 mM (**3c**); II – a concentration of 50 μg mL^{-1}, which corresponds to a concentration of 0.18 (**3a**), 0.12 (**3b**) and 0.11 mM (**3c**); III – a concentration of 10 μg mL^{-1}, which corresponds to a concentration of 0.04 (**3a**), 0.02 (**3b**) and 0.02 mM (**3c**)

Cell	Time of incubation / h	Growth inhibition factor, *GI* / %								
		Compound								
		3a			**3b**			**3c**		
		Dose								
		I	II	III	I	II	III	I	II	III
Human skin fibroblast HSF	24	0	0	0	5	5	0	0	0	5
	48	0	0	0	5	5	5	0	5	10
	72	0	0	0	5	5	5	5	5	10
Human lung cancer cell line A549	24	0	22	0	5	5	10	10	10	0
	48	0	25	0	5	20	10	25	25	0
	72	5	25	5	5	20	10	25	25	5
Human breast cancer cell line T47D	24	5	5	5	0	0	0	0	5	5
	48	5	10	10	0	10	10	5	5	5
	72	0	10	10	5	10	0	0	0	5

Antimicrobial activity

Selected compounds, **2a–c** and **3a–c**, were screened for their possible antimicrobial activities against *Staphylococcus aureus* ATCC 25923, *Klebsiella pneumoniae* ATCC 700603, *Enterococcus faecalis* ATCC 2912, *Escherichia coli* ATCC 25822, *Pseudomonas aeruginosa* ATCC 27853 and *Candida albicans* ATCC

90028, and clinical isolates of *C. albicans*, *C. parapsilosis*, *C. kefyr*, and *C. tropicalis*. The antimicrobial susceptibility to the tested compounds was determined by *MIC* (minimum inhibitory concentration) values and compared to amphotericin B and meropenem as standard drugs. All the studied bacterial species were classified as resistant to the standard meropenem, *MIC* > 1.0 μg mL^{-1},[28] and the studied species *Candida* spp. as resistant to the standard amphotericin B, *MIC* > > 16.0 μg mL^{-1}.[29] Compounds **3a** and **3b** at concentrations 3.75 and 1.87 μg mL^{-1}, respectively, were active against the tested *C. albicans* (clinical isolates, **3b**), *C. albicans* ATCC 90028 (**3b**) and *C. tropicalis* (**3a**, Table II). The other compounds were also found to inhibit growth of *Candida* spp. at a concentration of 7.5 μg mL^{-1}. All the tested derivatives showed *in vitro* effectiveness against the five reference species: *S. aureus* ATCC 25923, *K. pneumoniae* ATCC 700603, *E. faecalis* ATCC 2912, *E. coli* ATCC 25822 and *P. aeruginosa* ATCC 27853 at a concentration of 7.5 μg mL^{-1}.

TABLE II. Minimum inhibitory concentration (*MIC* / μg mL^{-1}) of compounds **2a–c** and **3a–c**; Ca* – *C. albicans* ATCC 90028, Ca - *C. albicans*, Cp - *C. parapsilosis*, Ck - *C. kefyr*, Ct- *C. tropicalis*, Sa- *S. aureus* ATCC 25923, Kp - *K. pneumoniae* ATCC 700603, Ef - *E. faecalis* ATCC 2912, Ec – *E. coli* ATCC 25822, Pa- *P. aeruginosa* ATCC 27853, ST - Standard: *amphotericin B, **meropenem

Compound	Microorganism									
	Ca*	Ca	Cp	Ck	Ct	Sa	Kp	Ef	Ec	Pa
2a	7.5	7.5	7.5	7.5	7.5	7.5	7.5	7.5	7.5	7.5
2b	7.5	7.5	7.5	7.5	7.5	7.5	7.5	7.5	7.5	7.5
2c	7.5	7.5	7.5	7.5	7.5	7.5	7.5	7.5	7.5	7.5
3a	7.5	7.5	7.5	7.5	3.75	7.5	7.5	7.5	7.5	7.5
3b	1.87	1.87	7.5	7.5	7.5	7.5	7.5	7.5	7.5	7.5
3c	7.5	7.5	7.5	7.5	7.5	7.5	7.5	7.5	7.5	7.5
ST	<0.5*	<0.5*	<0.5*	<0.5*	<0.5*	0.05**	0.05**	5.0**	0.5**	0.1**

EXPERIMENTAL

All chemicals were purchased from Merck or Alfa-Aesar and used without further purification. Melting points (m.p.) were determined in a Fisher-Johns block and are not corrected. The IR spectra were recorded in KBr discs using a Specord IR-75 spectrophotometer. The ^{1}H- and ^{13}C-NMR spectra were generally recorded at room temperature on a Bruker AC 200F instrument (300 MHz) in DMSO-d_6 with TMS as the internal standard. The mass spectra were obtained using an AMD-604 mass spectrometer with a 70 eV electron beam. The purity of the obtained compounds was checked by TLC on aluminum oxide 60 F_{254} plates (Merck) in $CHCl_3$/C_2H_5OH (10:1 and 10:2) solvent systems with UV or iodine visualization.

*General procedure for the synthesis of 1,6-bis{[(2-substituted hydrazinyl)carbonyl]amino}-hexanes **2a–g***

A mixture of an appropriate carboxylic acid hydrazide **1** (20 mmol) and 1,6-hexametylene diisocyanate (1.68 g, 10 mmol), and 10 mL of diethyl ether was kept at room tempera-

ture for 24 h. Then, the formed compound was filtered off, washed with diethyl ether and crystallized from ethanol.

*General procedure for the synthesis of 1,6-bis(3-substituted 1,5-dihydro-5-oxo-4*H*-1,2,4-triazol-4-yl)hexanes **3a–g***

The appropriate semicarbazide **2** (10 mmol) was placed in a round-bottomed flask equipped with reflux and 40–50 mL of a 2 % sodium hydroxide solution was added. The flask was heated for 10 h. After cooling, the solution was neutralized with dilute hydrochloric acid. The precipitate was filtered off and then crystallized from ethanol.

Proliferation of tumor cells assay

The synthesized compounds **3a–c** were evaluated for their anticancer activity in human tumor cell lines derived from lung and breast carcinoma cells. The studies was performed on A549 (ECACC 86012804 human lung epithelial) cells and T47D (ECACC 85102201 human breast epithelial). The influence of the newly synthesized triazoles on human skin fibroblast cells (HSF) was also determined. The cell lines were incubated at 10^4 cells per mL density on microtiter plates. The tested compounds were then added at three examined concentrations: 10, 50 and 100 μg mL^{-1}, and the cultures were incubated under standard conditions (37 °C, 5 % CO_2 and 90 % humidity) for 24, 48 and 72 h. The determinations were realized by 5-bromo-2'-deoxyuridine (BrdU) labeling [30,31] and detection kit (Roche) on an ELISA reader (BIO-TEC Instruments, USA). The viability of normal and carcinoma cells were evaluated spectrophotometrically. The results of all spectrophotometric measurements were registered as percent growth inhibition or growth stimulation. All experiments were repeated in triplicate.

Antifungal screening

Clinical isolates of *Candida albicans*, *C. parapsilosis*, *C. kefyr* and *C. tropicalis* and *C. albicans* ATCC 90028, all susceptible to amphotericin B (as determined by ATB fungitest-bioMerieux), were tested for their susceptibility to the newly obtained compounds. Stock solutions were prepared in dimethyl sulfoxide (DMSO), at a working concentration of 300 mg mL^{-1}. Final dilutions were prepared in RPMI 1640 medium (Sigma) buffered to pH 7.0, 0.165 M 4-morpholinepropanesulfonic acid (MOPS) buffer (Sigma) in 96-well plates (NUNC). The concentration of the *Candida* species in the final inoculums was $(1.5\pm1.0)\times10^3$ cells mL^{-1} RPMI 1640. All strains were incubated for 48 h at 35 °C.[32-34] As controls, DMSO and amphotericin B were used. The results were obtained spectrophotometrically (570 nm) and compared to the control results.[35]

Antibacterial screening

Antibacterial susceptibility was determined on following strains: *S. aureus* ATCC 25923, *K. pneumoniae* ATCC 700 603, *E. faecalis* ATCC 29 12, *E. coli* ATCC 25822 and *P. aeruginosa* ATCC 27853. Dilutions of the tested compounds were prepared from the stock solutions in DMSO. The susceptibilities of the bacterial strains 1.0 x 10^3 cells mL^{-1} to the tested compounds were determined by the CLSI microlitre broth dilution method,[22,36] performed in 96-well plates (NUNC) – 200 μL per well, at 35 °C for 24 h. As the control, meropenem at the same dilutions in DMSO was used for bacterial strains cultured under the same conditions. The results were obtained spectrophotometrically at 570 nm.

CONCLUSIONS

In the present study, novel series of 1,6-bis{[(2-substituted hydrazinyl)carbonyl]amino}hexanes and 1,6-bis(3-substituted 1,5-dihydro-5-oxo-4*H*-1,2,4-triazol-

-4-yl)hexanes were synthesized and characterized. The new derivatives **3a**–**c** were screened *in vitro* for their antiproliferative and anticancer activity in human tumor cell lines derived from breast and lung carcinoma cells. Compounds **3a** (at a concentration of 0.18 mM), **3b** (at concentrations of 0.12 and 0.02 mM) and **3c** (at concentrations of 0.23 and 0.11 mM) were found to be the most effective against the lung cell line. Compounds **2a**–**c** and **3a**–**c** were screened for their antimicrobial activities. All the tested derivatives showed *MIC* values in range 1.87–7.5 μg mL^{-1}.

SUPPLEMENTARY MATERIAL

Analytical and spectral data of synthesized compounds are available electronically from http://www.shd.org.rs/JSCS/, or from the corresponding author on request.

ИЗВОД

СИНТЕЗА 1,6-ХЕКСАНДИИЛ-БИС(СЕМИКАРБАЗИДА) И 1,6-ХЕКСАНДИИЛ-БИС-(1,2,4,-ТРИАЗОЛ-5-ОНА) И ЊИХОВА АНТИПРОЛИФЕРАТИВНА И АНТИБАКТЕРИЈСКА АКТИВНОСТ

M. PITUCHA[1], J. RZYMOWSKA[2], A. OLENDER[3] и L. GRZYBOWSKA-SZATKOWSKA[4]

[1]Department of Organic Chemistry, Medical University, 20-081 Lublin, Poland, [2]Department of Biology and Genetics, Medical University, 20-081 Lublin, Poland, [3]Chair and Department of Microbiology, Medical University, 20-093 Lublin, Poland u [4]Department of Oncology, Medical University, 20-090 Lublin, Poland

Синтетисана је серија 1,6-бис(3-супституисаних 1,5-дихидро-5-оксо-4*H*-1,2,4-триазол-4--ил)хексана **3a**–**g** реакцијом циклизације 1,6-бис{[(2-супституисаних хидразинил)карбо-нил]}хексана **2a**–**g** под базним условима. Испитана је *in vitro* антипролиферативна активност нових деривата **3a**–**3c** према ћелијским линијама хуманих тумора дојке и плућа. Утврђено је да су једињења **3a** (при концентрацији 0,18 mM), **3b** (при концентрацијама 0,12 и 0,02 mM) и **3c** (при концентрацијама 0,23 и 0,11 mM) најактивнија према ћелијској линији рака плућа. Једињење **3a** је најактивније према ћелијској линији рака дојке. Репрезентативним једињењима испитана је антимикробна активност. Сва испитана једињења показују *MIC* вредности у опсегу 1,87–7,5 μg/mL. Једињење **3b** је најактивније према *C. albicans* (*MIC* = = 1,87 μg/mL).

(Примљено 12. фебруара, ревидирано 14. августа 2011)

REFERENCES

1. D. L. Temple, US 4386091 (1983) (*CA* **99** 19529)
2. A. Catanese, E. Lisciari, *Boll. Chim. Farm.* **109** (1970) 369
3. Ş. G. Küçükgüzel, G. Rollas, O. Ötük-Saniş, I. Bayrak, T. Altuğ, J. P. Stables *Farmaco* **59** (2004) 893
4. B. S. Holla, B. Veerendra, M. K. Shivananada, B. Poojary, *Eur. J. Med. Chem*. **38** (2003) 759
5. S. Rolas, N. Kalyonuoglu, D. Sur-Altiner, Y. Yegenoglu, *Pharmazie* **48** (1993) 308
6. N. Gülerman, S. Rollas, M. Kiraz, A. C. Ekinci, A Vidin, *Farmaco* **52** (1997) 691
7. O. Bekircan, M. Kucuk, B. Kahveci, H. Bektas, *Z. Naturforsch.* **63b** (2008) 130
8. K. Sztanke, T. Tuzi mski, J. Rzymowska, K. Pasternak, M. Kandefer-Szerszeń, *Eur. J. Med. Chem.* **43** (2008) 404

9. M. Clemons, R.E. Coleman, S. Verma, *Cancer Treat. Rev*. **30** (2004) 325
10. N. Singhal, P.K Sharma, R. Dudhe, N. Kumar, *J. Chem. Pharm. Res.* **3** (2011) 126
11. A. Demirbas, D. Sahin, N. Demirbas, S. A. Karaoglu, *Eur. J. Med. Chem*. **44** (2009) 2896
12. H. Bektaş, N. Karaali, D. Şahin, A. Demirbaş, Ş.A. Karaoglu, N. Demirbaş, *Molecules* **15** (2010) 2427
13. M. Dobosz, *Annales UMCS, Lublin, Sectio AA* **34** (1979) 163
14. M. Dobosz, A. Pachuta-Stec, E. Tokarzewska-Wielosz, E. Jagiełło-Wójtowicz, *Acta Pol. Pharm.* **57** (2000) 205
15. M. Wujec, M. Pitucha, M. Dobosz, *Heterocycles* **68** (2006) 779
16. M. Koch, DE 3114314 (1983) (*CA* **98** 72110g)
17. A. Stunder, DE 3114349 (1983) (*CA* **98** 198249t)
18. A. A. Ikizler, K. Sancak, *Collect. Czech. Chem. Commun*. **60** (1995) 903
19. O. V. Fedorowa, G. G. Mordovskoi, G. L. Rusinov, I. G. Ovchinnikova, M. N. Zueva, M. A. Kravchenko, O. N. Chupakhin, *Pharm. Chem*. **32** (1998) 2
20. F. Azam, I.A. Alksakas, S.L. Khokra, O. Prakash, *Eur. J. Med. Chem* **44** (2009) 203
21. S. V. Andurkar, C. Beguin, J. P. Stables, H. Kohn, *J. Med. Chem*. **44** (2001) 1475
22. M. Pitucha, Z. Karczmarzyk, U. Kosikowska, A. Malm, *Z. Naturforsch*. **66b** (2011) 505
23. Z. Cui, Y. Ling, B. Li, Y. Li, C. Rui, J. Cui, Y. Shi, X. Yang, *Molecules* **15** (2010) 4267
24. M. Pitucha, B. Polak, R. Świeboda, U. Kosikowska, A. Malm, *Z. Naturforsch*. **64b** (2009) 570
25. M. Pitucha, A. Chodkow ska, M. Maciejewski, E. Jagie łło-Wójtowicz, A. Pachuta-Stec, *Monatsh. Chem*. **141** (2010) 199
26. M. Dobosz , M. Pitucha, M. Wujec *Acta Pol. Pharm*. **53** (1996) 31
27. M. Pitucha, M. Wujec, M. Dobosz, *Annales UMCS, Sectio AA* **59** (2004) 144
28. D. J. Diekema, S. A. Messer, L. B. Boyken, R. J. Hollis, J. Kroeger, S. Tendolkar, M. A. Pfaller. *J. Clin. Microbiol.* **47** (2009) 3170
29. Clinical and Laboratory Standards Institute (CLSI), *Performance Standards for Antimicrobial Susceptibility Testing, Twentieth Informational Supplement*, M100-S20-U, Wayne, PA, 2010
30. J. P. Magaud, I. Sarget, D.Y. Mason, *J. Immunol. Methods* **106** (1988) 95
31. D. Muris, S. Varon, M. Manthorpe, *Anal. Biochem*. **185** (1990) 377
32. M. P. Areval o, A. J. Carrillo-Munoz, J. Salg ado, D. Card enes, S. Brio, G. Quindos A. Espinel-Ingroff , *J. Antimicrob. Chemother*. **51** (2003) 163
33. M. R. Capoor, D. Nair, M. Dep, P. K. Verma, L. Srivastava, P. Aggarwaj, *Jpn. J. Infect. Dis*. **58** (2005) 344
34. F. Sabatelli, P. A. Mann, C. A. Mendrick, C. C. Norris, R. Hare, D. Loebenberg, T. A. Black, P. M. McNicholas, *Antimicrob. Agents. Chemother*. **50** (2006) 2009
35. K. L. Threse, R. Bagyalakshim, H. N. Madhavan, P. Deepa, *Indian J. Med. Microbiol*. **20** (2002) 160
36. Clinical and Laboratory Standards Institut e (CLSI), National Co mmittee for Clinical Laboratory Standards (NCLS), *Methods for Dilution Antimicrobial Susceptibility Test for Bacteria that Grow Aerobically*, Approved standard M7-A6, 6th ed., Wayne, PA, 2003.

Journal of the Serbian Chemical Society
JSCS@tmf.bg.ac.rs • www.shd.org.rs/JSCS
J. Serb. Chem. Soc. 77 (1) S1–S3 (2012) *Supplementary material*

SUPPLEMENTARY MATERIAL TO

Synthesis of 1,6-hexanediyl-bis(semicarbazides) and 1,6-hexanediyl-bis(1,2,4-triazol-5-ones) and their antiproliferative and antimicrobial activity

MONIKA PITUCHA1*, JOLANTA RZYMOWSKA2, ALINA OLENDER3 AND LUDMIŁA GRZYBOWSKA-SZATKOWSKA4

[1]Department of Organic Chemistry, Medical University, 20-081 Lublin, Poland, [2]Department of Biology and Genetics, Medical University, 20-081 Lublin, Poland, [3]Chair and Department of Medical Microbiology, Medical University, 20-093 Lublin, Poland and [4]Department of Oncology, Medical University, 20-090 Lublin, Poland

J. Serb. Chem. Soc. 77 (1) (2012) 1–8

ANALYTICAL AND SPECTRAL DATA OF THE SYNTHESIZED COMPOUNDS

*Acetic acid, 2,2'-[1,6-hexanediylbis(iminocarbonyl)]dihydrazide (**2a**)*. Yield: 78 %; m.p. 270–272 °C; Anal. Calcd. for $C_{12}H_{24}N_6O_4$ (FW: 316.36): C, 45.55; H, 7.64; N, 26.56 %. Found: C, 45.27; H, 7.58; N, 26.88 %; IR (KBr, cm^{-1}): 3312 (NH), 2937, 1470 (CH aliph.), 1641 (CO); ^{1}H-NMR (300 MHz, DMSO, δ / / ppm): 1.03–1.35 (8H, *m*, CH_2), 1.80 (6H, *s*, CH_3), 2.94–3.07 (4H, *m*, CH_2), 6.31 (2H, *s*, NH), 7.56 (2H, *s*, NH), 9,36 (2H, *s*, NH); ^{13}C-NMR (75 MHz, DMSO, δ / ppm): 19.24 (CH_3), 24.63, 28.45 (CH_2), 156.81, 167.80 (CO); MS (*m*/*z*, (%)): 152 (45), 113 (60), 102 (100), 99 (90), 56(85).

*Benzoic acid, 2,2'-[1,6-hexanediylbis(iminocarbonyl)]dihydrazide (**2b**)*. Yield: 79 %; m.p. 229–230 °C; Anal. Calcd. for $C_{22}H_{28}N_6O_4$ (FW: 440.49): C, 59.98; H, 6.40; N, 19.07 %. Found: C, 59.77; H, 6.38; N, 19.32 %; IR (KBr, cm^{-1}): 3304 (NH), 3116 (CH arom.), 2933, 1482 (CH aliph.), 1651 (CO); ^{1}H-NMR (300 MHz, DMSO, δ / ppm): 1.05–1.38 (8H, *m*, CH_2), 2.93–3.17 (4H, *m*, CH_2), 5.73 (2H, *s*, NH), 6.48 (2H, *s*, NH), 7.35–8.37 (10H, *m*, CH), 10.10 (2H, *s*, NH); ^{13}C-NMR (75 MHz, DMSO, δ / ppm): 24.74, 28.51 (CH_2), 126.20, 126.92, 130.27, 131.35 (CH arom.), 157.14 (C Ar), 165.08 (CO); MS (*m*/*z*, (%)): 284 (15), 143 (100), 98 (50), 86 (45).

*1-Methyl-1*H*-pyrrole-2-acetic acid, 2,2'-[1,6-hexanediylbis(iminocarbonyl)]-dihydrazide (**2c**)*. Yield: 80 %; m.p. 203–205 °C; Anal. Calcd. for $C_{22}H_{34}N_8O_4$ (FW: 474.56): C, 55.68; H, 7.22; N, 23.61 %. Found: C, 55.45; H, 7.42; N, 23.78 %; IR (KBr, cm^{-1}): 3349 (NH), 3030 (CH arom.), 2934, 1463 (CH aliph.), 1590

* Corresponding author. E-mail: monika.pitucha@umlub.pl

(CO); ^{1}H-NMR (300 MHz, DMSO, δ / ppm): 1.22–1.35 (8H, *m*, CH_2), 2.96–2.99 (4H, *m*, CH_2), 3.31 (4H, *s*, CH_2), 3.52 (6H, *s*, CH_3), 5.84 (2H, *s*, NH), 6.23–6.60 (6H, *m*, CH), 7.66 (2H, *s*, NH), 9.55 (2H, *s*, NH); ^{13}C-NMR (75 MHz, DMSO, δ / ppm): 22.33 (CH_3), 24.14, 24.35, 24.77, 26.72 (CH_2), 32.05 (CH_2), 104.98, 106.49, 121.06, 123.95 (CH arom), 143.73 (C arom), 153.76 (CO); MS *(m/z*, %): 277 (33), 94 (100).

*Formic acid, 2,2'-[1,6-hexanediylbis(iminocarbonyl)]dihydrazide (**2d**).* Yield: 77 %; m.p. 155–157 °C; Anal. Calcd. for $C_{10}H_{20}N_6O_4$ (FW: 288.30): C, 41.65; H, 6.99; N, 29.14 %. Found: C, 41.44; H, 7.03; N, 29.03 %; IR (KBr, cm^{-1}): 3351 (NH), 3032 (CH arom.), 2931, 1465 (CH aliph.) 1589 (CO); ^{1}H-NMR (300 MHz, DMSO, δ / ppm): 1.06–1.36 (8H, *m*, CH_2), 2.91–3.07 (4H, *m*, CH_2), 7.94 (1H, *s*, CH), 8.01 (1H, *s*, CH), 9.16 (2H, *d*, NH), 9.54 (2H, *d*, NH), 10.05 (2H, *s*, NH); ^{13}C-NMR (75 MHz, DMSO, δ / ppm): 24.57, 24.71, 27.79. 28.30 (CH_2), 63.57 (CH), 166.39 (CO).

*1-Naphthoic acid, 2,2'-[1,6-hexanediylbis(iminocarbonyl)]dihydrazide (**2e**).* Yield: 73 %; m.p. 138–140 °C; Anal. Calcd. for $C_{30}H_{32}N_6O_4$ (FW: 540.61): C, 66.65; H, 5.96; N, 15.54 %. Found: C, 66.73; H, 5.88; N, 15.34 %; IR (KBr, cm^{-1}): 3353 (NH), 3032 (CH arom.), 2937, 1465 (CH aliph.), 1587 (CO); ^{1}H-NMR (300 MHz, DMSO, δ / ppm): 1.33–1.56 (8H, *m*, CH_2), 3.32–3.37 (4H, *m*, CH_2), 6.44 (2H, *s*, NH), 7.49–8.06 (15H, *m*, CH), 8.34 (2H, *s*, NH), 10.01 (2H, *s*, NH).

*3-Isoquinolinecarboxylic acid, 2,2'-[1,6-hexanediylbis(iminocarbonyl)]dihydrazide (**2f**).* Yield: 71 % ; m.p. 242–244 °C; Anal. Calcd. for $C_{28}H_{30}N_8O_4$ (FW: 542.59): C, 61.98; H, 5.57; N, 20.65 %. Found: C, 61.81; H, 5.68; N, 20.46 %. IR (KBr, cm^{-1}): 3347 (NH), 3028 (CH arom.), 2933, 1459 (CH aliph.), 1594 (CO); ^{1}H-NMR (300 MHz, DMSO, δ / ppm): 1.06–1.57 (8H, *m*, CH_2), 3.32–3.36 (4H, *m*, CH_2), 6.42 (2H, *t*, NH), 7.80–8.57 (14H, *m*, CH), 9.40 (2H, *s*, NH), 10.26 (2H, *s*, NH); ^{13}C-NMR (75 MHz, DMSO, δ / ppm): 13.71, 24.70, 27.79, 28.31 (CH_2), 154.54, 156.41, 157.74, 158.80, 159.36, 160.27 (CH arom.), 165.51, 165.64 (C arom.), 166.39 (CO).

*Nicotinic acid, 2,2'-[1,6-hexanediylbis(iminocarbonyl)]dihydrazide (**2g**).* Yield: 66 %; m.p. 185–187 °C; Anal. Calcd. for $C_{20}H_{26}N_8O_4$ (FW: 442.47): C, 54.28; H, 5.92; N, 25.32 %. Found: C, 54.12; H, 5.98; N, 25.34 %; IR (KBr, cm^{-1}): 3353 (NH), 3028 (CH arom.), 2931, 1466 (CH aliph.), 1593 (CO); ^{1}H-NMR (300 MHz, DMSO, δ / ppm): 1.13–1.38 (8H, *m*, CH_2), 2.93–3.02 (4H, *m*, CH_2), 7.47––8.14 (8H, *m*, CH), 7.87 (2H, *s*, NH), 10.29 (4H, *s*, NH).

*4,4'-(1,6-Hexanediyl)bis[2,4-dihydro-5-methyl-3*H*-1,2,4-triazol-3-one] (**3a**).* Yield: 89 %; m.p. 235–237 °C.[18]

*4,4'-(1,6-Hexanediyl)bis[2,4-dihydro-5-phenyl-3*H*-1,2,4-triazol-3-one] (**3b**).* Yield: 70 %; m.p. 238–240 °C.[18]

*4,4'-(1,6-Hexanediyl)bis[2,4-dihydro-5-[(1*H*-pyrrol-2-yl)methyl]-3*H*-1,2,4-triazol-3-one] (**3c**).* Yield: 77 %; m.p. 228–230 °C; Calcd. for $C_{22}H_{30}N_8O_2$ (FW:

438.53): C, 60.25; H, 6.89; N, 25.55 %. Found: C, 60.33; H, 6.78; N, 25.34; IR (KBr, cm^{-1}): 3067 (CH arom.), 2928, 1496 (CH aliph.), 1698 (CO), 1575 (C=N), 1428 (C–N); ^{1}H-NMR (300 MHz, DMSO, δ / ppm): 1.09–1.26 (8H, *m*, CH_2), 3.39–3.44 (4H, *m*, CH_2), 3.49 (6H, *s*, CH_3), 3.89 (4H, *s*, CH_2), 5.69–6.64 (6H, *m*, CH), 11.44 (2H, *s*, NH); ^{13}C-NMR (75 MHz, DMSO, δ / ppm): 23.70 (CH_3), 25.50, 28.09, 33.41 (CH_2), 106.32, 107.84 (CH arom.), 145.05 (C arom.), 155.09 (CO); MS (*m*/*z*, (%)): 438 (54) [M^+], 177 (47), 94 (100).

*4,4'-(1,6-Hexanediyl)bis[2,4-dihydro-3*H*-1,2,4-triazol-3-one]* (***3d***). Yield: 71 %; m.p. 170–171 °C: Anal. Calcd. for $C_{10}H_{16}N_6O_4$ (FW: 284.27): C, 42.25; H, 5.67; N, 29.56 %. Found: C, 42.33; H, 5.77; N, 29.48 %; IR (KBr, cm^{-1}): 3072 (CH arom.), 2931, 1489 (CH aliph.), 1708 (CO), 1568 (C=N), 1430 (C–N); ^{1}H--NMR (300 MHz, DMSO, δ / ppm): 1.03–1.57 (8H, *m*, CH_2), 2.93–3.00 (4H, *m*, CH_2), 7.51 (1H, *s*, CH), 7.88 (1H, *s*, CH), 11.59 (2H, *s*, NH); ^{13}C-NMR (75 MHz, DMSO, δ / ppm): 25.32, 25.59, 28.55 (CH_2), 137.82 (CH), 154.53 (C arom.), 158.90 (CO).

*4,4'-(1,6-Hexanediyl)bis[2,4-dihydro-5-(1-naphthyl)-3*H*-1,2,4-triazol-3-one]* (***3e***). Yield: 68 % ; m.p. 160–161 °C; Anal. Calcd. for $C_{30}H_{28}N_6O_2$ (FW: 504.58): C, 71.40; H, 5.59; N, 16.65 %. Found: C, 71.22; H, 5.38; N, 16.73 %; IR (KBr, cm^{-1}): 3067 (CH arom.), 2928, 1496 (CH aliph.), 1698 (CO), 1575 (C=N), 1428 (C–N); ^{1}H-NMR (300 MHz, DMSO, δ / ppm): 0.89–1.57 (8H, *m*, CH_2), 2.72–3.39 (4H, *m*, CH_2), 7.31–8.35 (14H, *m*, CH), 10.01 (1H, *s*, NH), 12.05 (1H, *s*, NH); ^{13}C-NMR (75 MHz, DMSO, δ / ppm): 25.28, 25.49, 25.85, 26.11, 26.18, 28.02 (CH_2), 124.5–132.7 (CH), 133.1, 133.5, 145.3, 155.2 (C arom.), 168.7 (CO); MS (*m*/*z*, (%)): 212 (75), 155 (100), 127 (80).

*4,4'-(1,6-Hexanediyl)bis[2,4-dihydro-5-(1-isoquinolinyl)-3*H*-1,2,4-triazol-3--one]* (***3f***). Yield: 67 %; m.p. 150–152 °C; Anal. Calcd. for $C_{28}H_{26}N_8O_2$ (FW: 506.56): C, 66.38; H, 5.17; N, 22.12 %. Found: C, 66.24; H, 5.07; N, 22.34 %; IR (KBr, cm^{-1}): 3068 (CH arom.), 2929, 1702 (CH aliph.), 1573 (CO), 1495 (C=N), 1427 (C–N); ^{1}H-NMR (300 MHz, DMSO, δ / ppm): 1.11–1.58 (8H, *m*, CH_2), 3.89–4.11 (4H, *m*, CH_2), 7.48–8.69 (14H, *m*, CH), 12.12 (2H, *s*, NH); MS (*m*/*z*, (%)): 189 (22), 163 (39), 137 (100), 78 (57).

*4,4'-(1,6-Hexanediyl)bis[2,4-dihydro-5-(1-pyridinyl)-3*H*-1,2,4-triazol-3-one]* (***3g***). Yield: 66 % ; m.p. 125–126 °C; Anal. Calcd. for $C_{20}H_{22}N_8O_2$ (FW: 406.44): C, 59.10; H, 5.45; N, 27.56 %. Found: C, 59.32; H, 5.33; N, 27.43 %; ^{1}H-NMR (300 MHz, DMSO, δ / ppm): 1.08–1.41 (8H, *m*, CH_2), 3.59–3.71 (4H, *m*, CH_2), 7.53–68.84 (8H, *m*, CH), 11.80 (2H, *s*, NH); ^{13}C-NMR (75 MHz, DMSO, δ / ppm): 23.72, 24.15, 24.29, 24.76, 26.73 (CH_2), 122.02, 122.49, 133.87, 134.07, 142.72, 142.77 (CH arom.), 146.89, 149.55 (C arom.), 156.84, 163.42 (CO); MS (*m*/*z*, (%)): 406 (23) [M^+], 231 (65), 189 (67), 163 (100), 105 (65).

Journal of the Serbian Chemical Society
JSCS-info@shd.org.rs • www.shd.org.rs/JSCS
J. Serb. Chem. Soc. *77* (1) 9–16 (2012)
JSCS–4244
UDC 547.78+547.233+547.282.1:615.28–188
Original scientific paper

New oxadiazole derivatives of isonicotinohydrazide in the search for antimicrobial agents: Synthesis and *in vitro* evaluation

MANAV MALHOTRA[1], MOHIT SANDUJA[2], ABDUL SAMAD[3] and AAKASH DEEP[4]*

[1]*Department of Pharmaceutical Chemistry, Meerut Institute of Engineering and Technology, Bypass Road-Baghpat Crossing, Meerut-250005, Uttar Pradesh, India,* [2]*Department of Pharmaceutical Chemistry, ISF College of Pharmacy, Ferozepur Road, Moga-142001, India,* [3]*Department of Pharmaceutical Chemistry, College of Pharmacy in Al-Kharj, King Saud University, Riyadh, Saudi Arabia and* [4]*Department of Pharmaceutical Sciences, Maharshi Dayanand University, Rohtak-124001, India*

(Received 23 January, revised 24 June 2011)

Abstract: Structural modifications of the front line antitubercular drug isoniazid provide lipophilic adaptations of the drug in which the hydrazide moiety of isoniazid is replaced by 1,3,4-oxadiazole heterocycles to eliminate *in vivo* acetylation by arylamine *N*-acetyltransferase, which results in the formation of inactive acetylated drug. In the present study, a series of sixteen oxadiazole derivatives were synthesized and characterized by IR, ^{1}H-NMR, ^{13}C-NMR and mass spectral studies. All the synthesized compounds were evaluated for their antimicrobial activity by broth dilution method against two Gram-positive bacterial strains (*Bacillus subtilis* and *Staphylococcus aureus*), two Gram-negative bacterial strains (*Pseudomonas aeruginosa* and *Escherichia coli*) and two fungal strains (*Candida albicans* and *Aspergillus niger*). The minimum inhibitory concentrations of the compounds were in the range of 1.56–50 μg ml^{-1} against the bacterial and fungal strains. The results revealed that all the synthesized compounds have a significant biological activity against the tested microorganisms. Among the synthesized derivatives **4g**, **4h**, **4m** and **4p** were found to be the most effective antimicrobial compounds.

Keywords: 1,3,4-oxadiazoles; antimicrobial activity; isoniazid; Mannich bases; lipophilicity.

INTRODUCTION

One of the key objectives of organic and medicinal chemists is to design and synthesize molecules having potent therapeutic values.[1] The rapid development of resistance to existing antimicrobial drugs generates a serious challenge to the scientific community. Consequently, there is a vital need for the development of new antimicrobial agents having potent activity against the resistant microorga-

* Corresponding author. E-mail: aakashdeep82@gmail.com
doi: 10.2298/JSC110123155M

nism.[2–5] 1,3,4-Oxadiazoles have played an important role in medicinal chemistry, pesticide chemistry, polymer science and they are the building blocks in the construction of new molecular systems for biologically active molecules.[6] Many 1,3,4-oxadiazoles display a remarkable biological activity, such as anti microbial,[7,8] anti-HIV,[9] antitubercular,[10] antimalarial,[11] analgesic,[12] anti-inflammatory.[13] The oxadiazole pharmacophore has a key property that influences the ability of a drug to reach the target by transmembrane diffusion and show potent antimicrobial activity.[14] Inspired by the above facts and in continuation of an ongoing research program in the field of the synthesis and determination of the antimicrobial activity of medicinally important compounds,[15,16] the synthesis and antimicrobial evaluation of new oxadiazole derivatives are reported herein.

EXPERIMENTAL

Material and methods

Melting points of the synthesized compounds were determined in open-glass capillaries on Stuart SMP10 melting point apparatus and are uncorrected. The purity of the compounds was checked by thin layer chromatography (TLC). Silica gel, 0.25 m m, 60 GF_{254}, precoated sheets obtained from Merck, (Germany) were used for the TLC and the spots were visualized by iodine vapor/ultraviolet light. The IR spectra were obtained on a Perkin-Elmer 1600 FTIR spectrometer in KBr pellets. The ^{1}H-NMR spectra were recorded in DMSO-d_6 solutions on a Varian-Mercury 300 MHz spectrometer using tetramethylsilane as the internal reference. The ^{13}C-NMR spectra were recorded in DMSO-d_6 solutions on a Bruker Avance II 400 spectrometer at using tetramethylsilane as the internal reference. The mass spectra were recorded on a Shimadzu GCMS-QP 1000 EX. The elemental analyses were performed on an ECS 4010 elemental combustion system. The necessary chemicals were purchased from Loba Chemie, Fluka and Aldrich.

(E)-N'-*(2-Methoxybenzylidene)isonicotinohydrazide (**1a**)*

A mixture of 2-methoxybenzaldehyde (1.36 g, 0.01 mol) and isoniazid (1.37 g, 0.0100 mol) in 15 ml of absolute ethanol was refluxed for 7 h. The completion of reaction was confirmed by TLC. The reaction mixture was then poured into ice-cold water and the obtained precipitate was filtered and dried in an oven at a low temperature. The product was recrystallized from absolute ethanol.[17] Yield 68 %; m.p. 204–207 °C.

*(*E*)-N'-3-((Dimethylamino)methyl)-2-methoxybenzylidene)isonicotinohydrazide (**2a**)*

(*E*)-*N*'-(2-Methoxybenzylidene)isonicotinohydrazide (612 mg, 0.00240 mol) along with (0.10 ml, 0.0036 mol) of formaldehyde and (0.0024 mol) of dimethylamine was placed in 100 ml round bottom flask to which 50 ml of absolute ethanol was added. The pH was adjusted to 4 with hydrochloric acid and the mixture refluxed for 35 h. Completion of the reaction was confirmed by TLC. The reaction mixture was then poured into a beaker and concentrated on a water bath. The reaction mixture was allowed to cool to room temperature and then diethyl ether was added. The reaction mixture was kept for 3–5 h in a refrigerator, filtered and washed with *n*-hexane. The product was recrystallized from absolute ethanol. Yield 78 %; m.p. 222––225 °C.

*1-(2-(3-((Dimethylamino)methyl)-2-methoxyphenyl)-5-(pyridin-4-yl)-1,3,4-oxadiazol-3(2*H*)-yl)ethanone (**3a**)*

A mixture of (*E*)-*N*'-3-((dimethyamino)methyl)-2-methoxybenzylidene)isonicotinohydrazide (3.57 g, 0.0100 mol) with an excess of acetic anhydride was refluxed for 7 h until the completion of the reaction, which was confirmed by TLC. The excess acetic anhydride was distilled off and the residue was poured onto crushed ice. The solid thus obtained was filtered; washed with water and then recrystallized with aqueous methanol. Yield 75 %; m.p. 168–170 °C.

*General procedure for synthesis of the substituted oxadiazoles **4a**–**p***

A mixture of **3a** (0.010 mol) and an equimolar amount of an appropriate aromatic amine (0.010 mol) was added to 25 ml absolute ethanol with a drop of glacial acetic acid and heated under reflux for 7–9 h. The obtained precipitate was filtered off; washed with ethanol and recrystallized from absolute ethanol to obtain compounds **4a**–**p**.

Antimicrobial activity

The synthesized compounds were evaluated for their *in vitro* antimicrobial activity against the Gram-positive bacteria *Staphylococcus aureus* (MTCC 96) and *Bacillus subtilis* (MTCC 121), the Gram-negative bacteria *Escherichia coli* (MTCC 40) and *Pseudomonas aeruginosa* (MTCC 2453) and the fungal strains *Candida albicans* (MTCC 227) and *Aspergillus niger* (MTCC 8189). Antimicrobial activity was assessed by the serial two-fold dilution technique. Amoxicillin was used as the standard drug for the antibacterial activity and nystatin was used as the standard drug for the antifungal activity. All the compounds were dissolved in dimethyl sulfoxide to give a concentration of 10 μg ml^{-1}. The two-fold dilutions of the test and standard compounds were prepared in double strength nutrient broth I.P. (bacteria) or Sabouraud dextrose broth I.P. (fungi).[18] The stock solution was serially diluted to give concentrations of 50–0.78 μg ml^{-1} in the nutrient broth. The inoculum size was approximately 10^6 colony forming units (CFU ml^{-1}). The tubes were incubated at 37±1°C for 24 h (bacteria), 25 °C for *C. albicans* and 35°C for *A. niger* for 7 days. Subsequently, the inoculated culture tubes were macroscopically examined for turbidity. The culture tube showing turbidity (lower concentration) and the culture tube showing no turbidity (higher concentration) gave the minimum inhibitory concentration (*MIC*) for the compound.

RESULTS AND DISCUSSION

The syntheses of the target compounds were performed according to the outline given in Scheme 1. Compounds **4a**–**p** were readily prepared in good yield and purity. Firstly, an equimolar mixture of 2-methoxybenzaldehyde and isonicotinohydrazide was refluxed to form (*E*)-*N*'-(2-methoxybenzylidene)isonicotinohydrazide (**1a**), then its reaction with formaldehyde and dimethylamine formed (*E*)-*N*'-(3-((dimethyamino)methyl)-2-methoxybenzylidene)isonicotinohydrazide (**2a**), which on treatment with acetic anhydride yielded 1-(2-(3-((dimethylamino)methyl)-2-methoxyphenyl)-5-(pyridin-4-yl)-1,3,4-oxadiazol-3(2*H*)-yl)ethanone (**3a**) and in the last reaction with substituted aromatic amines, it afforded a series of (*Z*)-*N*-(1-(2-(3-((dimethylamino)methyl)-2-methoxyphenyl)-5-(pyridin-4-yl)-1,3,4-oxadiazol-3(2*H*)-yl)ethylidene)benzenamine derivatives (**4a**–**p**). The structure, melting points and yields the synthesized compounds **4a**–**p** are given in Table I. The purity of the compounds was checked by TLC and elemental analyses.

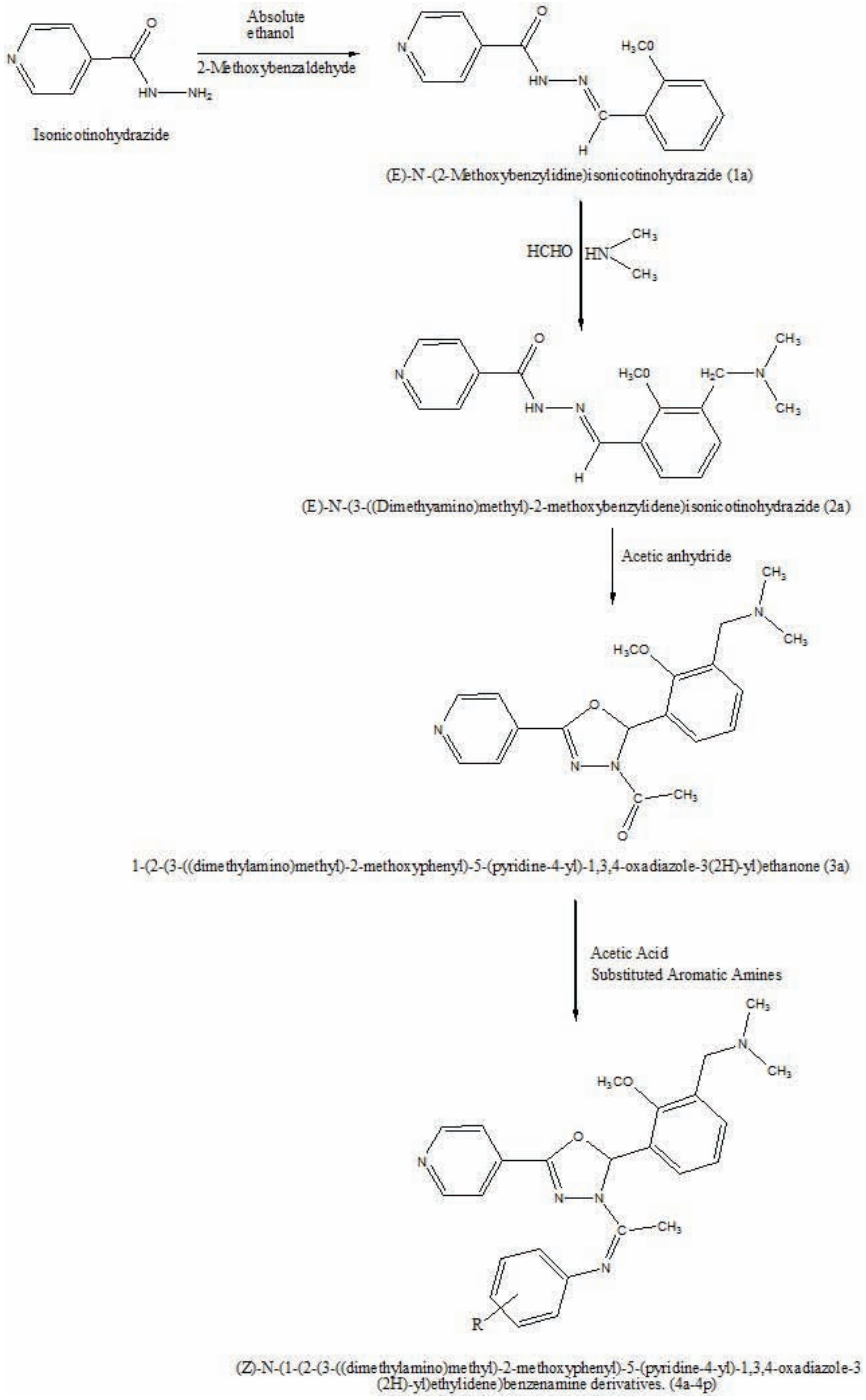

Scheme 1. Synthetic route for the formation of the title compounds.

TABLE I. Physical data of the synthesized compounds **4a**–**4p**

Compd.	R	Molecular formula	Molecular weight	Melting point, °C	Yield, %
4a	H	$C_{25}H_{27}N_5O_2$	429.5	205–207	72
4b	2-F	$C_{25}H_{26}FN_5O_2$	447.5	195–197	69
4c	3-F	$C_{25}H_{26}FN_5O_2$	447.5	187–189	72
4d	4-F	$C_{25}H_{26}FN_5O_2$	447.5	212–214	64
4e	2-Cl	$C_{25}H_{26}ClN_5O_2$	463.9	178–180	65
4f	3-Cl	$C_{25}H_{26}ClN_5O_2$	463.9	185–187	59
4g	4-Cl	$C_{25}H_{26}ClN_5O_2$	463.9	218–220	69
4h	2-Br	$C_{25}H_{26}BrN_5O_2$	508.4	228–230	77
4i	3-Br	$C_{25}H_{26}BrN_5O_2$	508.4	235–237	64
4j	4-Br	$C_{25}H_{26}BrN_5O_2$	508.4	215–217	65
4k	2-NO_2	$C_{25}H_{26}N_6O_4$	474.5	223–225	79
4l	3-NO_2	$C_{25}H_{26}N_6O_4$	474.5	210–212	65
4m	4-NO_2	$C_{25}H_{26}N_6O_4$	474.5	217–219	73
4n	2-OCH_3	$C_{26}H_{29}N_5O_3$	459.2	213–215	56
4o	3-OCH_3	$C_{26}H_{29}N_5O_3$	459.2	207–209	73
4p	4-OCH_3	$C_{26}H_{29}N_5O_3$	459.2	210–212	65

Nevertheless, the structures of all new compounds synthesized were confirmed by IR, ^{1}H-NMR and ^{13}C-NMR spectroscopy. The analytic and spectral data for all the compounds synthesized in this study are given in the Supplementary material to this paper. The IR spectra of all the compounds **4a**–**p** showed absorption bands at around 2993–2955, 2868–2839, 1679–1664, 1589–1557, 1189––1174, 1097–1018 cm^{-1} regions, confirming the presence of CH, CH_2, C=N, C=C, C–N, C–O groups, respectively. The, the chemical shifts, multiplicities, and coupling constants of the signals in the ^{1}H-NMR spectra of the respective derivatives **4a**–**p** verified their structures. The spectra of most compounds showed the characteristic 4H protons of pyridine at around δ 8.98–8.15 ppm, the characteristic protons of phenyl at δ 7.95–6.45 ppm, the 1H proton of oxadiazole at around δ 5.73–5.37 ppm, the 3H protons of O–CH_3 at around δ 3.88–3.64 ppm, the 2H protons of Ar–CH_2–N at around δ 3.69–3.52 ppm, the 6H protons of N–2CH_3 at around δ 2.49–2.26 ppm and the 3H protons of CH_3 at δ 1.21–1.05 ppm. The ^{13}C-NMR spectra of compounds **4a–p** exhibited characteristic signals of –N=**C**–CH_3 at around δ 164.77–164.18 ppm, phenyl at δ 155.87–119.15 ppm, pyridine at δ 149.78–124.11 ppm, oxadiazole at δ 155.17–154.13, O–CH_3 at δ 57.63–54.29, Ar–CH_2–N at δ 54.73–53.92 ppm, N-2CH_3 at δ 47.38–45.49 ppm and N–C–**C**H_3 at δ 22.77–15.13 ppm.

Antimicrobial activity

The compounds were evaluated for their antimicrobial properties in comparison to the control antibacterial drug amoxicillin and antifungal drug nystatin. The determined *MIC* values of compounds **4a**–**p** are listed in Table II. The investigation of antibacterial screening data revealed that all the tested compounds

showed moderate to good bacterial inhibition. The compounds **4g**, **4h**, **4m** and **4p** displayed excellent activity against the Gram-positive bacteria *B. subtilis* and *S. aureus* and good activity against the Gram-negative bacteria *P. aeruginosa* and *E. coli*. Compounds **4c**, **4d** and **4f** showed moderate antibacterial activity, while compounds **4a**, **4b**, **4e** and **4o** were less active against the tested bacterial strains. Of all the synthesized derivatives, compound **4a** was found to be the least active compound against most of the bacterial strain. From, these results, it could be generalized that the *p*-chloro-, *o*-bromo-, *p*-nitro- and *p*-methoxy-substituted oxadiazole derivatives showed higher antibacterial activity compared to the other analogues.

TABLE II. Antimicrobial screening results of the tested compounds (minimum inhibitory concentration, μg ml^{-1})

Compound	Gram-positive bacteria		Gram-negative bacteria		Fungal strain	
	B. subtilis (MTCC121)	*S. aureus* (MTCC96)	*P. aeruginosa* (MTCC2453)	*E. coli* (MTCC40)	*C. albicans* (MTCC227)	*A. nigar* (MTCC8189)
4a	6.25	12.5	50	3.12	12.5	25
4b	12.5	50	25	12.5	3.12	12.5
4c	6.25	6.25	12.5	3.12	6.25	3.12
4d	6.25	6.25	6.25	12.5	3.12	12.5
4e	12.5	6.25	3.12	12.5	6.25	12.5
4f	12.5	6.25	6.25	3.12	6.25	3.12
4g	3.12	1.56	1.56	3.12	6.25	3.12
4h	12.5	6.25	3.12	6.25	3.12	6.25
4i	3.12	12.5	12.5	25	50	12.5
4j	3.12	12.5	6.25	25	25	12.5
4k	6.25	25	12.5	6.25	12.5	25
4l	3.12	12.5	12.5	25	6.25	12.5
4m	1.56	3.12	3.12	1.56	6.25	12.5
4n	6.25	12.5	25	12.5	6.25	12.5
4o	25	12.5	12.5	6.25	12.5	6.25
4p	3.12	6.25	1.56	3.12	6.25	1.56
Amoxicillin	0.12	0.25	0.15	0.20	–	–
Nystatin	–	–	–	–	0.30	0.78

Concerning the antifungal activity of the tested compounds, only two fungal strains were selected *C. albicans* and *A. niger* and the result of antifungal screening data revealed that all the synthesized compounds showed variable degrees of inhibition against the tested fungi. The investigation of antibacterial screening data revealed that all the tested compounds showed moderate to good fungal inhibition as compare to standard drug nystatin. Of the screened compounds, **4g**, **4h**, **4m** and **4p** exhibited the highest antifungal activity against both fungal strains, while compounds **4e**, **4l** and **4n** showed moderate antifungal activity. Among all the synthesized derivatives, compound **4i** was found to be the least active com-

pound against the fungal strains. From these result, it could be generalized that the *p*-fluoro-, *o*-bromo-, *p*-nitro- and *m*-methoxy-substituted oxadiazole derivatives **4g**, **4h**, **4m** and **4p** showed higher antifungal activity than the other analogues. It was also observed that the derivatives having a chloro-, bromo-, nitro- and methoxy- substituent at the *ortho* and *meta* positions were not as potent as the derivatives having same substituent at the *para* position. Thus, from the obtained results it was found that the nature and position of the substituent had marked effects on antibacterial and antifungal activity.

SUPPLEMENTARY MATERIAL

Analytical and spectral data of synthesized compounds are available electronically from http://www.shd.org.rs/JSCS/, or from the corresponding author on request.

ИЗВОД

НОВИ ОКСАДИАЗОЛНИ ДЕРИВАТИ ИЗОНИКОТИНОХИДРАЗИДА У ПОТРАЗИ ЗА АНТИМИКРОБНИМ АГЕНСИМА: СИНТЕЗА И *IN VITRO* ЕВАЛУАЦИЈА

MANAV MALHOTRA[1], MOHIT SANDUJA[2], ABDUL SAMAD[3] и AAKASH DEEP[4]

[1]Department of Pharmaceutical Chemistry, Meerut Institute of Engineering and Technology, Bypass Road--Baghpat Crossing, Meerut-250005, Uttar Pradesh, India, [2]Department of Pharmaceutical Chemistry, ISF College of Pharmacy, Ferozepur Road, Moga-142001, India, [3]Department of Pharmaceutical Chemistry, College of Pharmacy in Al-Kharj, King Saud University, Riyadh, Saudi Arabia и [4]Department of Pharmaceutical Sciences, Maharshi Dayanand University, Rohtak-124001, India

Структурним модификацијама најважнијег лека против туберкулозе, изонијазида, добијени су деривати који имају израженије липофилне особине услед замене хидразидне функције 1,3,4-оксадиазолским хетероцикличним делом структуре. На тај начин се спречава *in vivo* ацетиловање ензимом ариламин-*N*-ацетилтрансфераза чиме су добијани неактивни ацетиловани деривати. У овом раду приказано је шеснаест нових оксадиазолских деривата који су окарактерисани спектралним анализама (IR, ^{1}H-NMR, ^{13}C-NMR и MS). Испитана је антимикробна активност синтетисаних деривата према Грам-позитивним (*Bacillus subtilis* и *Staphylococcus aureus*), Грам-негативним сојевима (*Pseudomonas aeruginosa* и *Escherichia coli*) и сојевима гљива (*Candida albicans* и *Aspergillus niger*). Минималне инхибиторне концентрација једињења налазе се у опсегу 1,56–50 μg ml $^{-1}$ према сојевима бактерија и гљива. Резултати показују да једињења показују изражену активност, од којих су најактивнији деривати **4g, 4h, 4m** и **4p**.

(Примљено 23. јануара , ревидирано 24. јуна 2011)

REFERENCES

1. A. Verma, S. K. Saraf, *Eur. J. Med. Chem.* **43** (2008) 897
2. M. Koca, S. Servi, C. Kirilimis, M. Ahmedzade, C. Kazaz, B. Ozbek, G. Otuk, *Eur. J. Med. Chem.* **40** (2005) 1351
3. C. Bonde, N. J. Gaikwad, *Bioorg. Med. Chem.* **12** (2004) 2151
4. O. Prakash, M. Kumar, R. Kumar, C. Sharma, K. R. Aneja, *Eur. J. Med. Chem.* **45** (2010) 4252
5. N. N. Farshori, M. R. Banday, A. Ahmad, A. U. Khan, A. Rauf, *Bioorg. Med. Chem. Lett.* **20** (2010) 1933

6. G. C. Ramaprasad, B. Kallurava, B. S. Kumar, R. K. Hunnur, *Eur. J. Med. Chem.* **45** (2010) 4587
7. K. Manjunthatha, B. Poojary, P. L. Lobo, J. Fernandes, N. S. Kumari, *Eur. J. Med. Chem.* **45** (2010) 5225
8. K. K. Jha, A. Samad, Y. Kumar, M. Shaharyar, K. L. Khosa, J. Jain, V. Kumar, P. Singh, *Eur. J. Med. Chem.* **45** (2010) 4963
9. A. A. El-Emam, O. A. Al-Deeb, M. Al-Omar, J. Lehmann, *Bioorg. Med. Chem.* **12** (2004) 5107
10. S. G. Kucukguzel, E. E. Oruc, S. Rollas, F. Sahin, A. Ozbek, *Eur. J. Med. Chem.* **37** (2002) 197
11. B. Chandrakantha, P. Shetty, V. Nambiyar, N. Isloor, A. M. Isloor, *Eur. J. Med. Chem.* **45** (2010) 1206
12. M. Akhter, A. Husain, B. Azad, M. Ajmal, *Eur. J. Med. Chem.* **44** (2009) 2372
13. V. Padmavathi, S. N. Reddy, G. D. Reddy, A. Padmaja, *Eur. J. Med. Chem.* **45** (2010) 4246
14. B. Testa, P. Crivori, M. Reist, P. A. Carrupt, *Perspect. Drug Discovery Des.* **19** (2000) 179
15. A. Madhukar, N. Kannappan, A. Deep, P. Kumar, M. Kumar, P. Verma, *Int. J. Chem. Tech. Res.* **1** (2009) 1376
16. A. Deep, S. Jain, P. C. Sharma, P. Verma, M. Kumar, C. P. Dora, *Acta Pol. Pharm.* **67** (2010) 255
17. M. Malhotra, R. Sharma, V. Monga, A. Deep, K. Sahu, A. Samad, *Lett. Drug Des. Discovery* **8** (2011) 579
18. *Pharmacopoeia of India*, Vol. II, Ministry of Health Department of India, New Delhi, 1996, p. A-88.

Journal of the Serbian Chemical Society
JSCS@tmf.bg.ac.rs • www.shd.org.rs/JSCS
J. Serb. Chem. Soc. 77 (1) S4–S9 (2012) *Supplementary material*

SUPPLEMENTARY MATERIAL TO

New oxadiazole derivatives of isonicotinohydrazide in the search for antimicrobial agents: Synthesis and *in vitro* evaluation

MANAV MALHOTRA[1], MOHIT SANDUJA[2], ABDUL SAMAD[3] and AAKASH DEEP[4]*

[1]*Department of Pharmaceutical Chemistry, Meerut Institute of Engineering and Technology, Bypass Road-Baghpat Crossing, Meerut-250005, Uttar Pradesh, India,* [2]*Department of Pharmaceutical Chemistry, ISF College of Pharmacy, Ferozepur Road, Moga-142001, India,* [3]*Department of Pharmaceutical Chemistry, College of Pharmacy in Al-Kharj, King Saud University, Riyadh, Saudi Arabia and* [4]*Department of Pharmaceutical Sciences, Maharshi Dayanand University, Rohtak-124001, India*

J. Serb. Chem. Soc. 77 (1) (2012) 9–16

ANALYTICAL AND SPECTRAL DATA OF THE SYNTHESIZED COMPOUNDS

(E)-N'-*(2-Methoxybenzylidene)isonicotinohydrazide* ***(1a)***. Anal. Calcd. for $C_{14}H_{13}N_3O_2$: C, 65.87; H, 5.13; N, 16.46 %. Found: C, 65.74; H, 5.18; N, 16.54 %; IR (KBr, cm^{-1}): 3261, 2926, 2865, 2838, 1674, 1652, 1561, 1116, 1064; ^{1}H--NMR (300 MHz, DMSO-d_6, δ / ppm): 12.05 (1H, *s*, –NH–N=), 8.82 (2H, *d*, *J* = = 4.7 Hz, pyridine), 8.7 4 (1H, *s*, –N=C–H), 7.88 (2H, *d*, *J* = 4.7 Hz, py ridine), 7.82 (2H, *d*, *J* = 9.2 Hz, benzylidene), 7.40 (2H, *d*, *J* = 8.9, benzylidene), 3.86 (3H, *s*, O–CH_3); ^{13}C-NMR (DMSO-d_6, δ / p pm): 163.45, 160.61, 149.81, 143.37, 139.24, 133.58, 131.74, 123.69, 121.31, 117.83, 113.77, 55.44.

(E)-N'-*3-((Dimethylamino)methyl)-2-methoxybenzylidene)isonicotinohydrazide* ***(2a)***. Anal. Calcd. for C $_{17}H_{20}N_4O_2$: C, 65 .37; H, 6.45; N, 17 .94 %. Found: C, 65.43; H, 6.44; N, 17.89 %; IR (KBr, cm^{-1}): 3258, 2952, 2858, 2840, 1668, 1654, 1545, 1121, 1072; ^{1}H-NMR (300 MHz, DMSO-d_6, δ / ppm): 11.92 (1H, *s*, –NH–N=), 8.74 (2H, *d*, *J* = 4.2 Hz, pyridine), 8.44 (1H, *s*, –N=C–H), 7.85 (2H, *d*, *J* = 3.9 Hz, pyridine), 7.54 (2H, *d*, *J* = 7.5 Hz, benzylidene), 7.19 (1H, *m*, *J* = 7.5 Hz, b enzylidene,), 3.84 (3H, *s*, O–CH_3), 3.32 (2H, *s*, Ar–CH_2–N), 0.98 (6H, *t*, 2CH_3); ^{13}C-NMR (DMSO-d_6, δ / ppm): 163.59, 160.71, 149.37, 143.45, 139.41, 133.52, 129.82, 122.64, 119.14, 117.38, 113.15, 55.61, 45.57. ESI-MS (*m*/*z*) = 297 (M+1).

*1-(2-(3-((Dimethylamino)methyl)-2-methoxyphenyl)-5-(pyridin-4-yl)-1,3,4--oxadiazol-3(2*H*)-yl) ethanone* ***(3a)***. Anal. Calcd. for C $_{19}H_{22}N_4O_3$: C, 64.39; H, 6.26; N, 15.81 %. Found: C, 64.35; H, 6.28; N, 15.83 5; IR (KBr, cm^{-1}): 2983,

* Corresponding author. E-mail: aakashdeep82@gmail.com

2861, 2842, 1673, 1565, 1185, 1059; ^{1}H-NMR (300 MHz, DMSO-d_6, δ / ppm): 8.94 (2H, *d*, *J* = 4.6 Hz, pyridine), 8.34 (2H, *d*, *J* = 4.2 Hz, pyridine), 7.35 (2H, *d*, *J* = 3.7 Hz, phenyl), 6.69 (1H, *m*, phenyl), 5.55 (1H, *s*, oxadiazole), 3.69 (3H, *s*, O–CH_3), 3.47 (2H, *s*, Ar–CH_2–N), 2.18 (6H, *s*, N–2CH_3), 1.13 (3H, *s*, N=C–CH_3); ^{13}C-NMR (DMSO-d_6, δ / ppm): 168.75, 154.88, 154.29, 149.53, 137.91, 126.37, 125.54, 123.91, 119.71, 118.63, 65.75, 55.26, 54.63, 45.12, 28.46; ESI-MS (*m*/z) = 355 (M+1).

(Z)-N-*(1-(2-(3-((Dimethylamino)methyl)-2-methoxyphenyl)-5-(pyridin-4-yl)-1,3,4-oxadiazol-3(2*H*)-yl)ethylidene)benzenamine* ***(4a)***. Anal. Calcd. for $C_{25}H_{27}N_5O_2$: C, 69.91; H, 6.34; N, 16.31 %. Found: C, 69.83; H, 6.35; N, 16.38 %; IR (KBr, cm^{-1}): 2955, 2863, 2841, 1678, 1571, 1182, 1079; ^{1}H-NMR (300 MHz, DMSO-d_6, δ / ppm): 8.98 (2H, *d*, *J* = 4.8 Hz, pyridine), 8.19 (2H, *d*, *J* = = 4.2 Hz, pyridine), 7.35–7.18 (8H, *m*, phenyl), 5.69 (1H, *s*, oxadiazole), 3.74 (3H, *s*, O–CH_3), 3.67 (2H, *s*, Ar–CH_2–N), 2.32 (6H, *s*, N–2CH_3), 1.13 (3H, *s*, N=C–CH_3); ^{13}C-NMR (DMSO-d_6, δ / ppm): 164.75, 155.48, 152.17, 149.17, 139.82, 137.15, 129.77, 127.74, 125.18, 124.28, 122.19, 119.75, 117.66, 68.53, 57.63, 54.73, 47.12, 18.46; ESI-MS (*m*/z) = 431 (M+1).

(Z)-N-*(1-(2-(3-((Dimethylamino)methyl)-2-methoxyphenyl)-5-(pyridin-4-yl)-1,3,4-oxadiazol-3(2*H*)-yl)ethylidene)-2-fluorobenzenamine* ***(4b)***. Anal. Calcd. for $C_{25}H_{26}FN_5O_2$: C, 67.10; H, 5.86; N, 4.25 %. Found: C, 66.92; H, 5.95; N, 4.34 %; IR (KBr, cm^{-1}): 2988, 2864, 2844, 1675, 1557, 1179, 1145, 1097; ^{1}H-NMR (300 MHz, DMSO-d_6, δ / ppm): 8.98 (2H, *d*, *J* = 4.5 Hz, pyridine), 8.75 (2H, *d*, *J* = 4.1 Hz, pyridine), 7.58 (2H, *d*, *J* = 3.7 Hz, phenyl), 7.26 (*d*, 2H, phenyl, *J* = 3.4 Hz), 6.82–6.67 (*m*, 3H, phenyl), 5.54 (*s*, 1H, oxadiazole), 3.84 (3H, *s*, O–CH_3), 3.56 (2H, *s*, Ar–CH_2–N), 2.33 (6H, *s*, N–2CH_3), 1.11 (s, 3H, N=C–CH_3); ^{13}C-NMR (DMSO-d_6, δ / ppm): 164.23, 155.87, 154.92, 154.13, 149.18, 137.53, 127.15, 126.19, 125.13, 124.88, 123.12, 121.22, 119.87, 115.38, 64.52, 55.18, 54.58, 45.91, 21.81. ESI-MS (*m*/z) = 449 (M+1).

(Z)-N-*(1-(2-(3-((Dimethylamino)methyl)-2-methoxyphenyl)-5-(pyridin-4-yl)-1,3,4-oxadiazol-3(2*H*)-yl)ethylidene)-3-fluorobenzenamine* ***(4c)***. Anal. Calcd. for $C_{25}H_{26}FN_5O_2$: C, 67.10; H, 5.86; N, 4.25 %. Found: C, 66.92; H, 5.95; N, 4.34 %; IR (KBr, cm^{-1}): 2975, 2863, 2845, 1679, 1583, 1188, 1139, 1075. ^{1}H-NMR (300 MHz, DMSO-d_6, δ / ppm): 8.92 (2H, *d*, *J* = 4.7 Hz, pyridine), 8.75 (2H, *d*, *J* = 4.1 Hz, pyridine), 7.21 (1H, *m*, phenyl), 7.18–7.10 (3H, *m*, phenyl), 6.88–6.72 (3H, *m*, phenyl), 5.59 (1H, *s*, oxadiazole), 3.71 (3H, *s*, O–CH_3), 3.62 (2H, *s*, Ar–CH_2–N), 2.35 (6H, *s*, N–2CH_3), 1.15 (3H, *s*, N=C–CH_3); ^{13}C-NMR (DMSO-d_6, δ / ppm): 164.37, 155.18, 154.72, 150.56, 149.78, 139.13, 130.14, 126.19, 125.15, 123.17, 119.91, 116.55, 115.18, 111.19, 66.12, 55.15, 54.27, 46.75, 22.75; ESI-MS (*m*/z) = 449 (M+1).

(Z)-N-*(1-(2-(3-((Dimethylamino)methyl)-2-methoxyphenyl)-5-(pyridin-4-yl)-1,3,4-oxadiazol-3(2*H*)-yl)ethylidene)-4-fluorobenzenamine* ***(4d)***. Anal. Calcd.

for $C_{25}H_{26}FN_5O_2$: C, 67.10; H, 5.86; N, 4.25 %. Found: C, 66.92; H, 5.95; N, 4.34 %; IR (KBr, cm^{-1}): 2967, 2861, 2845, 1673, 1574, 1188, 1156, 1072. ^{1}H-NMR (300 MHz, DMSO-d_6, δ / ppm): 8.95 (2H, *d*, *J* = 4.6 Hz, p yridine), 8.71 (2H, *d*, *J* = 4.1 Hz, pyridine), 7.45 (2H, *d*, *J* = 3.7 Hz, phenyl), 7.17 (2H, *d*, *J* = = 3.2 Hz, phenyl), 6.85–6.67 (3H, *m*, phenyl), 5.62 (1H, *s*, oxadiazole), 3.88 (3H, *s*, O–CH_3), 3.66 (2H, *s*, Ar–CH_2–N), 2.45 (6H, *s*, N–2CH_3), 1.05 (3H, *s*, N=C–CH_3); ^{13}C-NMR (DMSO-d_6, δ / ppm): 164.18, 161.42, 155.79, 155.17, 149.13, 144.54, 138.89, 126.17, 125.58, 124.72, 123.92, 121.11, 120.27, 116.85, 67.54, 56.15, 55.64, 46.28, 15.27; ESI-MS (*m*/*z*) = 449 (M+1).

(Z)-*2-Chloro*-N-*(1-(2-(3-((dimethylamino)methyl)-2-methoxyphenyl)-5-(pyridin-4-yl)-1,3,4-oxadiazol-3(2*H*)-yl)ethylidene)benzenamine* (***4e***). Anal. Calcd. for $C_{25}H_{26}ClN_5O_2$: C, 64.72; H, 5.65; N, 15.09 %. Found: C, 64.61; H, 5.72; N, 15.13 %; IR (KBr, cm^{-1}): 2983, 2859, 2838, 1669, 1561, 1181, 1018, 788. ^{1}H-NMR (300 MHz, DMSO-d_6, δ / ppm): 8.74 (2H, *d*, *J* = 4.4 Hz, p yridine), 8.71 (2H, *d*, *J* = 4.1, Hz pyridine), 7.83 (2H, *d*, *J* = 3.7 Hz, phenyl), 7.21 (2H, *d*, *J* = = 3.2 Hz, phenyl), 6.72–6.66 (3H, *m*, phenyl), 5.37 (1H, *s*, oxadiazole), 3.81 (3H, *s*, O–CH_3), 3.54 (2H, *s*, Ar–CH_2–N), 2.35 (6H, *s*, N–2CH_3), 1.13 (3H, *s*, N=C–CH_3); ^{13}C-NMR (DMSO-d_6, δ / ppm): 164.25, 155.85, 154.91, 153.88, 149.24, 137.18, 126.25, 125.18, 124.27, 123.94, 121.21, 119.86, 114.18, 64.51, 54.29, 53.92, 46.92, 21.85; ESI-MS (*m*/*z*) = 465 (M+1).

(Z)-*3-Chloro*-N-*(1-(2-(3-((dimethylamino)methyl)-2-methoxyphenyl)-5-(pyridin-4-yl)-1,3,4-oxadiazol-3(2*H*)-yl)ethylidene)benzenamine* (***4f***). Anal. Calcd. for $C_{25}H_{26}ClN_5O_2$: C, 64.72; H, 5.65; N, 15.09 %. Found: C, 64.61; H, 5.72; N, 15.13 %; IR (KBr, cm^{-1}): 2993, 2856, 2843, 1676, 1559, 1185, 1031, 759; ^{1}H-NMR (300 MHz, DMSO-d_6, δ / ppm): 8.88 (2H, *d*, *J* = 4.5 Hz, p yridine), 8.73 (2H, *d*, *J* = 4.1 Hz, pyridine), 7.28 (7H, *m*, phenyl), 5.45 (1H, *s*, oxadiazole), 3.75 (3H, *s*, O–CH_3), 3.65 (2H, *s*, Ar–CH_2–N), 2.35 (6H, *s*, N–2CH_3), 1.18 (3H, *s*, N=C–CH_3); ^{13}C-NMR (DMSO-d_6, δ / ppm): 164.31, 155.25, 154.77, 150.58, 149.72, 138.64, 130.19, 126.17, 124.39, 122.26, 119.93, 116.19, 114.74, 111.32, 67.19, 55.44, 54.13, 46.71, 22.77; ESI-MS (*m*/*z*) = 465 (M+1).

(Z)-*4-Chloro*-N-*(1-(2-(3-((dimethylamino)methyl)-2-methoxyphenyl)-5-(pyridin-4-yl)-1,3,4-oxadiazol-3(2*H*)-yl)ethylidene)benzenamine* (***4g***). Anal. Calcd. for $C_{25}H_{26}ClN_5O_2$: C, 64.72; H, 5.65; N, 15.09 %. Found: C, 64.61; H, 5.72; N, 15.13 %; IR (KBr, cm^{-1}): 2991, 2859, 2843, 1673, 1565, 1183, 1018, 755. ^{1}H-NMR (300 MHz, DMSO-d_6, δ / ppm): 8.88 (2H, *d*, *J* = 4.5 Hz, p yridine), 8.37 (2H, *d*, *J* = 4.1, Hz pyridine), 7.86 (2H, *d*, *J* = 3.8 Hz, phenyl), 7.49 (2H, *d*, *J* = = 3.3 Hz, phenyl), 6.77–6.59 (3H, *m*, phenyl), 5.55 (1H, *s*, oxadiazole), 3.79 (3H, *s*, O–CH_3), 3.67 (2H, *s*, Ar–CH_2–N), 2.39 (6H, *s*, N–2CH_3), 1.08 (3H, *s*, N=C–CH_3); ^{13}C-NMR (DMSO-d_6, δ / ppm): 164.35, 155.44, 154.78, 149.69, 147.18, 138.74, 132.33, 130.29, 127.19, 126.55, 124.37, 122.75, 121.63, 119.68, 66.56, 56.59, 55.27, 47.26, 15.88; ESI-MS (*m*/*z*) = 465 (M+1).

(Z)-*2-Bromo*-N-*(1-(2-(3-((dimethylamino)methyl)-2-methoxyphenyl)-5-(pyridin-4-yl)-1,3,4-oxadiazol-3(2*H)*-yl)ethylidene)benzenamine* (***4h***). Anal. Calcd. for $C_{25}H_{26}BrN_5O_2$: C, 59.06; H, 5.15; N, 13.77 %. Found: C, 58.96; H, 5.13; N, 13.89 %; IR (KBr, cm^{-1}): 2977, 2861, 2845, 1679, 1557, 1181, 1069, 589; ^{1}H-NMR (300 MHz, DMSO-d_6, δ / ppm): 8.81 (2H, *d*, *J* = 4.4 Hz, p yridine), 8.77 (2H, *d*, *J* = 3.9 Hz, pyridine), 7.59 (2H, *d*, *J* = 3.6 Hz, phenyl), 7.55 (2H, *d*, *J* = = 3.2 Hz, phenyl), 6.74–6.59 (3H, *m*, phenyl), 5.48 (1H, *s*, oxadiazole), 3.74 (3H, *s*, O–CH_3), 3.66 (2H, *s*, Ar–CH_2–N), 2.35 (6H, *s*, N–2CH_3), 1.18 (3H, *s*, N=C–CH_3); ^{13}C-NMR (DMSO-d_6, δ / ppm): 164.37, 155.38, 154.17, 149.75, 145.73, 135.14, 132.19, 128.19, 127.94, 126.88, 124.11, 119.91, 110.15, 66.72, 56.71, 55.53, 45.52, 21.72; ESI-MS (*m*/*z*) = 509 (M+1).

(Z)-*3-Bromo*-N-*(1-(2-(3-((dimethylamino)methyl)-2-methoxyphenyl)-5-(pyridin-4-yl)-1,3,4-oxadiazol-3(2*H)*-yl)ethylidene)benzenamine* (***4i***). Anal. Calcd. for $C_{25}H_{26}BrN_5O_2$: C, 59.06; H, 5.15; N, 13.77 %. Found: C, 59.11; H, 5.12; N, 13.75 %; IR (KBr, cm^{-1}): 2986, 2863, 2844, 1664, 1589, 1182, 1079, 584; ^{1}H-NMR (300 MHz, DMSO-d_6, δ / ppm): 8.85 (2H, *d*, *J* = 4.6 Hz, p yridine), 8.41 (2H, d, *J* = 4.2 Hz, pyridine), 7.73 (2H, *d*, *J* = 3.7 Hz, phenyl), 7.47 (2H, *d*, *J* = = 3.2 Hz, phenyl), 6.69–6.49 (3H, *m*, phenyl), 5.58 (1H, *s*, oxadiazole), 3.64 (3H, *s*, O–CH_3), 3.59 (2H, *s*, Ar–CH_2–N), 2.33 (6H, *s*, N–2CH_3), 1.15 (3H, *s*, N=C–CH_3); ^{13}C-NMR (DMSO-d_6, δ / ppm): 164.53, 155.51, 154.37, 149.62, 147.34, 137.92, 133.41, 129.53, 127.73, 127.32, 125.16, 124.72, 124.35, 121.72, 119.15, 65.53, 55.69, 54.38, 46.24, 21.34; ESI-MS (*m*/*z*) = 509 (M+1).

(Z)-*4-Bromo*-N-*(1-(2-(3-((dimethylamino)methyl)-2-methoxyphenyl)-5-(pyridin-4-yl)-1,3,4-oxadiazol-3(2*H)*-yl)ethylidene) benzenamine* (***4j***). Anal. Calcd. for $C_{25}H_{26}BrN_5O_2$: C, 59.06; H, 5.15; N, 13.77 %. Found: C, 58.95; H, 5.18; N, 13.85 %; IR (KBr; cm^{-1}): 2972, 2863, 2842, 1675, 1563, 1185, 1069, 839; ^{1}H-NMR (300 MHz, DMSO-d_6, δ / ppm): 8.79 (2H, *d*, *J* = 4.7, Hz p yridine), 8.44 (2H, *d*, *J* = 4.2 Hz, pyridine), 7.77 (2H, *d*, *J* = 3.9 Hz, phenyl), 7.55 (2H, *d*, *J* = = 3.3 Hz, phenyl), 6.71–6.48 (3H, *m*, phenyl), 5.59 (1H, *s*, oxadiazole), 3.71 (3H, *s*, O–CH_3), 3.64 (2H, *s*, Ar–CH_2–N), 2.34 (6H, *s*, N–2CH_3), 1.13 (3H, *s*, N=C–CH_3); ^{13}C-NMR (DMSO-d_6, δ / ppm): 164.45, 155.39, 154.18, 149.55, 147.64, 137.94, 133.38, 127.95, 125.72, 124.12, 121.72, 119.15, 65.29, 56.74, 55.18, 47.38, 15.34; ESI–MS (*m*/*z*) = 509 (M+1).

(Z)-N-*(1-(2-(3-((Dimethylamino)methyl)-2-methoxyphenyl)-5-(pyridin-4-yl)-1,3,4-oxadiazol-3(2*H)*-yl)ethylidene)-2-nitrobenzenamine* (***4k***). Anal. Calcd. for $C_{25}H_{26}N_6O_4$: C, 63.28; H, 5.52; N, 17.71 %. Found: C, 63.11; H, 5.65; N, 17.75 %; IR (KBr, cm^{-1}): 2987, 2859, 2842, 1676, 1569, 1547, 1357, 1189, 1059; ^{1}H-NMR (300 MHz, DMSO-d_6, δ / ppm): 8.91 (2H, *d*, *J* = 4.4 Hz, p yridine), 8.19 (2H, *d*, *J* = 4.1 Hz, pyridine), 7.93 (2H, *d*, *J* = 3.6 Hz, phenyl), 7.55 (2H, *d*, *J* = 3.2 Hz, phenyl), 6.82–6.75 (3H, *m*, phenyl), 5.51 (1H, *s*, oxadiazole), 3.66 (3H, *s*, O–CH_3), 3.59 (2H, *s*, Ar–CH_2–N), 2.31 (6H, *s*, N–2CH_3), 1.08 (3H, *s*,

N=C–CH_3); ^{13}C-NMR (DMSO-d_6, δ / ppm): 164.74, 155.19, 154.27, 149.37, 145.72, 141.18, 138.44, 135.53, 127.88, 125.72, 124.93, 123.15, 122.58, 121.18, 119.88, 65.71, 56.53, 55.34, 47.19, 21.13; ESI-MS (*m*/*z*) = 476 (M+1).

(Z)-N-*(1-(2-(3-((Dimethylamino)methyl)-2-methoxyphenyl)-5-(pyridin-4-yl)--1,3,4-oxadiazol-3(2*H*)-yl)ethylidene)-3-nitrobenzenamine* (***4l***). Anal. Calcd. for $C_{25}H_{26}N_6O_4$: C, 63.28; H, 5.52; N, 17.71 %. Found: C, 63.25; H, 5.51; N, 17.75 %; IR (KBr, cm^{-1}): 2979, 2855, 2843, 1677, 1564, 1545, 1355, 1184, 1056; ^{1}H--NMR (300 MHz, DMSO-d_6, δ / ppm): 8.83 (2H, *d*, *J* = 4.4 Hz, pyridine), 8.21 (2H, *d*, *J* = 4.1 Hz, pyridine), 7.93 (2H, *d*, *J* = 3.6 Hz, phenyl), 7.59 (2H, *d*, *J* = = 3.1 Hz, phenyl), 6.84–6.79 (3H, *m*, phenyl), 5.49 (1H, *s*, oxadiazole), 3.72 (3H, *s*, O–CH_3), 3.52 (2H, *s*, Ar–CH_2–N), 2.26 (6H, *s*, N–2CH_3), 1.19 (3H, *s*, N=C–CH_3); ^{13}C-NMR (DMSO-d_6, δ / ppm): 164.72, 155.79, 154.13, 149.75, 146.77, 138.44, 127.92, 125.72, 124.93, 123.12, 122.72, 121.19, 119.88, 66.24, 56.57, 55.19, 47.11, 15.13; ESI-MS (*m*/*z*) = 476 (M+1).

(Z)-N-*(1-(2-(3-((Dimethylamino)methyl)-2-methoxyphenyl)-5-(pyridin-4-yl)--1,3,4-oxadiazol-3(2*H*)-yl)ethylidene)-4-nitrobenzenamine* (***4m***). Anal. Calcd. for $C_{25}H_{26}N_6O_4$: C, 63.28; H, 5.52; N, 17.71 %. Found: C, 63.11; H, 5.65; N, 17.75 %; IR (KBr, cm^{-1}): 2985, 2858, 2839, 1673, 1564, 1184, 1055; ^{1}H-NMR (300 MHz, DMSO-d_6, δ / ppm): 8.95 (2H, *d*, *J* = 4.7 Hz, pyridine), 8.25 (2H, *d*, *J* = = 4.2 Hz, pyridine), 7.95 (2H, *d*, *J* = 3.8 Hz, phenyl), 7.55 (2H, *d*, *J* = 3.3 Hz, phenyl), 6.83–6.67 (3H, *m*, phenyl), 5.59 (1H, *s*, oxadiazole), 3.75 (3H, *s*, O–CH_3), 3.62 (2H, *s*, Ar–CH_2–N), 2.35 (6H, *s*, N–2CH_3), 1.13 (3H, *s*, N=C–CH_3); ^{13}C-NMR (DMSO-d_6, δ / ppm): 164.77, 155.84, 154.25, 149.38, 146.75, 137.94, 128.12, 125.57, 124.91, 123.17, 122.18, 121.37, 119.81, 65.92, 56.52, 55.29, 47.24, 15.87; ESI-MS (*m*/*z*) = 476 (M+1).

(Z)-N-*(1-(2-(3-((Dimethylamino)methyl)-2-methoxyphenyl)-5-(pyridin-4-yl)--1,3,4-oxadiazol-3(2*H*)-yl)ethylidene)-2-methoxybenzenamine* (***4n***). Anal. Calcd. for $C_{26}H_{29}N_5O_3$: C, 67.95; H, 6.36; N, 15.24 %. Found: C, 67.87; H, 6.34; N, 15.34 %; IR (KBr, cm^{-1}): 2977, 2858, 2843, 1679, 1561, 1174, 1076; ^{1}H-NMR (300 MHz, DMSO-d_6, δ / ppm): 8.77 (2H, *d*, *J* = 4.4 Hz, pyridine), 8.34 (2H, *d*, *J* = 4.1 Hz, pyridine), 7.69 (2H, *d*, *J* = 3.9 Hz, phenyl), 7.45 (2H, *d*, *J* = 3.2 Hz, phenyl), 6.66–6.51 (3H, *m*, phenyl), 5.73 (1H, *s*, oxadiazole), 3.77 (6H, *s*, O–2CH_3), 3.62 (2H, *s*, Ar–CH_2–N), 2.49 (6H, *s*, N–2CH_3), 1.09 (3H, *s*, N=C–CH_3); ^{13}C-NMR (DMSO-d_6, δ / ppm): 164.39, 155.17, 154.29, 149.21, 144.53, 140.77, 137.87, 135.91, 127.88, 126.29, 124.27, 123.27, 122.32, 120.74, 119.31, 65.42, 55.21, 54.37, 45.49, 15.55; ESI-MS (*m*/*z*) = 460 (M+1).

(Z)-N-*(1-(2-(3-((Dimethylamino)methyl)-2-methoxyphenyl)-5-(pyridin-4-yl)--1,3,4-oxadiazol-3(2*H*)-yl)ethylidene)-3-methoxybenzenamine* (***4o***). Anal. Calcd. for $C_{26}H_{29}N_5O_3$: C, 67.95; H, 6.36; N, 15.24 %. Found: C, 67.98; H, 6.27; N, 15.30 %; IR (KBr, cm^{-1}): 2975, 2861, 2839, 1674, 1568, 1188, 1072; ^{1}H-NMR (300 MHz, DMSO-d_6, δ / ppm): 8.74 (2H, *d*, *J* = 4.7 Hz, pyridine), 8.15 (2H, *d*,

J = 4.3 Hz, p yridine), 7.76 (2H, *d*, *J* = 3.5 Hz, phenyl), 7.36 (2H, *d*, *J* = 3.1 Hz, phenyl), 6.63–6.48 (3H, *m*, phenyl), 5.63 (1H, *s*, oxadiazole), 3.75 (6H, *s*, O–2CH_3), 3.68 (2H, *s*, Ar–CH_2–N), 2.44 (6H, *s*, N–2CH_3), 1.11 (3H, *s*, N=C–CH_3); ^{13}C-NMR (DMSO-d_6, δ / ppm): 164.52, 1 55.27, 154.37, 149.41, 148.87, 137.58, 131.55, 127.52, 126.89, 125.12, 124.43, 123.38, 120.63, 119.35, 115.55, 65.42, 55.27, 54.39, 46.77, 21.48. ESI-MS (*m*/z) = 460 (M+1).

(Z)-N-*(1-(2-(3-((Dimethylamino)methyl)-2-methoxyphenyl)-5-(pyridin-4-yl)--1,3,4-oxadiazol-3(2*H*)-yl) ethylidene)-4-methoxybenzenamine (**4p**)*. Anal. Calcd. for $C_{26}H_{29}N_5O_3$: C, 67.95; H, 6.36; N, 15.24 % . Found: C, 67. 83; H, 6.35; N, 15.37 %; IR (KBr, cm^{-1}): 2976, 2868, 2847, 1669, 1568, 1177, 1083; ^{1}H-NMR (300 MHz, DMSO-d_6, δ / ppm): 8.87 (2H, *d*, *J* = 4.5 Hz, pyridine), 8.28 (2H, *d*, *J* = 4.1 Hz, p yridine), 7.83 (2H, *d*, *J* = 3.8 Hz, phenyl), 7.36 (2H, *d*, *J* = 3.2 Hz, phenyl), 6.59–6.45 (3H, *m*, phenyl), 5.65 (1H, s , oxadiazole), 3.72 (6H, *s*, O–2CH_3), 3.69 (2H, *s*, Ar–CH_2–N), 2.49 (6H, *s*, N–2CH_3), 1.21 (3H, *s*, N=C–CH_3); ^{13}C-NMR (DMSO-d_6, δ / ppm): 164.75, 1 59.23, 155.17, 154.29, 149.27, 140.37, 137.93, 127.24, 126.19, 124.27, 123.17, 120.92, 119.33, 115.55, 55.42, 54.18, 46.24, 15.83; ESI-MS (*m*/z) = 460 (M+1).

J. Serb. Chem. Soc. 77 (1) 17–26 (2012) UDC 547.869+547.789+542.913:615.28–188
JSCS–4245 *Original scientific paper*

Synthesis and biological activity of 4-thiazolidinone derivatives of phenothiazine

RITU SHARMA*, PUSHKAL SAMADHIYA, SAVITRI D. SRIVASTAVA and SANTOSH K. SRIVASTAVA

Synthetic Organic Chemistry Laboratory, Department of Chemistry, Dr. H. S. Gour University (A Central University), Sagar-470003, India

(Received 24 September 2010, revised 24 April 2011)

Abstract: A new series of *N*-[3-(10*H*-phenothiazin-10-yl)propyl]-2-(substituted phenyl)-4-oxo-5-(substituted benzylidene)-3-thiazolidinecarboxamide, **5a**–**s** were synthesized. The reaction of thioglycolic acid with *N*-[3-(10*H*-phenothiazin-10-yl)propyl]-*N*'-[(substituted phenyl)methylidene]urea, **3a**–**s** in the presence of anhydrous $ZnCl_2$ afforded the new heterocyclic compounds *N*-[3-(10*H*-phenothiazin-10-yl)propyl]-2-(substituted phenyl)-4-oxo-3-thiazolidinecarboxamide, **4a**–**s**. The latter product on treatment with several selected substituted aromatic aldehydes in the presence of C_2H_5ONa underwent the Knoevenagel reaction to yield **5a**–**s**. The structure of compounds **1**, **2**, **3a**–**s**, **4a**–**s** and **5a**–**s** were confirmed by IR, ^{1}H-NMR, ^{13}C-NMR and FAB mass spectroscopy and by chemical analysis. All the above compounds were screened for their antimicrobial activity against some selected bacteria and fungi and for their antituberculosis activity, the compounds were screened against the bacterium *Mycobacterium tuberculosis*.

Keywords: synthesis; phenothiazine; 4-oxothiazolidine; antimicrobial; antitubercular.

INTRODUCTION

Thiazolidines have been shown to possess various remarkable biological activities such as analgesic,[1] amoebicidal,[2] nematocidal,[3] anaesthetic,[4] mosquito-repellent,[5] anti-HIV, anticancer,[6] antibacterial,[7–12] antifungal,[13–14] antiinflammatory,[16–19] antitubercular,[20–22] EGFR and HER-2 kinase inhibitor, [23] antiproliferative,[24,25] *etc*. Phenothiazine is also a bioactive heterocyclic compound of pharmaceutical importance and possesses different biological activities *viz*. antibacterial,[26,27] antifungal,[28] antitubercular,[29] and anti-inflammatory.[30] In the present study, compounds **1**, **2**, **3a**–**s**, **4a**–**s** and **5a**–**s** were synthesized as shown in Scheme 1. The starting material, phenothiazine with 1-bromo-3-chloropropane un-

* Corresponding author. E-mail: ritusharmaic@rediffmail.com
doi: 10.2298/JSC100924152S

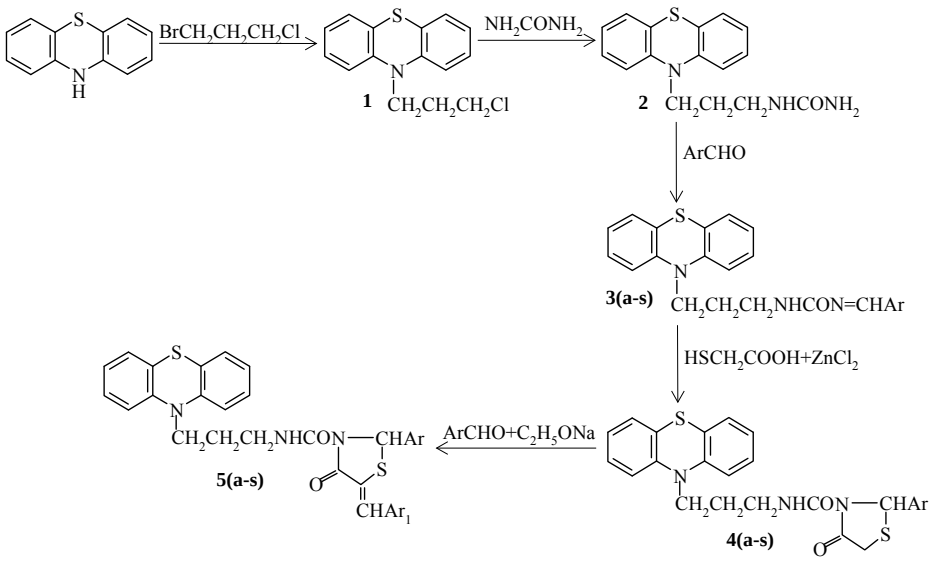

Ar= substituted phenyl ring

Compound	Ar = Ar_1	Compound	Ar = Ar_1	Compound	Ar = Ar_1
3a, **4a**, **5a**	C_6H_5	**3h**, **4h**, **5h**	4-$NO_2C_6H_4$	**3o**, **4o**, **5o**	3-$CH_3OC_6H_4$
3b, **4b**, **5b**	4-ClC_6H_4	**3i**, **4i**, **5i**	3-$NO_2C_6H_4$	**3p**, **4p**, **5p**	2-$CH_3OC_6H_4$
3c, **4c**, **5c**	3-ClC_6H_4	**3j**, **4j**, **5j**	2-$NO_2C_6H_4$	**3q**, **4q**, **5q**	4-HOC_6H_4
3d, **4d**, **5d**	2-ClC_6H_4	**3k**, **4k**, **5k**	4-$CH_3OC_6H_4$	**3r**, **4r**, **5r**	3-HOC_6H_4
3e, **4e**, **5e**	4-BrC_6H_4	**3l**, **4l**, **5l**	3-$CH_3OC_6H_4$	**3s**, **4s**, **5s**	2-HOC_6H_4
3f, **4f**, **5f**	3-BrC_6H_4	**3m**, **4m**, **5m**	2-$CH_3OC_6H_4$		
3g, **4g**, **5g**	2-BrC_6H_4	**3n**, **4n**, **5n**	4-$CH_3C_6H_4$		

Scheme 1. Reaction scheme for synthesis of compounds **1**–**5**.

derwent an nucleophilic substitution reaction yielding 10-(3-chloropropyl)-10*H*-phenothiazine, compound **1**. Compound **1** on reaction with urea afforded *N*-[3-(10*H*-phenothiazin-10-yl)propyl]urea, compound **2**. Compound **2** on reaction with several selected substituted benzaldehydes underwent a condensation reaction to afford *N*-[3-(10*H*-phenothiazin-10-yl)propyl]-*N*'-[(substituted phenyl)-methylidene]urea, compounds **3a**–**s**. The reaction of thioglycolic acid with compounds **3a**–**s** in the presence of anhydrous $ZnCl_2$ gave new heterocyclic compounds *N*-[3-(10*H*-phenothiazin-10-yl)propyl]-2-(substituted phenyl)-4-oxo-3-thiazolidinecarboxamide, compounds **4a**–**s**. Compounds **4a**–**s** on treatment with various selected substituted benzaldehydes in the presence of C_2H_5ONa underwent a Knoevenagel condensation reaction to yield the final products *N*-[3-(10*H*-phenothiazin-10-yl)propyl]-2-(substituted phenyl)-4-oxo-5-(substituted benzylidene)-3-thiazolidine-carboxamide, compounds **5a**–**s**. The structures of all the newly synthesized compounds **1**, **2**, **3a**–**s**, **4a**–**s** and **5a**–**s** were confirmed by IR, ^{1}H-NMR, ^{13}C-NMR and FAB mass spectroscopy and by chemical analysis. All

the above compounds were screened for their antimicrobial activity against some selected bacteria and fungi and an tituberculosis activity against *Mycobacterium tuberculosis*.

EXPERIMENTAL

Melting points were taken in open capillaries and are uncorrected. The progress of the reactions was monitored on silica gel-G coated TLC plates using MeOH : $CHCl_3$ (1:9). The spot was visualized by exposing the dry plate to iodine vapour. The IR spectra were recorded in KBr discs on a Shimadzu 8201 PC FTIR spectrophotometer (ν_{max} in cm^{-1}) and the ^{1}H- and ^{13}C-NMR spectra were measured on a Bruker DRX-300 spectrometer in $CDCl_3$ at 300 and 75 MHz, respectively, using TMS as an internal standard. All chemical shifts are reported on δ scales. The FAB mass spectra were recorded on a Jeol SX–102 mass spectrometer. Elemental analyses were realised on a Carlo Erba-1108 analyzer. The analytical data of all the compounds were highly satisfactory. For column chromatographic purification of the products, Merck silica Gel 60 (230–400 Mesh) was used. The employed reagent grade chemicals were purchased from commercial sources and further purified before use.

*Synthesis of 10-(3-chloropropyl)-10*H*-phenothiazine, compound **1***

Phenothiazine (0.301 mol) and 1-bromo-3-chloropropane (0.301 mol) in ethanol (100 ml) were stirred on a magnetic stirrer for 5.0 h at room temperature. Completion of the reaction was monitored on silica gel-G coated TLC plates. The product was filtered and purified over a silica gel packed column chromatography using $CHCl_3$:CH_3OH (8:2 v/v) as the eluant (120 ml). The purified product was dried under vacuum and recrystallized from acetone to yield compound **1** (Fig. 1).

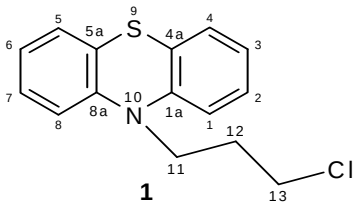

Fig. 1. Structure of compound **1**.

Synthesis of N-*[3-(10*H*-phenothiazin-10-yl)propyl]urea, compound **2***

Compound **1** (0.20 mol) and urea (0.20 mol) in ethanol (100 ml) were stirred on a magnetic stirrer for 4.0 h at room temperature. The completion of the reaction was monitored by silica gel-G coated TLC plates. The product was filtered and purified over a silica gel packed column chromatography using $CHCl_3$:CH_3OH (8:2 v/v) as eluant (120 ml). The purified product was dried under *vacuo* and recrystallized from ethanol to yield compound **2** (Fig. 2).

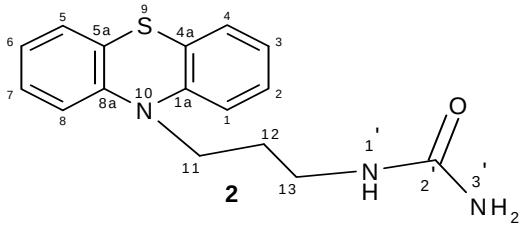

Fig. 2. Structure of compound **2**.

Synthesis of N-*[3-(10*H*-phenothiazin-10-yl)propyl]*-N*'-(phenylmethylidene)urea, compound **3a***

Compound **2** (0.026 mol) and benzaldehyde (0.026 mol) in ethanol (100 ml) in the presence of 2–4 drops glacial acetic acid were first stirred on a magnetic stirrer for 2.0 h at room temperature followed by refluxing on a steam bath at 80–90 °C for 3.3 h. The completion of the reaction was monitored using silica gel-G coated TLC plates. The product was filtered, cooled and purified over a silica gel packed column chromatography using CH_3OH:$CHCl_3$ (7:3 v/v) as eluant (90 ml). The purified product was dried under vacuum and recrystallized from acetone at room temperature to furnish compound **3a** (Fig. 3).

Compounds **3b**–**s** (Fig. 3) were synthesized using a similar method.

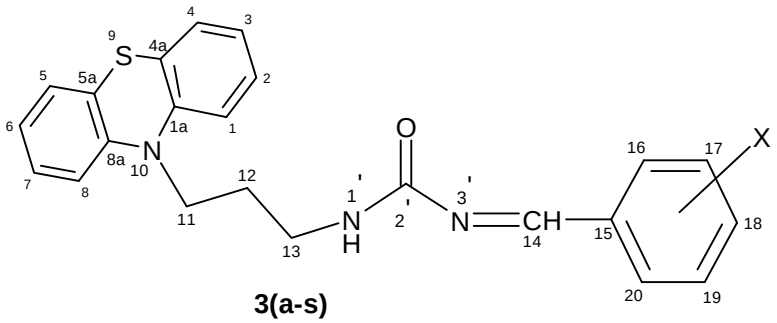

Fig. 3. Structure of compounds **3a**–**s**.

Synthesis of 4-oxo-N-*[3-(10*H*-phenothiazin-10-yl)propyl]-2-(phenyl)-3-thiazolidine-carboxamide, compound **4a***

Compound **3a** (0.0129 mol) and thioglycolic acid (0.0129 mol) in methanol (50 ml) in the presence of $ZnCl_2$ were first stirred on a magnetic stirrer for 2.0 h at room temperature followed by refluxing on a steam bath at 70–90 °C for 6.0 h. The completion of the reaction was monitored using silica gel-G coated TLC plates. The product was filtered, cooled and purified over a silica gel packed column chromatography using CH_3OH:$CHCl_3$ (7:3 v/v) as eluant (80 ml). The purified product was dried under vacuum and recrystallized from ethanol at room temperature to furnish compound **4a** (Fig. 4).

Compounds **4b**–**s** (Fig. 4) were synthesized using a similar method.

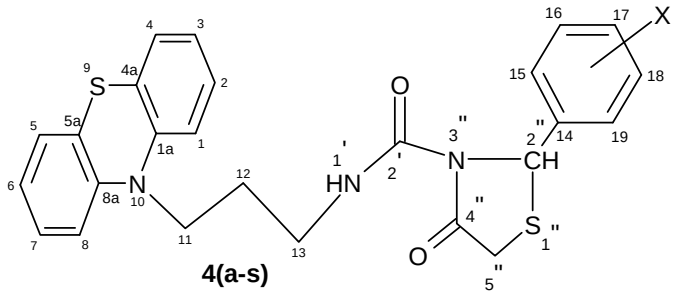

Fig. 4. Structure of compounds **4a**–**s**.

*Synthesis of 4-oxo-*N*-[3-(10*H*-phenothiazin-10-yl)-propyl]-2-phenyl-5-(phenylmethylidene)--3-thiazolidinecarboxamide, compound **5a***

Compound **4a** (0.008 mol) and benzaldehyde (0.008 mol) in ethanol (50 ml) in the presence of CH_3CH_2ONa were first stirred on a magnetic stirrer for 2.0 h at room temperature followed by refluxing on a steam bath at 80–90 °C for 5.0 h. Completion of the reaction was monitored using silica gel-G coated TLC plates. The product was filtered, cooled and purified by a silica gel packed column chromatography using CH_3OH:$CHCl_3$ (7:3 v/v) as eluant (70 ml). The purified product was dried under vacuum and recrystallized from ethanol at room temperature to furnish compound **5a**.

Compounds **5b**–**s** were synthesized using a similar method.

Biological study

The antibacterial, antifungal and antitubercular activities of compounds **1**, **2**, **3a**–**s**, **4a**–**s** and **5a**–**s** were assayed *in vitro* against selected bacteria, *i.e.*, *Escherichia coli*, *Bacillus subtilis*, *Staphylococus aureus*, and selected fungi, *Aspergillus flavus*, *Aspergillus niger* and *Candida albicans* H37Rv strain. The inhibition zone (mm) of compounds **1**, **2**, **3a**–**s**, **4a**–**s** and **5a**–**s** were determined using the filter paper disc diffusion method[31] (antibacterial and antifungal activity) at two concentration of 50 and 100 ppm and the percentage activity of compounds **1**, **2**, **3a**–**s**, **4a**–**s** and **5a**–**s** were determined using the L. J. medium (conventional) method (antitubercular activity) at 25 and 50 μg mL^{-1} and lower concentrations. Streptomycin and griseofulvin were used as the standard for the antibacterial and antifungal activity, respectively, and for the antitubercular activity, isoniazid and rifampicin were taken as standards.

RESULTS AND DISCUSSION

The analytical and spectral data of the synthesized compounds are given in the Supplementary material to this paper.

The reaction of 1-bromo-3-chloropropane with phenothiazine was performed in ethanol as solvent to afford compound **1**. The spectroscopic analyses of compound **1** showed absorption peaks for N–CH, C–Cl and C–S–C at 1272, 774 and 687 cm^{-1} in the IR spectrum. The IR spectrum confirms the formation of compound **1**. This fact was also supported by the disappearance of NH absorption of the phenothiazine.

Compound **1** on reaction with urea under continuous stirring at room temperature yielded compound **2**. In the spectroscopic analyses of compound **2**, three absorption peaks were found in the IR spectrum for NH, NH_2 and CO at 3342, 3412 and 1655 cm^{-1}, respectively while the absorption of C–Cl found in the spectrum of **1** had disappeared. This clearly indicated that compound **1** underwent substitution reaction with urea. This fact was also supported by the ^{1}H- and ^{13}C-NMR spectra as two signals appeared in the ^{1}H-NMR spectrum for NH and NH_2 at δ 5.83 and 5.99 ppm, respectively. The formation of compound **2** was fully supported by the signal for the CO group at δ 163.4 ppm in the ^{13}C-NMR spectrum. All the facts together were strong evidence for the synthesis of compound **2**.

Substituted benzaldehydes underwent condensation reaction with compound **2**, resulting in the formation of Schiff bases N=CH, which was confirmed by the IR, ^{1}H-NMR and ^{13}C-NMR spectra of compounds **3a**–**s**. In the IR spectra, an absorption was found in the range 1531–1584 cm^{-1}, while a strong signal appeared in the range of δ 7.84–8.34 and 143–158.4 ppm in the ^{1}H-NMR and ^{13}C-NMR spectra of compounds **3a**–**s**, respectively. These facts were also supported by the disappearance of the signal for NH_2 present in the ^{1}H-NMR spectrum of compound **2**.

Compounds **3a**–**s** on reaction with an equimolar amount of thioglycolic acid in the presence of $ZnCl_2$ underwent a reaction whereby a five-membered thiazolidinone ring was formed, compounds **4a**–**s**. Compounds **4a**–**s** showed a characteristic absorption for a cyclic carbonyl group in the range 1725–1758 cm^{-1} in the IR spectra. The ^{1}H-NMR spectra of compounds **4a**–**s** clearly indicated the presence of the active methylene group in the thiazolidine ring by exhibiting a signal in the range δ 3.26–3.68 ppm. The ^{13}C-NMR spectra of compounds **4a**–**s** also supported the fact that a cyclic carbonyl group was present by the signal that appeared in the range δ 160.4–178.8 ppm. These facts were supported by a) the disappearance of the N=CH proton and b) the appearance of a N–CH proton in the range of δ 5.23–5.82 ppm in the ^{1}H-NMR spectra of compounds **4a**–**s**.

Compounds **4a**–**s** underwent a Knoevenagel condensation reaction with substituted benzaldehydes in the presence of alkali metal alkoxide (C_2H_5ONa) to afford compounds **5a**–**s**. In the ^{1}H-NMR spectra of compounds **5a**–**s**, the two methylene protons of compounds **4a**–**s** were absent and a new signal for C=CH appeared in the range δ 6.32–6.77 ppm and in the ^{13}C-NMR spectra of compounds **5a**–**s**, two new signals for C=**C**H and **C**=CH appeared in the δ range 134.6–143.2 and 140.1–149.2 ppm, respectively. All these facts clearly confirmed the synthesis of all the final products.

Biological study

The results of the antimicrobial (antibacterial, antifungal and antitubercular) activities are summarized in Table I. All the compounds **1**, **2**, **3a**–**s**, **4a**–**s** and **5a**–**s** were screened for their antimicrobial activity against selected strains of bacteria and fungi and antitubercular activity against *M. tuberculosis* (H37Rv strain). The investigation of antimicrobial data revealed that compounds **5c**, **5d**, **5e**, **5f**, **5h**, **5i** and **5j** displayed high activity, compounds **4h**, **4j**, **5b**, **5g** and **5q** showed moderate activity and the other compounds showed less activity against all the strains compared with standard drugs.

The compounds exhibited a structure–activity relationship (SAR) because the activity of compounds varies with substitution. The nitro group-containing compounds **5h**, **5i** and **5j** showed higher activity than the chloro group- (**5c** and **5d**) or the bromo group-containing compounds (**5e** and **5f**). In addition, the

chloro- and bromo-derivatives also had a higher activity than the other tested compounds. Based on the SAR, it could be concluded that the activity of compounds depended on t he electron withdrawi ng nature of the substituent groups. The sequence of the activity is following:

$$NO_2 > Cl > Br > OCH_3 < OH > CH_3$$

TABLE I. Ant ibacterial, antifungal (inhibition zone in mm) and antitubercular activity of compounds **1**, **2**, **3a**–**s**, **4a**–**s** and **5a**–**s**

Compound	Antibacterial activity						Antifungal activity						Antitubercular activity, %	
	B. subtilis		*E. coli*		*S. aureus*		*A. niger*		*A. flavus*		*C. albicans*		*M. tuberculosis* H37Rv strain	
	c / ppm												*c* / μg mL^{-1}	
	50	100	50	100	50	100	50	100	50	100	50	100	25	50
1	–	7	–	5	4	7	–	8			4	6	–	5	13	20
2	2	9	–	7	2	6	5	8			4	7	3	6	10	18
3a	7	12	10	14	11	13			9	12	10	15	9	13	18	22
3b	10	20	11	18	13	19	10	17	13			17	11	14	25	32
3c	12	19	12	16	10	16	11	17	13			17	11	14	27	34
3d	10	13	14	17	12	19	13	20	14			20	13	17	30	35
3e	8	21	9	22			10	21	9	18	8	15	8	16	28	40
3f	9	20	10	21	11	20			8	14	6	13	6	17	27	50
3g	10	24	7	21			9	20	6	13	8	12	9	14	25	52
3h	13	26	10	24	13	27	10	18	12			25	14	22	32	65
3i	11	23	9	20			10	25	10	17	11	26	12	23	35	68
3j	13	27	10	24	12	26	10	18	10			24	11	22	38	66
3k	7	10	6	10			8	12	7	13	6	13	8	14	25	40
3l	8	12	6	13			7	13	6	14	7	13	7	12	28	42
3m	8	13	7	14			6	12	7	12	6	14	6	10	23	43
3n	4	10	5	12			4	11	6	13	5	9	4	10	20	38
3o	5	7	6	8	6			10	5	12	6	11	7	10	24	35
3p	5	8	5	9	4	7	6			10	5	9	6	11	25	38
3q	9	14	8	13			8	15	7	13	6	14	8	14	28	50
3r	10	16	9	14			8	13	7	12	7	15	9	14	30	52
3s	9	13	10	15			7	14	9	13	8	15	10	14	32	55
4a	15	20	13	19	14	20	10	15	12			20	10	14	20	35
4b	14	23	10	21	13	21	10	17	11			17	12	18	25	55
4c	10	27	10	28	12	27	11	20	10			19	11	21	30	60
4d	12	26	11	27	12	29	11	20			8	17	12	19	30	60
4e	10	29	10	27	10	28			9	21	8	17	10	19	30	68
4f	10	28	11	30	13	30	12	24	13			20	13	21	32	70
4g	17	30	8	31			10	30	7	20	8	21	10	22	30	75
4h	18	30	15	28	10	30	11	24			9	20	8	22	30	70
4i	10	22	13	24	12	28	10	12			9	19	8	20	32	68
4j	12	24	15	30	13	27	12	28	10			22	9	24	35	70

TABLE I. Continued

Compound	Antibacterial activity						Antifungal activity						Antitubercular activity, %	
	B. subtilis		*E. coli*		*S. aureus*		*A. niger*		*A. flavus*		*C. albicans*		*M. tuberculosis* H37Rv strain	
	c / ppm												*c* / μg mL^{-1}	
	50	100	50	100	50	100	50	100	50	100	50	100	25	50
4k	10	14	9	22	10	20	8	21	9	17	7	21	30	50
4l	11	15	8	20	10	21	8	20	8	15	6	15	32	53
4m	9	14	10	16	8	18	8	15	7	14	7	13	30	50
4n	8	10	8	12	8	14	7	13	9	13	7	13	29	41
4o	9	13	8	14	7	13	7	13	8	12	8	10	28	42
4p	8	14	9	17	8	15	7	16	7	13	8	14	30	45
4q	16	26	18	30	14	29	14	25	12	22	13	25	33	70
4r	17	24	15	30	15	27	13	24	13	21	10	21	34	70
4s	12	20	11	22	10	21	11	23	10	18	10	22	33	65
5a	18	25	07	22	10	23	07	15	07	12	10	14	22	45
5b	15	29	10	30	15	29	12	20	10	20	14	21	32	74
5c	13	34	12	32	14	31	15	24	17	25	14	23	36	80
5d	15	32	10	31	13	32	11	23	10	21	13	22	32	80
5e	12	33	12	31	15	31	10	22	12	23	15	23	30	78
5f	11	31	11	31	14	32	11	22	11	21	14	23	30	79
5g	20	27	10	28	10	28	10	19	10	20	10	20	29	76
5h	22	35	19	33	12	34	18	24	09	24	12	25	32	82
5i	20	34	10	32	12	35	12	25	10	23	12	24	27	83
5j	24	36	11	33	10	33	13	25	11	22	10	24	28	81
5k	08	28	09	21	08	27	11	18	10	14	11	17	28	60
5l	11	26	12	23	12	25	10	16	12	15	12	16	30	63
5m	13	27	15	25	14	26	13	15	13	15	12	12	31	65
5n	14	18	14	17	16	22	10	15	10	13	10	14	22	45
5o	12	19	14	15	15	20	09	14	09	12	11	15	18	49
5p	14	20	15	18	14	19	08	12	10	18	09	15	20	47
5q	12	29	13	28	12	30	14	20	13	16	12	21	24	76
5r	13	28	14	24	13	27	13	18	13	17	13	20	27	70
5s	11	30	12	21	11	29	12	18	10	15	11	19	25	65
Standard	28	37	26	34	27	35	20	26	18	25	19	26	100	100
	Streptomycin						Griseofulvin						Standards[a]	

[a]Standards for the antitubercular activity, isoniazid and rifampicin, showed 100 % activity at both tested concentrations

CONCLUSIONS

The present research study reports the successful synthesis of all the newly synthesized compounds **1**, **2**, **3a**–**s**, **4a**–**s** and **5a**–**s**. Some of the synthesized compounds displayed good biological activities while the others showed lower antimicrobial and antitubercular activities.

SUPPLEMENTARY MATERIAL

Analytical and spectral data of synthesized compounds are available electronically from http://www.shd.org.rs/JSCS/, or from the corresponding author on request.

Acknowledgements. The authors are thankful to SAIF , Central Drugs Research Institute, Lucknow (India) for providing the sp ectral and analytical data of the co mpounds. We are thankful to the Head, Depart ment of Biotec hnology, Dr. H . S. Gour University (A Central University), Sagar (India) for the antimicrobial (antibacterial and antifungal) results and the Microcare Laboratory and Tuberculosis Research Centre, Surat, Gujarat (India) for the ant i-tuberculosis activity results. We are also thank ful to the Head, Department of Chemistry, Dr. H. S. Gour Univ ersity (A Central University), Sagar (India) for providing the facilities for the realisation oft the work.

И З В О Д

СИНТЕЗА И БИОЛОШКА АКТИВНОСТ 4-ТИАЗОЛИДИНОНСКИХ ДЕРИВАТА ФЕНОТИАЗИНА

RITU SHARMA, PUSHKAL SAMADHIYA, SAVITRI D. SRIVASTAVA и SANTOSH K. SRIVASTAVA

Synthetic Organic Chemistry Laboratory, Department of Chemistry, Dr. H.S. Gour University (A Central University), Sagar-470003, India

Синтетисана је серија нових деривата *N*-[3-(10*H*-фенотиазин-10-ил)-пропил]-2-(супституисани фенил)-4-оксо-5-(супституисани бензилиден)-3-тиазолидин-карбоксамида **5a**–**s**. Реакција тиогликолне киселине и *N*-[3-(10*H*-фенотиазин-10-ил)-пропил]-*N*'-[(супституисани фенил)-метилиден]-уреа **3a–s**, у присуству анхидрованог $ZnCl_2$ даје нова хетероциклична једињења *N*-[3-(10*H*-фенотиазин-10-ил)-пропил]-2-(супституисани фенил)-4-оксо-3-тиазолидин-карбоксамиде, **4a**–**s**. Добијени производи у реакцији са одабраним супституисаним ароматични алдехидима, у присуству C_2H_5ONa подлежу Кневенагеловој реакцији и дају једињења **5a**–**s**. Једињења **1**, **2**, **3a–s**, **4a–s** и **5a–s** потврђнуте су IR, ^{1}H-NMR, ^{13}C-NMR, FAB MS инструменталним анализама и елементалној анализи. Испитана је антибактеријска, антифунгална и антитуберкулозна активност према *M. tuberculosis* синтетисаних једињења.

(Примљено 24. септембра 2010, ревидирано 24. априла 2011)

REFERENCES

1. J. Fraga-Dubrevil, J. P. Bazureau, *Tetrahedron* **59** (2003) 6121
2. A. Rao, A. Carbone, A. Chimirri, E. D. Clercq, A. M., Monforte, P. Monforte, C. Pannecouque, M. Zappala, *Farmaco* **57** (2002) 747
3. A. Rao, J. Balzarini, A. Carbone, A. Chimirri, E. D. Clercq, A. M. Monforte, M. Zappala, *Antiviral Res.* **63** (2004) 79
4. M. L. Barreca, A. Chimirri, L. D. Luca, A. -M. Monforte, P. Monforte, A. Rao, M. Zappalà, J. Balzarini, E. D. Clercq, C. Pannecouque, M. Witvrouw, *Bioorg. Med. Chem. Lett*. **11** (2001) 1793
5. N. B. Allens, A. S. Anderson, B. Fauber, A. Allen, L. E. Burgess, *Bioorg. Med. Chem. Lett*. **14** (2004) 1619
6. Y. S. Prabhaker, V. R. Solomon, R. K. Rawat, M. K. Gupta, S. B. Katti, *QSAR Comb. Sci.* **23** (2004) 234
7. S. K. Sonwane, S. D. Srivastava, *Proc. Nat. Acad. Sci. India* **78** (2008) 129

8. K. M. Mistry, K. R. Desai, *E-J. Chem*. **1** (2004) 189
9. M. Sayyed, S. Mokle, M. Bokhare, A. Mankar, S. Bhusare, Y. Vibhute, *Arkivoc* (2006) 187
10. P. Kohli, S. D. Srivastava, S. K. Srivastava, *J. Chin. Chem. Soc*. **54** (2007) 1003
11. V. V. Mulwad, A. M. Abid, *J. Korean Chem. Soc*. **52** (2008) 649
12. V. J. Sattigeri, A. Soni, S. Singhal, S. Khan, M. Pandya, P. Bhateja, T. Mathur, A. Rattan, J. M. Khanna, A. Mehta, *Arkivoc* (2005) 46
13. S. K. Sonwane, S.D. Srivastava, S.K. Srivastava, *J. Indian Counc. Chem*. **25** (2008) 15
14. H.-L. Liu, Z. Li, T. Anthonsen, *Molecules* **5** (2000) 1055
15. R. Yadav, S. D. Srivastava S. K. Srivastava, *Indian J. Chem., B* **44** (2005) 1262
16. R. Ottana, R. Maccari, M. L. Barreca,; G. Bruno, A. Rotondo, A. Rossi, G. Chiricosta, R. Di Paola, L. Sautebin, S. Cuzzocrea, M. G. Vigorita, *Bioorg. Med. Chem.* **13** (2005) 4243
17. P. Venkatesh, S. N. Pandeya, *E-J. Chem*. **6** (2009) 495
18. I. Vazzana, E. Terranova, F. Mattioli, F. Sparatore, *Arkivoc* (2004) 364
19. R. B. Patel, P. S. Desai, K. R. Desai, K. H. Chikhalia, *Indian J. Chem., B* **45** (2006) 773
20. T. Shrivastava, A. K. Gaikwad, W. Haq, S. Sinha, S. Katti, *Arkivoc* (2005) 120
21. A. S. Narute, P. B. Khedekar, K. P. Bhusari, *Indian J. Chem., B* **47** (2008) 586
22. P.-C. Lv, C.-F. Zhou, J. Chen, P.-G. Liu, K.-R. Wang, W.-J. Mao, H.-Q. Li, Y. Yang, J. Xiong, H.-L. Zhu, *Bioorg. Med. Chem*. **18** (2010) 314
23. R. Ottana, S. Carotti, R. Maccari, I. Landini, G. Chirico sta, B. Caciagli, M. G. Vigorita, E. Mini, *Bioorg. Med. Chem. Lett.* **15** (2005) 3930
24. J. P. Raval, K. R. Desai, *Arkivoc* (2005) 21
25. S. D. Srivastava, P. Kohli, *Proc. Natl. Acad. India* **77** (2007) 199
26. T. R. Rawat, S. D. Srivastava, *Indian J. Chem., B* **37** (1998) 91
27. A. R. Trivedi, A. B. Siddiqui, V. H. Shah, *Arkivoc* (2008) 210
28. F. Weng, J. Tan, *Acta Pharmacol. Sin.* **24** (2003) 1001
29. A. Rajasekaran, P. P. Tripathi, *Acta Pharm. Turc.* **45** (2003) 235
30. S. Kasmi-Mir, A. Djafri, L. Paquin, J. Hamelin, M. Rahmouni, *Molecules* **11** (2006) 597
31. R. Sharma, P. Samadhiya, S. D. Srivastava, S. K. Srivastava, *Acta Chim. Slov.* **58** (2011) 110.

Journal of the Serbian Chemical Society
JSCS@tmf.bg.ac.rs • www.shd.org.rs/JSCS
J. Serb. Chem. Soc. 77 (1) S10–S29 (2012) *Supplementary material*

SUPPLEMENTARY MATERIAL TO

Synthesis and biological activity of 4-thiazolidinone derivatives of phenothiazine

RITU SHARMA*, PUSHKAL SAMADHIYA, SAVITRI D. SRIVASTAVA and SANTOSH K. SRIVASTAVA

Synthetic Organic Chemistry Laboratory, Department of Chemistry Dr. H. S. Gour University (A Central University), Sagar, M. P. India 470003

J. Serb. Chem. Soc. 77 (1) (2012) 17–26

ANALYTICAL AND SPECTRAL DATA OF THE SYNTHESIZED COMPOUNDS

*10-(3-Chloropropyl)-10*H*-phenothiazine* ***(1)***. Yield: 60 %; m.p. 170–172 °C; Anal. Calcd. for $C_{15}H_{14}ClNS$: C, 65.32; H, 5.11; N, 5.07 %. Found: C, 65.27; H, 5.08; N, 4.97 %; IR (KBr, cm^{-1}): 687 (C–S–C), 774 (C–Cl), 1320 (N–C), 1552 (C=C), 1428, 2844, 2932 (CH_2), 3020 (CH–Ar); ^{1}H-NMR (300 MHz, $CDCl_3$, δ / / ppm): 2.09–2.15 (2H, *m*, H-12), 3.51 (2H, *t*, *J* = 7.65 Hz, H-13), 4.12 (2H, *t*, *J* = = 7.65 Hz, H-11), 6.31–7.75 (8H, *m*, Ar–H); ^{13}C-NMR (75 MHz, $CDCl_3$, δ / / ppm): 34.1 (C-12), 44.4 (C-13), 48.4 (C-11), 113.8 (C-4 and C-5), 119.2 (C-1 and C-8), 122.7 (C-2 and C-7), 124.3 (C-3 and C-6), 138. 2 (C-4a and C-5a), 146.7 (C-1a and C-8a); FAB mass (*m*/*z*): 275 [M^+].

N-*[3-(10*H*-Phenothiazin-10-yl)propyl]urea* ***(2)***. Yield: 71 %; m.p. 152–153 °C; Anal. Calcd. for $C_{16}H_{17}N_3OS$: C, 64.18; H, 5.72; N, 14.03 %. Found: C, 64.12; H, 5.65; N, 13.98 %; IR (KBr, cm^{-1}): 678 (C–S–C), 1228 (N–C), 1465 (C=C), 1655 (CO), 1434, 2837, 2892 (CH_2), 3025 (CH–Ar), 3342, 3413 (NH_2); ^{1}H-NMR (300 MHz, $CDCl_3$, δ / ppm): 2.16–2.25 (2H, *m*, H-12), 3.22–3.28 (2H, *m*, H-12), 4.16 (2H, *t*, *J* = 7.40 Hz, H-11), 5.83 (1H, *s*, H-1'), 5.99 (2H, *s*, H-3'), 6.44–7.73 (8H, *m*, Ar–H); ^{13}C-NMR (75 MHz, $CDCl_3$, δ / ppm): 34.0 (C-12), 44.2 (C-13), 48.9 (C-11), 114.0 (C-4 and C-5), 119.2 (C-1 and C-8), 122.7 (C-2 and C-7), 124.3 (C-3 and C-6), 138.2 (C-4a and C-5a), 145.3 (C-1a and C-8a) 163.4 (C-2'); FAB mass (*m*/*z*): 299 [M^+].

N-*[3-(10*H*-Phenothiazin-10-yl)propyl]*-N'*-(phenylmethylidene)urea* ***(3a)***. Yield: 61 %; m.p. 148–149 °C; Anal. Calcd. for $C_{23}H_{21}N_3OS$: C, 71.29; H, 5.46; N, 10.84 %. Found: C, 71.24; H, 5.38; N, 10.81 %; IR (KBr, cm^{-1}): 684 (C–S–C), 1332 (N–C), 1464 (C=C), 1547 (N=CH), 1652 (CO), 1430, 2836, 2894 (CH_2),

* Corresponding author. E-mail: ritusharmaic@rediffmail.com

3022 (CH–Ar), 335 6 (NH); ^{1}H-NMR (300 MHz, C DCl$_3$, δ / pp m): 2.28–2.35 (2H, *m*, H-12), 3.26–3.34 (2H, *m*, H-13), 4.18 (2H, *t*, *J* = 7.50 Hz, H-11), 5.88 (1H, *s*, H-1'), 7.84 (1H, *s*, H-14), 6.40 –7.81 (13H, *m*, Ar–H); ^{13}C-NMR (75 MHz, CDCl$_3$, δ / ppm): 33.5 (C-12), 43.6 (C-13), 49.3 (C-11), 115.3 (C-4 and C-5), 116.7 (C-1 and C-8), 120.8 (C-2 and C-7), 121.6 (C-3 and C-6), 123.6 (C-16 and C-20), 125.5 (C-17 and C-19), 126.8 (C-18), 135.6 (C-15), 136.9 (C-4a and 5a), 143.7 (C-1a and C-8a), 150.6 (C-14), 162.4 (C-2'); FAB mass (*m*/*z*): 387 [M$^+$].

N-*[(4-Chlorophenyl)methylidene]*-N'-*[3-(10*H-*phenothiazin-10-yl)propyl]urea* ***(3b)***. Yield: 66 %; m.p. 168–169 °C; Anal. Calcd. for C $_{23}$H$_{20}$ClN$_3$OS: C, 65.47; H, 4.77; N, 9.95 % . Found: C, 65.43; H, 4.65; N, 9.9 1 %; IR (KBr, cm^{-1}): 684 (C–S–C), 735 (C–Cl), 1303 (N–C), 1472 (C=C), 1569 (N=CH), 1661 (CO), 1448, 2869, 2913 (CH$_2$), 3031 (CH–Ar), 3373 (NH); ^{1}H-NMR (300 MHz, CDCl$_3$, δ / / ppm): 2.18–2.22 (*m*, 2H, H-12), 3.26–3.32 (*m*, 2H, H-13), 4.16 (t, 2H, *J* = 7.65 Hz, H-11), 5. 97 (1H, *s*, H-1'), 7.84 (1H, *s*, H-14), 6.29–7.75 (12H, *m*, Ar–H); ^{13}C-NMR (75 MHz, C DCl$_3$, δ / pp m): 35.0 (C-12), 44.7 (C-13), 50.0 (C-11), 115.8 (C-4 and C-5), 120. 4 (C-1 and C-8) , 124.5 (C-2 and C-7), 125. 4 (C-3 and C-6), 127.6 (C-16 and C-20), 126.5 (C-17 and C-19), 128.8 (C-18), 137.3 (C-15), 138.4 (C-4a and 5a), 147. 2 (C-1a and C-8a), 152.0 (C-14), 165.3 (C-2'); FAB mass (*m*/*z*): 421 [M$^+$].

N-*[(3-Chlorophenyl)methylidene]*-N'-*[3-(10*H-*phenothiazin-10-yl)propyl]urea* ***(3c)***. Yield: 67 %; m.p. 166–167 °C; Anal. Calcd. for C $_{23}$H$_{20}$ClN$_3$OS: C, 65.47; H, 4.77; N, 9.95 % . Found: C, 65.41; H, 4.71; N, 9.8 3 %; IR (KBr, cm^{-1}): 693 (C–S–C), 739 (C–Cl), 1344 (N–C), 1476 (C=C), 1572 (N=CH), 16 65 (CO), 1440, 2845, 2902 (CH$_2$), 3033 (CH–Ar), 3364 (NH); ^{1}H-NMR (300 M Hz, CDCl$_3$, δ / ppm): 2.20–2.25 (2H, *m*, H-12), 3.23–3.29 (2H, *m*, H-13), 4.20 (2H, *t*, *J* = 7.65 Hz, H-11), 5.9 8 (1H, *s*, H-1'), 7.84 (1H, *s*, H-14), 6.34–7.76 (12H, *m*, Ar–H); ^{13}C-NMR (75 MHz, CDCl$_3$, δ / ppm): 35.5 (C-12), 44.5 (C-13), 51.0 (C--11), 116.7 (C-4 and C-5), 120.3 (C-1 and C-8), 124.5 (C-2 and C-7), 125.6 (C-3 and C-6), 126.3 (C-16), 126.8 (C-20), 127.4 (C-17), 127.9 (C-19), 128.5 (C-18), 137.2 (C-15), 138.1 (C-4a and C-5a), 147.5 (C-1a and C-8a), 151.3 (C-14), 164.2 (C-2'); FAB mass (*m*/*z*): 421 [M$^+$].

N-*[(2-Chlorophenyl)methylidene]*-N'-*[3-(10*H-*phenothiazin-10-yl)propyl]urea* ***(3d)***. Yield 65 % ; m.p. 160–162 °C; Anal. Calcd. fo r C$_{23}$H$_{20}$ClN$_3$OS: C, 65.46; H, 4.77; N, 9.95 % . Found: C, 65.41; H, 4.72; N, 9.8 5 %; IR (KBr, cm^{-1}): 692 (C–S–C), 743 (C–Cl), 1338 (N–C), 1474 (C=C), 1578 (N=CH), 16 70 (CO), 1439, 2848, 2906 (CH$_2$), 3034 (CH–Ar), 3367 (NH); ^{1}H-NMR (300 M Hz, CDCl$_3$, δ / ppm): 2.18–2.25 (2H, *m*, H-12), 3.29–3.34 (2H, *m*, H-13), 4.19 (2H, *t*, *J* = 7.65 Hz, H-11), 5.9 1 (1H, *s*, H-1'), 7.87 (1H, *s*, H-14), 6.41–7.88 (12H, *m*, Ar–H); ^{13}C-NMR (75 MHz, CDCl$_3$, δ / ppm): 34.9 (C-12), 44.3 (C-13), 50.3 (C--11), 116.5 (C-4 and C-5), 119.4 (C-1 and C-8), 123.4 (C-2 and C-7), 124.1 (C-3 and C-6), 126.5 (C-16), 127.4 (C-20), 128.1 (C-17), 128.8 (C-19), 129.5 (C-18),

136.1 (C-15), 137.7 (C-4a and C-5a), 146.1 (C-1a and C-8a), 153.4 (C-14), 162.7 (C-2'); FAB mass (*m*/*z*): 421 [M^+].

N-*[(4-Bromophenyl)methylidene]*-N'-*[3-(10*H-phenothiazin-10-yl)propyl]urea (***3e***). Yield: 65 %; m.p. 159–161 °C; Anal. Calcd. for $C_{23}H_{20}BrN_3OS$: C, 59.23; H, 4.32; N, 9.00 % . Found: C, 59.15; H, 4.23; N, 8.9 4 %; IR (KBr, cm^{-1}): 631 (C–Br), 697 (C–S–C), 1342 (N–C), 1472 (C=C), 1574 (N=CH), 1663 (CO), 1441, 2850, 2907 (CH_2), 3037 (CH–Ar), 3371 (NH); ^{1}H-NMR (300 M Hz, $CDCl_3$, δ / ppm): 2.19–2.22 (2H, *m*, H-12), 3.21–3.26 (2H, *m*, H-13), 4.17 (2H, *t*, *J* = 7.60 Hz, H-11), 5.8 2 (1H, *s*, H-1'), 7.92 (1H, *s*, H-14), 6.39–7.68 (12H, *m*, Ar–H); ^{13}C-NMR (75 MHz, $CDCl_3$, δ / ppm): 35.0 (C-12), 43.8 (C-13), 50.2 (C--11), 115.1 (C-4 and C-5), 117.8 (C-1 and C-8), 122.7 (C-2 and C-7), 123.8 (C-3 and C-6), 124.4 (C-16 and C-20), 127.3 (C-17 and C-19), 128.8 (C-18), 140.8 (C-15), 141.2 (C-4a and C-5a), 146.4 (C-1a and C-8a), 153.8 (C-14), 16 2.1 (C--2'); FAB mass (*m*/*z*): 466 [M+1].

N-*[(3-Bromophenyl)methylidene]*-N'-*[3-(10*H-phenothiazin-10-yl)propyl]ure (***3f***). Yield: 64 %; m.p. 157–158 °C; Anal. Calcd. for $C_{23}H_{20}BrN_3OS$: C, 59.23; H, 4.32; N, 9.00 % . Found: C, 59.19; H, 4.31; N, 8.9 7 %; IR (KBr, cm^{-1}): 640 (C–Br), 691 (C–S–C), 1346 (N–C), 1479 (C=C), 1574 (N=CH), 1661 (CO), 1445, 2852, 2910 (CH_2), 3035 (CH–Ar), 3362 (NH); ^{1}H-NMR (300 MHz, $CDCl_3$, δ / / ppm): 2.16–2.23 (2H, *m*, H-12), 3.24-3.30 (2H, *m*, C-13), 4.21 (2H, *t*, *J* = 7.60 Hz, H-11), 5.88 (1H, *s*, H-1'), 7.93 (1H, *s*, H-14), 6.36–7.86 (12H, *m*, Ar–H); ^{13}C-NMR (75 MHz, $CDCl_3$, δ / ppm): 33.6 (C-12), 44.2 (C-13), 49.3 (C-11), 116.3 (C-4 and C-5), 117.5 (C-1 and C-8), 122.6 (C-2 and C-7), 123.4 (C-3 and C-6), 125.3 (C-16), 126.4 (C-20), 128.5 (C-17), 128.9 (C-19), 129.6 (C-18), 140.5 (C-15), 141.8 (C-4a and C-5a), 148.4 (C-1a and C-8a), 151.6 (C-14), 164.9 (C-2'); FAB mass (*m*/*z*): 466 [M+1].

N-*[(2-Bromophenyl)methylidene]*-N'-*[3-(10*H-phenothiazin-10-yl)propyl]urea (***3g***). Yield: 62 %; m.p. 161–163 °C; Anal. Calcd. for $C_{23}H_{20}BrN_3OS$: C, 59.23; H, 4.32; N, 9.00 % . Found: C, 59.15; H, 4.24; N, 8.9 2 %; IR (KBr, cm^{-1}): 623 (C–Br), 699 (C–S–C), 1339 (N–C), 1473 (C=C), 1584 (N=CH), 1666 (CO), 1438, 2846, 2904 (CH_2), 3040 (CH–Ar), 3361 (NH); ^{1}H-NMR (300 MHz, $CDCl_3$, δ / / ppm): 2.22–2.29 (2H, *m*, H-12), 3.27–3.36 (2H, *m*, H-13), 4.22 (2H, *t*, *J* = 7.65 Hz, H-11), 5.89 (1H, *s*, H-1'), 7.88 (1H, *s*, H-14), 6.23–7.83 (12H, *m*, Ar–H); ^{13}C-NMR (75 MHz, $CDCl_3$, δ / ppm): 33.2 (C-12), 45.0 (C-13), 51.2 (C-11), 116.8 (C-4 and C-5), 119.2 (C-1 and C-8), 123.5 (C-2 and C-7), 124.3 (C-3 and C-6), 125.9 (C-16 and C-20), 127.6 (C-17), 128.1 (C-19), 128.4 (C-18), 139.0 (C-15), 140.6 (C-4a and C-5a), 145.4 (C-1a and C-8a), 151.3 (C-14), 16 1.5 (C--2'); FAB mass (*m*/*z*): 466 [M+1].

N-*[(4-Nitrophenyl)methylidene]*-N'-*[3-(10*H-phenothiazin-10-yl)propyl]urea (***3h***). Yield: 66 %; m.p. 155–157 °C; Anal. Calcd. for $C_{23}H_{20}N_4O_3S$: C, 63.87; H, 4.66; N, 12.95 %. Found: C, 63.74; H, 4.61; N, 12.91 %; IR (KBr, cm^{-1}): 696

(C–S–C), 848 (C–N), 1478 (C=C), 1524 (N=O), 1559 (N=CH), 1669 (CO), 1444, 2851, 2909 (CH_2), 3036 (CH–Ar), 3351 (NH); ^{1}H-NMR (300 MHz, $CDCl_3$, δ / / ppm): 2.28–2.32 (2H, *m*, H-12), 3.25–3.31 (2H, *m*, H-13), 4.21 (2H, *t*, J = 7.60 Hz, H-11), 5.83 (1H, *s*, H-1'), 8.12 (1H, *s*, H-14), 6.24–7.89 (12H, *m*, Ar–H); ^{13}C-NMR (75 MHz, C DCl_3, δ / pp m): 38.7 (C-12), 46.4 (C-13), 47.3 (C-11), 116.8 (C-4 and C-5), 118.3 (C-1 and C-8), 124.0 (C-2 and C-7), 125.3 (C-3 and C-6), 126.6 (C-16 and C-20), 128.7 (C-17 and C-19), 129.3 (C-18), 139.9 (C-15), 140.5 (C-4a and C-5a), 149.2 (C-1a and C-8a), 153.7 (C-14), 165 (C-2'); FAB mass (*m*/*z*): 432 [M^+].

N-*[(3-Nitrophenyl)methylidene]*-N'-*[3-(10*H-phenothiazin-10-yl)propyl]urea ***(3i)***. Yield: 70 %; m.p. 157–159 °C; Anal. Calcd. for $C_{23}H_{20}N_4O_3S$: C, 63.87; H, 4.66; N, 12.95 %. Found: C, 63.75; H, 4.63; N, 12.87 %; IR (KBr, cm^{-1}): 694 (C–S–C), 845 (C–N), 1475 (C=C), 1534 (N=O), 1567 (N=CH), 1632 (CO), 1437, 2854, 2905 (CH_2), 3031 (CH–Ar), 3355 (NH); ^{1}H-NMR (300 MHz, $CDCl_3$, δ / / ppm): 2.25–2.29 (2H, *m*, H-12), 3.21–3.27 (2H, *m*, H-13), 4.18 (2H, *t*, J = 7.60 Hz, H-11), 6.13 (1H, *s*, H-1'), 7.84 (1H, *s*, H-14), 6.37–7.67 (12H, *m*, Ar–H); ^{13}C-NMR (75 MHz, C DCl_3, δ / pp m): 32.2 (C-12), 44.6 (C-13), 50.8 (C-11), 114.6 (C-4 and C-5), 119.6 (C-1 and C-8), 125.7 (C-2 and C-7), 126.1 (C-3 and C-6), 127.2 (C-16), 128.4 (C-20), 129.0 (C-17), 129.4 (C-19), 130.7 (C-18), 138.4 (C-15), 139.2 (C-4a and C-5a), 145.4 (C-1a and C-8a), 156.0 (C-14), 163.4 (C-2'); FAB mass (*m*/*z*): 432 [M^+].

N-*[(2-Nitrophenyl)methylidene]*-N'-*[3-(10*H-phenothiazin-10-yl)propyl]urea ***(3j)***. Yield: 61 %; m.p. 149–150 °C; Anal. Calcd. for $C_{23}H_{20}N_4O_3S$: C, 63.87; H, 4.66; N, 12.95 %. Found: C, 63.71; H, 4.61; N, 12.85 %; IR (KBr, cm^{-1}): 698 (C–S–C), 845 (C–NH), 1473 (C=C), 1531 (N=O), 1554 (N=CH), 1639 (CO), 1446, 2849, 2912 (CH_2), 3039 (CH–Ar), 3344 (NH); ^{1}H-NMR (300 MHz, $CDCl_3$, δ / / ppm): 2.21–2.24 (2H, *m*, H-12), 3.26–3.32 (2H, *m*, H-13), 4.21 (2H, *t*, J = 7.65 Hz, H-11), 6.08 (1H, *s*, H-1'), 8.23 (1H, *s*, H-14), 6.45-8.22 (12H, *m*, Ar–H); ^{13}C-NMR (75 MHz, C DCl_3, δ / pp m): 33.6 (C-12), 45.1 (C-13), 49.4 (C-11), 112.4 (C-4 and C-5), 118.2 (C-1 and C-8), 125.5 (C-2 and C-7), 126.4 (C-3 and C-6), 127.5 (C-16), 128.2 (C-20), 129.6 (C-17), 130.1 (C-19), 130.4 (C-18), 138.7 (C-15), 139.3 (C-4a and C-5a), 148.3 (C-1a and C-8a), 158.0 (C-14), 163.4 (C-2'); FAB mass (*m*/*z*): 432 [M^+].

N-*[(4-Methoxyphenyl)methylidene]*-N'-*[3-(10*H-phenothiazin-10-yl)propyl]-urea ***(3k)***. Yield: 61 %; m.p. 150–151 °C; Anal. Calcd. for $C_{24}H_{23}N_3O_2S$: C, 69.04; H, 5.55; N, 10.06 %. Found: C, 68.92; H, 5.48; N, 10.02 %; IR (KBr, cm^{-1}): 702 (C–S–C), 1336 (N–C), 1467 (C=C), 1546 (N=CH), 1667 (C O), 1433, 2839, 2895 (CH_2), 2943 (OCH_3), 3024 (CH–Ar), 3351 (NH); ^{1}H-NMR (300 M Hz, $CDCl_3$, δ / ppm): 2.12–2.16 (2H, *m*, H-12), 3.18–3.26 (2H, *m*, H-13), 3.61 (3H, *s*, OCH_3), 4.12 (2H, *t*, J = 7.55 Hz, H-11), 5.82 (1H, *s*, H-1'), 7.95 (1H, *s*, H-14), 6.35–7.89 (12H, *m*, Ar–H); ^{13}C-NMR (75 MHz, $CDCl_3$, δ / ppm): 32.0 (C-12),

42.5 (C-13), 48.4 (C-11), 53.0 (OCH_3),109.8 (C-4 and C-5), 116. 0 (C-1 and C--8), 121.7 (C-2 and C-7), 122.4 (C-3 and C-6), 124.8 (C-16 and C-20), 126.0 (C--17 and C-19), 127.7 (C-18), 136.6 (C-15), 137.0 (C-4a and C-5a), 158.0 (C-1 a and C-8a), 147.0 (C-14), 161.3 (C-2'); FAB mass (*m*/*z*): 417 [M^+].

N-*[(3-Methoxyphenyl)methylidene]*-N'-*[3-(10*H*-phenothiazin-10-yl)propyl]-urea* (***3l***). Yield: 62 %; m.p. 149–150 °C; Anal. Calcd. for $C_{24}H_{23}N_3O_2S$: C, 69.04; H, 5.55; N, 10.06 %. Found: C, 68.99; H, 5.51; N, 10.01 %; IR (KBr, cm^{-1}): 704 (C–S–C), 1332 (N–C), 1461 (C=C), 1534 (N=CH), 1667 (CO), 1436, 2834, 2897 (CH_2), 2941 (OCH_3), 3020 (CH–Ar), 3353 (NH); ^{1}H-NMR (300 MHz, $CDCl_3$, δ / ppm): 2.14–2.19 (2H, *m*, H-12), 3.18–3.25 (2H, *m*, H-13), 3.75 (3H, *s*, OCH_3), 4.16 (2H, *t*, *J* = 7.55 Hz, H-11), 5.84 (1H, *s*, H-1'), 7.88 (1H, *s*, H-14), 6.55–7.98 (12H, *m*, Ar–H); ^{13}C-NMR (75 MHz, $CDCl_3$, δ / ppm): 32.4 (C-12), 42.7 (C-13), 48.6 (C-11), 54.5 (OCH_3), 114.1 (C-4 and C-5), 117. 4 (C-1 and C--8), 120.3 (C-2 and C-7), 123.4 (C-3 and C-6), 125.5 (C-16), 126.2 (C-20), 126.5 (C-17), 127.3 (C-19), 128.9 (C-18), 135.6 (C-15), 138.6 (C-4a and C-5a), 158.7 (C-1a and C-8a), 146.0 (C-14), 163.9 (C-2'); FAB mass (*m*/*z*): 417 [M^+].

N-*[(2-Methoxyphenyl)methylidene]*-N'-*[3-(10*H*-phenothiazin-10-yl)propyl]-urea* (***3m***). Yield: 64 % ; m.p. 144–145 °C; Anal. Calcd. for $C_{24}H_{23}N_3O_2S$: C, 69.04; H, 5.55; N, 10.06 %. Found: C, 68.97; H, 5.51; N, 09.96 %; IR (KBr, cm^{-1}): 705 (C–S–C), 1339 (N–C), 1463 (C=C), 1531 (N=CH), 1665 (CO), 1431, 2836, 2899 (CH_2), 2941 (OCH_3), 3025 (CH–Ar), 3356 (NH); ^{1}H-NMR (300 MHz, $CDCl_3$, δ / ppm): 2.16–2.23 (2H, *m*, H-12), 3.20–3.28 (2H, *m*, H-13), 3.32 (3H, *s*, OCH_3), 4.12 (2H, *t*, *J* = 7.55 Hz, H-11), 5.73 (1H, *s*, H-1'), 8.15 (1H, *s*, H-14), 6.45–7.88 (12H, *m*, Ar–H); ^{13}C-NMR (75 MHz, $CDCl_3$, δ / ppm): 33.9 (C-12), 43.6 (C-13), 47.8 (CC-11), 52.0 (OCH_3), 115.4 (C-4 and C-5), 115.4 (C-1 and C--8), 120.7 (C-2 and C-7), 122.6 (C-3 and C-6), 124.3 (C-16), 125.4 (C-20), 126.0 (C-17), 126.8 (C-19), 127.5 (C-18), 138.6 (C-15), 141.0 (C-4a and 5a), 157.3 (C-1a and C-8a), 146.0 (C-14), 162.3 (C-2'); FAB–Mass (*m*/*z*): 417 [M^+].

N-*[(4-Methylphenyl)methylidene]*-N'-*[3-(10*H*-phenothiazin-10-yl)propyl]urea* (***3n***). Yield: 60 %; m.p. 141–142 °C; Anal. Calcd. for $C_{24}H_{23}N_3OS$: C, 71.79; H, 5.77; N, 10.46 %. Found: C, 71.69; H, 5.74; N, 10.37 %; IR (KBr, cm^{-1}): 699 (C–S–C), 1326 (N–C), 1460 (C=C), 1538 (N=CH), 1661 (CO), 1428, 2833, 2891 (CH_2), 2918 (CH_3), 3019 (CH–Ar), 3339 (NH); ^{1}H-NMR (300 MHz, $CDCl_3$, δ / / ppm): 2.11–2.19 (2H, *m*, H-12), 1.96 (3H, *s*, CH_3), 3.17–3.24 (2H, *m*, H-13), 4.06 (2H, *t*, *J* = 7.50 Hz, H-11), 5.82 (1H, *s*, H-1'), 8.14 (1H, *s*, H-14), 6.42-7.83 (12H, *m*, Ar-H); ^{13}C-NMR (75 MHz, $CDCl_3$, δ / ppm): 23.2 (CH_3), 33.0 (C-12), 45.5 (C-13), 51.8 (C-11), 112.9 (C-4 and C-5), 115.3 (C-1 and C-8), 120.4 (C-2 and C-7), 121.2 (C-3 and C-6), 123.4 (C-16 and C-20), 125.2 (C-17 and C-19), 126.3 (C-18), 135.4 (C-15), 136.3 (C-4a and C-5a), 145.9 (C-1a and C-8a), 151.0 (C-14), 162.3 (C-2'); FAB mass (*m*/*z*): 401 [M^+].

N-*[(3-Methylphenyl)methylidene]*-N'-*[3-(10*H-*phenothiazin-10-yl)propyl]urea* ***(3o)***. Yield: 61 %; m.p. 139–140 °C; Anal. for Calcd. $C_{24}H_{23}N_3OS$: C, 71.79; H, 5.77; N, 10.46 %. Found: C, 71.71; H, 5.69; N, 10.41 %; IR (KBr, cm^{-1}): 701 (C–S–C), 1323 (N–C), 1465 (C=C), 1536 (N=CH), 1663 (CO), 1425, 2838, 2892 (CH_2), 2920 (CH_3), 3014 (CH–Ar), 3354 (NH); ^{1}H-NMR (300 MHz, $CDCl_3$, δ / / ppm): 2.15–2.19 (2H, *m*, H-12), 2.01 (3H, *s*, CH_3), 3.21–3.29 (2H, *m*, H-13), 4.04 (2H, *t*, J = 7.45 Hz, H-11), 5.78 (1H, *s*, H-1'), 8.22 (1H, *s*, H-14), 6.41–7.81 (12H, *m*, Ar–H); ^{13}C-NMR (75 MHz, $CDCl_3$, δ / ppm): 24.0 (CH_3), 34.0 (C-12), 45.2 (C-13), 47.1 (C-11), 113.5 (C-4 and C-5), 116.6 (C-1 and C-8), 119.4 (C-2 and C-7), 122.4 (C-3 and C-6), 123.8 (C-16), 124.2 (C-20), 124.7 (C-17 and C--19), 126.7 (C-18), 139.4 (C-15), 142.3 (C-4a and C-5a), 146.8 (C-1a and C-8a), 148.0 (C-14), 162.2 (C-2'); FAB mass (*m*/*z*): 401 [M^+].

N-*[(2-Methylphenyl)methylidene]*-N'-*[3-(10*H-*phenothiazin-10-yl)propyl]urea* ***(3p)***. Yield: 62 %; m.p. 136–138 °C; Anal. Calcd. for $C_{24}H_{23}N_3OS$: C, 71.79; H, 5.77; N, 10.46 %. Found: C, 71.69; H, 5.67; N, 10.42 %; IR (KBr, cm^{-1}): 695 (C–S–C), 1323 (N–C), 1467 (C=C), 1531 (N=CH), 1665 (CO), 1426, 2830, 2894 (CH_2), 2910 (CH_3), 3017 (CH–Ar), 3345 (NH); ^{1}H-NMR (300 MHz, $CDCl_3$, δ / / ppm): 2.13–2.18 (2H, *m*, H-12), 2.05 (3H, *s*, CH_3), 3.18–3.26 (2H, *m*, H-13), 4.00 (2H, *t*, J = 7.50 Hz, H-11), 5.79 (1H, *s*, H-1'), 8.34 (1H, *s*, H-14), 6.34–7.85 (12H, *m*, Ar-H); ^{13}C-NMR (75 MHz, $CDCl_3$, δ / ppm): 21.6 (CH_3), 32.2 (C-12), 43.9 (C-13), 48.6 (C-11), 113.7 (C-4 and C-5), 116.5 (C-1 and C-8), 121.4 (C-2 and C-7), 122.4 (C-3 and C-6), 123.6 (C-16), 125.3 (C-20), 126.4 (C-17), 127.5 (C-19), 128.3 (C-18), 137.7 (C-15), 139.4 (C-4a and C-5a), 143.7 (C-1a and C--8a), 152.0 (C-14), 160.5 (C-2'); FAB mass (*m*/*z*): 401 [M^+].

N-*[(4-Hydroxyphenyl)methylidene]*-N'-*[3-(10*H-*phenothiazin-10-yl)propyl]-urea* ***(3q)***. Yield: 64 %; m.p. 162–164 °C; Anal. Calcd. for $C_{23}H_{21}N_3O_2S$: C, 68.46; H, 5.24; N, 10.41 %. Found: C, 68.41; H, 5.22; N, 10.35 %; IR (KBr, cm^{-1}): 702 (C–S–C), 1337 (N–C), 1468 (C=C), 1555 (N=CH), 1670 (CO), 1435, 2841, 2898 (CH_2), 3027 (CH–Ar), 3357 (NH), 3468 (OH); ^{1}H-NMR (300 MHz, $CDCl_3$, δ / ppm): 2.29–2.36 (2H, *m*, H-12), 3.07–3.14 (2H, *m*, H-13), 4.84 (1H, *s*, OH), 4.14 (2H, *t*, J = 7.45 Hz, H-11), 5.75 (1H, *s*, H-1'), 8.26 (1H, *s*, H-14), 6.52–7.79 (12H, *m*, Ar–H); ^{13}C-NMR (75 MHz, $CDCl_3$, δ / ppm): 32.4 (C-12), 43.6 (C-13), 51.3 (C-11), 114.7 (C-4 and C-5), 116.4 (C-1 and C-8), 121.6 (C-2 and C-7), 122.2 (C-3 and C-6), 124.6 (C-16 and C-20), 126.1 (C-17 and C-19), 127.4 (C-18), 136.5 (C-15), 137.2 (C-4a and C-5a), 154.6 (C-1a and C-8a), 146.0 (C-14), 157.0 (C-2'); FAB mass (*m*/*z*): 403 [M^+].

N-*[(3-Hydroxyphenyl)methylidene]*-N'-*[3-(10*H-*phenothiazin-10-yl)propyl]-urea* ***(3r)***. Yield: 60 % ; m.p. 166–167 °C; Anal. Calcd. for $C_{23}H_{21}N_3O_2S$: C, 68.46; H, 5.24; N, 10.41 %. Found: C, 68.32; H, 5.16; N, 10.38 %; IR (KBr, cm^{-1}): 706 (C–S–C), 1336 (N–C), 1465 (C=C), 1551 (N=CH), 1673 (CO), 1431, 2844, 2895 (CH_2), 3029 (CH–Ar), 3352 (NH), 3458 (OH); ^{1}H-NMR (300 MHz, $CDCl_3$,

δ / ppm): 2.31–2.36 (2H, *m*, H-12), 3.16–3.21 (2H, *m*, H-13), 4.78 (1H, *s*, OH), 4.20 (2H, *t*, *J* = 7.45 Hz, H-11), 5.81 (1H, *s*, H-1'), 7.99 (1H, *s*, H-14), 6.32–7.79 (m, 12H, Ar–H); ^{13}C NMR (75 MHz, $CDCl_3$, δ / ppm): 32.2 (C-12), 43.0 (C-13), 48.2 (C-11), 115.4 (C-4 and C-5), 1 19.5 (C-1 and C-8), 120.4 (C-2 and C-7), 123.7 (C-3 and C-6), 12 5.6 (C-16), 126.2 (C-20), 126.5 (C-17 and C-19), 129.7 (C-18), 135.6 (C-15), 139.2 (C-4a and C- 5a), 154.6 (C-1a and C-8a), 149.0 (C - -14), 155.7 (C-2'); FAB mass (*m*/z): 403 [M^+].

N-*[(2-Hydroxyphenyl)methylidene]*-N'-*[3-(10*H-phenothiazin-10-yl)propyl]-urea ***(3s)***. Yield: 62 % ; m.p. 160–162 °C; Anal. Calcd. for $C_{23}H_{21}N_3O_2S$: C, 68.46; H, 5.24; N, 10.41 %. Found: C, 68.33; H, 5.15; N, 10.37 %; IR (KBr, cm^{-1}): 703 (C–S–C), 1335 (N–C), 1473 (C=C), 1541 (N=CH), 1669 (CO), 1437, 2842, 2900 (CH_2), 3024 (CH–Ar), 3345 (NH), 3458 (OH); ^{1}H-NMR (300 MHz, $CDCl_3$, δ / ppm): 2.26–2.31 (2H, *m*, H-12), 3.14–3.19 (2H, *m*, H-13), 4.57 (1H, *s*, OH), 4.15 (2H, *t*, *J* = 7.45 Hz, H-11), 5.76 (1H, *s*, H-1'), 7.84 (1H, *s*, H-14), 6.35–7.85 (12H, *m*, Ar–H); ^{13}C-NMR (75 MHz, $CDCl_3$, δ / ppm): 32.4 (C-12), 42.3 (C-13), 49.4 (C-11), 114.2 (C-4 and C-5), 117.5 (C-1 and C-8), 122.4 (C-2 and C-7), 124.5 (C-3 and C-6), 126.3 (C-16), 126.9 (C-20), 127.4 (C-17), 128.4 (C-19), 130.3 (C-18), 138.6 (C-15), 143.5 (C-4a and C-5a), 154. 0 (C-1a and C- -8a), 152.0 (C-14), 157.2 (C-2'); FAB mass (*m*/z): 403 [M^+].

4-Oxo-N-*[3-(10*H-phenothiazin-10-yl)propyl]-2-phenyl-3-thiazolidinecarboxamide ***(4a)***. Yield: 64 %; m.p. 155–157 °C; Anal. Calcd. for $C_{25}H_{23}N_3O_2S_2$: C, 65.04; H, 5.02; N, 9.10 %. Found: C, 64.97; H, 4.93; N, 9.02 %; IR (KBr, cm^{-1}): 680 (C–S–C), 1330 (C–NH), 1457 (C=C), 1558, 1662 (CO), 1738 (CO cyclic), 1434, 2836, 2912 (CH_2), 2936 (S–CH_2), 3012 (CH–Ar), 3352 (NH); ^{1}H-NMR (300 MHz, $CDCl_3$, δ / ppm): 2.20–2.24 (2H, *m*, H-12), 3.43 (2H, *s*, H-5"), 3.35– –3.41 (2H, *m*, H-13), 4.24 (2H, *t*, *J* = 7.55 Hz, H-11), 5. 31 (1H, *s*, H-2"), 5.82 (1H, *s*, H-1'), 6.25–7.86 (13H, *m*, Ar–H); ^{13}C-NMR (75 MHz, $CDCl_3$, δ / ppm): 37.9 (C-12), 41.4 (C-5"), 46.6 (C-13), 51.7 (C-11), 63.2 (C-2"), 112.0 (C-4 and C-5), 119.7 (C-1 and C-8), 122.3 (C-2 and C-7), 123.7 (C-3 and C-6), 125.5 (C- -15 and C-19), 127.9 (C-16 and C-18), 128.4 (C-17), 137.9 (C-14), 138.7 (C-4a and C-5a), 145.0 (C-1a and C-8a), 162.2 (C-2'), 172.3 (C-4"); FAB mass (*m*/z): 462 [M^+].

2-(4-Chlorophenyl)-4-oxo-N-*[3-(10*H-phenothiazin-10-yl)propyl]-3-thiazolidinecarboxamide ***(4b)***. Yield: 71 %; m.p. 180–182 °C; Anal. Calcd. for $C_{25}H_{22}ClN_3O_2S_2$: C, 60.59; H, 4.4 7; N, 8.48 %. Found: C, 60.53; H, 4.43; N, 8.44 %; IR (KBr, cm^{-1}): 715 (C–S–C), 768 (C–Cl), 1340 (C–NH), 1462 (C=C), 1667 (CO), 1752 (CO cyclic), 1440, 2850, 2917 (CH_2), 2948 (S–CH_2), 3016 (CH–Ar), 3358 (NH); ^{1}H-NMR (300 MHz, $CDCl_3$, δ / ppm): 2.34–2.38 (2H, *m*, H-12), 3.68 (2H, *s*, H-5"), 3.44–3.49 (2H, *m*, H-13), 4.31 (2H, *t*, *J* = 7.45 Hz, H- -11), 5.39 (1H, *s*, H-2"), 5.90 (1H, *s*, H-1'), 6.44–8.05 (12H, *m*, Ar–H); ^{13}C- -NMR (75 MHz, $CDCl_3$, δ / ppm): 40.1 (C-12), 3 8.0 (C-5"), 48.3 (C-13), 55.5

(C-11), 59.0 (C-2”), 113.0 (C-4 and C-5), 121.1 (C-1 and C-8), 125.5 (C-2 and C-7), 126.5 (C-3 and C-6), 128.8 (C-15 and C-19), 129.4 (C-16 and C-18), 130.4 (C-17), 140.5 (C-14), 141.6 (C-4a and C-5a), 147.0 (C-1a and C-8a), 167.8 (C-2’), 176.5 (C-4”); FAB mass (*m*/*z*): 496 [M^+].

2-(3-Chlorophenyl)-4-oxo-N-*[3-(10*H*-phenothiazin-10-yl)propyl]-3-thiazolidinecarboxamide* ***(4c)***. Yield: 69 %; m.p. 178–179 °C; Anal. Calcd. for $C_{25}H_{22}ClN_3O_2S_2$: C, 60.59; H, 4.47; N, 8.48 %. Found: C, 60.53; H, 4.43; N, 8.41 %; IR (KBr, cm $^{-1}$): 687, 716 (C–S–C), 752 (C–Cl), 1343 (C–N), 1463 (C=C), 1670 (CO), 1750 (CO cyclic), 1444, 2836, 2918 (CH_2), 2954 (S–CH_2), 3027 (CH–Ar), 3362 (NH); ^{1}H-NMR (300 MHz, C DCl_3, δ / ppm): 2.35–2.40 (2H, *m*, H-12), 3.57 (2H, *s*, H-5”), 3.45–3.50 (2H, *m*, H-13), 4.37 (2H, *t*, J = 7.55 Hz, H-11), 5.57 (1H, *s*, H-2”), 5.92 (1H, *s*, H-1’), 6.32–7.65 (12H, *m*, Ar–H); ^{13}C-NMR (75 MHz, C DCl_3, δ / ppm): 40.4 (C-12), 32.0 (C-5”), 49.4 (C-13), 55.6 (C-11), 59.0 (C-2”), 115.0 (C-4 and C-5), 122.3 (C-1 and C-8), 125.5 (C-2 and C-7), 126.9 (C-3 and C-6), 130.3 (C-15), 131.2 (C-19), 132.1 (C-16), 132.7 (C-18), 133.7 (C-17), 141.5 (C-14), 142.6 (C-4a and C-5a), 146.0 (C-1a and C-8a), 163.6 (C-2’), 178.8 (C-4”); FAB mass (*m*/*z*): 496 [M^+].

2-(2-Chlorophenyl)-4-oxo-N-*[3-(10*H*-phenothiazin-10-yl)propyl]-3-thiazolidinecarboxamide* ***(4d)***. Yield: 68 %; m.p. 176–177 °C; Anal. Calcd. for $C_{25}H_{22}ClN_3O_2S_2$: C, 60.59; H, 4.47; N, 8.48 %. Found: C, 60.53; H, 4.43; N, 8.44 %; IR (KBr, cm $^{-1}$): 689, 710 (C–S–C), 760 (C–Cl), 1347 (C–N), 1472 (C=C), 1673 (CO), 1755 (CO cyclic), 1447, 2844, 2922 (CH_2), 2950 (S–CH_2), 3022 (CH–Ar), 3360 (NH); ^{1}H-NMR (300 MHz, C DCl_3, δ / ppm): 2.40–2.46 (2H, *m*, H-12), 3.61 (2H, *s*, H-5”), 3.41–3.47 (2H, *m*, H-13), 4.33 (2H, *t*, J = 7.40 Hz, H-11), 5.46 (1H, *s*, H-2”), 5.94 (1H, *s*, H-1’), 6.51–7.92 (12H, *m*, Ar–H); ^{13}C-NMR (75 MHz, C DCl_3, δ / ppm): 41.7 (C-12), 36.0 (C-5”), 46.3 (C-13), 53.1 (C-11), 61.0 (C-3”), 113.0 (C-4 and C-5), 119.7 (C-1 and C-8), 126.5 (C-2 and C-7), 127.2 (C-3 and C-6), 131.4 (C-15), 131.8 (C-19), 132.8 (C-16), 133.0 (C-18), 133.6 (C-17), 138.9 (C-14), 143.7 (C-4a and C-5a), 147.0 (C-1a and C-8a), 167.9 (C-2’), 175.0 (C-4”); FAB mass (*m*/*z*): 496 [M^+].

2-(4-Bromophenyl)-4-oxo-N-*[3-(10*H*-phenothiazin-10-yl)propyl]-3-thiazolidinecarboxamide* ***(4e)***. Yield: 70 %; m.p. 173–174 °C; Anal. Calcd. for $C_{25}H_{22}BrN_3O_2S_2$: C, 55.55; H, 4.10; N, 7.77 %. Found: C, 55.43; H, 4.04; N, 7.71 %; IR (KBr, cm^{-1}): 709 (C–S–C), 755 (C–Cl), 1338 (C–NH), 1466 (C=C), 1674 (CO), 1758 (CO cyclic), 1448, 2845, 2924 (CH_2), 2949 (S–CH_2), 3018 (CH–Ar), 3365 (NH); ^{1}H-NMR (300 MHz, $CDCl_3$, δ / ppm): 2.41–2.46 (2H, *m*, H-12), 3.51 (2H, *s*, H-5”), 3.47–3.53 (2H, *m*, H-13), 4.45 (2H, *t*, J = 7.45 Hz, H-11), 5.36 (1H, *s*, H-2”), 5.95 (1H, *s*, H-1’), 6.39–7.81 (12H, *m*, Ar–H); ^{13}C-NMR (75 MHz, $CDCl_3$, δ / ppm): 41.8 (C-12), 37.6 (C-5”), 46.3 (C-13), 53.4 (C-11), 62.6 (C-2”), 114.0 (C-4 and C-5), 121.3 (C-1 and C-8), 123.8 (C-2 and C-7), 124.6 (C-3 and C-6), 128.4 (C-15 and C-19), 130.3 (C-16 and C-18), 131.8

(C-17), 141.9 (C-14), 142.8 (C-4a and C- 5a), 148.0 (C-1a and C-8a), 164.0 (C - -2'), 176.0 (C-4"); FAB mass (*m*/*z*): 541 [M^+].

2-(3-Bromophenyl)-4-oxo-N-*[3-(10*H*-phenothiazin-10-yl)propyl]-3-thiazolidinecarboxamide* (***4f***). Yield: 69 %; m.p. 168–170 °C; Anal. Calcd. for $C_{25}H_{22}BrN_3O_2S_2$: C, 55.55; H, 4.10; N, 7.77 %. Found: C, 55 .45; H, 4.06; N, 7.72 %; IR (KBr, cm^{-1}): 705 (C–S–C), 749 (C–Cl), 1350 (C–N), 1467 (C=C), 1678 (CO), 1746 (CO cyclic), 1450, 2843, 2923 (CH_2), 2947 (S–CH_2), 3025 (CH–Ar), 3359 (NH); ^{1}H-NMR (300 MHz, $CDCl_3$, δ / ppm): 2.35–2.42 (2H, *m*, H-12), 3.49 (2H, *s*, H-5"), 3.45–3.51 (2H, *m*, H-13), 4.38 (2H, *t*, *J* = 7.60 Hz, H- -11), 5.62 (1H, *s*, H-2"), 5.98 (1H, *s*, H-1'), 6.25–7.79 (12H, *m*, Ar–H); ^{13}C- -NMR (75 MHz, $CDCl_3$, δ / ppm): 43.9 (C-12), 3 5.4 (C-5"), 48.6 (C-13), 5 4.1 (C-11), 64.3 (C-2"), 113.0 (C-4 and C-5), 121.7 (C-1 and C-8), 1 23.2 (C-2 and C-7), 124.3 (C-3 and C-6), 129.4 (C-15), 129.8 (C-19), 130.7 (C-16), 130.9 (C- -18), 131.3 (C-17), 139.1 (C-14), 140.9 (C-4a and C-5a), 148.0 (C-1a and C-8a), 165.5 (C-2'), 174.3 (C-4"); FAB mass (*m*/*z*): 541 [M^+].

2-(2-Bromophenyl)-4-oxo-N-*[3-(10*H*-phenothiazin-10-yl)propyl]-3-thiazolidinecarboxamide* (***4g***). Yield: 67 % ; m.p. 163–164 °C, Anal. Calcd. for $C_{25}H_{22}BrN_3O_2S_2$: C, 55.55; H, 4.10; N, 7.77 %. Found: C, 55 .43; H, 4.03; N, 7.73 %; IR (KBr, cm^{-1}): 702 (C–S–C), 748 (C–Cl), 1341 (C–N), 1468 (C=C), 1671 (CO), 1752 (CO cyclic), 1452, 2847, 2919 (CH_2), 2951 (S–CH_2), 3024 (CH–Ar), 3356 (NH); ^{1}H-NMR (300 MHz, $CDCl_3$, δ / ppm): 2.39–2.43 (2H, *m*, H-12), 3.34 (2H, *s*, H-5"), 3.42–3.48 (2H, *m*, H-13), 4.40 (2H, *t*, *J* = 7.50 Hz, H- -11), 5.51 (1H, *s*, H-2"), 5.93 (1H, *s*, H-1'), 6.35–7.92 (12H, *m*, Ar–H); ^{13}C- -NMR (75 MHz, $CDCl_3$, δ / ppm): 32.3 (C-12), 3 7.0 (C-5"), 45.1 (C-13), 4 9.2 (C-11), 65.1 (C-2"), 114.0 (C-4 and C-5), 120.2 (C-1 and C-8), 1 26.4 (C-2 and C-7), 127.2 (C-3 and C-6), 130.8 (C-15), 131.4 (C-19), 131.9 (C-16), 132.2 (C- -18), 132.8 (C-17), 139.1 (C-14), 140.6 (C-4a and C-5a), 145.0 (C-1a and C-8a), 166.7 (C-2'), 171.4 (C-4"); FAB mass (*m*/*z*): 541 [M^+].

2-(4-Nitrophenyl)-4-oxo-N-*[3-(10*H*-phenothiazin-10-yl)propyl]-3-thiazolidinecarboxamide* (***4h***). Yield: 74 % ; m.p. 167–168 °C; Anal. Calcd. for $C_{25}H_{22}N_4O_4S_2$: C, 59.27; H, 4.37; N, 11.05 %. Found: C, 59.1 8; H, 4.32; N, 10.99 %; IR (cm^{-1}): 692 (C–S–C), 870 (C–NO), 1324 (C–N), 1540 (N=O), 1464 (C=C), 1672 (CO), 1748 (CO cyclic), 1453, 2841, 2921 (CH_2), 2955 (S–CH_2), 3019 (CH–Ar), 336 1 (NH); ^{1}H-NMR (300 MHz, C DCl_3, δ / pp m): 2.41–2.45 (2H, *m*, H-12), 3.52 (2H, *s*, H-5"), 3.50–3.57 (2H, *m*, H-13), 4.36 (2H, *t*, *J* = 7.55 Hz, H-11), 5 .39 (1H, *s*, H-2"), 6.01 (1H, *s*, H-1'), 6.45–7 .94 (12H, *m*, Ar–H); ^{13}C-NMR (75 MHz, C DCl_3, δ / pp m): 42.2 (C-12), 37.6 (C-5"), 47.5 (C-13), 56.6 (C-11), 63.0 (C-2"), 116.0 (C-4 and C-5), 122.0 (C-1 and C-8), 126.8 (C-2 and C-7), 127.6 (C-3 and C-6), 131.5 (C-15 and C-19), 132.7 (C-16 and C-18), 133.1 (C-17), 140.2 (C-14), 141.6 (C-4a and C-5a), 149.0 (C-1a and C-8a), 164.4 (C-2'), 162.2 (C-4"); FAB mass (*m*/*z*): 507 [M^+].

2-(3-Nitrophenyl)-4-oxo-N-*[3-(10*H*-phenothiazin-10-yl)propyl]-3-thiazolidinecarboxamide* ***(4i)***. Yield: 72 % ; m.p. 164–165 °C; Anal. Calcd. for $C_{25}H_{22}N_4O_4S_2$: C, 59.27; H, 4.37; N, 11.05 %. Found: C, 59.18; H, 4.32; N, 10.99 %; IR (KBr, cm^{-1}): 698 (C–S–C), 865 (C–NO), 1324 (C–N), 1545 (N=O), 1470 (C=C), 1679 (CO), 1752 (CO cyclic), 1454, 2840, 2925 (CH_2), 2945 (S–CH_2), 3024 (CH–Ar), 3363 (NH); ^{1}H-NMR (300 MHz, $CDCl_3$, δ / ppm): 2.32–2.37 (2H, *m*, H-12), 3.64 (2H, *s*, H-5”), 3.46–3.52 (2H, *m*, H-13), 4.42 (2H, *t*, *J* = 7.45 Hz, H-11), 5.69 (1H, *s*, H-2”), 6.00 (1H, *s*, H-1’), 6.35–7.84 (12H, *m*, Ar-H); ^{13}C-NMR (75 MHz, $CDCl_3$, δ / ppm): 43.3 (C-12), 38.6 (C-5”), 47.9 (C-13), 54.8 (C-11), 63.4 (C-2”), 116.0 (C-4 and C-5), 119.6 (C-1 and C-8), 124.8 (C-2 and C-7), 125.7 (C-3 and C-6), 131.6 (C-15), 130.5 (C-19), 129.1 (C-16), 129.7 (C-18), 130.4 (C-17), 141.7 (C-14), 142.7 (C-4a and C-5a), 148.0 (C-1a and C-8a), 165.4 (C-2’), 173.0 (C-4”); FAB mass (*m*/*z*): 507 [M^+].

2-(2-Nitrophenyl)-4-oxo-N-*[3-(10*H*-phenothiazin-10-yl)propyl]-3-thiazolidinecarboxamide* ***(4j)***. Yield: 73 % ; m.p. 162–163 °C; Anal. Calcd. for $C_{25}H_{22}N_4O_4S_2$: C, 59.27; H, 4.37; N, 11.05 %. Found: C, 59.19; H, 4.34; N, 10.97 %; IR (KBr, cm^{-1}): 655 (C–S–C), 1325 (C–N), 1489 (C=C), 1496 (N=O), 1680 (CO), 1745 (CO cyclic), 1446, 2851, 2924 (CH_2), 2948 (S–CH_2), 3020 (CH–Ar), 3362 (NH); ^{1}H-NMR (300 MHz, $CDCl_3$, δ / ppm): 2.35–2.41 (2H, *m*, H-12), 3.38 (2H, *s*, H-5”), 3.41–3.46 (2H, *m*, H-13), 4.37 (2H, *t*, *J* = 7.50 Hz, H-11), 5.26 (1H, *s*, H-2”), 5.93 (1H, *s*, H-1’), 6.29–7.97 (12H, *m*, Ar–H); ^{13}C-NMR (75 MHz, $CDCl_3$, δ / ppm): 41.0 (C-12), 42.9 (C-5”), 48.2 (C-13), 56.4 (C-11), 63.6 (C-2”), 112.0 (C-4 and C-5), 120.3 (C-1 and C-8), 124.6 (C-2 and C-7), 125.9 (C-3 and C-6), 129.7 (C-15), 130.2 (C-19), 131.2 (C-16), 132.6 (C-18), 142.4 (C-17), 143.6 (C-14), 148.6 (C-4a and C-5a), 146.0 (C-1a and C-8a), 162.2 (C-2’), 163.4 (C-4”); FAB mass (*m*/*z*): 507 [M^+].

2-(4-Methoxyphenyl)-4-oxo-N-*[3-(10*H*-phenothiazin-10-yl)propyl]-3-thiazolidinecarboxamide* ***(4k)***. Yield: 66 %; m.p. 157–159 °C; Anal. Calcd. for $C_{26}H_{25}N_3O_3S_2$: C, 63.51; H, 5.12; N, 8.54 %. Found: C, 63.38; H, 5.08; N, 8.49 %; IR (KBr, cm^{-1}): 688 (C–S–C), 1065 (C–O), 1331 (C–N), 1458 (C=C), 1664 (CO), 1729 (CO cyclic), 1435, 2837, 2913 (CH_2), 2949 (S–CH_2), 2958 (OCH_3), 3014 (CH–Ar), 3354 (NH); ^{1}H-NMR (300 MHz, $CDCl_3$, δ / ppm): 2.29–2.33 (2H, *m*, H-12), 3.39 (2H, *s*, H-5”), 3.42–3.47 (2H, *m*, H-13), 3.56 (3H, *s*, OCH_3), 4.27 (2H, *t*, *J* = 7.45 Hz, H-11), 5.42 (1H, *s*, H-2”), 5.85 (1H, *s*, H-1’), 6.36–7.85 (12H, *m*, Ar–H); ^{13}C-NMR (75 MHz, $CDCl_3$, δ / ppm): 39.5 (C-12), 38.0 (C-5”), 45.7 (C-13), 52.4 (C-11), 60.3 (C-2”), 52.0 (OCH_3), 116.0 (C-4 and C-5), 118.1 (C-1 and C-8), 122.3 (C-2 and C-7), 123.4 (C-3 and C-6), 126.5 (C-15 and C-19), 128.5 (C-16 and C-18), 129.7 (C-17), 138.4 (C-14), 142.4 (C-4a and C-5a), 158.0 (C-1a and C-8a), 163.9 (C-2’), 162.0 (C-4”); FAB mass (*m*/*z*): 492 [M^+].

2-(3-Methoxyphenyl)-4-oxo-N-*[3-(10*H*-phenothiazin-10-yl)propyl]-3-thiazolidinecarboxamide* ***(4l)***. Yield: 64 %; m.p. 154–155 °C; Anal. Calcd. for

$C_{26}H_{25}N_3O_3S_2$: C, 63.51; H, 5.12; N, 8.54 %. Found: C, 63.37; H, 5.05; N, 8.44 %; IR (KBr, cm^{-1}): 688 (C–S–C), 1028 (C–O), 1336 (C–N), 1453 (C=C), 1669 (CO), 1752 (CO cyclic), 1433, 2838, 2911 (CH_2), 2948 (S–CH_2), 2951 (OCH_3), 3015 (CH–Ar), 3359 (NH); ^{1}H-NMR (300 MHz, C DCl_3, δ / ppm): 2.25–2.30 (2H, *m*, H-12), 3.46 (2H, *s*, H-5"), 3.45–3.49 (2H, *m*, H-13), 3.49 (3H, *s*, OCH_3), 4.28 (2H, *t*, *J* = 7.45 Hz, H-11), 5.33 (1H, *s*, H-2"), 5.88 (1H, *s*, H-1'), 6.52–7.84 (12H, *m*, Ar–H); ^{13}C-NMR (75 MHz, $CDCl_3$, δ / ppm): 38.4 (C-12), 34.0 (C-5"), 44.8 (C-13), 52.1 (C-11), 59.6 (C-2"), 54.3 (OCH_3), 118.2 (C-4 and C-5), 120.4 (C-1 and C-8), 123.9 (C-2 and C-7), 124.6 (C-3 and C-6), 126.8 (C-15), 128.4 (C-19), 129.4 (C-16), 131.1 (C-18), 132.4 (C-17), 137.3 (C-14), 144.1 (C-4a and C-5a), 156.0 (C-1a and C-8a), 159.9 (C-2'), 161.0 (C-4"); FAB mass (*m*/*z*): 492 [M^+].

2-(2-Methoxyphenyl)-4-oxo-N-*[3-(10*H*-phenothiazin-10-yl)propyl]-3-thiazolidinecarboxamide* (***4m***). Yield: 61 % ; m.p. 156–158 °C; An al. Calcd. for $C_{26}H_{25}N_3O_3S_2$: C, 63.51; H, 5.12; N, 8.54 %. Found: C, 63.42; H, 5.09; N, 8.51 %; IR (KBr, cm^{-1}): 687 (C–S–C), 1055 (C–O), 1335 (C–N), 1455 (C=C), 1663 (CO), 1725 (CO cyclic), 1438, 2834, 2919 (CH_2), 2943 (S–CH_2), 2945 (OCH_3), 3016 (CH–Ar), 3350 (NH); ^{1}H-NMR (300 MHz, C DCl_3, δ / ppm): 2.21–2.27 (2H, *m*, H-12), 3.35 (2H, *s*, H-5"), 3.39–3.45 (2H, *m*, H-13), 3.52 (3H, *s*, OCH_3), 4.24 (2H, *t*, *J* = 7.45 Hz, H-11), 5.21 (1H, *s*, H-2"), 5.80 (1H, *s*, H-1'), 6.46–7.86 (12H, *m*, Ar–H); ^{13}C-NMR (75 MHz, $CDCl_3$, δ / ppm): 37.3 (C-12), 33.1 (C-5"), 43.9 (C-13), 53.6 (C-11), 61.2 (C-2"), 56.2 (OCH_3), 119.0 (C-4 and C-5), 120.3 (C-1 and C-8), 121.6 (C-2 and C-7), 125.7 (C-3 and C-6), 127.5 (C-15), 129.2 (C-19), 130.4 (C-16), 131.5 (C-18), 133.8 (C-17), 140.3 (C-14), 146.1 (C-4a and C-5a), 155.0 (C-1a and C-8a), 162.4 (C-2'), 161.2 (C-4"); FAB mass (*m*/*z*): 492 [M^+].

2-(4-Methylphenyl)-4-oxo-N-*[3-(10*H*-phenothiazin-10-yl)propyl]-3-thiazolidinecarboxamide* (***4n***). Yield: 68 % ; m.p. 148–151 °C; Anal. Calcd. for $C_{26}H_{25}N_3O_2S_2$: C, 65.65; H, 5.29; N, 8.83 %. Found: C, 65.48; H, 5.22; N, 8.73 %; IR (KBr, cm^{-1}): 672 (C–S–C), 1326 (C–N), 1456 (C=C), 1660 (CO), 1728 (CO cyclic), 1433, 2835, 2910 (CH_2), 2942 (S–CH_2), 3011 (CH–Ar), 2898 (CH_3), 3350 (NH); ^{1}H-NMR (300 MHz, $CDCl_3$, δ / ppm): 2.02 (3H, *s*, CH_3), 2.20–2.24 (2H, *m*, H-12), 3.49 (2H, *s*, H-5"), 3.39–3.45 (2H, *m*, H-13), 4.21 (2H, *t*, *J* = 7.40 Hz, H-11), 5.64 (1H, *s*, H-2"), 5.80 (1H, *s*, H-1'), 6.35–7.90 (12H, *m*, Ar–H); ^{13}C-NMR (75 MHz, $CDCl_3$, δ / ppm): 20.5 (CH_3), 38.1 (C-12), 33.5 (C--5"), 43.3 (C-13), 51.1 (C-11), 63.0 (C-2"), 117.0 (C-4 and C-5), 118.7 (C-1 and C-8), 122.1 (C-2 and C-7), 123.2 (C-3 and C-6), 124.8 (C-15 and C-19), 127.4 (C-16 and C-18), 128.5 (C-17), 137.6 (C-14), 138.5 (C-4a and C-5a), 149.0 (C-1a and C-8a), 161.7 (C-2'), 160.0 (C-4"); FAB mass (*m*/*z*): 476 [M^+].

2-(3-Methylphenyl)-4-oxo-N-*[3-(10*H*-phenothiazin-10-yl)propyl]-3-thiazolidinecarboxamide* (***4o***). Yield: 66 % ; m.p. 147–148 °C; Anal. Calcd. for

$C_{26}H_{25}N_3O_2S_2$: C, 65.65; H, 5.29; N, 8.83 %. Found: C, 65.46; H, 5.20; N, 8.75 %; IR (KBr, cm^{-1}): 679 (C–S–C), 1325 (C–N), 1458 (C=C), 1663 (CO), 1727 (CO cyclic), 1439, 2833, 2917 (CH_2), 2945 (S–CH_2), 3017 (CH–Ar), 2888 (CH_3), 3353 (NH); ^{1}H-NMR (300 MHz, $CDCl_3$, δ / ppm): 1.95 (3H, *s*, CH_3), 2.23–2.27 (2H, *m*, H-12), 3.64 (2H, *s*, H-5"), 3.41–3.48 (2H, *m*, H-13), 4.24 (2H, *t*, *J* = 7.40 Hz, H-11), 5.39 (1H, *s*, H-2"), 5.87 (1H, *s*, H-1'), 6.35–7.82 (12H, *m*, Ar–H); ^{13}C-NMR (75 MHz, $CDCl_3$, δ / ppm): 23.8 (CH_3), 35.5 (C-12), 37.6 (C--5"), 44.7 (C-13), 55.6 (C-11), 62.0 (C-2"), 115.0 (C-4 and C-5), 119.5 (C-1 and C-8), 120.3 (C-2 and C-7), 124.8 (C-3 and C-6), 126.3 (C-15), 127.1 (C-19), 127.7 (C-16), 129.3 (C-18), 131.4 (C-17), 136.5 (C-14), 142.7 (C-4a and C-5a), 147.0 (C-1a and C-8a), 160.0 (C-2'), 161.4 (C-4"); FAB mass (*m*/*z*): 476 [M^+].

2-(2-Methylphenyl)-4-oxo-N-*[3-(10*H*-phenothiazin-10-yl)propyl]-3-thiazolidinecarboxamide* (***4p***). Yield: 64 % ; m.p. 144–145 °C; Anal. Calcd. for $C_{26}H_{25}N_3O_2S_2$: C, 65.65; H, 5.29; N, 8.83 %. Found: C, 65.40; H, 5.19; N, 8.71 %; IR (KBr, cm^{-1}): 681 (C–S–C), 1324 (C–N), 1457 (C=C), 1663 (CO), 1730 (CO cyclic), 1438, 2834, 2917 (CH_2), 2945 (S–CH_2), 3018 (CH–Ar), 2882 (CH_3), 3354 (NH); ^{1}H-NMR (300 MHz, $CDCl_3$, δ / ppm): 2.07 (3H, *s*, CH_3), 2.23–2.29 (2H, *m*, H-12), 3.39 (2H, *s*, H-5"), 3.33–3.38 (2H, *m*, H-13), 4.24 (2H, *t*, *J* = 7.40 Hz, H-11), 5.82 (1H, *s*, H-2"), 5.86 (1H, *s*, H-1'), 6.54–7.85 (12H, *m*, Ar–H); ^{13}C-NMR (75 MHz, $CDCl_3$, δ / ppm): 22.5 (CH_3), 35.6 (C-12), 37.5 (C--5"), 47.4 (C-13), 54.5 (C-11), 62.2 (C-2"), 117.0 (C-4 and C-5), 119.7 (C-1 and C-8), 121.5 (C-2 and C-7), 122.7 (C-3 and C-6), 126.4 (C-15), 127.4 (C-19), 128.5 (C-16), 129.8 (C-18), 131.1 (C-17), 136.5 (C-14), 139.4 (C-4a and C-5a), 150.0 (C-1a and C-8a), 161.1 (C-2'), 162.8 (C-4"); FAB mass (*m*/*z*): 476 [M^+].

2-(4-Hydroxyphenyl)-4-oxo-N-*[3-(10*H*-phenothiazin-10-yl)propyl]-3-thiazolidinecarboxamide* (***4q***). Yield: 62 %; m.p. 170–172 °C; Anal. Calcd. for $C_{25}H_{23}N_3O_3S_2$: C, 62.87; H, 4.85; N, 8.79 %. Found: C, 62.72; H, 4.81; N, 8.75 %; IR (KBr, cm^{-1}): 687 (C–S–C), 1332 (C–NH), 1460 (C=C), 1666 (CO), 1757 (CO cyclic), 1438, 2838, 2915 (CH_2), 2950 (S–CH_2), 3015 (CH–Ar), 3355 (NH), 3498 (OH); ^{1}H-NMR (300 MHz, $CDCl_3$, δ / ppm): 2.32–2.36 (2H, *m*, H-12), 3.39 (2H, *s*, H-5"), 3.44–3.50 (2H, *m*, H-13), 4.29 (2H, *t*, *J* = 7.45 Hz, H-8), 4.57 (1H, *s*, OH), 5.35 (1H, *s*, H-2"), 5.87 (1H, *s*, H-1'), 6.36–7.92 (12H, *m*, Ar–H); ^{13}C-NMR (75 MHz, $CDCl_3$, δ / ppm): 35.3 (C-12), 37.0 (C-5"), 46.6 (C-13), 52.3 (C-11), 62.0 (C-2"), 118.0 (C-4 and C-5), 119.7 (C-1 and C-8), 125.6 (C-2 and C-7), 127.2 (C-3 and C-6), 128.4 (C-15 and C-19), 130.2 (C-16 and C-18), 131.9 (C-17), 138.9 (C-14), 142.4 (C-4a and C-5a), 154.0 (C-1a and C-8a), 163.9 (C-2'), 162.3 (C-4"); FAB–Mass (*m*/*z*): 478 [M^+].

2-(3-Hydroxyphenyl)-4-oxo-N-*[3-(10*H*-phenothiazin-10-yl)propyl]-3-thiazolidinecarboxamide* (***4r***). Yield: 61 %; m.p. 168–170 °C; Anal. Calcd. for $C_{25}H_{23}N_3O_3S_2$: C, 62.87; H, 4.85; N, 8.79 %. Found: C, 62.75; H, 4.79; N, 8.73 %; IR (KBr, cm^{-1}): 689 (C–S–C), 1335 (C–NH), 1463 (C=C), 1668 (CO), 1752

(CO cyclic), 1434, 2838, 2913 (CH_2), 2957 (S–CH_2), 3013 (CH–Ar), 3358 (NH), 3504 (OH); ^{1}H-NMR (300 MHz, $CDCl_3$, δ / ppm): 2.36–2.41 (2H, *m*, H-12), 3.45 (2H, *s*, H-5"), 3.43–3.48 (2H, *m*, H-13), 4.32 (2H, *t*, *J* = 7.45 Hz, H-8), 4.50 (1H, *s*, OH), 5.52 (1H, *s*, H-2"), 5.84 (1H, *s*, H-1'), 6.36–7.78 (12H, *m*, Ar–H); ^{13}C-NMR (75 MHz, $CDCl_3$, δ / ppm): 32.2 (C-12), 37.6 (C-5"), 41.8 (C-13), 47.5 (C-11), 63.0 (C-2"), 116.0 (C-4 and C-5), 120.1 (C-1 and C-8), 124.7 (C-2 and C-7), 126.8 (C-3 and C-6), 130.3 (C-15), 131.2 (C-19), 132.7 (C-16), 133.4 (C-18), 134.2 (C-17), 140.5 (C-14), 146.8 (C-4a and C-5a), 153. 0 (C-1a and C--8a), 160.1 (C-2'), 162.1 (C-4"); FAB–Mass (*m*/*z*): 478 [M^+].

2-(2-Hydroxyphenyl)-4-oxo-N-*[3-(10*H*-phenothiazin-10-yl)propyl]-3-thiazolidinecarboxamide* (***4s***). Yield: 64 %; m.p. 171–172 °C; Anal. Calcd. for $C_{25}H_{23}N_3O_3S_2$: C, 62.87; H, 4.85; N, 8.79 %. Found: C, 62.81; H, 4.77; N, 8.69 %; IR (KBr, cm^{-1}): 697 (C–S–C), 1329 (C–NH), 1458 (C=C), 1664 (CO), 1751 (CO cyclic), 1432, 2835, 2918 (CH_2), 2953 (S–CH_2), 3019 (CH–Ar), 3351 (NH), 3505 (OH); ^{1}H-NMR (300 MHz, $CDCl_3$, δ / ppm): 2.30–2.35 (2H, *m*, H-12), 3.33 (2H, *s*, H-5"), 3.47–3.52 (2H, *m*, H-13), 4.35 (2H, *t*, *J* = 7.45 Hz, H-8), 4.52 (1H, *s*, OH), 5.45 (1H, *s*, H-2"), 5.91 (1H, *s*, H-1'), 6.38–7.83 (12H, *m*, Ar–H); ^{13}C-NMR (75 MHz, $CDCl_3$, δ / ppm): 36.1 (C-12), 37.6 (C-5"), 46.9 (C-13), 50.5 (C-11), 62.0 (C-2"), 114.0 (C-4 and C-5), 118.4 (C-1 and C-8), 123.8 (C-2 and C-7), 126.3 (C-3 and C-6), 129.5 (C-15), 130.1 (C-19), 130.4 (C-16), 131.4 (C-18), 134.5 (C-17), 140.6 (C-14), 141.5 (C-4a and C-5a), 154. 0 (C-1a and C--8a), 159.2 (C-2'), 162.0 (C-4"); FAB–Mass *(m/z):* 478 [M^+].

5-(Benzylidene)-4-oxo-N-*[3-(10*H*-phenothiazin-10-yl)propyl]-2-phenyl-3-thiazolidinecarboxamide* (***5a***). Yield: 64 %; m.p. 145–146 °C; Anal. Calcd. fo r $C_{32}H_{27}N_3O_2S_2$: C, 69.91; H, 4.95; N, 7.64 %. Found: C, 69.83; H, 4.91; N, 7.61 %; IR (KBr, cm^{-1}): 689 (C–S–C), 1335 (C–N), 1595 (C=C), 1467 (C=CH), 1673 (CO), 1740 (CO cyclic), 2987 (C=CH), 1444, 2845, 2921 (CH_2), 3028 (CH–Ar), 3371 (NH); ^{1}H-NMR (300 MHz, $CDCl_3$, δ / ppm): 2.18–2.22 (2H, *m*, H-12), 3.45–3.50 (2H, *m*, H-13), 4.33 (2H, *t*, *J* = 7.45 Hz, H-11), 5.2 5 (1H, *s*, H-2"), 5.90 (1H, *s*, H-1'), 6.45 (1H, *s*, H-20), 6.36–7.85 (18H, *m*, Ar–H); ^{13}C-NMR (75 MHz, $CDCl_3$, δ / ppm): 39.4 (C-12), 45.4 (C-13), 52.8 (C-11), 63.4 (C-2"), 114.0 (C-4 and C-5), 118.7 (C-1 and C-8), 123. 7 (C-2 and C-7), 124.9 (C-3 and C-6), 125.8 (C-15 and C-19), 126.9 (C-22 and C-26), 127.7 (C-16 and C-18), 128.6 (C--23 and C-25), 129.8 (C-17), 130.7 (C-24), 131.6 (C-14), 141.2 (C-5"), 134.8 (C--21), 139.9 (C-4a and C-5a), 136.0 (C-20), 148.0 (C-1a and C-8a), 163. 0 (C-2'), 168.6 (C-4"); FAB mass (*m*/*z*): 550 [M^+].

5-(4-Chlorobenzylidene)-2-(4-chlorophenyl)-4-oxo-N-*[3-(10*H*-phenothiazin--10-yl)propyl]-3-thiazolidinecarboxamide* (***5b***). Yield: 67 % ; m.p.160–162 °C; Anal. Calcd. for $C_{32}H_{25}Cl_2N_3O_2S_2$: C, 62.13; H, 4.07; N, 6.79 %. Found: C, 62.05; H, 4.01; N, 6.73 %; IR (KBr, cm^{-1}): 698, 755 (C–Cl), 1339 (C–N), 1625 (C=CH), 1683 (CO), 1748 (CO cy clic), 3012 (C=CH), 1445, 28 55, 2928 (CH_2),

3034 (CH–Ar), 3390 (NH); ^{1}H-NMR (300 MHz, C DCl$_3$, δ / ppm): 2.32–2.38 (2H, *m*, H-12), 3.65–3.70 (2H, *m*, H-13), 4.38 (2H, *t*, *J* = 7.50 Hz, H-11), 5.96 (1H, *s*, H-1'), 5.30 (1H, *s*, H-2"), 6.74 (1H, *s*, H-20), 6.41–8.15 (16H, *m*, Ar–H); ^{13}C-NMR (75 MHz, CDCl$_3$, δ / ppm): 42.6 (C-12), 146.3 (C-5"), 50.7 (C-13), 55.5 (C-11), 66.3 (C-2"), 115.0 (C-4 and C-5), 123.7 (C-1 and C-8), 126.4 (C-2 and C-7), 127.5 (C-3 and C-6), 128.7 (C-15 and C-19), 129.5 (C-22 and C-26), 130.1 (C-16 and C-18), 131.6 (C-23 and C-25), 132.2 (C-17), 133.5 (C-24), 134.0 (C-14), 139.7 (C-21), 140.0 (C-20), 142.3 (C-4a and C-5a), 146. 0 (C-1a and C-8a), 165.3 (C-2'), 172.2 (C-4"); FAB mass (*m*/*z*): 618 [M$^+$].

5-(3-Chlorobenzylidene)-2-(3-chlorophenyl)-4-oxo-N-*[3-(10*H*-phenothiazin--10-yl)propyl]-3-thiazolidinecarboxamide (**5c**)*. Yield: 66 % ; m.p. 158–159 °C; Anal. Calcd. for $C_{32}H_{25}Cl_2N_3O_2S_2$: C, 62.13; H, 4.07; N, 6.79 %. Found: C, 62.08; H, 4.03; N, 6.75 %; IR (KBr, cm^{-1}): 696 (C–S–C), 741 (C–Cl), 1342 (C–N), 1622 (C=CH), 1688 (CO), 1747 (CO cyclic), 3009 (C=CH), 1456, 2857 , 2932 (CH_2), 3034 (CH–Ar), 3386 (NH); ^{1}H-NMR (300 MHz, CDCl$_3$, δ / ppm): 2.35––2.40 (2H, *m*, H-12), 3.60–3.67 (2H, *m*, H-13), 4.40 (2H, *t*, *J* = 7.55 Hz, H-11), 6.00 (1H, *s*, H-1'), 5.32 (1H, *s*, H-2"), 6.72 (1H, *s*, H-20), 6.32–7.99 (16H, *m*, Ar–H); ^{13}C-NMR (75 MHz, CDCl$_3$, δ / ppm) δ: 43.3 (C-12), 146.3 (C-5"), 48.6 (C-13), 55.3 (C-11), 66.7 (C-2"), 113.0 (C-4 and C-5), 122. 3 (C-1 and C-8), 125.5 (C-2 and C-7), 126.6 (C-3 and C-6), 127.5 (C-15), 127.9 (C-19), 128.9 (C--22), 129.2 (C-26), 129. 4 (C-16), 129 .8 (C-18), 130.2 (C-23), 130.7 (C-25), 131.1 (C-17), 131.7 (C-24), 132.5 (C-14), 139.5 (C-21), 141.0 (C-20), 143.3 (C--4a and C-5a), 143. 0 (C-1a and C-8a), 168.2 (C-2'), 174.4 (C-4"); FAB mass (*m*/*z*): 618 [M$^+$].

5-(2-Chlorobenzylidene)-2-(2-chlorophenyl)-4-oxo-N-*[3-(10*H*-phenothiazin--10-yl)propyl]-3-thiazolidinecarboxamide (**5d**)*. Yield: 67 %; m.p. 156–157 °C; Anal. Calcd. for $C_{32}H_{25}Cl_2N_3O_2S_2$: C, 62.13; H, 4.07; N, 6.79 %. Found: C, 62.02; H, 4. 04; N, 6. 76 %; IR (KBr, cm^{-1}): 739 (C–Cl), 1347 (C–N), 1610 (C=C), 1684 (CO), 1755 (CO cyclic), 2999 (C=CH), 1447, 28 52, 2929 (CH_2), 3039 (CH–Ar), 3383 (NH); ^{1}H-NMR (300 MHz, C DCl$_3$, δ / ppm): 2.37–2.42 (2H, *m*, H-12), 3.59–3.63 (2H, *m*, H-13), 4.43 (2H, *t*, *J* = 7.50 Hz, H-11), 6.07 (1H, *s*, H-1'), 5.34 (1H, *s*, H-2"), 6.73 (1H, *s*, H-20), 6.49–8.14 (16H, *m*, Ar–H); ^{13}C-NMR (75 MHz, CDCl$_3$, δ / ppm): 41.3 (C-12), 145.8 (C-5"), 50.7 (C-13), 54.8 (C-11), 65.1 (C-2"), 117.0 (C-4 and C-5), 120.6 (C-1 and C-8), 125.2 (C-2 and C-7), 126.9 (C-3 and C-6), 127.4 (C-15), 127.8 (C-19), 128.4 (C-22), 128.8 (C-26), 129.8 (C-16), 130. 0 (C-18), 130.4 (C-23), 130.7 (C-25), 131.6 (C-17), 132.7 (C-24), 133.3 (C-14), 136.9 (C-21), 141.5 (C-20), 141.2 (C-4a and C-5a), 146.0 (C-1a and C-8a), 167.3 (C-2'), 177.8 (C-4"); FAB mass (*m*/*z*): 618 [M$^+$].

5-(4-Bromobenzylidene)-2-(4-bromophenyl)-4-oxo-N-*[3-(10*H*-phenothiazin--10-yl)propyl]-3-thiazolidinecarboxamide (**5e**)*. Yield: 65 % ; m.p. 152–153 °C; Anal. Calcd. for $C_{32}H_{25}Br_2N_3O_2S_2$: C, 54.32; H, 3,56; N, 5. 93 %. Found: C,

54.23; H, 3.51; N, 5.88 %; IR (KBr, cm^{-1}): 563 (C–Br), 1610 (C=CH), 1350 (C–H), 1678 (CO), 1745 (CO cyclic), 2995 (C=CH), 1448, 285 9, 2935 (CH_2), 3035 (CH–Ar), 3384 (NH); ^{1}H-NMR (300 MHz, $CDCl_3$, δ / ppm): 2.33–2.37 (2H, *m*, H-12), 3.67–3.71 (2H, *m*, H-13), 4.45 (2H, *t*, *J* = 7.55 Hz, H-11), 6.03 (1H, *s*, H--1'), 5.37 (1H, *s*, H-2"), 6.70 (1H, *s*, H-20), 6.32–8.03 (16H, *m*, Ar–H); ^{13}C--NMR (75 MHz, $CDCl_3$, δ / ppm): 44.2 (C-12), 143.2 (C-5"), 46.6 (C-13), 54.9 (C-11), 65.4 (C-2"), 112.0 (C-4 and C-5), 122.5 (C-1 and C-8), 1 24.4 (C-2 and C-7), 125.8 (C-3 and C-6), 126.3 (C-15 and C-19), 127.3 (C-22 and C-26), 128.6 (C-16 and C-18), 129.5 (C-23 and C-2 5), 130.8 (C-17), 131.6 (C-24), 132.8 (C--14), 137.1 (C-21), 139.8 (C-20), 143.6 (C-4a and C-5a), 150.0 (C-1a and C-8a), 165.2 (C-2'), 1174.4 (C-4"); FAB mass (*m*/*z*): 707 [M^+].

5-(3-Bromobenzylidene)-2-(3-bromophenyl)-4-oxo-N-*[3-(10*H-*phenothiazin--10-yl)propyl]-3-thiazolidinecarboxamide (**5f**)*. Yield: 63 % ; m.p. 154–156 °C; Anal. Calcd. for $C_{32}H_{25}Br_2N_3O_2S_2$: C, 54.32; H, 3,56; N, 5. 93 %. Found: C, 54.27; H, 3. 53; N, 5.8 6 %; IR (KBr, cm^{-1}): 570 (C–Br), 1350 (C–N), 158 7 (C=CH), 1681 (CO), 1750 (CO cy clic), 2989 (C=CH), 1453, 28 54, 2934 (CH_2), 3045 (CH–Ar), 338 1 (NH); ^{1}H-NMR (300 MHz, C DCl_3, δ / pp m): 2.34–2.39 (2H, *m*, H-12), 3.70–3.75 (2H, *m*, H-13), 4.41 (2H, *t*, *J* = 7.60 Hz, H-11), 5.97 (1H, *s*, H-1'), 5.38 (1H, *s*, H-2"), 6.68 (1H, *s*, H-20), 6.22–7.79 (16H, *m*, Ar–H); ^{13}C-NMR (75 MHz, $CDCl_3$, δ / ppm): 40.2 (C-12), 144.0 (C-5"), 49.5 (C-13), 56.7 (C-11), 67.5 (C-2"), 113.0 (C-4 and C-5), 119.2 (C-1 and C-8), 127.6 (C-2 and C-7), 128.2 (C-3 and C-6), 129.1 (C-15), 130.2 (C-19), 130.6 (C-22), 131.1 (C-26), 131.6 (C-16), 131. 9 (C-18), 13 2.7 (C-23), 1 32.9 (C-25), 133.2 (C-17), 133.9 (C-24), 134.7 (C-14), 138.6 (C-21), 138.9 (C-20), 142.9 (C-4a and C-5a), 148.0 (C-1a and C-8a), 167.7 (C-2'), 175.3 (C-4"); FAB mass (*m*/*z*): 707 [M^+].

5-(2-Bromobenzylidene)-2-(2-bromophenyl)-4-oxo-N-*[3-(10*H-*phenothiazin--10-yl)propyl]-3-thiazolidinecarboxamide (**5g**)*. Yield: 64 %; m.p. 151–152 °C; Anal. Calcd. for $C_{32}H_{25}Br_2N_3O_2S_2$: C, 54.32; H, 3,56; N, 5. 93 %. Found: C, 54.25; H, 3. 52; N, 5.8 3 %; IR (KBr, cm^{-1}): 577 (C–Br), 134 8 (C–NH), 1597 (C=C), 1686 (CO), 1753 (CO cyclic), 2988 (C=CH), 1450, 28 55, 2926 (CH_2), 3042 (CH–Ar), 338 0 (NH); ^{1}H-NMR (300 MHz, C DCl_3, δ / pp m): 2.36–2.40 (2H, *m*, H-12), 3.72–3.76 (2H, *m*, H-13), 4.42 (2H, *t*, *J* = 7.55 Hz, H-11), 5.98 (1H, *s*, H-1'), 5.40 (1H, *s*, H-2"), 6.65 (1H, *s*, H-20), 6.37–7.88 (16H, *m*, Ar–H); ^{13}C-NMR (75 MHz, $CDCl_3$, δ / ppm): 43.7 (C-12), 143.2 (C-5"), 49.4 (C-13), 56.3 (C-11), 67.2 (C-2"), 117.0 (C-4 and C-5), 123.4 (C-1 and C-8), 126.9 (C-2 and C-7), 127.5 (C-3 and C-6), 128.7 (C-15), 129.1 (C-19), 129.5 (C-22), 129.8 (C-26), 130.4 (C-16), 130. 8 (C-18), 13 1.9 (C-23), 1 32.1 (C-25), 132.5 (C-17), 133.6 (C-24), 134.9 (C-14), 138.7 (C-21), 139.8 (C-20), 144.4 (C-4a and C-5a), 147.0 (C-1a and C-8a), 165.1 (C-2'), 177.3 (C-4"); FAB mass (*m*/*z*): 707 [M^+].

5-(4-Nitrobenzylidene)-2-(4-nitrophenyl)-4-oxo-N-*[3-(10*H-*phenothiazin-10--yl)propyl]-3-thiazolidinecarboxamide (**5h**)*. Yield: 70 %; m.p. 149–151 °C;

Anal. Calcd. for $C_{32}H_{25}N_5O_6S_2$: C, 60.08; H, 3, 93; N, 10. 94 %. Found: C, 60.04; H, 3.89; N, 10.91 %; IR (KBr, c m^{-1}): 695 (C–S–C), 870 (C–NO), 1347 (C–NH), 1521 (N=O), 1 588 (C=CH), 1680 (CO), 1754 (CO cy clic), 3014 (C=CH), 1450, 285 3, 2933 (CH_2), 3036 (CH–Ar), 3382 (NH); ^{1}H-NMR (300 MHz, $CDCl_3$, δ / ppm): 2.31–2.36 (2H, *m*, H-12), 3.74–3.80 (2H, *m*, H-13), 4.37 (2H, *t*, *J* = 7.50 Hz, H-11), 6.04 (1H, *s*, H-1'), 5.29 (1H, *s*, H-2"), 6.62 (1H, *s*, H--20), 6.29–797 (16H, *m*, Ar–H); ^{13}C-NMR (75 MHz, $CDCl_3$, δ / ppm): 42.9 (C--12), 142.0 (C-5"), 47.3 (C-13), 57.4 (C-11), 64.5 (C-2"), 115.0 (C-4 and C-5), 121.4 (C-1 and C-8), 127.5 (C-2 and C-7), 128.6 (C-3 and C-6), 129.8 (C-15 and C-19), 130.4 (C-22 and C-26), 13 1.5 (C-16 and C-18), 132.6 (C-23 and C-25), 133.2 (C-17), 134.5 (C-24), 134.9 (C-14), 138.4 (C-21), 139.0 (C-20), 144.2 (C--4a and C-5a), 146. 0 (C-1a and C-8a), 168.8 (C-2'), 177.4 (C-4"); FAB mass (*m*/*z*): 639 [M^+].

5-(3-Nitrobenzylidene)-2-(3-nitrophenyl)-4-oxo-N-*[3-(10*H*-phenothiazin-10--yl)propyl]-3-thiazolidinecarboxamide (**5i**)*. Yield: 72 %; m.p. 150–151 °C; Anal. Calcd. for $C_{32}H_{25}N_5O_6S_2$: C, 60.08; H, 3,93; N, 10.94 %. Found: C, 60.06; H, 3.90; N, 10.89 %; IR (KBr, cm^{-1}): 679 (C–S–C), 868 (C–NO), 1351 (C–N), 1594 (C=CH), 1511 (N=O), 1685 (CO), 1750 (CO cyclic), 3011 (C=CH), 1449, 2852, 2930 (CH_2), 3041 (CH–Ar), 3384 (NH); ^{1}H-NMR (300 MHz, $CDCl_3$, δ / ppm): 2.33–2.38 (2H, *m*, H-12), 3.72–3.77 (2H, *m*, H-13), 4.39 (2H, *t*, *J* = 7.50 Hz, H--11), 5.99 (1H, *s*, H-1'), 5.36 (1H, *s*, H-2"), 6.58 (1H, *s*, H-20), 6.38–7.95 (16H, *m*, Ar–H); ^{13}C-NMR (75 MHz, $CDCl_3$, δ / ppm): 44.8 (C-12), 144.5 (C-5"), 48.7 (C-13), 57.6 (C-11), 65.5 (C-2"), 114.0 (C-4 and C-5), 121. 3 (C-1 and C-8), 125.7 (C-2 and C-7), 126.4 (C-3 and C-6), 127.5 (C-15), 128.2 (C-19), 128.7 (C--22), 129.1 (C-26), 129. 6 (C-16), 129 .8 (C-18), 130.3 (C-23), 130.8 (C-25), 131.6 (C-17), 132.5 (C-24), 133.6 (C-14), 137.9 (C-21), 140.0 (C-20), 145.5 (C--4a and C-5a), 147. 0 (C-1a and C-8a), 166.3 (C-2'), 178.6 (C-4"); FAB mass (*m*/*z*): 639 [M^+].

5-(2-Nitrobenzylidene)-2-(2-nitrophenyl)-4-oxo-N-*[3-(10*H*-phenothiazin-10--yl)propyl]-3-thiazolidinecarboxamide (**5j**)*. Yield: 69 %; m.p. 153–155 °C; Anal. Calcd. for $C_{32}H_{25}N_5O_6S_2$: C, 60.08; H, 3,93; N, 10.94 %. Found: C, 60.02; H, 3.88; N, 10.92 %; IR (KBr, cm^{-1}): 697 (C–S–C), 8 72 (C–NO), 1356 (C–NH), 1509 (N=O), 1584 (C=CH), 1679 (CO), 1751 (CO cy clic), 2980 (C=CH), 1457, 2860, 2931 (CH_2), 3040 (CH–Ar), 3388 (NH); ^{1}H-NMR (300 MHz, $CDCl_3$, δ / / ppm): 2.32–2.37 (2H, *m*, H-12), 3.64–3.68 (2H, *m*, H-13), 4.44 (2H, *t*, *J* = 7.55 Hz, H-11), 6.05 (1H, *s*, H-1'), 5.38 (1H, *s*, H-2"), 6.69 (1H, *s*, H-20), 6.31–7.83 (16H, *m*, Ar–H); ^{13}C-NMR (75 MHz, $CDCl_3$, δ / ppm): 41.3 (C-12), 145.6 (C--5"), 47.2 (C-13), 57.1 (C-11), 66.5 (C-2"), 113.0 (C-4 and C-5), 120.1 (C-1 and C-8), 126.5 (C-2 and C-7), 127.6 (C-3 and C-6), 128.2 (C-15), 128.9 (C-19), 129.6 (C-22), 129.9 (C-26), 130.1 (C-16), 130.7 (C-18), 131.4 (C-23), 131.8 (C--25), 132.1 (C-17), 133. 6 (C-24), 133 .8 (C-14), 137.5 (C-21), 140.1 (C-20),

144.7 (C-4a and C-5a), 14 5.0 (C-1a and C-8a), 168.8 (C-2'), 176.4 (C-4"); FAB mass (*m*/*z*): 639 [M^+].

5-(4-Methoxybenzylidene)-2-(4-methoxyphenyl)-4-oxo-N-*[3-(10*H*-phenothiazin-10-yl)propyl]-3-thiazolidinecarboxamide (**5k**)*. Yield: 63 %; m.p. 146–147 °C; Anal. Calcd. for $C_{33}H_{31}N_3O_2S_2$: C, 66.97; H, 5.12; N, 6.8 9 %. Found: C, 66.89; H, 5.08; N, 6.82 %; IR (KBr, cm^{-1}): 692 (C–S–C), 1085 (C–O), 1341 (C–N), 1590 (C=CH), 1675 (CO), 1741 (CO cy clic), 2995 (C=CH), 1443, 2846 , 2923 (CH_2), 2965 (OCH_3), 3030 (CH–Ar), 3 373 (NH); ^{1}H-NMR (300 MHz, $CDCl_3$, δ / ppm): 2.32–2.36 (2H, *m*, H-12), 3.22 (6H, *s*, 2×OCH_3), 3.64–3.69 (2H, *m*, H--13), 4.35 (2H, *t*, *J* = 7.40 Hz, H-11), 5.27 (1H, *s*, H-2"), 5.95 (1H, *s*, H-1'), 6.66 (1H, *s*, H-20), 6.35–7.68 (16H, *m*, Ar–H); ^{13}C-NMR (75 MHz, $CDCl_3$, δ / ppm): 40.3 (C-12), 145.8 (C-5"), 45.3 (C-13), 53.1 (C-11), 52.4 (2×OCH_3), 64.5 (C-2"), 112.0 (C-4 and C-5), 118. 9 (C-1 and C-8), 124.3 (C-2 and C-7), 125. 1 (C-3 and C-6), 126.1 (C-15 and C- 19), 127.7 (C-22 and C- 26), 128.6 (C-16 and C- 18), 129.5 (C-23 and C-25), 130.1 (C-17), 131.3 (C-24), 131.8 (C-14), 137.2 (C-21), 139.5 (C-20), 141.2 (C-4a and C-5a), 144.0 (C-1a and C-8a), 164.7 (C-2'), 170.5 (C-4"); FAB mass (*m*/*z*): 609 [M^+].

5-(3-Methoxybenzylidene)-2-(3-methoxyphenyl)-4-oxo-N-*[3-(10*H*-phenothiazin-10-yl)propyl]-3-thiazolidinecarboxamide (**5l**)*. Yield: 62 %; m.p. 142–144 °C; Anal. Calcd. for $C_{33}H_{31}N_3O_2S_2$: C, 66.97; H, 5.12; N, 6.89 %. Found: C, 66.86; H, 5.05; N, 6.80 %; IR (KBr, cm^{-1}): 690 (C–S–C), 1089 (C–O), 134 6 (C–N), 1594 (C=CH), 1673 (CO), 1744 (CO cy clic), 2982 (C=CH), 1447, 2849 , 2925 (CH_2), 2958 (OCH_3), 3033 (CH–Ar), 3 377 (NH); ^{1}H-NMR (300 MHz, $CDCl_3$, δ / ppm): 2.35–2.41 (2H, *m*, H-12), 3.65 (6H, *s*, 2×OCH_3), 3.65–3.73 (2H, *m*, H--13), 4.38 (2H, *t*, *J* = 7.40 Hz, H-11), 5.26 (1H, *s*, H-2"), 5.97 (1H, *s*, H-1'), 6.70 (1H, *s*, H-20), 6.22–7.73 (16H, *m*, Ar–H); ^{13}C-NMR (75 MHz, $CDCl_3$, δ / ppm): 44.6 (C-12), 145.2 (C-5"), 48.4 (C-13), 55.8 (C-11), 55.4 (2×OCH_3), 66.8 (C-2"), 113.0 (C-4 and C-5), 119. 5 (C-1 and C-8), 123.5 (C-2 and C-7), 124. 5 (C-3 and C-6), 125.7 (C-15), 126.4 (C-19), 12 8.5 (C-22), 128.9 (C-26), 129.4 (C-1 6), 129.9 (C-18), 130.2 (C-23), 130.8 (C-25), 131.6 (C-17), 132.5 (C-24), 132.9 (C--14), 134.2 (C-21), 137.5 (C-20), 144.7 (C-4a and C-5a), 148.0 (C-1a and C-8a), 166.8 (C-2'), 171.7 (C-4"); FAB mass (*m*/*z*): 609 [M^+].

5-(2-Methoxybenzylidene)-2-(2-methoxyphenyl)-4-oxo-N-*[3-(10*H*-phenothiazin-10-yl)propyl]-3-thiazolidinecarboxamide (**5m**)*. Yield: 61 % ; m.p. 148–150 °C; Anal. for Calcd. $C_{33}H_{31}N_3O_2S_2$: C, 66.97; H, 5.12; N, 6.89 %. Found: C, 66.87; H, 5.04; N, 6.79 %; IR (KBr, cm^{-1}): 699 (C–S–C), 1088 (C–O), 134 5 (C–N), 1598 (C=CH), 1671 (CO), 1743 (CO cy clic), 2986 (C=CH), 1442, 2845 , 2927 (CH_2), 2966 (OCH_3), 3032 (CH–Ar), 3 377 (NH); ^{1}H-NMR (300 MHz, $CDCl_3$, δ / ppm): 2.37–2.44 (2H, *m*, H-12), 3.54 (6H, *s*, 2×OCH_3), 3.69–3.75 (2H, *m*, H--13), 4.38 (2H, *t*, *J* = 7.40 Hz, H-11), 5.31 (1H, *s*, H-2"), 5.97 (1H, *s*, H-1'), 6.45 (1H, *s*, H-20), 6.55–7.92 (16H, *m*, Ar–H); ^{13}C-NMR (75 MHz, $CDCl_3$, δ / ppm):

41.9 (C-12), 46.2 (C-13), 52.7 (C-11), 56.4 (2×OCH_3), 61.3 (C-2"), 116.0 (C -4 and C-5), 118.3 (C-1 and C-8), 124.9 (C-2 and C-7), 125.4 (C-3 and C-6), 126.7 (C-15), 126.8 (C-19), 127.2 (C-22), 127.8 (C-26), 128.9 (C-16), 129.1 (C-18), 129.4 (C-23), 130.2 (C-25), 131.9 (C-17), 132.7 (C-24), 133.5 (C-14), 134.6 (C--21), 136.5 (C-20), 140.9 (C-4a and C-5a), 142.0 (C-5"), 145.0 (C-1a and C-8a), 163.7 (C-2'), 172.3 (C-4"); FAB mass (*m*/*z*): 609 [M^+].

5-(4-Metylbenzylidene)-2-(4-methylphenyl)-4-oxo-N-*[3-(10*H-*phenothiazin--10-yl)propyl]-3-thiazolidinecarboxamide (**5n**)*. Yield: 62 % ; m.p. 136–138 °C; Anal. Calcd. for $C_{34}H_{31}N_3O_2S_2$: C, 70.68; H, 5.40; N, 7.27 %. Found: C, 70.65; H, 4.37; N, 7.21 %; IR (KBr, cm^{-1}): 687 (C–S–C), 1336 (C–N), 1580 (C=CH), 1672 (CO), 1738 (CO cyclic), 2991 (C=CH), 1440, 2842, 2919 (CH_2), 2992 (CH_3), 3027 (CH–Ar), 3370 (NH); ^{1}H-NMR (300 MHz, $CDCl_3$, δ / ppm): 2.04 (6H, *s*, 2×CH_3), 2.27–2.30 (2H, *m*, H-12), 3.58–3.62 (2H, *m*, H-13), 4.29 (2H, *t*, *J* = 7.45 Hz, H-11), 5.23 (1H, *s*, H-2"), 5.89 (1H, *s*, H-1'), 6.49 (1H, *s*, H-20), 6.42–7.74 (16H, *m*, Ar–H); ^{13}C-NMR (75 MHz, $CDCl_3$, δ / ppm): 22.5 (2×CH_3), 39.7 (C-12), 140.2 (C-5"), 45.1 (C-13), 52.4 (C-11), 63.1 (C-2"), 116.0 (C-4 and C-5), 118.5 (C-1 and C-8), 123.4 (C-2 and C-7), 124.7 (C-3 and C-6), 125.3 (C--15 and C-19), 126.6 (C-22 and C-26), 127.1 (C-16 and C-18), 128.0 (C-23 and C-25), 129.5 (C-17), 130.4 (C-24), 131.1 (C-14), 137.5 (C-21), 137.6 (C-20), 139.6 (C-4a and C-5a), 148.0 (C-1a and C-8a), 163.3 (C-2'), 167.5 (C-4"); FAB mass (*m*/*z*): 577 [M^+].

5-(3-Metylbenzylidene)-2-(3-methylphenyl)-4-oxo-N-*[3-(10*H-*phenothiazin--10-yl)propyl]-3-thiazolidinecarboxamide (**5o**)*. Yield: 65 %; m.p. 141–142 °C; Anal. Calcd. for $C_{34}H_{31}N_3O_2S_2$: C, 70.68; H, 5.40; N, 7.27 %. Found: C, 70.61; H, 4.33; N, 7.19 %; IR (KBr, cm^{-1}): 684 (C–S–C), 1332 (C–N), 1586 (C=CH), 1677 (CO), 1740 (CO cyclic), 2989 (C=CH), 1443, 2847, 2915 (CH_2), 2878 (CH_3), 3030 (CH–Ar), 3373 (NH); ^{1}H-NMR (300 MHz, $CDCl_3$, δ / ppm): 2.00 (6H, *s*, 2×CH_3), 2.26–2.32 (2H, *m*, H-12), 3.55–3.61 (2H, *m*, H-13), 4.25 (2H, *t*, *J* = 7.45 Hz, H-11), 5.21 (1H, *s*, H-2"), 5.86 (1H, *s*, H-1'), 6.42 (1H, *s*, H-20), 6.29-7.71 (16H, *m*, Ar-H); ^{13}C-NMR (75 MHz, $CDCl_3$, δ / ppm): 23.1 (2×CH_3), 37.6 (C-12), 43.5 (C-13), 54.7 (C-11), 65.4 (C-2"), 118.0 (C-4 and C-5), 119.5 (C-1 and C-8), 122.3 (C-2 and C-7), 123.7 (C-3 and C-6), 124.5 (C-15), 124.9 (C-19), 125.2 (C-22), 125.8 (C-26), 126.7 (C-16), 127.1 (C-18), 127.4 (C-23), 127.9 (C-25), 128.7 (C-17), 129.4 (C-24), 130.8 (C-14), 133.2 (C-21), 135.1 (C--20), 138.9 (C-4a and C-5a), 141.1 (C-5"), 151.0 (C-1a and C-8a), 164.6 (C-2'), 168.5 (C-4"); FAB mass (*m*/*z*): 577 [M^+].

5-(2-Metylbenzylidene)-2-(2-methylphenyl)-4-oxo-N-*[3-(10*H-*phenothiazin--10-yl)propyl]-3-thiazolidinecarboxamide (**5p**)*. Yield: 62 %; m.p. 138–139 °C; Anal. Calcd. for $C_{34}H_{31}N_3O_2S_2$: C, 70.68; H, 5.40; N, 7.27 %. Found: C, 70.60; H, 4.31; N, 7.24 %; IR (KBr, cm^{-1}): 686 (C–S–C), 1339 (C–N), 1594 (C=CH), 1674 (CO), 1736 (CO cyclic), 2989 (C=CH), 1443, 2848, 2914 (CH_2), 2875

(CH_3), 3023 (CH–Ar), 3377 (NH); ^{1}H-NMR (300 MHz, $CDCl_3$, δ / ppm): 2.05 (6H, *s*, 2×CH_3), 2.24–2.28 (2H, *m*, H-12), 3.53–3.68 (2H, *m*, H-13), 4.30 (2H, *t*, *J* = 7.45 Hz, H-11), 5.25 (1H, *s*, H-2"), 5.83 (1H, *s*, H-1'), 6.39 (1H, *s*, H-20), 6.44–7.80 (16H, *m*, Ar–H); ^{13}C-NMR (75 MHz, $CDCl_3$, δ / ppm): 22.1 (2×CH_3), 38.5 (C-12), 45.1 (C-13), 52.9 (C-11), 65.7 (C-2"), 116.0 (C-4 and C-5), 117.4 (C-1 and C-8), 122.5 (C-2 and C-7), 123.6 (C-3 and C-6), 125.4 (C-15), 125.8 (C-19), 126.2 (C-22), 126.9 (C-26), 127.6 (C-16), 127.9 (C-18), 128.3 (C-23), 129.7 (C-25), 130.1 (C-17), 131.9 (C-24), 132.4 (C-14), 136.4 (C-21), 134.6 (C-20), 138.4 (C-4a and C-5a), 142.1 (C-5"), 154.4 (C-1a and C-8a), 161.6 (C-2'), 168.4 (C-4"); FAB mass (*m*/z): 577 [M^+].

5-(4-Hydroxybenzylidene)-2-(4-hydroxylphenyl)-4-oxo-N-*[3-(10*H*-phenothiazin-10-yl)propyl]-3-thiazolidinecarboxamide (**5q**)*. Yield: 60 %; m.p. 154–155 °C; Anal. Calcd. for $C_{32}H_{27}N_3O_4S_2$: C, 66.07; H, 4.67; N, 7.22 %. Found: C, 65.97; H, 4.62; N, 7.18 %; IR (KBr, cm^{-1}): 693 (C–S–C), 1134 (C–O), 1344 (C–N), 1602 (C=CH), 1677 (CO), 1743 (CO cyclic), 2981 (C=CH), 1444, 2848, 2925 (CH_2), 3031 (CH–Ar), 3374 (NH), 3487 (OH); ^{1}H-NMR (300 MHz, $CDCl_3$, δ / / ppm): 2.33–2.37 (2H, *m*, H-12), 3.75–3.80 (2H, *m*, H-13), 4.35 (2H, *t*, *J* = 7.40 Hz, H-11), 5.85 (1H, *s*, H-1'), 4.52 (2H, *s*, 2×OH), 6.58 (1H, *s*, H-20), 6.32–7.86 (16H, *m*, Ar–H); ^{13}C-NMR (75 MHz, $CDCl_3$, δ / ppm): 40.7 (C-12), 142.3 (C-5"), 46.5 (C-13), 53.6 (C-11), 64.2 (C-2"), 115.0 (C-4 and C-5), 119.8 (C-1 and C-8), 124.6 (C-2 and C-7), 125.4 (C-3 and C-6), 126.9 (C-15 and C-19), 127.6 (C-22 and C-26), 128.6 (C-16 and C-18), 129.8 (C-23 and C-25), 130.3 (C-17), 131.7 (C-24), 132.2 (C-14), 137.7 (C-21), 139.2 (C-20), 140.6 (C-4a and C-5a), 155.0 (C-1a and C-8a), 164.1 (C-2'), 171.5 (C-4"); FAB mass (*m*/z): 581 [M^+].

5-(3-Hydroxybenzylidene)-2-(3-hydroxylphenyl)-4-oxo-N-*[3-(10*H*-phenothiazin-10-yl)propyl]-3-thiazolidinecarboxamide (**5r**)*. Yield: 63 %; m.p. 158–160 °C; Anal. Calcd. for $C_{32}H_{27}N_3O_4S_2$: C, 66.07; H, 4.67; N, 7.22 %. Found: C, 66.03; H, 4.60; N, 7.16 %; IR (KBr, cm^{-1}): 696 (C–S–C), 1133 (C–O), 1348 (C–N), 1617 (C=CH), 1673 (CO), 1749 (CO cyclic), 2998 (C=CH), 1440, 2847, 2921 (CH_2), 3038 (CH–Ar), 3378 (NH), 3486 (OH); ^{1}H-NMR (300 MHz, $CDCl_3$, δ / / ppm): 2.32–2.39 (2H, *m*, H-12), 3.73–3.82 (2H, *m*, H-13), 4.37 (2H, *t*, *J* = 7.40 Hz, H-11), 5.82 (1H, *s*, H-1'), 4.72 (2H, *s*, 2×OH), 6.62 (1H, *s*, H-20), 6.35–7.87 (16H, *m*, Ar–H); ^{13}C-NMR (75 MHz, $CDCl_3$, δ / ppm): 40.1 (C-12), 49.3 (C-13), 51.5 (C-11), 65.6 (C-2"), 115.0 (C-4 and C-5), 117.3 (C-1 and C-8), 122.3 (C-2 and C-7), 124.7 (C-3 and C-6), 127.3 (C-15), 127.9 (C-19), 128.9 (C-22), 129.1 (C-26), 129.3 (C-16), 130.4 (C-18), 130.8 (C-23), 131.8 (C-25), 132.4 (C-17), 133.5 (C-24), 135.3 (C-14), 139.3 (C-21), 140.2 (C-20), 143.5 (C-4a and C-5a), 145.2 (C-5"), 153.0 (C-1a and C-8a), 165.1 (C-2'), 171.3 (C-4"); FAB mass (*m*/z): 581 [M^+].

5-(2-Hydroxybenzylidene)-2-(2-hydroxylphenyl)-4-oxo-N-*[3-(10*H*-phenothiazin-10-yl)propyl]-3-thiazolidinecarboxamide (**5s**)*. Yield: 60 %; m.p. 162–164 °C;

Anal. Calcd. for $C_{32}H_{27}N_3O_4S_2$: C, 66.07; H, 4.67; N, 7.22 %. Found: C, 66.05; H, 4.59; N, 7.15 %; IR (KBr, cm^{-1}): 695 (C–S–C), 1138 (C–O), 1341 (C–N), 1612 (C=CH), 1674 (CO), 1748 (CO cyclic), 2987 (C=CH), 1449, 2842, 2925 (CH_2), 3037 (CH–Ar), 3378 (NH), 3480 (OH); ^{1}H-NMR (300 MHz, $CDCl_3$, δ / / ppm): 2.31–2.36 (2H, *m*, H-12), 3.72–3.73 (2H, *m*, H-13), 4.38 (2H, *t*, J = 7.40 Hz, H-11), 5.80 (1H, *s*, H-1'), 4.55 (2H, *s*, 2×OH), 6.68 (1H, *s*, H-20), 6.36–7.91 (16H, *m*, Ar–H); ^{13}C-NMR (75 MHz, $CDCl_3$, δ / ppm): 45.8 (C-12), 46.5 (C-13), 55.8 (C-11), 62.9 (C-2"), 114.0 (C-4 and C-5), 116.7 (C-1 and C-8), 122.5 (C-2 and C-7), 123.6 (C-3 and C-6), 126.5 (C-15), 126.8 (C-19), 127.9 (C-22), 128.3 (C-26), 128.6 (C-16), 128.9 (C-18), 129.5 (C-23), 130.2 (C-25), 131.6 (C-17), 132.7 (C-24), 134.6 (C-14), 138.4 (C-21), 139.9 (C-20), 142.4 (C-4a and C-5a), 144.6 (C-5"), 154.5 (C-1a and C-8a), 163. 1 (C-2'), 170.2 (C-4"); FAB mass (*m*/*z*): 581 [M^+].

Journal of the Serbian Chemical Society
JSCS-info@shd.org.rs • www.shd.org.rs/JSCS
J. Serb. Chem. Soc. 77 (1) 27–42 (2012)
JSCS–4246
UDC *Pseudomonas aeruginosa* san-ai: 577.115.002.2
Original scientific paper

Production and characterization of rhamnolipids from *Pseudomonas aeruginosa* san-ai

MILENA G. RIKALOVIĆ[1], GORDANA GOJGIĆ-CVIJOVIĆ[2], MIROSLAV M. VRVIĆ[1,2] and IVANKA KARADŽIĆ[3]*

[1]*Faculty of Chemistry, University of Belgrade, Studentski trg 12–16, Belgrade, Serbia,* [2]*Department of Chemistry, ICTM, University of Belgrade, Njegoševa 12, Belgrade, Serbia and* [3]*School of Medicine, Department of Chemistry, University of Belgrade, Višegradska 26, Belgrade, Serbia*

(Received 11 February, revised 3 August 2011)

Abstract: The production and characteristics of rhamnolipid biosurfactant obtained by the strain *Pseudomonas aeruginosa* san-ai were investigated. With regard to the carbon and nitrogen sources, several media were tested to enhance the production of rhamnolipids. Phosphate-limited proteose peptone–ammonium salt (PPAS) medium supplemented with sunflower oil as a source of carbon and mineral ammonium chloride and peptone as nitrogen sources greatly improved the production of rhamnolipid, from 0.15 on basic PPAS (C/N ratio 4.0) to 3 g L^{-1} on optimized PPAS medium (C/N ratio 7.7). Response surface methodology analysis was used for testing the effect of three factors, *i.e.*, temperature, concentration of carbon and nitrogen source (mass %), in the optimized PPAS medium on the production of rhamnolipid. The isolated rhamnolipids were characterized by infrared (IR) spectroscopy and electrospray ionization mass spectrometry (ESI–MS). The IR spectra confirmed that the isolated compound corresponded to the rhamnolipid structure, whereas MS indicated that the isolated preparation was a mixture of mono-rhamno-mono-lipidic, mono-rhamno-di-lipidic and di-rhamno-di-lipidic congeners.

Keywords: rhamnolipids; *Pseudomonas aeruginosa*; renewable sources.

INTRODUCTION

Biosurfactants are microbial secondary metabolites that appear to play a role whenever a microbe encounters an interface.[1] Biosurfactants are important for motility, cell–cell interactions (biofilm formation, maintenance and maturation, quorum sensing, amensalism and pathogenicity) and cellular differentiation, substrate accession (*via* direct interfacial contact and pseudosolubilization of substrates), as well as avoidance of toxic elements and compounds. They may also

* Corresponding author. E-mail: ikaradzic@med.bg.ac.rs
doi: 10.2298/JSC110211156R

be used as carbon and energy storage molecules, as a protective mechanism against high ionic strength, and may simply be byproducts released in response to environmental changes (*e.g.*, extracellular coverings).[2]

Almost all surfactants currently in use are chemically derived from petroleum. However, biosurfactants have several advantages over the chemical surfactants, such as lower toxicity, higher biodegradability, better environmental compatibility, higher foaming, high selectivity and specific activity at extreme temperatures, pH and salinity, and the ability to be synthesized from renewable feedstock.[1] Due to these properties, biosurfactants are becoming important biotechnology products for industrial and medical applications.[3] They can be used as emulsifiers, de-emulsifiers, wetting and foaming agents, functional food ingredients and as detergents in petroleum, petrochemicals, environmental management, agrochemicals, foods and beverages, cosmetics and pharmaceuticals, and in the mining and metallurgical industries. Surfactants also play an important role in enhanced oil recovery by increasing the apparent solubility of petroleum components and effectively reducing the interfacial tensions of oil and water *in situ*.[4]

The main factor limiting commercialization of biosurfactants is associated with their non-economic large-scale production. To overcome this obstacle and to compete with synthetic surfactants, an inexpensive substrate and effective microorganism have to be intensively developed for biosurfactant production. Agro-industrial wastes are considered as promising substrates for biosurfactant production, which could alleviate many processing industrial waste management problems.[5] The fact should be noted that although the literature mentions a number of microbe producers with potential to be advantageous for increasing production and efficiency, in practice, this has only been confirmed for a few genera such as *Bacillus*, *Candida* and *Pseudomonas*.[1] Regardless of these problems, the production of microbial surfactants follows the trend of green chemistry and forms the basis of modern industrial processes. The creation of an ecological society, which is in harmony with its surroundings, is now, with green chemistry, the greatest challenge for science and mankind.

Biosurfactants can be divided into two classes: low-molecular-mass molecules, which efficiently lower surface and interfacial tension, and high-molecular-mass polymers, which are more effective as emulsion stabilizing agents. The classes of low-mass surfactants include glycolipids, lipopeptides and phospholipids, whereas high-mass ones include polymeric and particulate surfactants. Most biosurfactants are either anionic or nonionic and the hydrophobic moiety is based on long-chain fatty acids or their derivatives whereas the hydrophilic portion can be a carbohydrate, amino acid, phosphate or cyclic peptide. Bacteria are the predominant group of surfactant-producing organisms.[3] *Pseudomonas* species synthesize both classes of surfactants, low- and high-molecular-mass molecules, but are commonly mentioned as rhamnolipid (RL) producers.[2,6]

Rhamnolipids (RLs) belong to class of low-molecular-mass molecules. The principal rhamnolipids: mono-rhamno-di-lipidic congener and di-rhamno-di-lipidic congener, consist of one or two L-rhamnose units and two units of β-hydroxydecanoic acid (RL1 and RL2 in Fig. 1), while mono-rhamno-mono-lipidic congener and di-rhamno-mono-lipidic congener, consisting of one or two L-rhamnose and one unit of β-hydroxydecanoic acid, are biosynthesized only under certain cultivation conditions (RL3 and RL 4 in Fig. 1). [7] Rhamnolipids are secondary metabolites, and as such, their production coincides with the onset of the stationary phase of microbial growth .[8] Rhamnolipid production seems possible from most carbon sources supporting bacterial growth. Nevertheless, oil of vegetable origin, such as soybean, corn, canola, and olive, provides the highest productivity. Elevated C/N and C/P ratios promote the production of rhamnolipids, while high concentrations of divalent cations, especially iron, are inhibitory. Production of rhamnolipids is inhibited by the presence of NH_4^+, glutamine, asparagine, and arginine as nitrogen source and promoted by NO_3^-, glutamate and aspartate.[9]

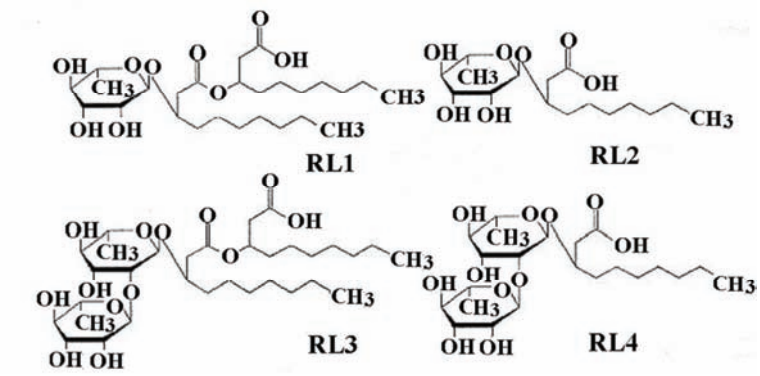

Fig. 1. Structure of rhamnolipid: RL1 (mono-rhamno-di-lipidic congener), RL2 (mono-rhamno-mono-lipidic congener), RL3 (di-rhamno-di-lipidic congener) and RL4 (di-rhamno-mono-lipidic congener).

Pseudomonas sp. are well known for their ability to produce rhamnolipid biosurfactants with potential surface active properties when grown on different carbon substrates and, therefore, are promising candidates for large scale production of biosurfactants.[6,7] In addition to tensioactive properties, rhamnolipids are compounds which play a vital role in regulating the cell population density-dependent control of genes expression, termed quorum sensing (QS) or cell-to-cell communication.[10] Except these, biosurfactants in the mentioned physiological process are involved as transcription factors, signal molecules and as a range of other secondary metabolites, among others extracellular lipase, the expression of which on a genetic level is regulated together with the rhamnolipids themselves.[11]

The aim of this research was to optimize the medium with regard to sources of carbon and nitrogen for improved production of rhamnolipids by the strain *P. aeruginosa* san-ai and to characterize the obtained rhamnolipids by FTIR and MS analysis. This is the first investigation of the production of rhamnolipids by a strain isolated from an unusual environment, *i.e.*, an extremely alkaline environment with a high amount of hydrocarbons. The dynamics of the production of RL by *P. aeruginosa* san-ai during submerged growth, as well comparison of the productivity of a referent strain and strains isolated from similar environments, was also investigated.

EXPERIMENTAL

Microorganisms

P. aeruginosa san-ai strain was isolated from industrial mineral metal-cutting oil.[12] *P. aeruginosa* 67 was isolated from a biopile constructed in Oil Refinery Pančevo,[13] Serbia, whereas *P. aeruginosa* ATCC 27853 was used as the referent strain.

Culture conditions

The strains were cultivated on nutrient agar (Torlak, Serbia) at 30 °C for 24 h and transferred to a 500 mL Erlenmeyer flask, containing 100 mL of Kay's mineral medium (3 g L^{-1} $NH_4H_2PO_4$, 2 g L^{-1} K_2HPO_4, 2 g L^{-1} glucose, 0.5 mg L^{-1} $FeSO_4$ and 1 g L^{-1} $MgSO_4$).[14] The flask was incubated at 30 °C for 20 h and shaken at 250 cycles min^{-1} on a horizontal shaker Kuhner (Switzerland). An actively growing culture was used to inoculate the basic medium.

Selection of the basic medium

Investigation of production media was realized in three steps: *i*) selection of the basic medium, *ii*) selection of the sources of N and C and *iii*) final optimization of the C and N ratio by the response surface methodology (RSM).

To select the basic medium, an actively growing culture from Kay's medium was dispensed (1 %) into 500 mL Erlenmeyer flasks containing 100 mL of one of three media: LB (Lurie–Bertani), MSM (mineral salt medium) and PPAS (phosphate-limited proteose peptone––ammonium salt) as a modification of PPGAS (phosphate-limited peptone–glucose–ammonium salt).[14] The composition of the LB medium was 5 g L^{-1} NaCl, 5 g L^{-1} yeast extract and 10 g L^{-1} peptone I.[12] The MSM medium contained 4 g L^{-1} NH_4NO_3, 4.08 g L^{-1} KH_2PO_4, 5.68 g L^{-1} Na_2HPO_4, 7.77×10^{-4} g L^{-1} $CaCl_2$, 0.2 g L^{-1} $MgSO_4\cdot7H_2O$, 1.49×10^{-3} g L^{-1} ethylenediaminetetraacetate disodium salt (sodium EDTA) and 5.56×10^{-4} g L^{-1} $FeSO_4\cdot7H_2O$.[15] The PPAS medium consisted of 1.07 g L^{-1} NH_4Cl, 1.49 g L^{-1} KCl, 14.54 g L^{-1} Tris HCl, 0.20 g L^{-1} $MgSO_4$ and 10 g L^{-1} peptone.[14] As a source of carbon, 0.7 % of olive oil (Carapelli, Italy) was added to all the listed basic media[7] and fermentation was realized at 30 °C for 96 h.

Selection of optimal type of nitrogen and carbon source

The effect of different sources of carbon and nitrogen was investigated using PPAS, as the basic medium selected in the previous step. To elucidate the effects of C-sources (2 % w/w), glucose, sunflower oil (Vital, Serbia), olive oil, metal cutting oil, kerosene, frying sunflower oil, ethanol, glycerol, or sunflower mill effluent (Plima M, Serbia) were investigated. Two fractions from sunflower mill effluent were tested: the oil emulsion (residue after oil degumming, composed of water, oil and phosphatides), and the fatty acids after neutralization

and saponification (composed of neutral oil, fatty acids and waxes.) For selection of optimal nitrogen source, peptone I (Torlak, Serbia) from the PPAS medium (with 2 % of olive oil) was replaced with (1 % w/w): whey, meat extract, yeast extract, soy flour (Soja Vita, Serbia) and tryptone (Torlak, Serbia).

An actively growing culture from Kay's medium was dispensed (1 %) into 500 mL Erlenmeyer flasks containing 100 mL of medium and the fermentation was performed at 30 °C for 96 h. All experiments were realized in tetraplicate.

Determination of the carbon and nitrogen contents of the media

The total contents of carbon and nitrogen were determined using a Vario EL III CHNS/O elemental analyzer (Germany).

Growth of bacterial strains

Bacterial growth was monitored as the change of optical density (*OD*) at 580 nm, measured on a Gilford 250 spectrophotometer (Oberlin, Ohio, USA), using sterile medium as the reference.[16]

Determination of the RL concentration

After removal of the biomass, 0.25 mL of 500 mM glycine buffer, pH 2, was added to 0.25 mL of supernatant. The mixture was well stirred and centrifuged for 10 min at 10000 rpm (Denver Instrument, USA). The supernatant was discarded and precipitate resuspended in 0.5 mL of a mixture of chloroform/methanol (2:1), with intense agitation for 5 min. The suspension was centrifuged for 5 min at 10000 rpm and 0.25 mL of supernatant was transferred to a new Eppendorf tube. After evaporation of the solvent mixture, the precipitate remaining was dissolved in water. The concentration of RL (c_{rl}) was determined spectrophotometrically by the orcinol reaction using rhamnose as a standard. The orcinol reagent (0.19 % orcinol in 53 % (v/v) sulfuric acid) was prepared immediately before use. The reaction mixture, composed of 150 μL of sample and 1350 μL of reagents, was well stirred, warmed for 30 min at 80 °C, and kept for 15 min at room temperature. The absorbance was measured at 421 nm using a Gilford 250 instrument. c_{rl} was calculated based on the assumption that 1 μg of rhamnose corresponds to 2.5 μg of RL.[17,18]

Isolation of RL

RL was isolated from the fermentation broth after separation of the bacterial cells by centrifugation. The crude preparation of RL was obtained by acidic precipitation using 1 M HCl (final pH: 2). The precipitate was collected by centrifugation at 5 000 rpm for 10 min (Sorvall, rotor SS-1, UK) and the RLs were dissolved in a mixture of chloroform and methanol (2:1). Clear supernatant obtained after centrifugation at 5000 rpm for 10 min (Janetzki T32c, Germany)[16] was vacuumed to dryness and used for FTIR and MS analysis.

Response surface methodology (RSM)

Response surface methodology (RSM) was applied for data analysis using Design Expert software (version 8.0.5). The PPAS medium with sunflower oil as the carbon source and peptone I as the nitrogen source was used. The plan applied in this study involved 17 experiments conducted according a Box–Behnken design.[19] The effects of the concentrations of the C and N sources and temperature were tested in following ranges: concentration of sunflower oil, as the carbon source (1–6 %), concentration of peptone I, as the nitrogen source (0.5–4 %) and temperature (20–40 °C). The response value was the concentration of rhamnolipid (c_{rl}) expressed as g L^{-1}. The concentration of rhamnolipid was measured on the fourth day of fermentation.

Lipase enzyme assay

The lipase activity (c_e) was measured spectrophotometrically using an assay based on the hydrolysis of *p*-nitrophenyl palmitate (pNPP, Sigma Aldrich, USA) at a concentration of 0.79 mmol pNPP mL^{-1}. The reaction mixture was composed of 900 µL of pNPP solution and 100 µL of lipase solution. The pNPP solution was prepared as follows: 30 mg of pNPP in 10 mL of 2-propanol was added to 90 mL of 0.05 M phosphate buffer pH 8.0 supplemented with 207 mg of Na-deoxycholate and 100 mg of gum arabic. The enzyme reaction mixture was incubated at 30 °C and the absorbance measured at 410 nm during the first 3 min of reaction. One unit (1 U) is defined as that quantity of enzyme that (under the test conditions) liberates 1 µmol pNPP min^{-1}.[12]

FTIR analysis

The IR spectra were recorded on a Perkin-Elmer 31725 X FTIR spectrophotometer using KBr discs.

HPLC–MS-ESI analysis

Mass spectra of RL were recorded on MS system consisting of an HPLC (Agilent 1200 Series, Agilent Technologies) and a 6210 Time-of-Flight LC/MS (Agilent Technologies), using Zorbax Eclipse Plus C18 column and a DAD detector. The mobile phase was a mixture of solvent A (0.2 % formic acid in water) and B (acetonitrile) in a gradient mode: 0–1.5 min 95 % A, 1.5–12 min 95–5 % A, 12–15 min 5 % A, 15–16 min 5–95 % A. The data were processed by means of a Mass Hunter Workstation.

RESULTS AND DISCUSSION

Strain *P. aeruginosa* san-ai, isolated from an unusual extremely alkaline environment with high content of hydrocarbons (mineral cutting oil), was investigated to determine its capability to produce rhamnolipids (RLs) on different sources of carbon and nitrogen.[12] Potential of *P. aeruginosa* san ai to produce RLs was compared to that of a referent strain ATCC 27853 and the strain *P. aeruginosa* 67, isolated from a biopile with a high level of petroleum hydrocarbons.

Selection of the basic medium

Pseudomonas sp. produce rhamnolipids as secondary metabolites and the production, among other things, depends on the general medium composition, particularly on the sources of carbon and nitrogen, as well as the total C/N ratio.[8,20–24] LB, MSM and PPAS medium were investigated to find the optimal base for testing the influence of carbon and nitrogen sources on the production of RLs by *P. aeruginosa* san-ai. All media were supplemented with olive oil as a source of carbon, which according to the literature provides the greatest production of rhamnolipids.[8] The production of rhamnolipids on LB, MSM, and PPAS medium was found to be 15.5, 10.7, and 1010.4 mg L^{-1}, respectively, indicating that PPAS is the optimal base to improve rhamnolipid production, which is in good agreement with previously reported data.[14]

Influence of carbon source on the production of RL

Results obtained by testing sunflower oil, olive oil, metal cutting oil, kerosene, frying sunflower oil, ethanol, glucose, glycerol, a combination of glucose and sunflower, and sunflower mill effluent on the production of RL by *P. aeruginosa* san-ai in PPAS medium are shown in Fig. 2a. The histogram shows that the yield of RL was the highest on sunflower (1.35 g L^{-1}) and olive oil (1.01 g L^{-1}). A high production of RL was achieved on the frying sunflower oil (0.96 g L^{-1}), suggesting the possibility of using this substrate as a renewable source. Low producti on

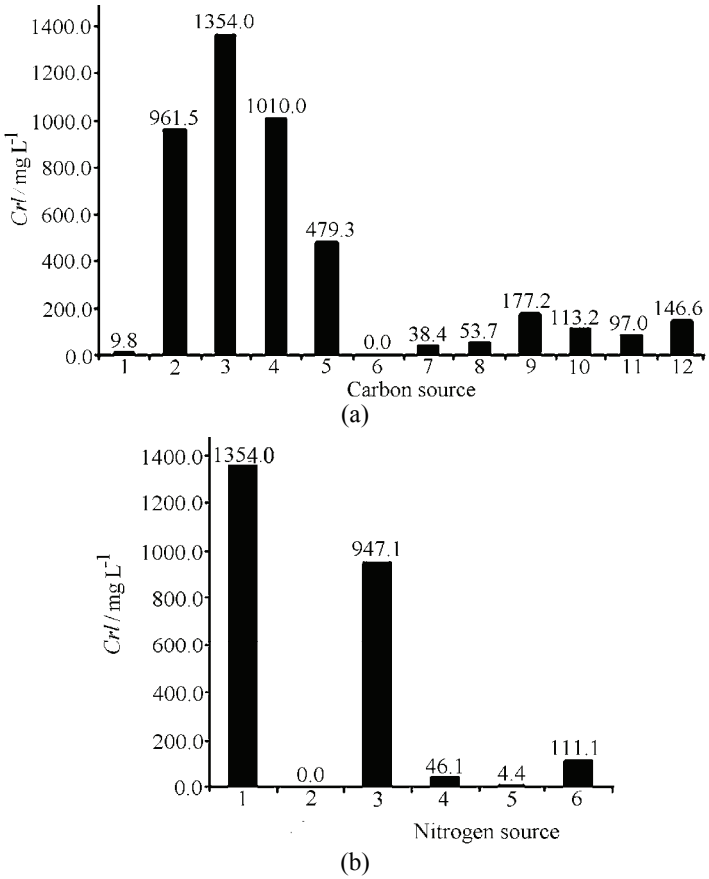

Fig. 2. a) Effect of different sources of carbon on the production of RL by *P. aeruginosa* san-ai. PPAS medium with (2 %): 1 – kerosene, 2 – frying sunflower oil, 3 – sunflower oil, 4 – olive oil, 5 – sunflower oil and glucose, 6 – metal cutting oil and glucose, 7 – ethanol, 8 – glycerol, 9 – glucose, 10 – sunflower mill effluent suspension, 11 – sunflower mill effluent emulsion; 12 – 0.5 % glucose (basic PPAS[14]). b) Effect of different sources of nitrogen on the production of RL by *P. aeruginosa* san-ai. PPAS medium with 2 % of sunflower oil, supplemented with (1 %): 1 – peptone I (control), 2 – whey, 3 – meat extract, 4 – yeast extract, 5 – soy flour, 6 – tryptone.

was detected on sunflower oil mill effluent and the other sources of carbon (kerosene, ethanol, glycerol, metal cutting oil, a combination of sugar and sunflower oil, glucose). Thus, sunflower oil was selected as the optimal carbon source.

Using PPAS medium supplemented with sunflower oil as a source of carbon and six different nitrogen sources: whey, meat extract, yeast extract, soybean flour, tryptone, peptone I, their effect on the production of RL by *P. aeruginosa* san-ai was tested. Preliminary experiments (data not shown) with urea, sodium nitrate and ammonium chloride as unique N-sources, showed that these sources were not suitable for a minimal growth of the culture, giving extremely low productions of RL. Fig. 2b shows that the highest production of rhamnolipid was achieved using peptone I (1.35 g L^{-1}) and meat extract (0.95 g L^{-1}). Production of RL on yeast extract, soy flour, tryptone and the whey was low or undetectable. Therefore, peptone I was selected as the optimal nitrogen source.

After selection of the optimal carbon (sunflower oil) and the optimal nitrogen sources (peptone I), *P. aeruginosa* san-ai on improved PPAS medium gave an RL production of 3.1 g L^{-1}. Under the same conditions, the productions of RL by *P. aeruginosa* ATCC 27853 and *P. aeruginosa* 67 were found to be 1.2 and 0.8 g L^{-1}, respectively. Compared to *P. aeruginosa* san-ai, both strains exhibited lower productions of RL. Interestingly, despite being isolated from an environment with a high content of hydrocarbon derivates (similar to the natural environment of *P. aeruginosa* san-ai), strain 67 produced less RL than strain san-ai.

This study showed that good substrates for the production of RL were vegetable oils, including oil wastes, as a carbon source and peptone I as an organic nitrogen source, which differs significantly from producing strains reported in the literature. Namely, glucose, glycerol and olive oil in combination with inorganic nitrogen were found to be preferential sources for RL production giving a high yield of 1.2–7.65 g L^{-1} of RL, respectively.[22–27] In addition, industrial waste and byproducts, such as whey waste, with yield of 0.92 g L^{-1} of RL, and molasses and corn steep liquor, both with yield of 0.25 g L^{-1} of RL, showed themselves to be relatively good substrates.

Comparison of the production of rhamnolipids by *P. aeruginosa* grown in LB, as a commonly used medium and the optimized PPAS medium, which were found to be 15 and 3000 mg L^{-1}, respectively, clearly shows the potential of *P. aeruginosa* san-ai for enhanced RL production.

Dynamics of fermentation on optimized medium

Production of RL by *P. aeruginosa* san-ai on optimized medium (PPAS supplemented with sunflower oil, as carbon source and ammonium chloride and peptone I as nitrogen sources) for a period of 8 days was monitored and the results are shown in Fig. 3a. Obviously, a significant production of RL begins after the third day of fermentation, when the bacterial population is in a stationary phase of growth, which is consistent with the fact that RL, as a secondary metabolite,

was produced after the phase of intensive growth. c_{rl} varied considerably during the fermentation with a maximum production of RL on the fourth day (3.0 g L^{-1}) with an *OD* of 2.2, while on the seventh day, the yield of 4.6 g L^{-1} RL, with a culture *OD* of 0.25, was the result of cell lysis.

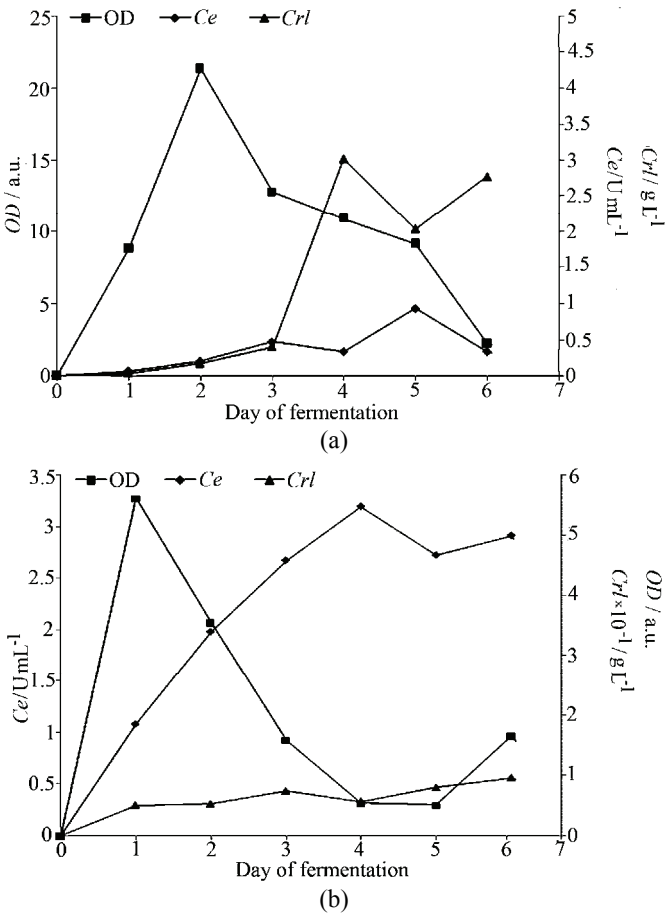

Fig. 3. Dynamics of the growth (*OD*), production of RL (c_{rl}) and lipase activity (c_e) of *P. aeruginosa* san-ai on: a) optimized PPAS medium (sunflower oil and peptone I) and b) LB medium.

Comparison of the dynamics of the fermentation (*OD*, c_{rl} and c_e) on the optimized PPAS medium (Fig. 3a) and the commonly used LB medium (Fig. 3b) showed differences. The bacterial culture was more active on the optimized medium, giving five times higher growth and favoring rhamnolipid production (30 times higher) than the LB medium. Interesting, on the other hand, the composition of the LB medium was more suitable for enzyme synthesis, giving a higher lipase production. The observed differences between the growth of the culture

and the production of rhamnolipids and lipase are related to cell-to-cell communication. Namely, rhamnolipids play a vital role in regulating the cell population density-dependent control of genes expression, termed quorum sensing (QS).[10] Observed cell density changes and exchanged activity of extracellular lipase, as indicators of QS response on environmental change clearly suggest that the effect of nutritional compounds should be considered in the context of environmental regulation of the *P. aeruginosa* QS system.[28]

RSM Analysis

The highest production of RL achieved by the one-factor-at-a-time approach was found to be 3 g L^{-1}. Analysis of the effect of temperature and the concentrations of the carbon and nitrogen sources on RL production on the optimized PPAS medium was made by the RSM experimental design methodology. A similar approach based on the combination of the one-factor-at-a-time and the statistical experimental design methodology for enhanced RL production was recently reported.[19] For the RSM analysis, 17 experiments were conducted under a three-factorial Box–Behnken (BC) design. The value of the *F*-test of 3.51 and *P* value of 0.0389 indicate that the model was adequate for describing the obtained experimental results, the *P* value BC model term (combination of temperature and concentration of nitrogen source) of 0.0167 was significant. The equation of the statistical model is:

$$Y = 1.42 - 0.50A - 0.78B - 0.36C + 1.06AB + 0.37AC + 1.44BC$$

where *A*, *B*, *C* and *Y* correspond to the sunflower oil and peptone I content, %, temperature, °C, and c_{rl}, g L^{-1}, respectively. The results of the experimental runs and points are given in Table I. The 3D response surface shows the effect of pep-

TABLE I. Experimental RSM design according to the Box–Behnken method, for rhamnolipid production on optimized medium with a total C/N ratio of medium per run

Run	Carbon source %	Nitrogen source %	Temperature °C	Total C/N ratio	c_{rl} / g L^{-1}
1	6.00	4.00	30	9.78	0.36
2, 4, 9,12, 14	3.50	2.25	30	8.73	1.59
3	3.50	0.50	20	12.83	4.07
5	6.00	0.50	30	19.51	0
6	3.50	4.00	20	7.10	0.83
7	6.00	2.25	20	12.55	0.26
8	1.00	2.25	20	4.83	0.68
10	3.50	4.00	40	7.10	1.56
11	6.00	2.25	40	12.55	1.72
13	1.00	0.50	30	5.68	3.00
15	3.50	0.50	40	12.83	0.05
16	1.00	2.25	40	4.83	0.67
17	1.00	4.00	30	4.39	0.56

tone I and temperature (sunflower oil, 3.5 %) (Fig. 4). The optimal response predicted by the RSM was found to be 4.07 g L^{-1} of RL, obtained with 3.5 % sunflower oil and 0.5 % peptone I (C/N ratio 12.83), at 20 °C. With 1 % sunflower oil and 0.5 % peptone I (C/N ratio 5.68) at 30 °C, a rhamnolipid concentration of 3.00 g L^{-1} was achieved.

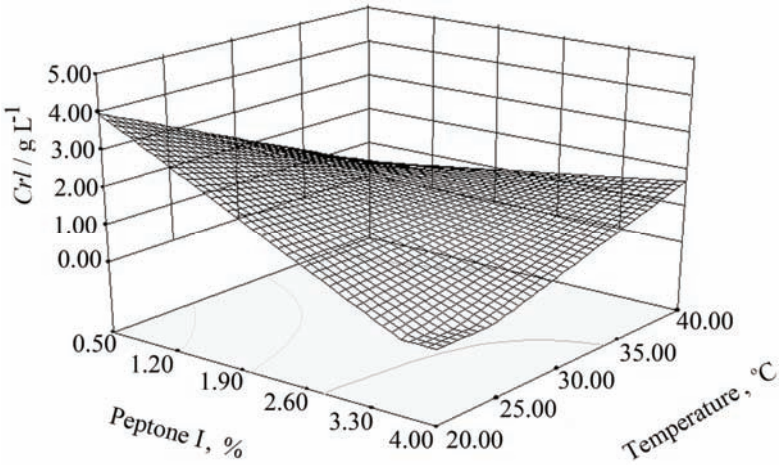

Fig. 4. 3D surface graph: effect of temperature and concentration of nitrogen source, with a 3.5 % concentration of the carbon source, on rhamnolipid production by *P. aeruginosa* san-ai.

Comparison of C/N ratio in the basic, one-factor-at-a-time optimized and RSM optimized PPAS medium for the highest yield showed a C/N ratio of 4.0, 7.7 to 12.83, respectively. This correlates with the fact that the evaluated C/N conditions gave higher yield of rhamnolipids.[7–9] However, this C/N ratio is strongly affected by temperature, as Table I indicates.

A previously reported optimization of rhamnolipid production by *P. aeruginosa* san-ai on LB medium using RSM analysis gave a yield of only 138 mg L^{-1}.[29] Thus, the present combined one-factor-at-a-time and statistical approach to enhance the production of RL gave an over 30 times better yield than using only RSM on a single basic medium.

Characterization of the RL

IR analysis. The IR spectrum of rhamnolipid from *P. aeruginosa* san-ai is shown in Fig. 5. The fingerprint areas between 400–1500 cm^{-1} showed the deformation C–OH band at 1384 cm^{-1}, the O–H in plane deformation at 1315 cm^{-1}, the O–C–O symmetric band at 1047 cm^{-1}, the C–O stretching at 1168, 1127 and 1047 cm^{-1}, C–H deformations at 1451, 1238 and 808 cm^{-1} and CH_3 rocking at 983 cm^{-1} for RL. There are also the typical stretching vibrations of the COO^- group. The strong symmetric stretching C=O band of the carboxylate group of

RL was at 1739 cm^{-1}. The IR spectra of RL gave absorption bands at 3360 cm^{-1} for symmetric O–H stretching. The spectrum also showed vibrations at 2928 cm^{-1} and 2856 cm^{-1} typical for the C–H stretching vibrations of CH_2 and CH_3 groups. The results are in a good agreement with a typical IR spectrum of rhamnolipids.[30]

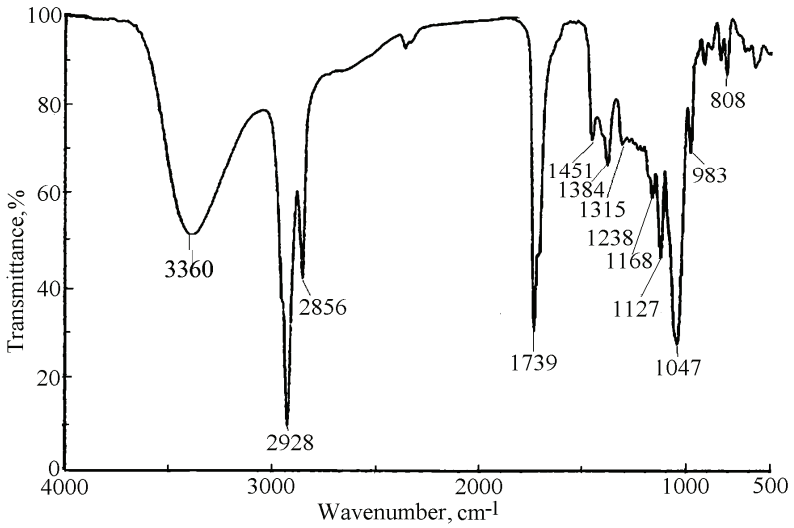

Fig. 5. IR Spectrum of rhamnolipid showing the following vibrations: C–H stretching asym. (2928 and 2856 cm^{-1}), C=O stretching (1739 cm^{-1}), C–H deformations (1451, 1238 and 808 cm^{-1}), C–H/O–H deformation (1384 cm^{-1}), O–H in plane deformation (1315 cm^{-1}), C–O stretching (1168, 1127 and 1047 cm^{-1}), CH_3 rocking (983 cm^{-1}).

HPLC–ESI-MS analysis. A list of the rhamnolipid congeners detected by HPLC–MS-ESI analysis with their molecular formulas, molecular weights, retention time and abundance of M^- and $[M–H]^-$ is given in Table II. The mass spectra of Rha-C10, Rha-C10- C10:1/Rha-C10:1-C10 and Rha-Rha-C10-C12:1/Rha--Rha-C12:1-C10 observed by ESI–MS in the negative mode are given in Figs. 6–8. Table II shows a list of the detected rhamnolipid congeners with their molecular formulas, weights and relative abundance of M^- and $[M–H]^-$. The strain *P. aeruginosa* san ai produces a unique mixture of rhamnolipids composed of: Rha-C8, Rha-C10, Rha-C12, Rha-C8-C10/Rha-C8-C10, Rha-C10-C10:1/Rha-C10:1-C10, Rha-C8-C12/Rha-C12-C8//Rha-C10-C10, Rha-C10-C12:1/Rha-C12:1-C10, Rha-C10-C12/Rha-C12-C10, Rha-C10-C14/Rha-C14-C10//Rha-C12-C12, Rha-C10-C10-CH3, Rha-Rha-C10-C10, Rha-Rha-C10-C12/Rha-Rha-C12-C10, Rha-Rha-C10-C12:1/Rha-Rha-C12:1-C10, Rha-Rha-C10-C14:1/Rha-Rha-C14:1-C10//Rha-Rha-C12-C12:1 and Rha-Rha-C10-C10-CH3. Thus, the most frequent were mono-rhamno-di-lipidic (7 detected), followed by di-rhamno-di-lipidic (5

detected) and mono-rhamno-mono-lipidic (3 detected) congeners. The relative abundance of M^- and $[M–H]^-$ of mono-rhamno-mono-lipidic, mono-rhamno-di-lipidic and di-rhamno-di-lipidic structures were 1.83, 53.15 and 44.77 %, respectively.[31] The most abundant (12 %) individual congeners were ions of Rha-C8-C10/Rha-C8-C10, Rha-C8-C12/Rha-C12-C8//Rha-C10-C10, Rha-C10-C12//Rha-C12-C10, Rha-Rha-C10-C10, Rha-Rha-C10-C12:1/Rha-Rha-C12:1-C10.

TABLE II. List of rhamnolipid congeners detected by HPLC–MS-ESI analysis with their molecular formulas, molecular weights, retention time and abundance of M^- and $[M–H]^-$

Rhamnolipid congener	Molecular formula	Molecular weight g mol^{-1}	Retention time, min	Relative abundance of M^- + $[M–H]^-$, %
Rha-C8	$C_{14}H_{26}O_7$	306.17	10.29	0.06
Rha-C10	$C_{16}H_{30}O_7$	334.20	8.05	1.61
Rha-C12	$C_{18}H_{34}O_7$	362.23	9.22	0.16
Rha-C8-C10/Rha-C10-C8	$C_{24}H_{44}O_9$	476.30	11.16	12.64
Rha-C10-C10:1/Rha-C10:1-C10	$C_{26}H_{46}O_9$	502.31	11.88	6.95
Rha-C8-C12/Rha-C12-C8//Rha-C10-C10	$C_{26}H_{48}O_9$	504.33	12.34	12.71
Rha-C10-C12:1/Rha-C12:1-C10	$C_{28}H_{50}O_9$	530.34	12.98	4.40
Rha-C10-C12/Rha-C12-C10	$C_{28}H_{52}O_9$	532.36	13.43	12.48
Rha-C10-C14/Rha-C14-C10//Rha-C12-C12	$C_{30}H_{56}O_9$	560.39	14.40	1.50
Rha-C10-C10-CH3	$C_{27}H_{50}O_9$	518.34	12.89	2.47
Rha-Rha-C10-C10	$C_{32}H_{58}O_{13}$	650.39	11.55	12.47
Rha-Rha-C10-C12:1/Rha-Rha-C12:1-C10	$C_{34}H_{60}O_{13}$	676.40	11.98	12.32
Rha-Rha-C10-C12/Rha-Rha-C12-C10	$C_{34}H_{62}O_{13}$	678.42	13.30	0.13
Rha-Rha-C10-C10-CH3	$C_{33}H_{60}O_{13}$	664.40	12.11	8.64
Rha-Rha-C10-C14:1/Rha-Rha-C14:1-C10//Rha-Rha-C12-C12:1	$C_{36}H_{64}O_{13}$	704.43	13.76	11.21

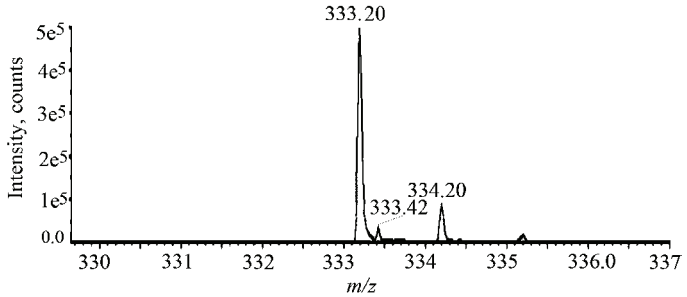

Fig. 6. MS spectrum of mono-rhamno-mono-lipidic Rha-C10 rhamnolipid congener detected in the rhamnolipid mixture produced by *P. aeruginosa* san-ai.

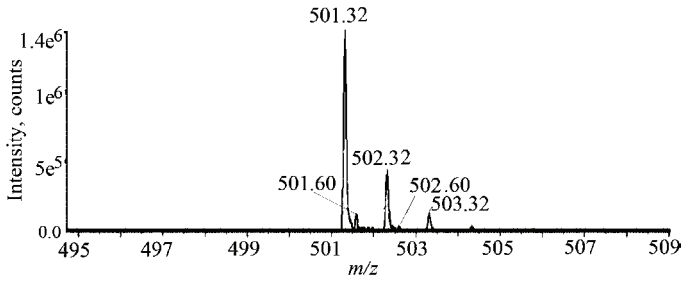

Fig. 7. MS spectrum of mono-rhamno-di-lipidic Rha-C10-C10:1/Rha-C10:1-C10 rhamnolipid congener detected in the rhamnolipid mixture produced by *P. aeruginosa* san-ai.

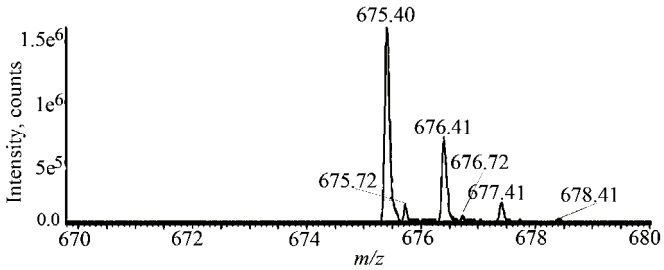

Fig. 8. MS spectrum of di-rhamno-di-lipidic Rha-Rha-C10-C12:1/Rha-Rha-C12:1-C10 rhamnolipid congener detected in the rhamnolipid mixture produced by *P. aeruginosa* san-ai.

CONCLUSIONS

Rhamnolipid production by the *P. aeruginosa* san-ai strain was significantly enhanced on optimized PPAS medium. The tested carbon and nitrogen sources indicated that the strain *P. aeruginosa* san-ai also grew and produced RL on waste raw materials (oil from the fryers and sunflower mill effluent). PPAS medium supplemented with sunflower oil as a source of carbon and ammonium chloride and peptone as nitrogen sources greatly improved rhamnolipid production, from 0.15 g L^{-1} on basic PPAS (C/N ratio 4.0) to 3 g L^{-1} on the optimized PPAS medium (C/N ratio 7.7). A comparison of the production of rhamnolipids by *P. aeruginosa* grown in LB, a commonly used medium, and optimized PPAS showed the production to 15 and 3000 mg L^{-1}, respectively, clearly showing the potential of *P. aeruginosa* san-ai for enhanced RL production. Further elevation of RL production on optimized PPAS was achieved by RSM analysis of the concentrations of the carbon and nitrogen sources, and temperature. The best yield of 4.07 g L^{-1} was achieved at 20 °C with a carbon concentration of 3.5 % and a 0.5 % concentration of nitrogen sources with a C/N ratio of 12.83. Compared to the referent *P. aeruginosa* ATCC 27853 strain and strain 67 isolated from biopile, the strain *P. aeruginosa* san-ai has a much better potential for RL production.

As confirmed by MS analysis, the rhamnolipid produced by *P. aeruginosa* san-ai is a mixture of different rhamnolipidic congeners (mono-rhamno-mono-

-lipidic, mono-rhamno-di-lipidic and di-rhamno-di-lipidic). The mono-rhamno--di-lipidic congener had the highest relative abundance of M^- and $[M–H]^-$.

Acknowledgment. This work was supported by the Ministry of Education and Science of the Republic of Serbia through Project No. III 43004. Authors thank Dr. D. Bezbradica from the Faculty of Technology and Metallurgy, Belgrade, for his assistance with the RSM analysis, Milka Jadranin, M. Sc., from the Department of Chemistry, ICTM, Belgrade, for the MS–ESI analysis and Dr. N. Fujiwara from the Institute for Technological Research (TRI), Osaka, Japan for the donation of the strain *P. aeruginosa* san-ai.

ИЗВОД

ПРОДУКЦИЈА И КАРАКТЕРИЗАЦИЈА РАМНОЛИПИДА СОЈА *Pseudomonas aeruginosa* SAN-AI

МИЛЕНА Г. РИКАЛОВИЋ[1], ГОРДАНА ГОЈГИЋ-ЦВИЈОВИЋ[2], МИРОСЛАВ М. ВРВИЋ[1,2] и ИВАНКА КАРАЦИЋ[3]

[1]Хемијски факултет, Универзитет у Београду, Студентски трг 12–16, Београд, [2]Центар за хемију ИХТМ, Универзитет у Београду, Његошева 12, Београд и [3]Медицински факултет, Хемијски институт, Универзитет у Београду, Вишеградска 26, Београд

У овом раду је описана продукција и карактеризација рамнолипидног биосурфактанта соја *Pseudomonas aeruginosa* san-ai. Испитан је утицај различитих извора угљеника и азота на продукцију рамнолипида. Подлога протеозе пептон-амонијум соли са ограниченом количином фосфата (PPAS) са сунцокретовим уљем као извором угљеника и амонијум-хлоридом и пептоном као извором азота, знатно повећава продукцију рамнолипида, од 0,15, на PPAS са стандардним саставом (однос C/N 4,0), до 3 g L^{-1} на оптимизованој PPAS подлози (однос C/N 7,7). Методом планираног експеримента (*response surface methodology*) испитан је ефекат три параметра: температуре, концентрације извора угљеника и азота на оптимизованој подлози. Карактеризација изолованог препарата рамнолипида урађена је помоћу IR и ESI-MS анализа. IR анализа је потврдила присуство структурних елемената карактеристичних за рамнолипиде. MS анализа показала је да реч о смеши у којој су присутне моно-рамно-моно-липидне, ди-рамно-моно-липидне и ди-рамно-ди-липидне компоненте.

(Примљено 11. фебруара, ревидирано 3. августа 2011)

REFERENCES

1. J. D. Desai, I. M. Banat, *Microbiol. Mol. Biol. Rev*. **61** (1997) 47
2. J. D. Van Hamme, A. Singh, O. P. Ward, *Biotechnol. Adv*. **24** (2006) 604
3. M. Nitschke, S. G. V. A. O. Costa, *Trends Food Sci. Technol*. **18** (2007) 252
4. A. Singh, J. D. Van Hamme, O. P. Ward, *Biotechnol. Adv*. **25** (2007) 99
5. S. Maneerat, *Songklanakarin J. Sci. Technol.* **27** (2005) 676
6. K. Muthusamy, S. Gopalakrishnan, T. K. Ravi, P. Sivachidambaram, *Curr. Sci*. **94** (2008) 736
7. A. Tahzibi, F. Kamal, M. M. Assadi, *Iran Biomed. J*. **8** (2004) 25
8. G. Soberón-Chávez, F. Lépine, E. Déziel, *Appl. Microbiol. Biotechnol*. **68** (2005) 718
9. C. Chayabutra, J. Wu, L. K. Ju, *Biotechnol. Bioeng*. **72** (2001) 25
10. K. Duan, M. G. Surette, *J. Bacteriol*. **189** (2007) 4827
11. K. Heurlier, F. Williams, S. Heeb, C. Dormond, G. Pessi, D. Singer, M. Cámara, P. Williams, D. Haas, *J. Bacteriol.* **186** (2004)
12. I. Karadzic, A. Masui, N. Fujiwara, *J. Biosci. Bioeng*. **98** (2004) 145

13. V. P. Beskoski, G. Dj. Gojgic-Cvijovic, J. Milic, M. Ilic, S. B. Miletic, T. M. Solevic, M. M. Vrvic, *Chemosphere* **83** (2011) 34
14. N. W. Gunther, A. Nunez A, W. Fett, D. K. Y. Solaiman, *Appl. Environ. Microbiol.* **71** (2005) 2288
15. J. Y. Wu, K. L. Yeh, W. B. Lu, C. L. Lin, J. S. Chang, *Bioresour. Technol*. **99** (2008) 1157
16. M. Heyd, A. Kohnert, T. H. Tan, M. Nusser, F. Kirschhöfer, G. Brenner-Weiss, M. Franzreb, S. Berensmeier, *Anal. Bioanal. Chem*. **391** (2008) 1579
17. Q. Wang, X. Fang, B. Bai, X. Liang, P. J. Shuler, W. A. Goddard III, Y. Tang, *Biotechnol. Bioeng*. **98** (2007) 842
18. S. Wilhelm, A. Gdynia, P. Tielen, F. Rosenau, K. E. Jaeger, *J. Bacteriol*. 189 (2007) 6695
19. Y. H. Wei, C. L. Cheng, C. C. Chien, H. M. Wan, *Process Biochem*. **43** (2008) 769
20. E. R. B. Moore, B. J. Tindall, V. A. P. Martins dos Santos, D. H. Pieper, J. L. Ramos, N. J. Palleroni, *Prokaryotes*, Springer, Singapore, 2006, p. 646
21. M. Abouseoud, R. Maachi, A. Amrane, S. Boudergua, A. Nabi, *Desalination* **223** (2008) 143
22. M. Robert, E. Mercado, I. P. Bosch, J. L. Parra, M. J. Espuny, M. A. Manresa, J. Guinea, *Biotechnol. Lett*. **2** (1989) 871
23. H. Rashedi, E. Jamshidi, M. Mazaheri Assadi, B. Bonakdarpour, *Iranian J. Chem. Eng*. **25** (2006) 25
24. L. M. Santa Anna, G. V. Sebastian, E. P. Menezes, T. L. Alves, A. S. Santos, N. Pereira, D. M. G. Fereire, *Braz. J. Chem. Eng*. **19** (2002) 154
25. K. Dubey, A. Juwarkar, *Indian J. Biotechnol*. **3** (2004) 74
26. R. M. Patel, A. J. Desai, *Lett. Appl. Microbiol.* **25** (1997) 91
27. E. Haba, M. J. Espuny, M. Busquets, A. Manresa, *J. Appl. Microbiol*. **88** (2000) 379
28. F. Leitermann, C. Syldatk, R. Hausmann, *J. Biol. Eng.* **2** (2008) 13
29. D. Bezbradica, S. Jankovetic, S. Grbavcic, N. Avramovic, N. Milosavic, Z. Knezevic-Jugovic, I. Karadzic, in *Proceeding of the 47th Meeting of the Serbian Chemical Society*, (2009), Proceedings, Serbian Chemical Society, Belgrade, Serbia, 2009, p. 168
30. A. M. Abdel-Mawgoud, F. Lépine, E. Déziel, *Appl. Microbiol. Biotechnol*. **86** (2010) 1323
31. J. Arutchelvi, M. Doble, *Lett. Appl. Microbiol*. **51** (2010) 75.

Journal of the Serbian Chemical Society
JSCS-info@shd.org.rs • www.shd.org.rs/JSCS
J. Serb. Chem. Soc. *77* (1) 43–52 (2012)
JSCS–4247
UDC *Escherichia coli*:634.773:547.455.623
Original scientific paper

Optimization of the heterologous expression of banana glucanase in *Escherichia coli*

MOHAMED ABUGHREN[1], MILICA POPOVIĆ[1], RAJNA DIMITRIJEVIĆ[2#], LIDIJA BURAZER[3], MILICA GROZDANOVIĆ[1#], MARINA ATANASKOVIĆ-MARKOVIĆ[4] and MARIJA GAVROVIĆ-JANKULOVIĆ[1*#]

[1]*Faculty of Chemistry, University of Belgrade, Belgrade, Serbia,* [2]*Innovation Center of the Faculty of Chemistry, University of Belgrade, Belgrade, Serbia,* [3]*Institute of Virology, Vaccines and Sera, Torlak, Belgrade, Serbia and* [4]*University Children's Hospital, Medical Faculty, University of Belgrade, Belgrade, Serbia*

(Received 9 March, revised 21 June 2011)

Abstract: For the heterologous production of a banana glucanase in *Escherichia coli*, its gene (GenBank GQ268963) was cloned into a pG EX-4T expression vector as a fusion protein wit h glutathione-*S*-transferase (GST). BL21 cells transformed with the GST-Mus a 5 con struct were employed for production of the protein induced by 1 mM isopropyl-*β*-D-thiogalactopyranoside (IPTG). The conditions for protein expression were opti mized by varying the tem perature (25, 30 and 37 °C) and duration of protein expression (3, 6 and 12 h). The level of protein production was analyzed by densitometry of the sodium dodecyl sulfate–polyacrylamide gel (SDS–PAG) after electrophoretic resolution of the respective cell lysates. The optimal protein expression for downstream processing was obtained after 12 h of cell growth at 25 °C upon addition of IPTG. Recombinant GST-Mus a 5 purified by glutathione affinity chromatography revealed a molecular mass of a bout 60 kDa. The IgE and IgG reactivity of the rGST-Mus a 5 was confirmed by dot blot an alysis with sera of individual patients from subjects with banana allergy and polyclonal rabbit antibodies against banana extract, respectively. The purified reco mbinant glucanase is a potential candidate for banana allergy diagnosis.

Keywords: food allergen; protein expression; glucanase.

INTRODUCTION

Immunoglobulin E (IgE)-mediated allergy affects more that 25 % of the world's population, and b elongs to the most chronic disorders in m odern society.[1] The key issue for the treat ment of allergies is the em ployment of reliable diagnostic reagents. The allergen extracts currently employed for diagnosis re-

* Corresponding author. E-mail: mgavrov@chem.bg.ac.rs
# Serbian Chemical Society member.
doi: 10.2298/JSC110309158A

present mixtures of allergens and non-allergenic material. Diagnostic tests for food allergy frequently have poor specificity and sensitivity,[2] as the quality of allergen extracts from fruits and other plant-derived foods can vary due to the inherent presence of proteolytic enzymes, the ripening stage and/or storage conditions of the allergenic source materials.[3,4] Therefore, replacement of allergen extracts with a panel of IgE reactive molecules from an allergen source is a promising strategy for the improvement of allergy diagnostics. A panel of three cherry recombinant allergens was superior to diagnostic methods based on cherry extract.[5] In this respect, the evaluation of allergenic properties of a particular allergen candidate for component-resolved diagnostics needs to be performed.

Allergy to banana fruit has been reported as an isolated allergy, but sometimes it is associated with pollen or latex allergy.[6] Component-resolved diagnostics (CRD) of allergy to plant foods is essential for the clinical management of allergic patients.[7] Specific IgE immunodetection has enabled the identification of several IgE binding components in banana fruit, covering a wide range of molecular sizes. However, putative allergens of 30–37 kDa are the most frequently recognized in the sera from allergic patients.[8–10] The molecular basis of banana allergy has been ascribed to five IUIS (www.allergen.org) nominated allergens: profilin (Mus a 1), class I chitinase (Mus a 2), non-specific lipid transfer protein (Mus a 3), thaumatin-like protein (Mus a 4) and beta-1,3-glucanase (Mus a 5).

Most fruit allergens are structurally and evolutionary related to "pathogenesis-related proteins" (PR-proteins).[11] Beta-1,3-glucanase belongs to the PR-2 family of proteins and is involved not only in plant defense, but also in diverse physiological and developmental processes. Besides banana fruit,[12] IgE reactive beta-1,3-glucanases were found in several pollens (olive, ash and birch), vegetables (tomato, potato and bell pepper) and latex.[13,14] Palomares *et al.* showed that beta-1,3-glucanases contribute to the latex–pollen–vegetable food cross-reactivity,[14] In addition, an occupational allergy due to Ole e 9, glucanase from olive pollen has been reported.[15] The crystal structure of the banana glucanase has been revealed and its three-dimensional structure exhibits a canonical $(\beta/\alpha)_8$ TIM-barrel motif found in other glucan endohydrolases.[16]

The aim of this work was to optimize the procedure for recombinant banana glucanase (Mus a 5) production in *E. coli* and its downstream processing for potential application in component-resolved allergy diagnostics.

EXPERIMENTAL

Bacterial strain and construct

E. coli BL21-CodonPlus (DE3)-RIPL cells, kindly provided by Dr Knud Poulsen (University of Aarhus, Denmark), were transformed with the construct pGEX-4T-glucanase denoted as rGST-Mus a 5. The cloning strategy was to produce recombinant Mus a 5 (GenBank GQ268963) with glutathione-*S*-transferase as an expression tag on the *N*-terminal. Total RNA was isolated from banana fruit by an RNeasy Plant Mini Kit (Qiagen, Hilden, Germany)

according to the manufacturer's instructions. Cyclic-DNA (cDNA) was transcribed by a RevertAid^{TM} First Strand cDNA synthesis kit (Fermentas UAB, Vilnius, Lithuania). For amplification of the mature gene of Musa 5, sense and antisense – specific primers with EcoR I and Xho I restriction sites (marked in italic) 5'-GAATTCATTGGTGTCTGCTACGG-3' and 5'-CTCGAGCTAAAAGCTTATTTGGTAGAC-3' were used, respectively. The amplified Musa 5-encoding fragment, was cloned into a pGEX-4T vector. The construct was verified by DNA sequencing.

Cell growth and induction of protein expression

Inocula were prepared from transformed BL21 cells that were grown overnight at 37 °C in LB medium (1 g L^{-1} tryptone, 5 g L^{-1} yeast extract, 5 g L^{-1} NaCl, 2 g L^{-1} glucose) containing 100 mg L^{-1} ampicillin, 25 mg L^{-1} chloramphenicol and 25 mg L^{-1} kanamycin. The culture (0.5 mL) was introduced into 10 mL of LB medium containing the respective antibiotics. Once the absorbance (OD_{600}) reached a value of 0.6 following an initial growth phase, protein expression was induced with 1 mM IPTG (Fermentas), and the cells were grown at 25, 30 or 37 °C. Following induction of protein expression, aliquots (1 mL) were taken after 3, 6 and 12 h.

SDS–PAGE analysis

The GST-Musa 5 protein expression was analyzed in cell lysates of induced and non-induced bacteria by SDS–PAG electrophoresis under reducing conditions, as outlined by Laemmli.[17] In brief, prior to separation on 14 % SDS–PAG, cell lysates (100 μg) were incubated in sample buffer (6 mM Tris–HCl, 5 % 2-mercaptoethanol, 2 % SDS and 25 % glycerol) for 5 min at 95 °C and centrifuged (14000×g, 1 min). After electrophoresis, the proteins in the gel were stained with Coomassie brilliant blue (CBB-R250, Serva, Germany). For comparison of the level of rGST-Musa 5 protein expression under different experimental conditions, the SDS–PAG was scanned for densitometric quantification using GelPro Analyzer 3.1 (Media Cybernetics).

Isolation of rGST-Musa 5

Recombinant GST-Musa 5 was purified from a BL21 cell culture (100 mL), after 12 h of protein expression at 25 °C. The cells were harvested by centrifugation (3000×*g*, 15 min), and the pellet was suspended in 25 mL of ice-cold L buffer (5 mM Tris–HCl, pH 8.0, 10 mM NaCl, 5 mM EDTA, 0.1 % NaN_3 and 0.1 % Na-deoxycholate). Immediately before use, PMSF (0.1 mM) and DTT (1 mM) were added to the L buffer. After sonication (3×20 s, 20 rms, Branson Sonifier 150), $MgSO_4$ (1 mM), benzonase (0.01 mg mL^{-1}, Novagen) and lysozyme (0.1 mg mL^{-1}, Serva, Germany) were added to the cell lysate, which was further incubated at RT for 15 min. To collect the insoluble fraction (IF), the cell lysate was centrifuged (3000×*g*, for 15 min). After two washings with the buffer (5 mM Tris–HCl, pH 8.0, 10 mM NaCl, 5 mM EDTA, 0.1 % NaN_3), the IF was solubilized in S buffer (10 mM Tris, 5 mM glycine, 6 M urea, pH 8.0). Protein refolding was achieved by rapid mixing of denatured protein solution with R buffer (30 mM NaCl, 2 mM Na_2HPO_4, 3.6 mM KH_2PO_4, pH 7.50; 1:7, v:v), in which a cocktail of protease inhibitors (1 mL L^{-1} of buffer) and oxidized (0.3 mM GSSG) and reduced glutathione (3 mM GSH) were added. The rGST-Musa 5 solution was applied onto a pre-equilibrated GST-Bind® resin (Novagen) according to the manufacturer's instruction.[18] The concentration of the rGST-Musa 5 protein was determined using a molar extinction coefficient of 1.434, which was calculated from the amino acid sequence by ProtParam (http://expasy.org/cgi-bin/protparam).

Production of the polyclonal antibodies to banana extract

Two rabbits were immunized according to the protocol described by Harlow and Lane.[19] In brief, 0.25 mL of banana extract (0.5 mg mL^{-1}) which was prepared according to Gavrović-Jankulović *et al.*[20] was mixed with 0.25 mL CFA (complete Freunds adjuvant) for the first immunization. Every 15 days, for four months, the rabbits were boosted with a mixture of 0.25 mL of the banana extract and 0.25 mL of IFA (incomplete Freunds adjuvant). Each rabbit was subcutaneously immunized with 0.5 mL of the emulsion. After four months, sera were collected and the antibodies were pooled and fractionated by ammonium sulfate (50% saturation). After dialysis against phosphate buffer saline (PBS) antibodies were aliquoted and stored in 20% glycerol at –20°C.

Dot blot

Six sera from persons with positive clinical history to banana allergy and positive skin prick test to banana extract were used for the evaluation of IgE reactivity of rGST-Mus a 5 in dot blot. A pool of three sera from persons without banana allergy was used as a control. Purified rGST-Mus a 5 (5 μg) was applied to a nitrocellulose membrane (NC) using 96-well dot blot hybridization manifold (VWR, Vienna, Austria). To discriminate IgE reactivity of the GST tag from IgE reactivity of glucanase, rGST was applied onto the NC membrane as a control. Membranes were blocked using 30 mM Tris buffer saline (TBS) pH 7.4, containing 5% w/v skimmed milk for 1 h at RT. Membranes were incubated with the pooled sera in 1 % skimmed milk in TBS (dilution, 1:3, v:v) overnight at RT. Goat anti-human IgE (dilution 1:10000, v:v) was used for detection of IgE binding. Alkaline phosphatase-labeled rabbit anti-goat IgE antibodies (dilution 1: 30000, v:v, Sigma) were used as the tertiary antibody. IgE reactive spots were visualized with BCIP/NBT solution.

For detection of IgG reactivity of rGST-Mus a 5, rabbit antibodies against banana extract were employed. After blocking, the membrane was incubated with the primary antibodies (dilution 1:5000) for 2 h at room temperature. After three washings, the membrane was incubated with alkaline phosphatase anti-rabbit antibodies (dilution 1:30000, Sigma–Aldrich, Missouri, USA) as previously described.[21]

IgG inhibition assay

For IgG inhibition assays natural Mus a 5[22] (5 μg) was applied to the NC membrane according to previously described procedure. After blocking, the respective membranes were incubated overnight with anti-banana rabbit antibodies, which had been previously incubated for 2 h with two different concentrations of rGST-Mus a 5 (5 and 50 μg mL^{-1}).

RESULTS AND DISCUSSION

Optimization of rGST-Mus a 5 expression

Structural homogeneity, batch-to-batch consistency and unlimited availability makes recombinantly produced proteins advantageous over their natural counterparts. Various expression systems have been adopted for recombinant protein production. Natural banana glucanase is a 32 kDa protein that possesses no post-translational modifications,[12] making prokaryotic cells a suitable option for its expression. Protein purification with a glutathione-*S*-transferase (GST) affinity tag, which was introduced in 1988 by Smith and Johnson,[23] is based on the strong affinity of GST for glutathione-covered matrices. In the GST gene fu-

sion system, expression is under the control of the *tac* promoter, which is induced using the lactose analogue IPTG. Induced cultures are allowed to express GST fusion proteins for several hours before the cells are harvested. *E. coli* BL21 is a protease-deficient strain specifically selected to give high efficiency transformation and high level of expression of GST fusion proteins.[24]

The cloning strategy of Mus a 5 into the pGEX expression vector is given in Fig. 1. For the optimization of the expression of a given protein construct, a time-course analysis of the level of protein expression in recommended.[25] Therefore, for the optimization of rGST-Mus a 5 expression upon induction of protein synthesis, BL21 (DE3) cells were grown at different temperatures, *i.e.*, 25, 30 and 37 °C. Aliquots taken after 3, 6 and 12 h upon rGST-Mus a 5 induction were analyzed by SDS–PAG electrophoresis. Densitometric comparison of the intensity of the rGST-Mus a 5 band with all other constitutively expressed proteins per line, revealed that the highest yield of expression was obtained after 12 h of induction of protein synthesis under all the tested temperatures (Fig. 2). The band of about

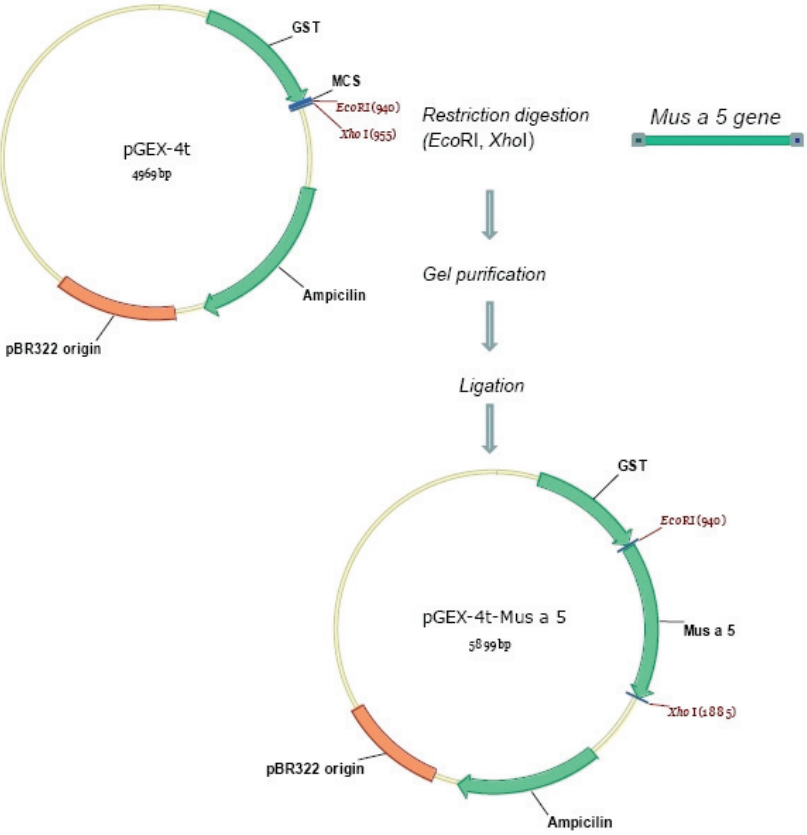

Fig. 1. Cloning of banana glucanase gene into the pGEX-4T vector.

60 kDa, representing rGST-Mus a 5, is predominant in all tested samples, except in the non-induced cells with the pGEX-4T-glucanase plasmid (Fig. 2, lane 1) and after 3 h of induction of protein synthesis at 25 °C (Fig. 2, lane 2). Taking into consideration the presence of other proteins in the cell lysates, the optimal conditions for the protein expression and further downstream purification was protein synthesis for 12 h at 25 °C.

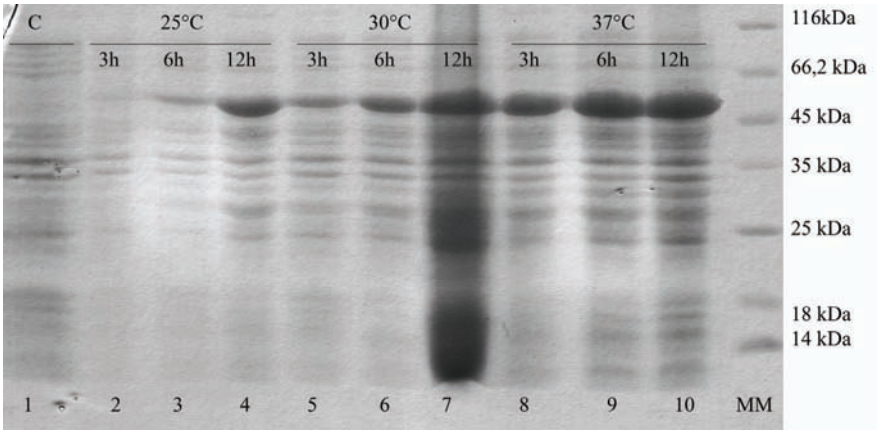

Fig. 2. Time course of rGST-Mus a 5 expression at 25, 30 and 37 °C. Expression of rGST-Mus a 5 was induced with 1 mM IPTG. Aliquots were removed at the times indicated. Proteins were visualized by Coomassie brilliant blue staining; line 1: control, MM: molecular markers.

Isolation of rGST-Mus a 5

Recombinant GST-Mus a 5 was isolated from BL21 cells by glutathione affinity chromatography. Prior to affinity purification, the cells were harvested by centrifugation and after resuspension were lysed with lysozyme. Benzonase was employed to reduce the viscosity of the cell lysate caused by nucleic acids. Further SDS–PAG electrophoresis revealed that rGST-Mus a 5 was accumulated in the insoluble fraction of the cell lysate, and its solubilization was achieved with 6 M urea. Prior to separation, denatured rGST-Mus a 5 was refolded by rapid batch dilution and subsequently applied onto an affinity column. The homogeneity of the isolated rGST-Mus a 5 was assessed by SDS-PAG electrophoresis, revealing a protein band of about 60 kDa (Fig. 3). The yield of the purified rGST-Mus a 5 was about 35 mg L^{-1} of LB, as calculated using the molar extinction coefficient for rGST-Mus a 5.

IgE and IgG reactivity of rGST-Mus a 5

The IgE reactivity of the rGST-Mus a 5 was examined by dot blot analysis using the sera of six banana allergic patients. To evaluate the IgE reactivity of the fusion tag, recombinant GST was also tested as a control. IgE reactivity was

detected only for the rGST-Mus a 5 (Fig. 4), while no IgE binding was found for GST. Although the correct protein folding should be confirmed by a thorough structural characterization, the IgE reactivity of the rGST-Mus a 5 suggests that this protein could find application as a diagnostic reagent in banana allergy.

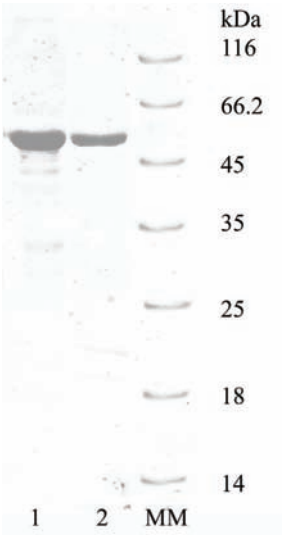

Fig. 3. SDS-PAG electrophoresis of purified rGST-Mus a 5 produced in *E. coli*: 1 – solubilized rGST-Mus a 5 fraction; 2 – rGST-Mus a 5 eluted from the affinity matrix; MM – molecular markers.

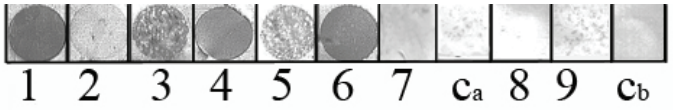

Fig. 4. IgE reactivity of rGST-Mus a 5: 1–6 – individual sera from banana allergic persons, 7 – pool of sera from 3 healthy individuals, c_a – control of secondary antibody; IgE reactivity of rGST: 8 – pool of sera from 6 banana allergic persons, 9 – pool of sera from 3 healthy individuals and c_b – control of secondary antibody.

The IgG reactivity of rGST-Mus a 5 was shown by dot blot analysis with anti-banana rabbit antibodies (Fig. 5).

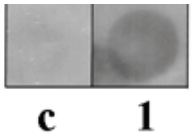

Fig. 5. IgG reactivity of rGST-Mus a 5: c – control, 1 – rGST-Mus a 5.

IgG inhibition assay

To evaluate the IgG reactivity of the rGST-Mus a 5, an inhibition assay with anti-banana rabbit antibodies was performed. Compared to the positive control, IgG binding to natural Mus a 5 was reduced with 5 μg of rGST-Mus a 5. Complete inhibition was achieved by pre-incubation of the antibodies with 50 μg of

inhibitor (Fig. 6), suggesting that the rGST-Mus a 5 shares immunodominant epitopes with natural Mus a 5.

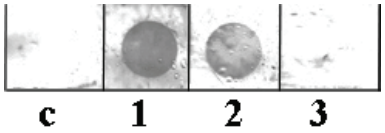

Fig. 6. Inhibition of IgG binding to natural Mus a 5 by rGST-Mus a 5. The membranes were incubated with c – secondary antibodies, 1 – anti-banana antibodies, 2 – anti-banana antibodies pre-incubated with 5 μg rGST-Mus a 5, 3 – anti-banana antibodies pre-incu–bated with 50 μg rGST-Mus a 5.

CONCLUSIONS

An optimization of expression of recombinant banana glucanase - Mus a 5 in a prokaryotic expression system with a GST fusion tag is reported. Optimal expression of rGST-Mus a 5 in *E. coli* BL21(DE3) cells was established (12 h protein expression at 25 °C), and the protein was isolated by glutathione affinity chromatography. The rGST-Mus a 5 showed IgE reactivity with five out of six individual sera of banana allergic subjects. A dot blot inhibition assay with anti--banana rabbit antibodies revealed that the rGST-Mus a 5 shares immunodominant epitopes with natural Mus a 5. Further structural and immunological characterization should assess the applicability of the recombinant banana glucanase for the diagnosis of banana allergy.

Acknowledgements. This work was supported by Grant 172049 from the Ministry of Education and Science of the Republic of Serbia.

ИЗВОД

ОПТИМИЗАЦИЈА ХЕТЕРОЛОГЕ ПРОИЗВОДЊЕ ГЛУКАНАЗЕ ИЗ БАНАНЕ У *E. coli*

МОНАМЕД ABUGHREN[1], МИЛИЦА ПОПОВИЋ[1], РАЈНА ДИМИТРИЈЕВИЋ[2], ЛИДИЈА БУРАЗЕР[3], МАРИНА АТАНАСКОВИЋ-МАРКОВИЋ[4] и МАРИЈА ГАВРОВИЋ-ЈАНКУЛОВИЋ[1]

[1]*Катедра за биохемију, Хемијски факултет Универзитета у Београду,* [2]*Иновациони центар Хемијског факултета Универзитета у Београду,* [3]*Институт за вирусологију, вакцине и серуме, Торлак, Београд и* [4]*Универзитетска дечја клиника, Медицински факултет Универзитета у Београду*

За потребе производње у *Escherichia coli* ген глуканазе из банане (GenBank GQ268963) је уклониран у експресиони вектор pGEX-4T са глутатион-*S*-трансферазом (GST). Производња овог протеина у ћелијама је индукована 1 mM изопропил-β-D-тиогалактопиранозидом (IPTG). Услови за експресију протеина су оптимизовани варирањем температуре (25, 30 и 37 °C) и дужине трајања протеинске синтезе (3, 6 и 12 h). Ниво производње протеина је анализиран денситометријом SDS–PA гела након електрофоретског раздвајања ћелијских лизата. Оптимална производња протеина за његово даље процесовање је добијена гајењем ћелија након додатка IPTG на 25 °C током 12 h. Рекомбинантни GST-Mus a 5 пречишћен афинитетном хроматографијом са глутатионом показује молекулску масу од 60 kDa. IgE и IgG реактивност изоловане глуканазе потврђена је у "dot blot" са појединачним серумима особа алергичних на банану, и са поликлонским зечијим антителима на екстракт банане, редом. Пречишћена рекомбинантна глуканаза је потенцијалан кандидат за дијагнозу алергије на банану.

(Примљено 9. марта, ревидирано 21. јуна 2011)

REFERENCES

1. J. Lidholm, K. Ballmer-Weber, A. Mari, S. Vieths, *Curr. Opin. Allergy Immunol.* **6** (2006) 234
2. R. van Ree, J. Akkerdaas, A. van Leeuwen, M. Fernandez-Rivas, *Allergy Clin. Immunol. Int.* **12** (2000) 7
3. M. A. Ciardiello, I. Giangrieco, L. Tuppo, M. Tamburrini, M. Buccheri, P. Palazzo, M. L. Bernardi, R. Ferrara, A. Mari, *J. Agric. Food Chem.* **57** (2009) 1565
4. M. Gavrovic-Jankulovic, N. Polovic, S. Prisic, R. M. Jankov, M. Atanaskovic-Markovic, O. Vuckovic, T. Cirkovic Velickovic, *Food Agric. Immunol*. **16** (2005) 117
5. A. Reuter, J. Lidholm, K. Andersson, J. Ostling, M. Lundberg, S. Scheurer, E. Enrique, A. Cistero-Bahima, M. San Miguel-Moncin, B. K. Ballmer-Weber, S. Vieths, *Clin. Exp. Allergy* **36** (2006) 815
6. R. Sanchez-Monge, C. Blanco, A. Diaz-Perales, C. Collada, T. Carrillo, C. Aragoncillo, G. Salcedo, *Clin. Exp. Allergy* **2** (1999) 673
7. M. Bublin, M. Pfister, C. Radauer, C. Oberhuber, S. Bulley, A. M. Dewitt, J. Lidholm, G. Reese, S. Vieths, H. Breitened er, K. Hoffmann-Sommergruber, B. K. Ballmer-Weber, *J. Allergy Clin. Immunol*. **125** (2010) 687
8. M. F. Delbourg, L. Guilloux, D. A. Monere t-Vautrin, G. Ville, *Ann. Allergy Asthma Immunol*. **76** (1996) 321
9. H. Alenius, S. Makinen-Kiljunen, M. Ahlroth, K. Turjanmaa, T. Reunala, T. Polosuo, *Clin. Exp. Allergy* **26** (1996) 341
10. A. A. Wadee, L. A. Boting, A. R. Rabson, *J. Allergy Clin. Immunol*. 85 (1990) 801
11. H. Breiteneder, C. Ebner, *J. Allergy Clin. Immunol.* **106** (2000) 27
12. V. Receveur-Brechot, M. Czjzek, A. Barre, A. Roussel, W. J. Peumans, E. J. M. van Damme, P. Rouge, *Proteins* **63** (2006) 235
13. A. Palacin, S. Quirce, R. Sanchez-Monge, I. Bobolea, A. Diaz-Perales, F. Martin-Munoz, C. Pascual, G. Salcedo, *Pediatric Allergy Immunol*. **22** (2011) 186
14. O. Palomares, M. Villalba, J. Quiralte, F. Polo, R. Rodriguez, *Clin. Exp. Allergy* **35** (2005) 345
15. S. Wagner, C. Radauer, C. Hafner, H. Fuchs, E. Jansen-Jarolim, B. Wuthrich, O. Scheiner, H. Breiteneder, *Clin. Exp. Allergy* **35** (2004) 1739
16. O. Palomares, M. Fernandez-Nieto, M. Villalba, R. Rodriguez, J. Cuesta-Herranz, *Allergy* **63** (2008) 784
17. U. K. Laemmli, *Nature* **227** (1970) 680
18. Novagen, *Protein Purification and Detection Tools*, 220018-2006EURO, p. 32
19. E. Harlow, D. Lane, *Antibodies A Laboratory Manual*, Cold Spring Harbor Laboratory, New York, 1988, p. 410
20. M. Gavrovic-Jankulovic, M. Spasic, T. Cirkovic Velickovic, M. Stojanovic, A. Inic-Kanada, L. Dimitrijevic, B. Lindner, A. Petersen, W. Becker, R. Jankov, *Mol. Nutr. Food Res.* **52** (2008) 701
21. R. Dimitrijevic, M. Jadranin, L. Burazer, S. Ostojic, M. Gavrovic-Jankulovic, *Food Chem*. **120** (2010) 1113
22. I. Aleksic, R. Dimitrijevic, M. Popovic, E. Vassilopoulou, N. Sinaniotis, M. Atanaskovic-Markovic, B. Lindner, A. Petersen, N. Papadopoulos, M. Gavrovic-Jankulovic, in *Proceedings of 28th Symposium of the Collegium Internationale Allergologicum*, Ischia, Italy, 2010, pp. 73

23. D. B. Smith, K. S. Johnson, *Gene* **67** (1988) 31
24. *The Recombinant Protein Handbook*, Amersham Pharmacia Biotech, Piscataway, NJ, 18-1142-75
25. The QIAexpressionistTM, 1024473, *Qiagen*, p.49.

Journal of the Serbian Chemical Society
JSCS-info@shd.org.rs • www.shd.org.rs/JSCS
J. Serb. Chem. Soc. *77* (1) 53–66 (2012)
JSCS–4248
UDC 547.496.2+546.776+547.7:
532.74:615.28–188
Original scientific paper

Spectroscopic properties and antimicrobial activity of dioxomolybdenum(VI) complexes with heterocyclic *S,S'*-ligands

SOFIJA P. SOVILJ[1]*#, DRAGANA MITIĆ[1#], BRANKO J. DRAKULIĆ[2] and MARINA MILENKOVIĆ[3]

[1]*Faculty of Chemistry, P. O. Box 118, 11158 Belgrade, Serbia,* [2]*ICTM, Department of Chemistry, Njegoševa 12, 11001 Belgrade, Serbia and* [3]*Department of Microbiology and Immunology, Faculty of Pharmacy, University of Belgrade, Vojvode Stepe 450, Belgrade, Serbia*

(Received 28 March, revised 26 August 2011)

Abstract: Five new dioxomolybdenum(VI) complexes of the general formula $[MoO_2(Rdtc)_2]$, **1–5**, where Rdtc⁻ refer to piperidine (Pipdtc), 4-morpholine (Morphdtc), 4-thiomorpholine (Timdtc), piperazine (Pzdtc) or *N*-methylpiperazine (*N*-Mepzdtc) dithiocarbamates, respectively, have been prepared. The complexes were characterized by elemental analysis, conductometric measurements, electronic, IR and NMR spectroscopy. The complexes **1**–**5** contain a *cis*-MoO_2 group and have an octahedral geometry. Two dithiocarbamato ions join as bidentates with both the sulfur atoms to the molybdenum atom. The presence of different heteroatoms in the piperidino moiety influences the ν(C=N) and ν(C=S) vibrations, which wavelengths decrease in the order: Pipdtc > *N*-Mepzdtc > Morphdtc > Pzdtc > Timdtc ligands. Based on their spectral data, the molecular structures of complexes **1**–**5** were optimized at the semi-empirical molecular-orbital level, and the geometries, as obtained from calculations, are described. The antimicrobial activities of the complexes were tested against nine different laboratory control strains of bacteria and two strains of the yeast *Candida albicans*. All the tested strains were sensitive. Complexes bearing heteroatom in position 4 of piperidine moiety were significantly more potent against the tested bacteria compared to the corresponding ligands.

Keywords: dithiocarbamates; molybdenum(VI) complexes; MoO_2^{2+} group; geometry optimization.

INTRODUCTION

Molybdenum complexes with organic ligands are compounds of great theoretical and practical interest, especially valuable as model systems for biochemi-

* Corresponding author. E-mail: ssovilj@chem.bg.ac.rs
# Serbian Chemical Society member.
doi: 10.2298/JSC110328160S

cal processes. The presence of $[Mo^{VI}O_2]^{2+}$ groups can serve as oxygen atom transfer agents and is of importance in the fully oxidized states of a number of redox enzymes, in which their active site consists of a *cis*-molybdenum dioxo moiety.[1,2] In recent years, their antimicrobial potency has gained special attention against both human and plant pathogenic microorganisms.[3,4]

Moreover, dithiocarbamato ($Rdtc^-$) ligands are known to form stable complexes with many transition metals.[5–14] Interest in dithiocarbamate complexes arises because of their versatile structures, depending on the manner of coordination,[15–19] and the type of their biological activity.[20–24] Additionally, these coordination compounds have intriguing properties, being good corrosion inhibitors in acidic media.[23–27]

The aim of the present study was to synthesize dioxomolybdenum(VI) complexes with piperidine- (Pipdtc), 4-morpholine- (Morphdtc), 4-thiomorpholine- (Timdtc), piperazine- (Pzdtc) and *N*-methylpiperazine- (*N*-Mepzdtc) dithiocarbamato ligands. As a contribution to the problem of the coordination behavior of heteroalicyclic dithiocarbamates, their mode of coordination was determined and, particularly, the spectrochemical properties of these compounds are discussed. In order to obtain further insight of the electronic structure of the complexes, the effect of heteroatom variation in the piperidino moiety on the C–N, and the C–S bonds, as well as on the electronic structure of the complexes was examined. Molecular modeling is a powerful tool to add chemical and physical information to the information obtained by other techniques.[28–32] For these reasons, based on the available spectral data, the molecular structures of all the prepared complexes, **1**–**5**, was optimized and a description of the structural parameters is given. Finally, the complexes were examined as potential antimicrobial agents.

EXPERIMENTAL

*Syntheses of the $[MoO_2(Rdtc)_2]$ complexes **1**–**5***

All the used chemicals were commercial products of analytical reagent grade. The starting acetylacetonato complex $[MoO_2(acac)_2]$ and the sodium salts of $Rdtc^-$ were prepared as described in the literature.[12,33]

To a methanolic solution (5 cm^3) of $MoO_2(acac)_2$ (330 mg, 1.0 mmol) was added dropwise 2.0 mmol of the corresponding $NaRdtc{\cdot}2H_2O$ ligand (*i.e.*, 468 mg of Pipdtc; 452 mg of Morphdtc; 484 mg of Timdtc; 450 mg of Pzdtc or 478 mg of *N*-Mepzdtc) dissolved in water (5 cm^3), during 1 h under stirring and thermostating at 40 °C. The mixture was then continuously stirred under reflux for about 2 h. The filtrate was concentrated under vacuum to 10 cm^3. Upon cooling the mixture for two days in a refrigerator, the crude products precipitated. After recrystallization from a 1-heptene/toluene mixture (1:1, v/v), light brown crystalline substances of the corresponding complexes were obtained.

Materials and methods

Elemental analyses (C, H, N) were performed by standard micro methods at the Department of Instrumental Analyses of the Institute of Chemistry, Technology and Metallurgy (ICTM), Belgrade. The molar conductivity of methanolic solutions (1.0×10^{-3} mol dm^{-3}) was

measured at 20 °C using a Jenway-4009 conductometer. The electronic spectra of methanol solutions (1.0×10^{-3} M) were recorded on a GBC UV/VIS 911A spectrophotometer. The IR spectra in the 4000–400 cm^{-1} ranges were measured on a Perkin Elmer 31725x FTIR spectrophotometer, using KBr discs. The ^{1}H- and ^{13}C-NMR spectra were taken on a Varian Gemini 200 instrument at 200/50 MHz in DMSO-d_6, at room temperature. All chemical shifts are reported in ppm downfield from tetramethylsilane (TMS), used as the internal standard.

Molecular modeling was realized by MOPAC2009,[34] a general-purpose semi-empirical molecular orbital package for the study of the solid state and molecular structures. The semi-empirical molecular-orbital (MO) PM6 method[35] was used. Geometry optimizations (full optimization of bond angles and bond distances), without any input constraints, were performed by Eigenvector following optimization with a convergence limit of 0.001 kcal mol^{-1} $Å^{-1}$. Geometry optimization of the complexes **1**–**5** were realized in vacuum and by using implicit solvation in water (COSMO).[36] The IR spectra of the representative complex **1** was obtained from the initial structure assessed by the semi-empirical MO PM6 method additionally optimized on the DFT level (B3LYP) using the LanL2DZ basis set, without any constraint. The ^{1}H- and ^{13}C-NMR spectra were calculated by the Gauge-Independent Atomic Orbital (GIAO) method,[37] using single point calculation (B3LYP/LanL2DZ) and implicit solvation in dimethyl sulfoxide (PCM)[38] on the structure assessed by the semi-empirical MO PM6 method. All calculations on the DFT level were realized by the Gausian03 suit of programs.[39] Superimposition of the calculated structures for complexes **1** and **3** with the experimentally obtained crystal structures of similar ones taken from literature was realized by VegaZZ 2.4.0.[40] The complexes and their molecular orbitals were visualized by Jmol.[41] All computations were performed on AMD Athlon 64 x2 Dual Core Processors, in Windows or Linux environments.

Antimicrobial activity

The antimicrobial activities of the synthesized complexes were evaluated using nine laboratory control strains of bacteria, *i.e.*, the Gram-positive: *Staphylococcus aureus* (ATCC 25923), *S. epidermidis* (ATCC 12228), *Micrococcus luteus* (ATCC 9341), *M. flavus* (10240), *Enterococcus faecalis* (ATCC 29212), *Bacillus subtilis* (ATCC 6633) and the Gram-negative: *Escherichia coli* (ATCC 25922), *Klebsiella pneumoniae* (NCIMB 9111), *Pseudomonas aeruginosa* (ATCC 27853), and two strains of yeast, *i.e.*, *Candida albicans* (ATCC 24433 and ATCC 10259). The microorganisms were provided by the Institute for Immunology and Virology, Torlak, Belgrade, Serbia. A broth microdilution method was used to determine the minimal inhibitory concentration (*MIC*) of complexes **1**–**5**, according to the Clinical and Laboratory Standards Institute (CLSI 2005).

All tests were performed in Müller Hinton broth for the bacterial strains and in Sabouraud dextrose broth for the yeasts. Overnight broth cultures of each strain were prepared, and the final concentration in each well was adjusted to 2×10^{6} CFU ml^{-1} for the bacteria and 2×10^{5} CFU ml^{-1} for the yeasts. The investigated compounds were dissolved in 1 % dimethyl sulfoxide (DMSO) and then diluted to the highest concentration. Serial doubling dilutions of the compounds were prepared in a 96-well microtiter plate over the concentration range 31.25–1000 μg ml^{-1}. In the tests, triphenyl tetrazolium chloride (TTC) (Aldrich Chemical Company Inc., USA) was also added to the culture medium as a growth indicator. The final concentration of TTC after inoculation was 0.05 %. The microbial growth was determined from the absorbance at 600 nm, using a universal microplate reader after 24 h incubation at 37 °C for the bacteria and after 48 h incubation at 25 °C for the fungi. The *MIC* is defined as the lowest concentration of the compound at which no visible growth of microorganism is observed. All determinations were performed in duplicate and two positive growth controls were

included.[42] To resolve structure–activity trends, the *MIC* values of complexes **1**–**5**, the corresponding ligands and $[MoO_2(acac)_2]$ used for comparison, originally determined in mass concentration (μg ml^{-1}), were converted to molar concentrations (M).

RESULTS AND DISCUSSION

Syntheses and physico–chemical properties of the complexes

Complexes **1**–**5** were obtained by mixing the reactants in a 1:2 molar ratio, in a substitution reaction of the two acetylacetonato anions in the $[MoO_2(acac)_2]$ complex by $Rdtc^-$ ligands:

$$[MoO_2(acac)_2] + 2RdtcNa{\cdot}2H_2O \rightarrow [MoO_2(Rdtc)_2] + 2acacNa + 2H_2O$$

The obtained complexes were light brown microcrystalline substances, stable under atmospheric conditions and soluble in methanol, ethanol, 1-heptene, toluene and dimethyl sulfoxide and insoluble in water, chloroform, dichloromethane and benzene.

The analytical results confirmed the proposed composition:

$[MoO_2(Pipdtc)_2]$ ***(1)***. Yield: 106 mg (17 %); Anal. Calcd. for $C_{12}H_{20}MoN_2O_2S_4$ (FW: 448.30): C, 32.14; H, 4.49; N, 6.25 %. Found: C, 32.31; H, 4.80; N, 6.38 %;

$[MoO_2(Morphdtc)_2]$ ***(2)***. Yield: 90 mg (19.8 %); Anal. Calcd. for $C_{10}H_{16}MoN_2O_4S_4$ (FW: 452.05): C, 26.55; H, 3.57; N, 6.19 %. Found: C, 27.02; H, 4.11; N, 6.20 %;

$[MoO_2(Timdtc)_2]$ ***(3)***. Yield: 52 m g (10.8 %); Anal. Calcd. for $C_{10}H_{16}MoN_2O_2S_6$ (FW: 484.05): C, 24.79; H, 4.33; N, 5.79 %. Found: C, 24.44; H, 4.17; N, 5.80 %;

$[MoO_2(Pzdtc)_2]$ ***(4)***. Yield: 153 m g (33.8 %); Anal. Calcd. for $C_{10}H_{18}MoN_4O_2S_4$ (FW: 450.08): C, 26.6 6; H, 4.03; N, 12.45 %. Found: C, 26.39; H, 4.31; N, 11.54 %;

$[MoO_2$(N-Mepzdtc)$_2]$ ***(5)***. Yield: 130 m g (27.1 %); Anal. Calcd. for $C_{12}H_{22}MoN_4O_2S_4$ (FW: 478.10): C, 35.1 2; H, 4.64; N, 11.71 %. Found: C, 35.37; H, 4.77; N, 11.77 %.

The non-electrolyte nature of the complexes was confirmed by their low molar conductivities[43] (λ_M = 45.30; 17.80; 25.90; 33.30 and 13.70 Ω^{-1} cm^2 mol^{-1} for complexes **1**–**5**, respectively).

Spectroscopic properties

Electronic absorption spectra. The complexes are diamagnetic, as expected for the $4d^0$ configuration. Since there are no d electrons, splitting from d–d transitions was not discernible. The absorptions appearing in the electronic spectra in the range of 280–400 nm arise from charge transfer and intraligand transitions, especially due to the NCS_2 chromophore, but the assignments of charge-transfer spectra are controversial.[44]

IR Spectra. The pertinent IR data, *i.e.*, ν(C–N), ν(C–S) vibrations of the free and coordinated Rdtc⁻ ligands, ν(Mo–S) bands, as well as the MoO_2^{2+} core vibrations of the complexes **1**–**5** are collected in Table I.

TABLE I. IR spectral data (cm^{-1}) for complexes **1**–**5**, and for the Rdtc⁻ ligands (abbreviations: *vs*, very strong; *s*, strong; *m*, medium; *w*, weak)

Compound	ν(C=N)	ν(C=S)	ν(Mo–S)	ν_s(Mo=O)	ν_{as}(Mo=S)
1	1442_s	948_s	437_m	880_m	907_m
2	1455_s	985_s	429_m	870_s	897_s
3	1465_s	997_s	436_m	815_m	948_s
4	1458_s	986_s	439_w	875_w	899_m
5	1448_s	975_s	430_w	860_m	908_s
PipdtcNa	1465_{vs}	965_s	–	–	–
MorphdtcNa	1449_{vs}	990_s	–	– –	
TimdtcNa	1465_{vs}	995_s	–	– –	
PzdtcNa	1460_{vs}	1000_s	–	– –	
N-MepzdtcNa	1450_{vs}	995_s	–	– –	

Concerning the electronic and structural characteristics of the described compounds, there are several regions of considerable interest in the IR spectra. The 1390–1430 cm^{-1} region is associated primarily with the thioureide vibration and is attributed to the ν(C=N) vibrations of the $S_2C=NR_2$ bond[12,14] (Table I). This indicates a significant increase in double bond character of the C=N bond, resulting in higher frequencies compared with the free Rdtc⁻ ligands. All the complexes exhibit ν(C=N) bands in the 1470–1480 cm^{-1} range, which lie between ν(C=N) and ν(C–N), in the 1640–1690 and 1250–1350 cm^{-1} range,[9] respectively. The 950–1100 cm^{-1} region is associated with ν(CSS) vibrations and has been effectively used to differentiate between monodentate and bidentate Rdtc⁻ ligands.[9,14] In the IR spectra of the obtained complexes, the presence of only one strong band in this region supports a symmetrical bidentate coordination of the dithio ligands, while a doublet expected in the case of monodentate coordination[9] was absent. New absorption bands in the 420–440 cm^{-1} region, absent in the spectra of the free Rdtc⁻ ligands, are in good agreement with the available literature data.[10,14] The heteroatoms (N, O, S) in the piperidino moiety influence both the ν(C=N) and ν(C=S) values that increase in the order of the complexes with: Pipdtc > *N*-Mepzdtc > Morphdtc > Pzdtc > Timdtc ligands (Table I). This band, however, demonstrates the partial double bond character of the C=S bond on consideration of its position between ν(C=S) (1080–1200 cm^{-1}) and the ν(C–S) bond (600–800 cm^{-1}). This behavior can be attributed to the electron releasing ability of the heterocyclic atom that forces a high electron density towards the SCS group.[45,46] The symmetric and antisymmetric stretching vibrations observed near 900 cm^{-1} can be attributed to a *cis*-$[MoO_2]^{2+}$ core.[47] Generally, the wave

numbers of ν_{sym}(Mo=O) vibrations are higher than t hose of ν_{asym}(Mo=O).[48,49] Finally, the skeletal pyperidine bands are located at *ca.* 1610 cm^{-1}.

The recorded and calculated (see Experimental) IR sp ectra of complex **1** are shown in Fig. S1 in the Supplementary material. Fair agreement can be visually observed.

NMR spectra. Although molybdenum(VI) complexes were well characterized in the s olid state, their charact erization in solution is necess ary in order to evaluate the stability of the obtained co mplexes under biologically relevant conditions. However, the poor solubility of the molybdenum(VI) complexes **1**–**5** and the related free ligands hampered NMR experiments in an aqueous environment; therefore, the spectra were recorded in DMSO-d_6. The structure enumeration for the structure–spectra assignments are as given in Scheme 1.

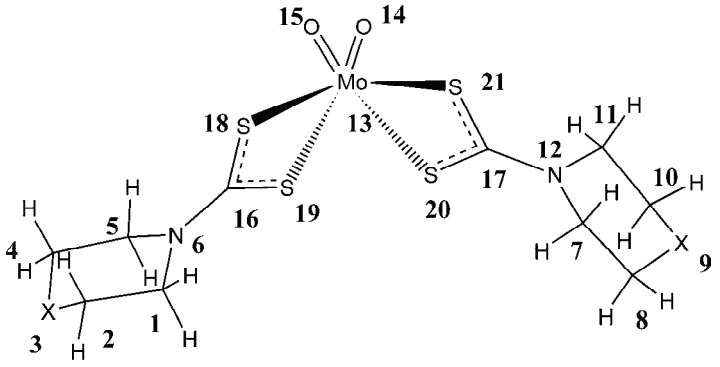

X = -CH_2- (1), -O- (2), -S-(3), -NH-(4), -N(Me)-(5)

Scheme 1. Numbering of the non-hydrogen atoms that correspond to the labels in Table II.

TABLE II. ^{1}H- and ^{13}C-NMR chemical shifts for c omplexes **1–5** in ppm downfield from TMS. Assignment of the atoms given according to the Scheme 1

Complex	δ^1H	δ^{13}C	δ^{13}C
1	2.51 (2H, *t* (C1)); 1.91 (2H, *s* (C2)); 1.68 (2H, *s* (C3)); 2.00 (2H, *s* (C4)); 3.36 (2H, *s* (C5))	S_2CN, 190.91	C1(C5), 52.35; C2, 22.13; C3, 25.97; C4, 23.54
2	2.73 (2H, *s* (C1)); 3.51 (2H, *m* (C2)); 3.67 (2H, *s* (C4)); 3.17 (2H, *s* (C5))	S_2CN, 195.42	C1(C5), 51.82; C2, 66.5; C4, 66.5
3	3.27 (2H, *t* (C1)); 2.58 (2H, *s* (C2)); 2.82 (2H, *m* (C4)); 3.27(2H, *t* (C5))	S_2CN, 201.66	C1(C5), 53.88; C2, 29.54; C4, 29.54
4	2.92(2H, *s* (C1)); 2.51 (2H, *t* (C2)); 1.91 (H, *s* (C3)); 2.46 (2H, *s* (C4)); 2.99 (2H, *s* (C5))	S_2CN, 201.93	C1(C5), 66.42; C2, 45.43; C4, 45.43
5	3.39 (2H, *s* (C1)); 2.51 (2H, *d* (C2)); 2.25 (3H, *t* (C3)); 2.40 (2H, *s* (C4)); 3.39 (2H, *s* (C5))	S_2CN, 197.40	C1(C5), 49.13; C2, 54.96; C4, 54.96; C6, 45.71

The absence of S–H protons and a slight downfield shift of the protons in the NMR spectra of all complexes, with respect to the corresponding ligands, were observed. This indicates that the ligands are coordinated to molybdenum through sulfur atoms.[50] In the ^{1}H-NMR spectra (Table II), signals of five protons, which belong to the Rdtc$^-$ ligand, were found for complex **1**. The position and multiplicity of the proton signals for complexes **2**–**5** depend on the type of heteroatom in position four of the piperidinyl moiety. In the ^{13}C-NMR spectrum for complex **1**, there are signals at 52.35, 22.13, 25.97 and 23.64 ppm that belong to the Rdtc$^-$ ligand (Table II). Two signals for complexes **2**, **3** and **4** originated from the symmetrical Rdtc$^-$ ligands. The last signal, C6, in the spectrum of complex **5** is ascribed to the methyl carbon *N*-Me of *N*-methylpiperidine. Only one signal that corresponds to the CS_2 moieties of Rdtc$^-$ was observed in the spectrum of each complex, indicating that the chemical environments of the CS_2 moieties of the two Rdtc$^-$ ligands bound to the *cis*-MoO_2 center are equivalent to each other.[51,52] The experimentally obtained ^{1}H- and ^{13}C-NMR spectra for complex **1** and the Pipdtc ligand, and the calculated NMR spectra for complex **1** are given in the Supplementary material. Fair agreement between the calculated and experimentally obtained spectra can be seen (Figs. S2–S4 in the Supplementary material).

Molecular modeling

Data of the total energy and heat of formation for each system, as well as selected bond distances and angles of the calculated geometry for complexes **1–5**, as accessed by the geometry optimization, are presented in Table III. The optimized structures of the complexes **1** and **3** are shown in Figs. 1a and 1b, respectively.

TABLE III. Selected bond distances and bond angle values for complexes **1**–**5**, as obtained by the semi-empirical MO PM6 method in vacuum

PM6	**1**	**2**	**3**	**4**	**5**
Total energy, eV	–3579.16	–3861.72	–3628.15	–3665.11	–3964.50
ΔH_f / kJ mol^{-1}, vacuum implicit	–496.64	–727.48	–399.42	–350.89	–364.40
water model	–593.34	–838.31	–504.80	–496.38	–479.33
Distance N6–C16 (N12–C17), Å	1.331	1.333	1.338	1.331	1.331
	(1.331)	(1.333)	(1.338)	(1.331)	(1.331)
Angle S18–Mo13–S20, °	82.152	87.400	87.432	87.321	87.334
Angle S19–Mo13–S21, °	148.494	148.60	148.545	148.453	148.502
Angle S19–Mo13–S18	68.642	68.788	68.698	68.705	68.713
(S21–Mo13–S20), °	(68.641)	(68.782)	(68.695)	(68.705)	(68.713)
Angle O15–Mo13–O14, °	107.508	107.531	107.672	107.493	107.476
Distance O15–Mo13 (O14–Mo13), Å	1.681	1.680	1.680	1.680	1.681
	(1.681)	(1.680)	(1.680)	(1.680)	(1.681)
Distance S18–Mo13 (S20–Mo13), Å	2.635	2.636	2.636	2.638	2.639
	(2.635)	(2.637)	(2.635)	(2.638)	(2.639)

TABLE III. Continued

PM6	**1**	**2**	**3**	**4**	**5**
Distance S19–Mo13 (S21–Mo13), Å	2.456 (2.456)	2.457 (2.456)	2.456 (2.455)	2.457 (2.457)	2.457 (2.457)
Distance C16–S19 (S18–C16), Å	1.742 (1.710)	1.740 (1.707)	1.739 (1.706)	1.740 (1.709)	1.741 (1.709)
Distance C17–S21 (C17–S20), Å	1.742 (1.710)	1.740 (1.707)	1.737 (1.706)	1.740 (1.709)	1.741 (1.709)
Angle O15–Mo13–S19 (O15–Mo13–S20), °	104.068 (160.266)	103.809 (160.562)	103.712 (160.548)	103.987 (160.386)	104.012 (160.381)
Angle O15–Mo13–S18 (O15–Mo13–S21), °	87.166 (97.432)	86.976 (94.671)	86.876 (94.769)	87.150 (94.569)	87.135 (94.530)
Angle O14–Mo13–S21 (O14–Mo13–S18), °	104.130 (160.250)	103.804 (160.566)	103.700 (160.528)	104.000 (160.394)	104.222 (160.378)
Angle O14–Mo13–S19 (O14–Mo13–S20), °	94.451 (87.125)	94.656 (86.956)	94.749 (86.871)	94.573 (87.133)	94.530 (87.142)
Angle S19–C16–S18 (S21–C17–S20), °	112.754 (112.764)	113.380 (113.380)	113.261 (113.255)	113.140 (113.142)	113.111 (113.112)

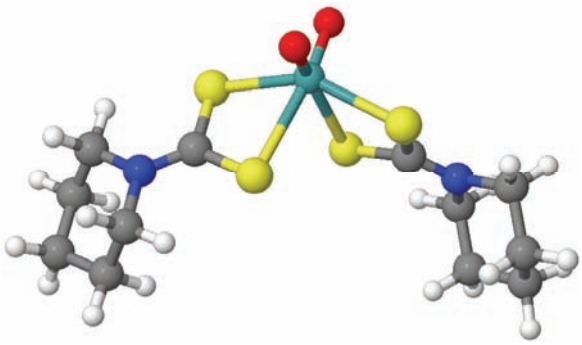

(a)

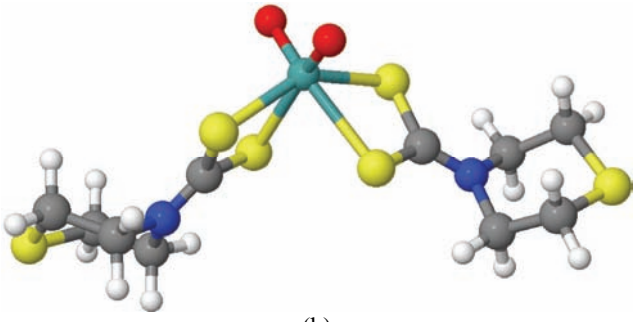

(b)

Fig. 1. Opti mized geometry of the complexes obtained by the semi-empirical MO PM6 method:
a) $[MoO_2(Pipdtc)_2]$ (**1**);
b) $[MoO_2(Timdtc)_2]$ (**3**).

The non-hydrogen atoms numbering in Table III correspond to the labels as given in Scheme 1. The complexes **1**–**5** represent a deformed octahedral structure around the metal atom with the two oxygen atoms in the *cis*-position. The S–Mo–S

chelate angle of 69° is in agreement with X-ray crystal structures for this type of complexes.[51,53] Length difference between Mo13–S18 (Mo13–S20) and Mo13–S19 (Mo13–S21) is a consequence of the *trans* influence of the oxo--group.[45] The two $Rdtc^-$ ligands are oriented in the *cis*-position toward each other coordinated to metal ion *via* their deprotonated dithiocarbamato (CS_2^-) groups, as presented in Figs. 1a and 1b for complexes **1** and **3**, respectively. The short N–C distance indicates a significant double bond character of these bonds.

In all the complexes, the heteroalicyclic parts of both ligands are in the chair conformation. The improper torsion angle in the heteroalicyclic part of the ligands, defined by the angle between the bonds C1–C2 and C5–C6 (C7–C8 and C11–C12) smaller than 1°, demonstrate an almost ideal chair conformation for the ligands in all the complexes. The planes of the cyclic part of the ligands, in the chair conformation, are oriented to each other at an angle of *ca.* 180°. The obtained results of molecular modeling demonstrate C2 symmetry for all the complexes. Degree of deformation from an ideal octahedral structure is represented by the bond and torsion angles in the coordination sphere (Table III). The HOMO (highest occupied molecular orbital), HOMO-1 and HOMO-2 orbitals are located almost exclusively on the dioxo oxygen atoms and the dithiocarbamato sulfur atoms, as exemplified for complex **1** in Fig. 2, indicating involve-

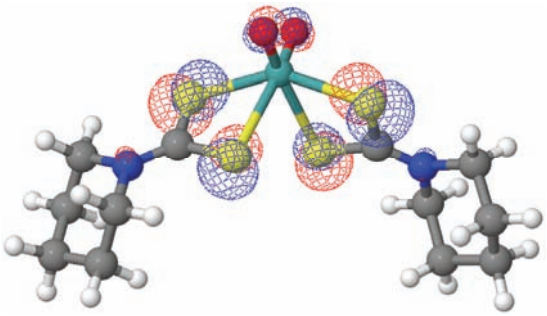

(a)

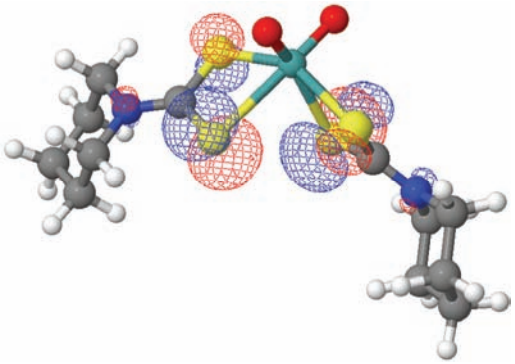

(b)

Fig. 2. a) HOMO (–8.31 eV) and b) HOMO-1 (–8.38 eV) of complex **1**.

ments of molybdenum $d_{x^2-y^2}$ and d_{z^2} orbitals in the coordination. All the complexes appear to be somewhat more stable (have a more negative heat of formation) in the implicit water model than in vacuum, probably due to favorable electrostatic interactions of the heteratoms (N, O, S), accessible to the solvent. Calculated structures of complexes **1** and **3** were superimposed on similar[53] or the same[51] experimentally obtained structures taken from the literature (Fig. S5 in the Supplementary material). For the superimposition, the coordination sphere (MoO_2=S_2C–) and the heteroalicyclic N connected to dithiocarbamato moiety were used. The very good agreement should be noted. The calculated structure of complex **1** and the literature dioxomolybdenum di-(dithiocarbamato-*N*-pyrrolo) complex (CSD code 153544) superimpose their coordination spheres with a root-mean square deviation of 0.147. The calculated structure of complex **3** and the same experimentally obtained structures taken from literature superimpose their coordination spheres with a root-mean square deviation of 0.113. It should be noted that the symmetrically oriented thiomorpholino part of the ligands for complex **3**, as obtained by semi-empirical calculations, appears somewhat more stable both in solution and in vacuum than the asymmetrically oriented ones found in the crystal structure.

Suggested structure

The important features of the IR spectra provide a consistent picture that the $Rdtc^-$ ligands are bound through the both sulfur atoms to the molybdenum atom, as it can also be seen from the chemical environments of the CS_2 moieties in the NMR spectra. This bidentate *S*,*S*' structure is again the most favorable in comparison with a monodentate one. The geometry of the MoO_2S_4 core is a distorted octahedron (Fig. 1) with the two terminal oxo ligands lying invariably in a *cis*--position to each other, usual for dioxomolybdenum(VI) complexes,[51–53] while the two $Rdtc^-$ ligands complete the distorted octahedral coordination. Based on the above calculation (Table III), the influence of the variation of the heteroatom in position 4 of the piperidine moiety on the coordination sphere can be straightforwardly elucidated.

Antimicrobial activity

The results of the obtained antimicrobial activities of $[MoO_2(acac)_2]$, the five $Rdtc^-$ ligands, complexes **1**–**5**, standard antibiotics and nystatin are presented in Tables IV and V. Generally, the complexes were more potent than the corresponding ligands and $[MoO_2(acac)_2]$. Obviously, the introduction of a heteroatom in position 4 of the piperidino moiety makes the complexes significantly more potent in respect to the corresponding ligands. A higher potency of the ligand compared to the complex was only observed in the data of complex **1**, for some of the tested microbial strains (Table IV).

TABLE IV. Minimal inhibitory concentrations (*MIC*) of the tested compounds

Microorganism	$[MoO_2(acac)_2]$	Complexes/corresponding ligand				
		1/L	**2**/L	**3**/L	**4**/L	**5**/L
S. aureus ATCC 25923[a]	3.81	5.56/6.21	5.53/22.8	2.58/45.6	2.78/11.4	10.5/10.7
S. epidermidis ATCC 12228	7.62	2.79/6.21	2.76/22.8	2.58/22.8	1.39/11.4	2.61/10.7
M. luteus ATCC 9341	13.81	5.56/1.24	5.53/22.8	2.58/22.8	2.78/11.4	2.61/5.38
M. flavus ATCC 10240	3.81	5.56/1.24	2.76/22.8	2.58/45.6	2.78/11.4	2.61/5.38
E. faecalis ATCC 29212	7.62	5.56/49.6	2.76/45.6	2.58/45.6	2.78/11.4	2.61/10.7
B. subtilis ATCC 6633	7.62	5.56/1.24	2.76/22.8	2.58/22.8	2.78/11.4	2.61/10.7
E. coli ATCC 25922	7.62	5.56/6.21	2.76/45.6	2.58/45.6	2.78/11.4	2.61/10.7
K. pneumoniae NCIMB 9111[b]	7.62	5.56/6.21	2.76/45.6	2.58/45.6	2.78/11.4	2.61/10.7
P. aeruginosa ATCC 27853	7.62	5.56/49.6	5.53/45.6	5.16/45.6	5.55/22.9	2.61/10.7
C. albicans ATCC 10259	7.62	2.79/2.48	11.2/11.38	2.58/22.8	2.78/5.72	2.61/5.38
C. albicans ATCC 24433	7.62	2.79/2.48	11.2 /5.69	2.58 /22.8	2.78/5.72	2.61/5.38

[a]American Type Culture Collection (http://www.atcc.org/); [b]National Collections of Industrial Food and Marine Bacteria: NCIMB Ltd, UK

TABLE V. Minimal inhibitory concentrations (*MIC*) of the standard antibiotics against the tested microbial strains (n.t. – not tested)

Microorganism	Amikacin	Ampicillin	Vancomycin	Nystatin
S. aureus ATCC 25923	3.42	2.86	1.52	n.t.
S. epidermidis ATCC 12228	n.t.	n.t.	1.38	n.t.
M. luteus ATCC 9341	n.t.	10.3 n.t.		n.t.
M. flavus ATCC 10240	n.t.	12.0 n.t.		n.t.
E. faecalis ATCC 29212	4.09	n.t.	n.t. n.t.	
E. coli ATCC 25922	14.7	12.6	n.t.	n.t.
K. pneumoniae NCIMB 9111	10.9	n.t.	n.t. n.t.	
P. aeruginosa ATCC 27853	4.78	n.t.	n.t. n.t.	
C. albicans ATCC 10259	n.t.	n.t.	n.t.	4.1
C. albicans ATCC 24433	n.t.	n.t.	n.t.	6.69

It should be noted that all the complexes were active against *S. epidermidis*, as well as against *P. aeruginosa*, which is one of the most resistant human pathogen.

CONCLUSIONS

The present study demonstrates simple synthetic routes to five new dioxomolybdenum(VI) complexes with heterocyclic dithiocarbamates. The employed spectroscopic techniques suggest that the coordination in all $[MoO_2(Rdtc)_2]$ complexes yielded an octahedral geometry through both sulfur donating atoms, the NCSS group coordinating the metal center in a bidentate symmetrical mode. The geometries of **1**–**5**, obtained on semi-empirical MO PM6 levels are in good agreement with similar complexes for which X-ray structure data can be found in the literature. The dioxomolybdenumdithiocarbamates were capable of inhibiting bacterial growth to a certain degree.

SUPPLEMENTARY MATERIAL

IR, ^{1}H- and ^{13}C-NMR spectra of synthesized compounds are available electronically from http://www.shd.org.rs/JSCS/, or from the corresponding author on request.

Acknowledgments. This research was supported by the Ministry of Education and Science of the Republic Serbia (No. 172014).

И З В О Д

СПЕКТРОСКОПСКА СВОЈСТВА И АНТИМИКРОБНА АКТИВНОСТ ДИОКСОМОЛИБДЕН(VI) КОМПЛЕКСА СА ХЕТЕРОЦИКЛИЧНИМ *S,S'*-ЛИГАНДИМА

СОФИЈА П. СОВИЉ[1], ДРАГАНА МИТИЋ[1], БРАНКО Ј. ДРАКУЛИЋ[2] и МАРИНА МИЛЕНКОВИЋ[3]

[1]Хемијски факултет Универзитета у Београду, п. пр. 118, 11158 Београд, [2]Институт за хемију, технологију и металургију – Центар за хемију, Његошева 12, 11001 Београд и [3]Фармацеутски факултет, Универзитет у Београду, Војводе Степе 450, 11000 Београд

Синтетисано је пет нових диоксомолибден(VI) комплекса, опште формуле $[MoO_2(Rdtc^-)_2]$, са $Rdtc^-$ лигандима: пиперидин- (Pipdtc), 4-морфолин- (Morphdtc), 4-тиоморфолин- (Timdtc), пиперазин- (Pzdtc) и *N*-метилпиперазин- (*N*-Mepzdtc) дитиокарбаматима. Комплекси су окарактерисани елементалном анализом, IR и NMR спектроскопијом као и мерењем моларне проводљивости. Претпостављена геометрија свих комплекса је октаедарска. $Rdtc^-$ лиганди су бидентатно координовани преко оба атома сумпора за атом молибдена. Присуство различитих хетероатома утиче на промену положаја ν(C=H) и ν(C=S) вибрација, чији опада следећим редом лиганада: Pipdtc > *N*-Mepzdtc > Morphdt > Pzdtc > Timdtc. На основу спектралних података, структуре свих комплекса су оптимизоване на семиемпиријском молекулско-орбиталном нивоу употребом PM6 метода. Антимикробна активност испитивана је на једанаест различитих патогена. Уочено је да комплекси који имају хетероатом у положају 4 пиперидинског прстена испољавају значајно већу јачину антимикробног дејства према бактеријама, у поређењу са одговарајућим лигандима.

(Примљено 28. марта, ревидирано 26. августа 2011)

REFERENCES

1. R. R. Mendel, F. Bittner, *Biochim. Biophys. Acta, Mol. Cell Res.* **1763** (2006) 621
2. A. Sigel, H. Sigel, Eds., *Metal Ions in Biological Systems 39, Molybdenum and Tungsten: Their Roles in Biological Processes*, Marcel Dekker, New York, 2002
3. J. Davis, *Science* **264** (1994) 375

4. R. F. Service, *Science* **270** (1995) 724
5. C. D. Brondino, M. G. Rivas, M. J. Romao, J. G. Jose, I. Moura, *Acc. Chem. Res.* **39** (2006) 788
6. G. Schwarz, R. R. Mendel, *Annu. Rev. Plant Biol.* **57** (2006) 623
7. J. H. Enemark, A. V. Astashkin, A. M. Raitsimring, *Dalton Trans.* **29** (2006) 3501
8. P. Nag, R. Bohra, R. C. Mehrotra, R. Ratnani, *Synth. React. Inorg. Met.-Org. Chem.* **32** (2002) 1549
9. D. Coucouvanis, *Prog. Inorg. Chem.* **26** (1989) 301
10. S. P. Sovilj, G. Vučković, K. Babić, S. Macura, N. Juranić, *J. Coord. Chem.* **41** (1997) 19
11. S. P. Sovilj, K. Babić-Samardžija, *Synth. React. Inorg. Met.-Org. Chem.* **29** (1999) 1655
12. L. I. Victoriano, *Coord. Chem. Rev.* **196** (2000) 383 (and references cited therein)
13. S. P. Sovilj , N. Avra mović, D. Poleti, D. Djoković, *Bull. Chem. Technol. Maced.* **19** (2000) 139
14. S. P. Sovilj, N. Avramović, N. Katsaros, *Transition Met. Chem.* **29** (2004) 737
15. K. B. Pandeya, B. B. Kaul, *Synth. React. Inorg. Met.-Org. Chem.* **12** (1982) 259
16. S. O. Pinheiro, J. R. de Sousa, M. O. Santiago, I. M. Carvalho, Y. Hao, W. Perez-Segarra, Q. Shi, A. Wei, *J. Am. Chem. Soc.* **127** (2005) 7328
17. J. D. E. T. Wilton-Ely, D. Solanki, G. Hogarth, *Eur. J. Inorg. Chem.* (2005) 4027
18. A. L. R. Silva, A. A. Batista, E. E. Castellano, J. Ellena, I. S. Moreira, I. C. N. Diogenes, *Inorg. Chim. Acta* **359** (2006) 391
19. S. P. Sovilj, D. Mitić, V. M. Leovac, *Asian J. Chem.* **15** (2003) 165
20. C. Bolzati, M. C. Ceccato, S. Agostini, F. Refosco, Y. Y amamichi, S. Tokunaga, D. Carta, N. Salvarese, D. Bernardini, G. Bandoli, *Bioconjugate Chem.* **21** (2010) 928
21. H. Li, C. S. Lai, J. Wu, P. C. Ho, D. de Vos, E. R. T. Tiekink, *J. Inorg. Biochem.* **101** (2007) 809
22. Z. A. Kaplancikli, G. Turan-Zitouni, G. Revial, G. Iscan, *Phosphorus, Sulfur Silicon Relat. Elem.* **179** (2004) 1449
23. N. K. Kaushik, B. Bushan, A. K. Sharma, *Transition Met. Chem.* **9** (1984) 250
24. N. Katsaros, M. Katsaroua, S. P. Sovil j, K. Babić-Samardžija, D. M. Mitić, *Bioinorg. Chem. App.* **2** (2004) 193
25. N. Hackerman, D. D. Justice, E. McCofferty, *Corrosion* **31** (1975) 240
26. V. M. Jovanović, K. Babić-Samardžija, S. P. Sovilj, *Electroanalysis* **13** (2001) 1129
27. V. M. Jovanović, K. Babić-Samardžija, S. P. Sovilj, *J. Serb. Chem. Soc.* **70** (2005) 51
28. S. P. Sovilj, B. J. Drakulić, D. Lj. Stojić, N. Katsaros, *Mater. Sci. Forum* **518** (2006) 411
29. E. Farkas, H. Csoka, G. Bell, D. A. Brown, L. P. Cuffe, N. J. Fitzpatrick, W. K. Glass, *J. Chem. Soc., Dalton Trans.* **16** (1999) 2789
30. A. C. Stergiou, S. Bladenopoulou, C. Tsiamis, *Inorg. Chim. Acta* **217** (1994) 61
31. B. B. Kaul, J. H. Enemark, S. L. Merbs, J. T. Spence, *J. Am. Chem. Soc.* **107** (1985) 2885
32. K. Babić-Samardžija, S. P. Sovilj, N. Katsaros, *J. Molec. Struct.* **694** (2004) 165
33. M. M. Jones, *J. Am. Chem. Soc.* **81** (1959) 3188
34. a) J. J. P. Stewart, *J. Comput.-Aided Mol. Des.* **4** (1990) 1; b) J. J. P Stewart, MOPAC2009, Stewart Computational Chemistry, Colorado Springs, CO, 20 09, http://OpenMOPAC.net (accessed on 17/03/2011)
35. J. J. P. Stewart, *J. Mol. Model.* **13** (2007) 1173
36. A. Klamt, G. Schüümann, *J. Chem. Soc., Perkin Trans. 2* (1993) 799
37. K. Wolinski, J. F. Hilton, P. Pulay, *J. Am. Chem. Soc.* **112** (1990) 8251

38. S. Miertus, E. Scrocco, J. Tomasi, *Chem. Phys.* **55** (1981) 117
39. *GAUSSIAN 03, Revision C.02*, Gaussian, Inc., Pittsburgh, PA, 2003
40. A. Pedretti, L. Villa, G. Vistoli, *J. Comput.-Aided Mol. Des.* **18** (2004) 167
41. *Jmol: an open-source Java Viewer for Chemical Structures in 3D, Jmol v.11.2.1*, http://www.jmol.org/ (accessed on 17/03/2011)
42. Clinical and Laboratory Standards Institute (CLSI), *Performance Standards for Antimicrobial Susceptibility Testing: 15th Informational Supplement*, CLSI Document M100-S15, Wayne, PA, USA, 2005
43. W. J. Geary, *Coord. Chem. Rev.* **7** (1971) 81
44. R. J. H. Clark, T. J. Dines, M. J. Wolf, *J. Chem. Soc., Faraday Trans. 2* **78** (1982) 679
45. H. O. Desseyn, A. C. Fabretti, F. Forghieri, C. Preti, *Spectrochim. Acta, Part A* **41** (1985) 1105
46. A. C. Fabretti, F. Forghieri, A. Giusti, C. Preti, G. Tosi, *Inorg. Chim. Acta* **85** (1984) 127
47. L. J. Willis, T. M. Loehr, K. F. Miller, A. E. Bruce, E. I. Stiefl, *Inorg. Chem.* **25** (1986) 4289
48. F. A. Cotton, G. Wilkinson, C. A. Murillo, M. Boch mann, *Advanced Inorganic Chemistry*, 6th ed., Wiley, New York, 1999, Chap. 18, p. 944
49. K. Nakamoto, *Infrared and Raman Spectra of Inorganic and Coordination Compounds*, 5th ed., Wiley, New York, 1988, p. 82
50. G. Faraglia, S. Sitran, *Inorg. Chim. Acta* **176** (1990) 67
51. K. Unoura, A. Yamazaky, A. Nagasawa, H. Itoh, H. Kudo, Y. Fukuda, *Inorg. Chim. Acta* **269** (1998) 260
52. L. Stelzig, S. Kotte, B. Krebs, *J. Chem. Soc., Dalton Trans.* **17** (1998) 2921
53. H. Teruel, Y. C. Gorrin, L. R. Falvello, *Inorg. Chim. Acta* **316** (2001) 1.

Journal of the Serbian Chemical Society
JSCS@tmf.bg.ac.rs • www.shd.org.rs/JSCS
J. Serb. Chem. Soc. 77 (1) S30–S35 (2012) *Supplementary material*

SUPPLEMENTARY MATERIAL TO

Spectroscopic properties and antimicrobial activity of dioxomolybdenum(VI) complexes with heterocyclic *S,S'*-ligands

SOFIJA P. SOVILJ[1]*, DRAGANA MITIĆ[1], BRANKO J. DRAKULIĆ[2] and MARINA MILENKOVIĆ[3]

[1]Faculty of Chemistry, P. O. Box 118, 11158 Belgrade, Serbia, [2]ICTM, Department of Chemistry, Njegoševa 12, 11001 Belgrade, Serbia and [3]Department of Microbiology and Immunology, Faculty of Pharmacy, University of Belgrade, Vojvode Stepe 450, Belgrade, Serbia

J. Serb. Chem. Soc. 77 (1) (2012) 53–66

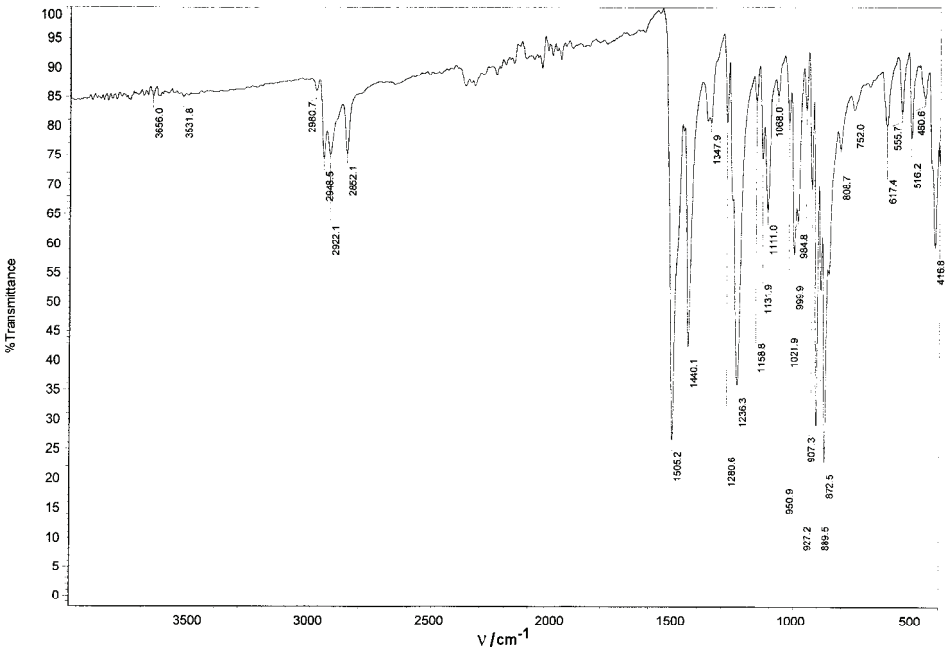

Fig. S1a. Recorded IR spectrum for the complex **1**.

* Corresponding author. E-mail: ssovilj@chem.bg.ac.rs

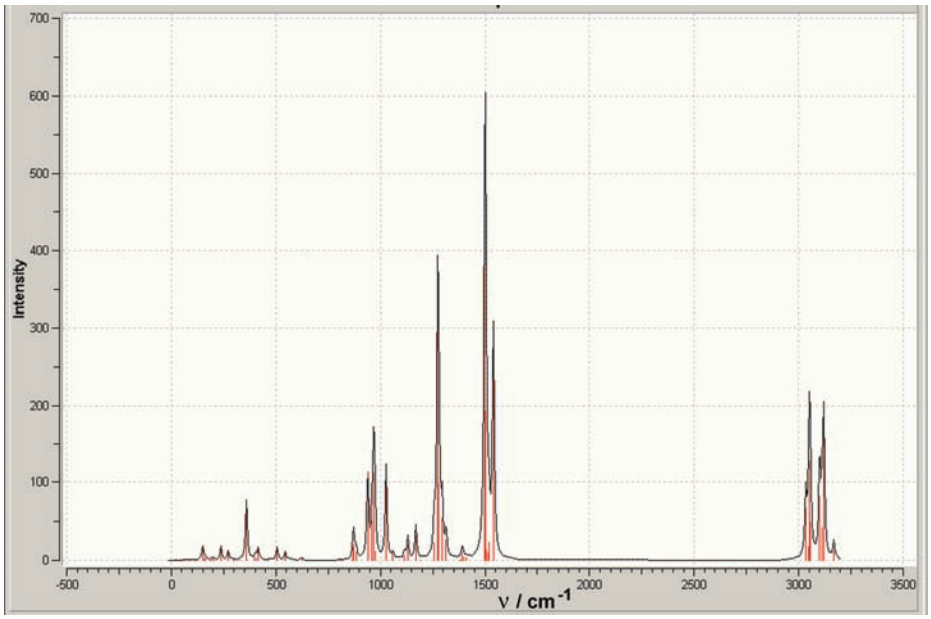

Fig. S1b. Calculated IR spectrum for the complex **1**.

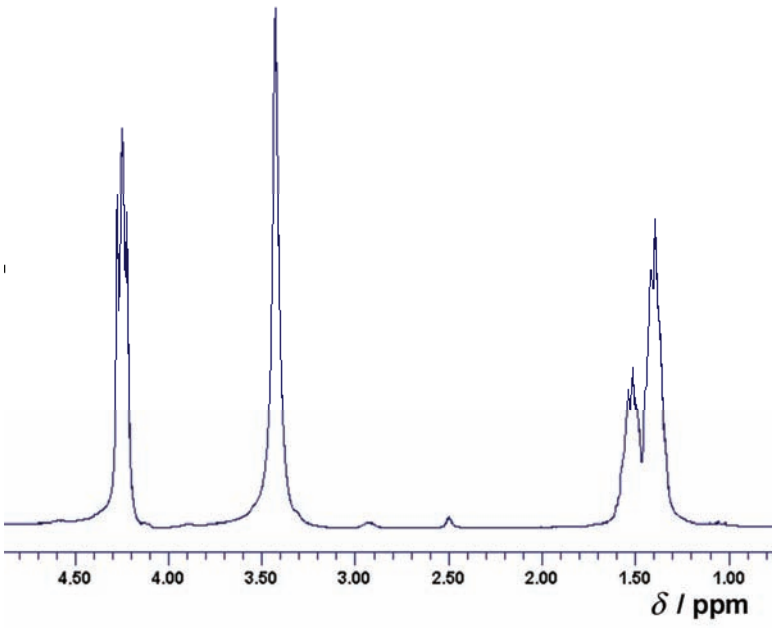

Fig. S2a. ^{1}H-NMR spectrum of Pipdtc.

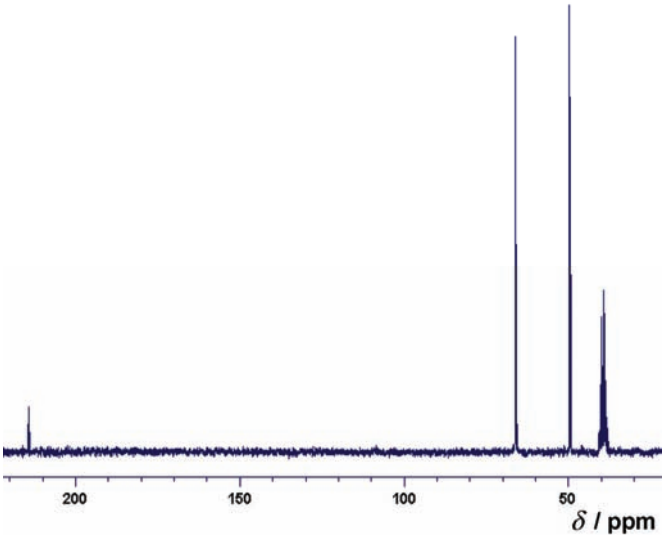

Fig. S2b. ^{13}C-NMR spectrum of Pipdtc.

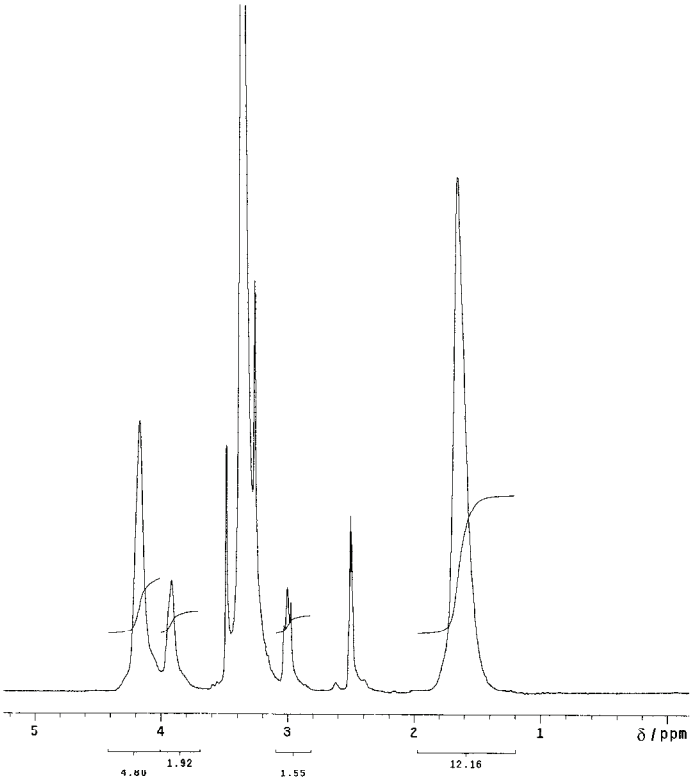

Fig. S3a. Experimentally obtained ^{1}H-NMR spectrum of complex **1**.

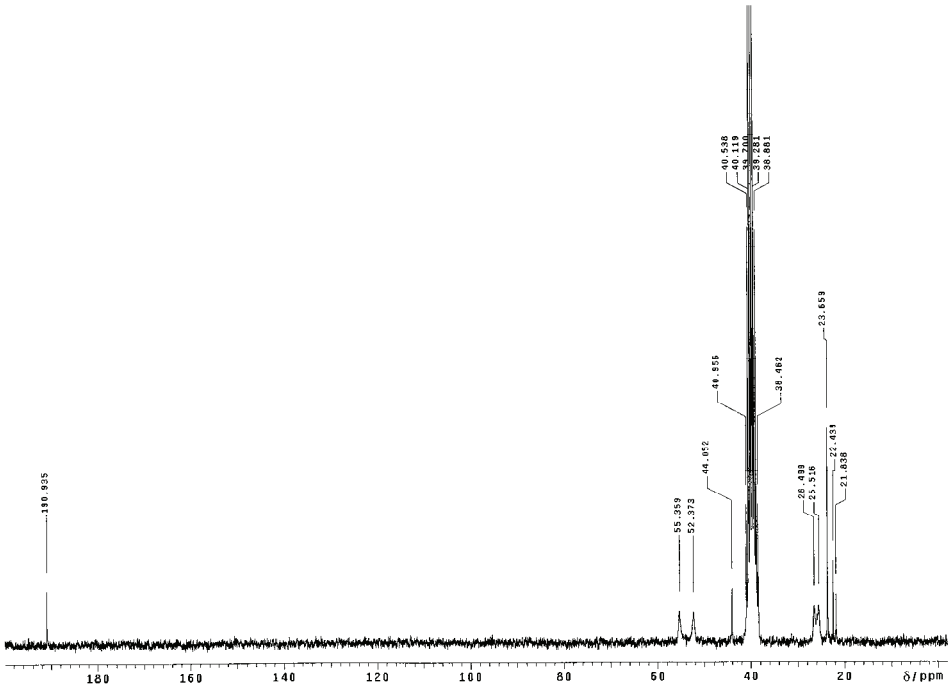

Fig. S3b. Experimentally obtained ^{13}C-NMR spectrum of complex **1**.

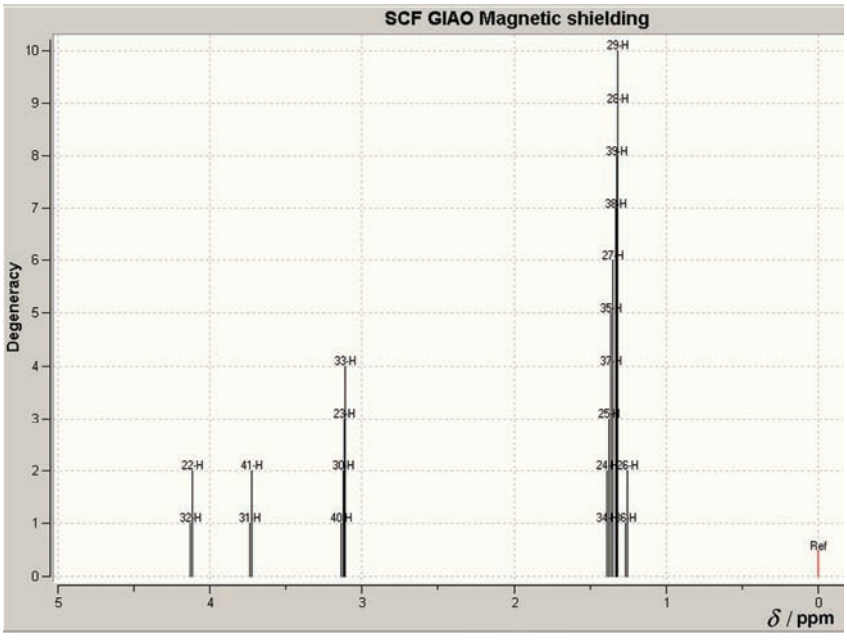

Fig. S3c. Calculated ^{1}H-NMR spectrum of complex **1**.

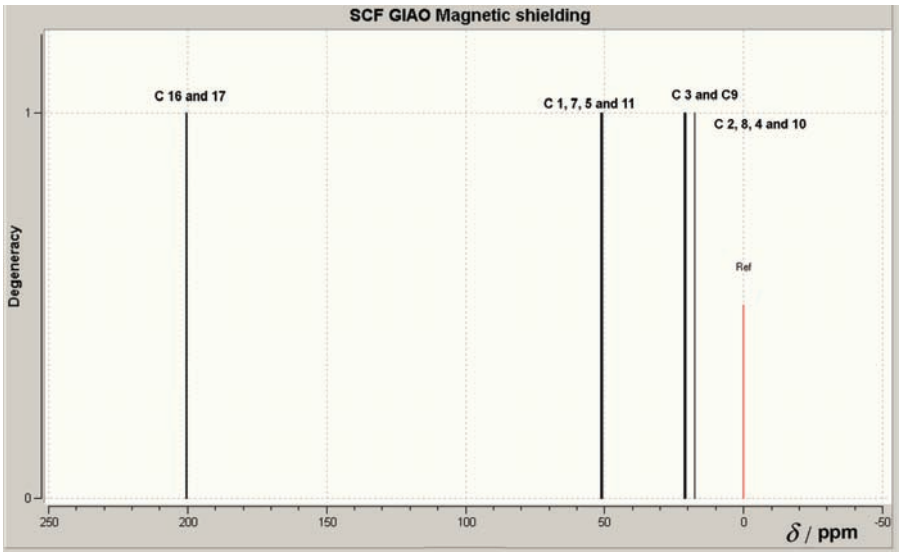

Fig. S3d. Calculated ^{13}C-NMR spectrum of complex **1**.

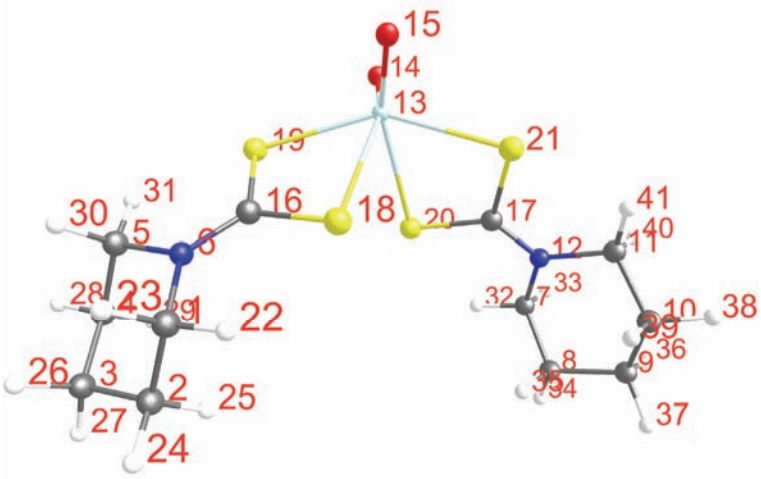

Fig. S4. Atoms enumeration that correspond to assignation given on calculated spectra for complex **1**, Fig. S3.

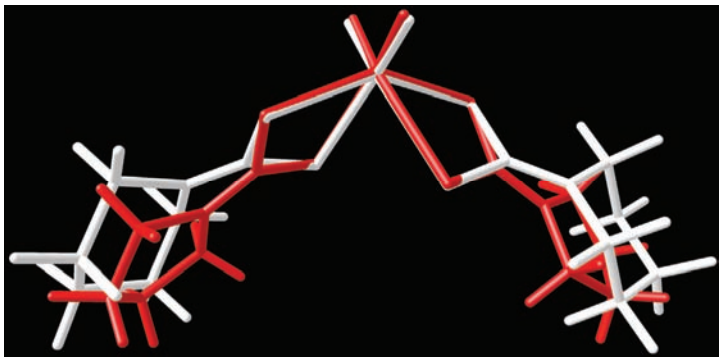

(a)

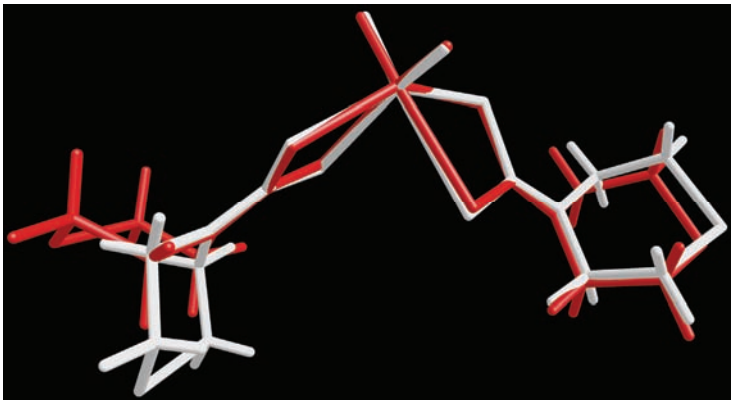

(b)

Fig. S5. Superimposed structures of: a) calculated complex **1** to CSD entry 153544 taken from reference 49; and b) calculated complex **3** to crystal structure taken from reference 47 (see References in the paper).

Journal of the Serbian Chemical Society
JSCS-info@shd.org.rs • www.shd.org.rs/JSCS
J. Serb. Chem. Soc. *77* (1) 67–73 (2012)
JSCS–4249
UDC 546.56:541.64+547.86+547.586.7+547.233'821
Original scientific paper

X-Ray structure of a 1D-coordination polymer of copper(II) bearing pyrazine-2,3-dicarboxylic acid and 2-aminopyrimidine

MASOUD MIRZAEI[1]*, HOSSEIN ESHTIAGH-HOSSEINI[1], AZAM HASSANPOOR[1] and VICTOR BARBA[2]

[1]*Department of Chemistry, Ferdowsi University of Mashhad, 917791436 Mashhad, Iran and* [2]*Centro de Investigaciones Químicas, UAEM, Av. Universidad 1001, 62209 Cuernavaca, México*

(Received 15 November 2010, revised 28 September 2011)

Abstract: A new 1D-coordination polymer of Cu(II) ions, $\{(2\text{-apymH})_2[Cu(pyzdc)_2]\cdot 6H_2O\}_n$, (2-apym = 2-aminopyrimidine, $pyzdcH_2$ = pyrazine-2,3-dicarboxylic acid), was synthesized based on the proton transfer mechanism and characterized by elemental analysis, infrared spectroscopy and single crystal X-ray diffraction. The coordination polymer consists of infinite chains of $[Cu(pyzdc)_2]^{2-}$ bridged across a double chain running along the *a*-axis and discrete $(2\text{-apymH})^+$ fragments. The Cu(II) ion is located on the inversion centre in the basal plane of an elongated octahedron with two oxygen atoms from adjacent $(pyzdc)^{2-}$ ligands occupying the axial positions. The interaction between oxygen atoms of water molecules with the dicarboxylic acid plays an important role in the overall supramolecular assembly.

Key words: copper; pyrazine-2,3-dicarboxylic acid; 2-aminopyrimidine; proton transfer; hydrogen bond; coordination polymer; water cluster.

INTRODUCTION

The field of coordination polymer particles has received much attention in coordination chemistry in recent years owing to their novel and diverse topologies and potential applications in host–guest chemistry, catalysis, biomedical applications, magnetism, and non-linear optics.[1–4] By selecting appropriate metal ions and organic linkers, coordination polymers with various structures, such as 1D chains ladders,[5–7] 2D grids[8] and 3D networks[9] can be obtained. Polycarboxylic acids represent supramolecular connectors that can generate infinite networks and metal–organic frameworks.[10] The carboxylate group may present various coordination modes, leading to the formation of *mono*-nuclear, *di*-nuclear,

* Corresponding author. E-mail: mirzaeesh@um.ac.ir
doi: 10.2298/JSC101115153M

metal–organic frameworks or coordination polymers.[11] In particular, pyrazinedicarboxylic acids have many different modes of coordination to metal ions. For example, it coordinated to the Cu(II) ion as a monodentate ligand in the $[Cu(pyzdc)(H_2O)(en)_2]$ (en = ethylene diamine) complex.[12] In another instance, $pyzdcH_2$ behaved as a bidentate ligand *via* the oxygen atom of carboxylate and the nitrogen atom of 1,4-pyrazine ring in the $(ampyH)_2[Cu(pyzdc)_2(H_2O)_2]\cdot 6H_2O$ (ampy = 2-amino-4-methylpyridine) coordination compound.[13] Moreover, $pyzdcH_2$ is well known to act as a bridging ligand, especially in the design and construction of metal–organic frameworks and coordination polymers.[11] It acts as multidentate bridges between metal ions forming 1D-network chains. For example, $pyzdcH_2$ coordinated to the metal ions as a tridentate and tetradentate ligand in $\{(acrH)_2[Zn(pyzdc)_2]\}_n$ (acr = acridine) and $\{[Mn(pyzdc)(H_2O)]\cdot 2H_2O\}_n$ complexes.[14–16] In the mentioned complexes, the coordination sites for each $(pyzdc)^{2-}$ are, respectively, three and four O atoms of carboxylate groups and one N atom of the 1,4-pyrazine ring. In this work, the synthesis and identification of $\{(2\text{-apymH})_2[Cu(pyzdc)_2]\cdot 6H_2O\}_n$ by elemental analysis, infrared spectroscopy, and crystal structure determination are described.

EXPERIMENTAL

Materials and physical measurements

All reagents used in the synthesis were purchased from commercial sources and were used as received without further purification. The infrared spectrum in the range (4000–600 cm^{-1}) was recorded on a Buck 500 scientific spectrometer using a KBr disc. Elemental analyses were performed using a Thermo Finnigan Flash-1112EA microanalyzer. The X-ray diffraction studies were performed on a Bruker-APEX diffractometer with a CCD area detector, using Mo K_α-radiation, (λ = 0.71073 Å), and a graphite monochromator. Frames were collected at T = 100 K *via* ω/ϕ-rotation at 10 s per frame (SMART).[17] The measured intensities were reduced to F^2 and corrected for adsorption with SADABS (SAINT-NT).[18] Corrections were made for Lorentz and polarization effects. Structure solution, refinement, and data output were realised with the SHELXTL-NT program package.[19] Non-hydrogen atoms were refined anisotropically. C−H hydrogen atoms were placed in the geometrically calculated positions using a riding model. O−H and N−H hydrogen atoms were localized by difference Fourier maps.

*Preparation of $\{(2\text{-apymH})_2[Cu(pyzdc)_2]\cdot 6H_2O\}_n$ (**1**)*

A mixture of $pyzdcH_2$ (0.18 mmol, 0.030 g) and 2-apym (0.36 mmol, 0.030 g) in water (10 mL) was refluxed for 1 h, then $CuCl_2\cdot 2H_2O$ (0.060 mmol, 0.010 g) was added and refluxing was continued for 6 h, whereby a green solution was obtained. This solution gave green needle crystals of **1** in a yield of approximate 60 % (based on copper) after slow evaporation of the solvent at room temperature. Anal. Calcd. for $C_{20}H_{28}CuN_{10}O_{14}$: C, 34.56; H, 4.03; N, 20.16 %. Found: C, 34.15; H, 3.93; N, 21.05 %; IR (KBr, cm^{-1}): 3400, 1651, 1607, 1554, 1437, 1362, 1283, 1174, 1127, 1060, 975, 880, 842.

RESULTS AND DISCUSSION

*X-Ray crystallographic study of {(2-apymH)$_2$[Cu(pyzdc)$_2$]·6H$_2$O}$_n$ (**1**)*

The crystallographic data of the title compound is given in Table I. The molecular structure of **1** contains a discrete coordination polymer of the $[Cu(pyzdc)_2]^{2-}$, organic species of $(2\text{-apymH})^+$ and crystallization water molecules in a 1:2:6 molar ratio (Fig. 1). In the polymeric chain of $[Cu(pyzdc)_2]^{2-}$, the copper ion is six-coordinated showing CuN_2O_4 bound set by two N and four O atoms belonging to two $(pyzdc)^{2-}$ ligands which are related by an inversion centre (the N1−Cu−N1^i bond angle is 180°). This arrangement causes the formation of a distorted octahedral geometry. The equatorial plane around the Cu(II) ion consists of a five-membered chelate ring with N (Cu−N1, 1.991(2) Å) and O (Cu−O1, 1.959(17) Å) as donor atoms while the axial positions are occupied by two oxygen atoms (Cu−O3, 2.427(19) Å) belonging to the remaining carboxylate group. The bonds length in the title compound can be compared with two 1D--coordination polymers, *i.e.*, $\{Cu(pzdc)(H_2O)_2\cdot H_2O\}_n$ (**a**)[20] and {[Cu(μ--pzdc)(bipy)]·$H_2O\}_n$ (**b**)[21] (bipy = bipyridine). The axial bond distance in **1** is

TABLE I. Selected crystallographic data and structure refinement parameters of **1**

Empirical formula		$C_{20}H_{28}CuN_{10}O_{14}$
Formula weight, g mol^{-1}		696.07
Temperature, K		293(2)
Wavelength λ, Å		0.71073
Crystal system		Monoclinic
Space group		P21/c
a / Å		6.625 (3)
b / Å		11.600 (5)
c / Å		18.438 (8)
β / °		82.901 (8)
V / Å^3		1395.4 (11)
Z		2
D_c / kg m^{-3}		1657
F_{000}		718
μ / mm^{-1}		0.87
Crystal size, mm		0.45×0.32×0.26
Space range, °		$2.1 < \theta < 23.4$
Reciprocal lattice segments:	h	$-7 \rightarrow 7$,
	k	$-12 \rightarrow 12$,
	l	$-20 \rightarrow 20$
Reflections collected		11294
Reflection independent		2026
R_1, $wR_2[I > 2\sigma(I)]$		0.0317, 0.0752
R_1, wR_2 (all data)		0.0350, 0.0770
Goodness-of-fit on F^2		1.061
Largest differences peak and hole, e Å^{-3}		0.31 and –0.29

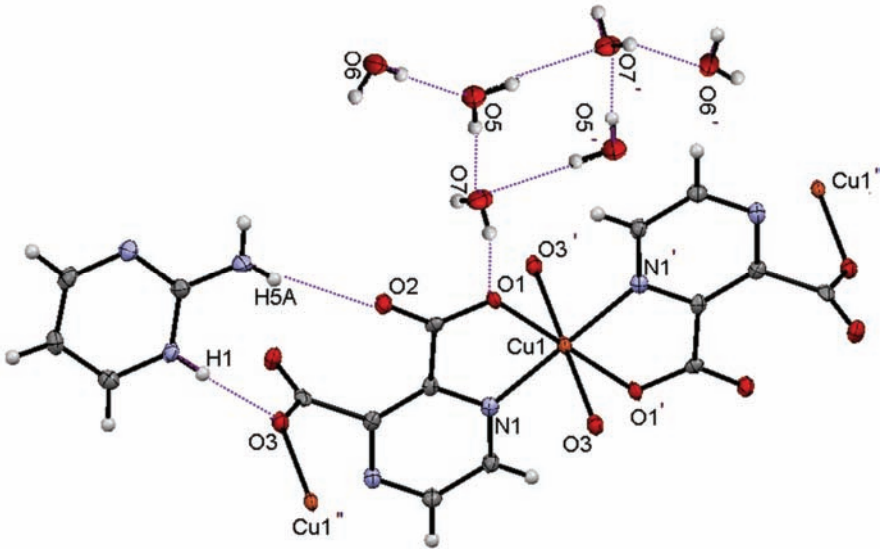

Fig. 1. The coordination environment of the Cu(II) ion with atom numbering, showing displacement ellipsoids at the 50 % probability level. Hydrogen bonds shown as dashed line. Atom symmetry operators: O6, 1–*x*, –*y*, 1–*z*; O7, 1+*x*, 1/2–*y*, 1/2+*z*; O5, 1+*x*, 1/2–*y*, 1/2+*z*; O7', 2–*x*, –1/2+*y*, 1.5–*z*; O5', 2–*x*, –1/2+*y*, 1.5–*z*; O6', 2–*x*, –*y*, 1–*z*; O4, 2–*x*, –*y*, 1–*z*; O1', 1–*x*, –*y*, 1–*z*; O3', 1–*x*, –*y*, 1–*z*; N1', 1–*x*, –*y*, 1–*z*; Cu1', 1+*x*, *y*, *z*; Cu1", –1+*x*, *y*, *z*.

longer than in **a** (2.306(3) Å) and **b** (2.151(3) Å), while the equatorial Cu−O bond distance is shorter than the respective bond (1.987(3) and 1.963(3) Å) in **a** and **b**, respectively. In addition to the covalent coordinative bonds in the crystalline network that cause the formation of a 1D-chain-like polymer, cooperatively there are intriguing intermolecular hydrogen bonds that join together to create various motifs and chains of solvent water molecules. The N5−H5A···O2 and N4−H1···O3 interactions between $[Cu(pyzdc)_2]^{2-}$ polymeric species and protonated moiety resulted in the formation of hetero synthon $R_2^2(11)$. One of the most significant points in this study is the molecules of crystallization water, which play an important role in expanding the title polymer to give a 3D supramolecular architecture. In fact, these water molecules, which are linked by hydrogen bonds to form tapes comprised of an alternating sequence of fused hexamer and tetramer water clusters, act as a gluing factor for connecting adjacent polymeric chains by the establishment of hydrogen bonding interactions.[22] In 2006, Castillo and co-workers reported the synthesis of a coordination polymer, $\{(H_2bpe)[Cu(\mu\text{-}pyzdc)_2]\cdot 2H_2O\}_n$, (bpe = 1,2-bis(4-pyridyl)ethylene), that is similar to compound **1**.[23] In both structures, the cations and water molecules are inserted between two parallel arrays of chains giving rise to a pillared structure which acts as a hydrogen-bond donor linking the upper and lower arrays of chains (Fig. 2). However, the difference in reaction conditions and type of the

cationic entities leads to a change in the crystalline network, the packing diagram and the hydrogen bonding interactions. One of the significant diff erences within **1** in comparison to the Castillo compound is the presence of water clusters in the former and their absence in the latter.

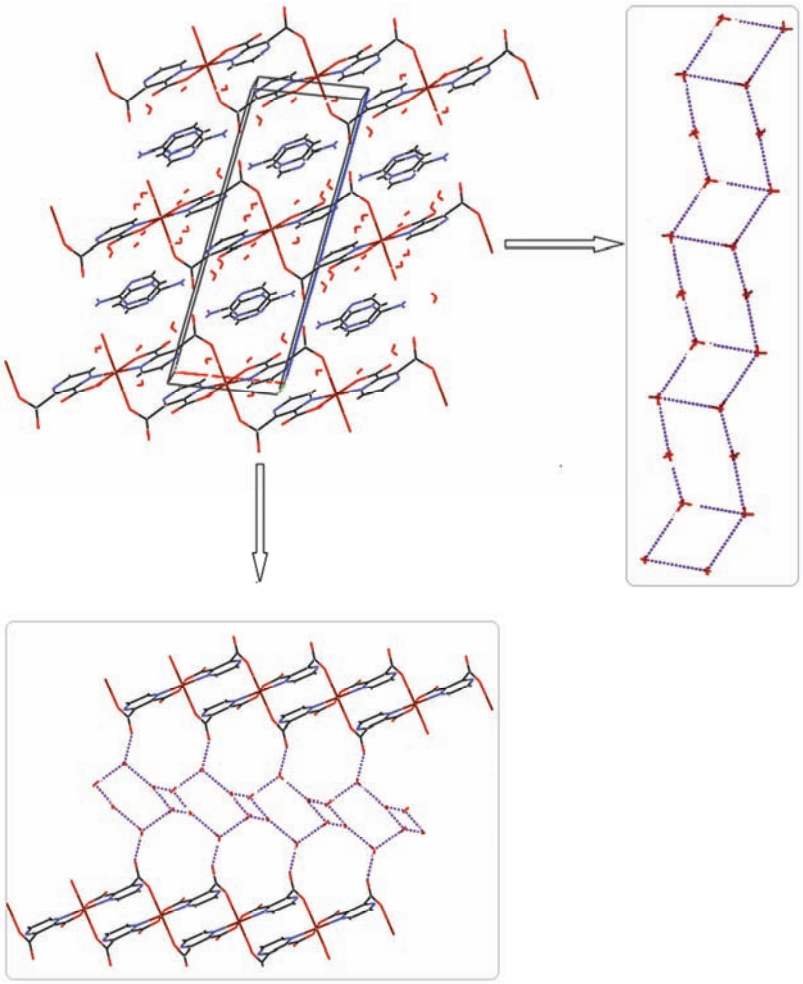

Fig. 2. View of the network including non-coordinated water molecules formed by N–H···O and O–H···O bonds.

CONCLUSIONS

A new 1D-Cu(II) coordination poly mer was sy nthesized and structurally characterized by means of elemental analysis, infrared spectroscopy and single crystal X-ray diffraction. A novel topological net with channels was prepared by using a flexible ligand. The cry stal structure of **1** consists of a 1 D-polymer and

shows a coordination number of six for the Cu(II) ions. Presently, other complexes are being explored with much more flexible polycarboxylate ligands and relationships between their coordination mode and the structures obtained *via* the proton transfer mechanism are being studied.[24] Many aspects of these categories of coordination polymer with a proton transfer ligand and their complexes, such as their solid phase fluorescence and biological activity, as well as further studies employing SEM and/or TEM techniques with the view of obtaining layered coordination metal–organic frameworks in nano-size regime using sonochemical irradiation, for comparing with the routine methods, remain to be investigated, which are our aims for the near future.

SUPPLEMENTARY DATA

CCDC 785660 contains the supplementary crystallographic data for this paper. These data can be obtained free of charge *via* www.ccdc.cam.ac.uk/conts/retrieving.html (or from the Cambridge Crystallographic Data Centre, 12, Union Road, Cambridge CB2 1EZ, UK; fax: +44 1223 336033).

Acknowledgement. The authors wish to thank to the Ferdowsi University of Mashhad, Iran, for financial support of this article (Grant No. P/2106).

ИЗВОД

МОЛЕКУЛСКА СТРУКТУРА 1D-КООРДИНАЦИОНОГ ПОЛИМЕРА БАКРА(II) СА ПИРАЗИН-2,3-ДИКАРБОКСИЛНОМ КИСЕЛИНОМ И 2-АМИНОПИРИМИДИНОМ

MASOUD MIRZAEI[1], HOSSEIN ESHTIAGH-HOSSEINI[1], AZAM HASSANPOOR[1] и VICTOR BARBA[2]

[1]Department of Chemistry, Ferdowsi University of Mashhad, 917791436 Mashhad, Iran и [2]Centro de Investigaciones Químicas, UAEM, Av. Universidad 1001, 62209 Cuernavaca, México

На основу протон-трансфер механизма синтетизован је нови 1D-координациони полимер бакар(II) јона, $\{(2\text{-apymH})_2[Cu(pyzdc)_2]\cdot 6H_2O\}_n$, (2-apym = 2-аминопиримидин, $pyzdcH_2$ = = пиразин-2,3-дикарбоксилна киселина). За карактеризацију овог полимера употребљени су елементална микроанализа, инфрацрвена спектроскопија и дифракција X-зрака са монокристала. Координациони полимер садржи непрекидне полимерне ланце од $[Cu(pyzdc)_2]^{2-}$, где су два ланца међусобно мосно повезана дуж *a*-осе, и дискретних $(2\text{-apymH})^+$ фрагмената. Бакар(II) јон се налази у инверзионом центру основне равни издуженог октаедра, док су два кисеоникова атома суседних $(pyzdc)^{2-}$ лиганада у аксијалном положају актаедра. Интеракције између атома кисеоника из молекула воде заједно са дикарбоксилном киселином имају значајну улогу у грађењу супрамолекулске структуре.

(Примљено 15. новембра 2010, ревидирано 28. септембра 2011)

REFERENCES

1. T. Uemura, N. Yanai, S. Kitagawa, *Chem. Soc. Rev*. **38** (2009) 1228
2. A. U. Czaja, N. Trukhan, U. Muller, *Chem. Soc. Rev*. **38** (2009) 1284
3. L. Ma, C. Abney, W. Lin, *Chem. Soc. Rev*. **38** (2009) 1248
4. A. M. Spokoyny, D. Kim, A. Sumrein, C. A. Mirkin, *Chem. Soc. Rev*. **38** (2009) 1218
5. D. M. Shin, I. S. Lee, Y. A. Lee, Y. K. Chung, *Inorg. Chem*. **42** (2003) 297

6. M. A. Withersby, A. J. Blake, N. R. Champness, P. A. Cooke, P. Hubberstey, W. S. Li, M. Schröder, *Inorg. Chem.* **38** (1999)
7. Y. Ma, Y. K. He, L. T. Zhang, J. Q. Gao, Z. B. Han, *J. Chem. Crystallogr*. **38** (2008) 267
8. D. M. Shin, I. S. Lee, Y. K. Chung, M. S. Lah, *Inorg. Chem*. **42** (2003) 5459
9. B. Q. Ma, H. L. Sun, S. Gao, *Inorg. Chem*. **44** (2005) 837
10. a) G. B. Deacon, R. J. Phillips, *Coord. Chem. Rev*. **33** (1980) 251; b) D. J. Tranchemontagne, J. L. Mendoza-Cortés, M. O'Keeffe, O. M. Yaghi, *Chem. Soc. Rev*. **38** (2009) 1257
11. T. L. Che, Q. C. Gao, W. P. Zhang, Z. X. Nan, H. Z. Li, Y. Q. Cai, J. S. Zhao, *Russ. J. Coord. Chem*. **35** (2009) 723
12. O. Z. Yeşilel, A. Mutlu, O. Büyükgüngör, *Polyhedron* **27** (2008) 2471
13. H. Eshtiagh-Hosseini, F. Gschwind, N. Alfi, M. Mirzaei, *Acta Crystallogr., E* **66** (2010) 826
14. a) H. Eshtiagh-Hosseini, H. Aghabozorg, M. Mirzaei, *Acta Crystallogr., E* **66** (2010) 882; b) H. Eshtiagh-Hosseini, H. Aghabozorg, M. Shamsipur, M. Mirzaei, M. Ghanbari, *J. Iran. Chem. Soc*. **8** (2011) 762
15. H. Eshtiagh-Hosseini, A. Hassanpoor, N. Alfi, M. Mirzaei, K. M. Fromm, A. Shokrollahi, F. Gschwind, E. Karami, *J. Coord. Chem*. **63** (2010) 3175
16. C. D. Ene, F. Tuna, O. Fabelo, C. Ruiz-Pérez, A. M. Madalan, H. W. Roesky, M. Andruh, *Polyhedron* **27** (2008) 574
17. Bruker Analytical X-ray Systems, *SMART: Bruker Molecular Analysis Research Tool, versions 5.057 and 5.618*, 1997 and 2000
18. Bruker Analytical X-ray Systems, *SAINT + NT, versions 6.01 and 6.04*, 1999 and 2001
19. G.M. Sheldrick, *Acta Crystallogr., A* **64** (2008) 112
20. S. Konar, S. Chandra Manna, E. Zangrando, N. Ray Chaudhuri, *Inorg. Chim. Acta* **357** (2004) 1593
21. O. Z. Yeşilel, A. Mutlu, O. Büyükgüngör, *Polyhedron* **28** (2009) 437
22. H. Aghabozorg, H. Eshtiagh-Hosseini, A. R. Salimi, M. Mirzaei, *J. Iran. Chem. Soc*. **7** (2010) 289
23. G. Beobide, O. Castillo, A. Luque, U. Garc ía-Couceiro, J. P. García-Terán, P. Rom án, *Inorg. Chem*. **45** (2006) 5367
24. M. Mirzaei, H. Aghabozorg, H. Eshtiagh-Hosseini, *J. Iran. Chem. Soc*. **8** (2011) 580.

Journal of the Serbian Chemical Society
JSCS-info@shd.org.rs • www.shd.org.rs/JSCS
J. Serb. Chem. Soc. 77 (1) 75–81 (2012) UDC 546.28+547.7+547.313.2:66.095.252.091.7
JSCS–4250 *Original scientific paper*

Ab initio study of mechanism of the formation of a silicic bis-heterocyclic compound in the reaction of silylenesilylene (H_2Si=Si:) with ethene

XIUHUI LU*, LEYI SHI, YONGQING LI and ZHINA WANG

School of Chemistry and Chemical Engineering, University of Jinan, Jinan, Shandong, 250022, People's Republic of China

(Received 15 January, revised 4 october 2011)

Abstract: The mechanism of the cycloaddition reaction of the formation of a silicic bis-heterocyclic compound between singlet state silylenesilylene (H_2Si=Si:) and ethene was investigated by the CCSD(T)//MP2/6-31G* method. From the potential energy profile, it can be predicted that the reaction has one dominant reaction pathway. The presented rule of the dominant reaction pathway is that the [2+2] cycloaddition effect of the two reactants leads to the formation of a four-membered ring silylene (INT1). When the four-membered ring silylene (INT1) interacts with ethene, due to sp^3 hybridization of the Si: atom in four-membered ring silylene (INT1), the four-membered ring silylene (INT1) further combines with ethene to form a silicic bis-heterocyclic compound (P2).

Keywords: silylenesilylene (H_2Si=Si:); cycloaddition reaction; potential energy profile.

INTRODUCTION

In recent years, silylene as an important active intermediate has attracted much attention in various fields of chemistry [1,2] and has led to a varied chemistry concerning silylenes. Reactions of silylene are regarded as an effective method in the synthesis of new bonds and heterocyclic compounds containing Si, which have long been some of the most interesting topics for organo–silicon chemists. There have been many theoretical and experimental investigations on addition reactions to saturated silylene.[3–9] For example, the rate constant for the reaction of SiH_2 ($\tilde{X}^1A$) and C_2H_4 is 9.7×10^{-11} cm^3 mol^{-1} s^{-1}, measured by Inoue and Suzuki using the laser photolysis–laser-induced fluorescence method at 298 K and 1 Torr.[6]

Becerra *et al.*[9] obtained the following Arrhenius parameters: log (A / cm^3 mol^{-1} s^{-1}) = –10.10±0.06, E_a = –3.91±0.47 kJ mol^{-1}, and the Arrhenius Equa-

* Corresponding author. E-mail: lxh@ujn.edu.cn
doi: 10.2298/JSC110115119L

tion: log (k / cm^3 mol^{-1} s^{-1}) = (–10.10±0.06) + (3.91±0.47 kJ mol^{-1}) / RTln 10, by using laser flash photol ysis to gener ate SiH_2 and monitoring the reaction of SiH_2 with acetaldehy de over the pressure range 1–100 T orr and tem perature range 297–599 K. Some studies were performed on th e cycloaddition reaction of saturated silylene.[10–13] In addition, the cycloaddition reaction of u nsaturated silylenes were preliminarily studied,[14–18] but these studies wer e always limited to the cycloaddition reaction of silylidene and its derivatives (R_1R_2C=Si: (R_1, R_2 = = H, Me, F , Cl, Br, Ph, Ar, *etc.*)). Hitherto, there are no reports on the cycloaddition reaction of sil ylene silylene and its derivati ves (R_1R_2 Si=Si: (R_1, R_2 = H, Me, F, Cl, Br, Ph, Ar, *etc.*)); hence, this is a new study field of the cy cloaddition reaction of unsatura ted silylene. In order to explore the rules of the c yclo-addition reactions between silylenesilylene or its derivatives and symmetric π--bonded compounds, silylenesilylene (H_2Si=Si:) and ethene were chosen as model molecules, and it's the mechanism of their reaction was investigated and analyzed theoretically. The results showed that this c ycloaddition reaction has two possible pathways (considering the hydrogen transfer simultaneously) as follows:

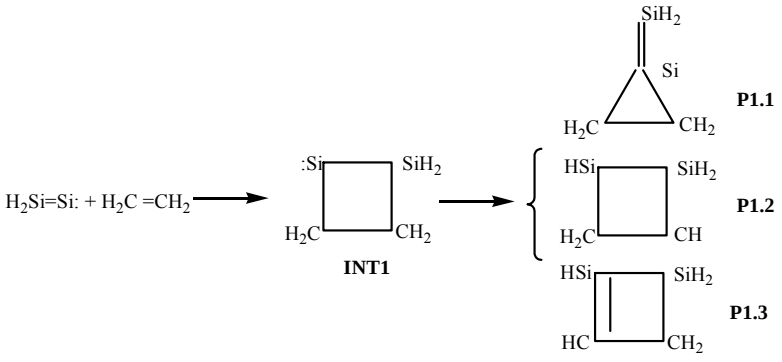

(1)

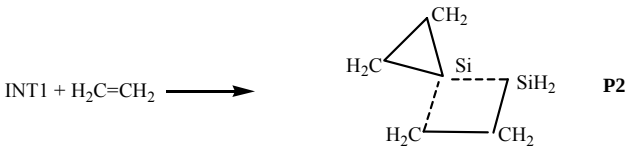

(2)

The research result indicates the laws of the cy cloaddition reaction between silylenesilylene (H_2Si=Si:) and its derivatives and sy mmetric π-bonded compounds, which are significant for the s ynthesis of small-ring and b is-heterocyclic compounds with Si. This study extends the resear ch area of the reactions of ethene with R_2C=C:[19,20] and heteroatom substituted ylenes (Si and Ge)[14,17,21–25], and especially enriches the research knowledge of silylene chemistry.

CALCULATION METHOD

MP2/6-31G*[26] implemented in the Gaussian 98 package was employed to locate all the stationary points along the reaction pathways. Full optimization and vibrational analysis were realized for the stationary points on the reaction profile. Zero point energy and CCSD(T) corrections were included in the energy calculations. In order to explicitly establish the relevant species, the intrinsic reaction coordinate (IRC)[27,28] was also calculated for all the transition states appearing on the cycloaddition energy profile.

RESULTS AND DISCUSSION

The geometric parameters of the four-membered ring silylene (INT1), the transition states (TS1.1, TS1.2 and TS1.3) and the products (P1.1, P1.2, P1.3 and P2) which appear in the cycloaddition reactions (1) and (2) between silylene-silylene (R1) and ethene (R2) are given in Fig. 1. The energies are listed in Table I, and the potential energy profile for the cycloaddition reaction is shown in Fig. 2. The results of the IRC calculation for TS1.1, TS1.2 and TS1.3 are given in Fig. 3. According to the calculations of the IRC of TS1.1, TS1.2 and TS1.3 and further optimization for the primary IRC results, TS1.1 connects IN T1 with P1.1; TS1.2 connects INT1 with P1.2 and TS1.3 connects INT1 with P1.3. According to Fig. 2, it can be seen that reaction (1) consists of four steps: 1) the two reactants (R1 and R2) form a four-membered ring silylene (INT1), which is a barrier-free exothermic reaction of 509.6 kJ mol^{-1}; 2) INT1 isomerizes to a three-membered ring product (P1.1) through transition state (TS1.1) with an energy barrier of 72.7 kJ mol^{-1}; 3) and 4) INT1 undergoes hydrogen transfer, *via* either transition state TS1.2 and TS1.3 with energy barriers of 60.1 and 116.0 kJ mol^{-1}, resulting in the formation of product P1.2 and P1.3, respectively. According to Fig. 2, because the energy of P1.1 is 51.5 kJ mol^{-1} higher than that of INT1, the reaction of INT1→P1.1 is thermodynamically prohibited at normal temperatures and pressure. INT1→P1.2 and INT1→P1.3 are mutually competing reactions but because the energy of TS1.3 is 55.9 kJ mol^{-1} higher than that of TS1.2, P1.2 is the main product of reaction (1).

In reaction (2), INT1 further reacts with ethene (R2) to form a silicic bis-heterocyclic compound (P2). According to Fig. 2, this reaction is a barrier-free exothermic reaction of 141.7 kJ mol^{-1}. A careful and detailed study of this reaction, for which no intermediates or transition states exist, was performed. It was believed that when INT1 interacts with ethene, due to the large radius of the Si atom, sp^3 hybridization the Si(2) atom in INT1 occurs before INT1 and ethene could form intermediate and transition states, and thus INT1 combines with ethene to form the silicic bis-heterocyclic compound (P2).

According to Fig. 2, INT1→P1.2 and reaction (2) are two mutually competitive reactions and as the reaction INT1 →P1.2 has a barrier of 60.1 kJ mol^{-1} while the reaction INT1+R2→P2 directly reduces the system energy by 141.7 kJ mol^{-1}, reaction (2) should be the main reaction pathway.

According to the above analysis, the dominant reaction channel of the cyclo-addition reaction between singlet silylenesilylene and ethene is as follows:

$$R1 + R2 \longrightarrow INT1 \xrightarrow{R2} P2$$

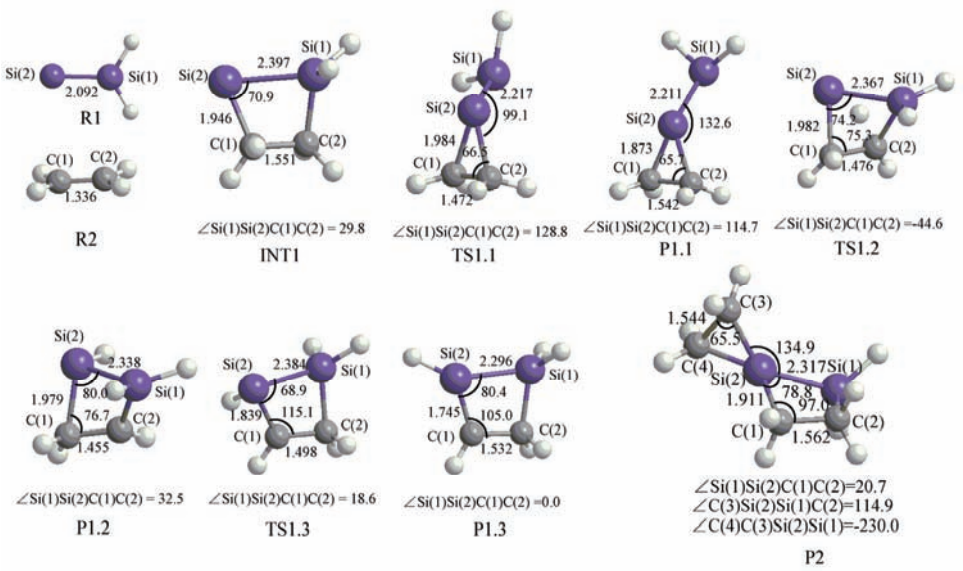

Fig.1. Optimized MP2/6-31G* geometrical parameters and the atomic numbering for the species in cycloaddition reactions (1) and (2). Bond lengths and bond angles are in angstroms and degrees, respectively.

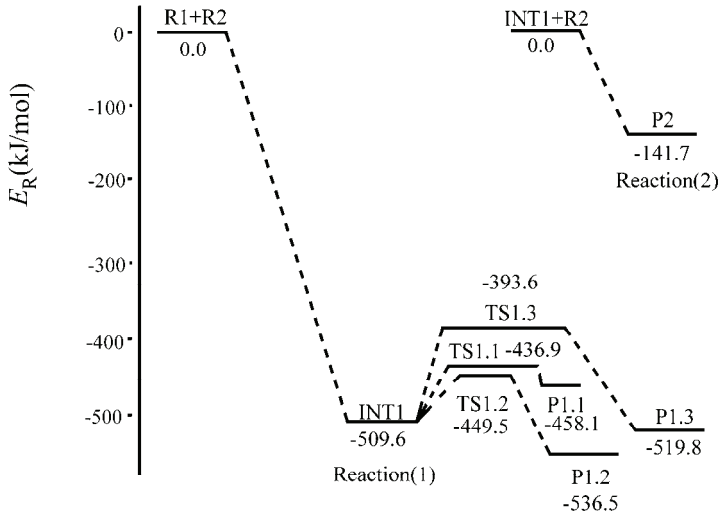

Fig. 2. The potential energy profile for the cycloaddition reactions between $H_2Si{=}Si$: and ethene with CCSD (T)//MP2/6-31G*.

The mechanism of the dominant reaction pathway can be explained by the molecular orbital diagrams (Figs. 4 and 5) and Fig. 1. According to the NBO analysis of INT1, the natural electron configuration of the Si(2) atom in INT1 is [core] 3s(1.69) 3p(1.62) 3d(0.02). Hence, it is certain that the hybridization of Si(2) atom in INT1 is sp (Fig. 5). According to Figs. 1 and 4, when the silylenesilylene (R1) interacts with ethane (R2), due to the [2+2] cycloaddition effect of the two π-bonds in silylenesilylene (R1) and ethene, a four-membered ring silylene (INT1) is formed. As INT1 is still an active intermediate, INT1 may further react with ethene to form a silicic bis-heterocyclic compound (P2). The mechanism of this reaction can be explained with Figs. 1 and 5. When INT1 interacts with ethene, due to the large radius of the Si atom, sp^3 hybridization of the Si(2) atom in INT1 occurs before any intermediate or transition states could be formed. Thus INT1 combined with ethene to form a silicic bis-heterocyclic compound (P2). According to the NBO analysis of P2, the Si(2) atom is $sp^{2.53}$ in the Si(2)–C(1) bond, the Si(2) atom is $sp^{2.54}$ in the Si(2)–Si(1) bond, the Si(2) atom is $sp^{3.81}$ in the Si(2)–C(3) bond, the Si(2) atom is $sp^{3.24}$ in the Si(2)–C(4) bond. Thus, it is certain that the Si(2) atom in INT1 undergoes sp^3 hybridization, when INT1 interacts with ethene.

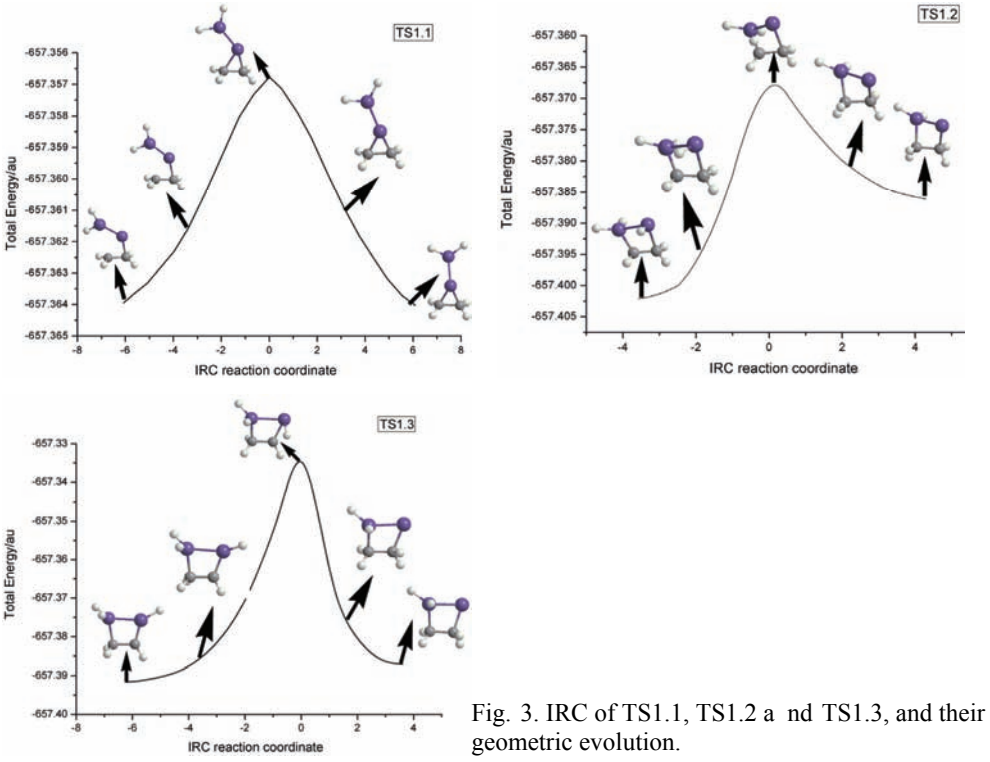

Fig. 3. IRC of TS1.1, TS1.2 and TS1.3, and their geometric evolution.

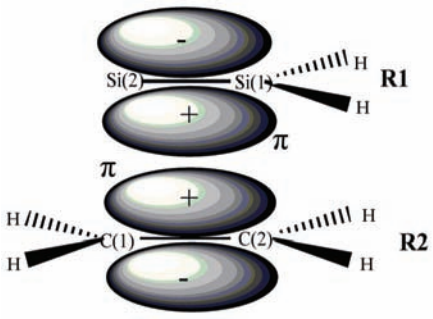

Fig. 4. A schematic interaction diagram for the frontier orbitals of H_2Si=Si: (R1) and H_2C=CH_2 (R2).

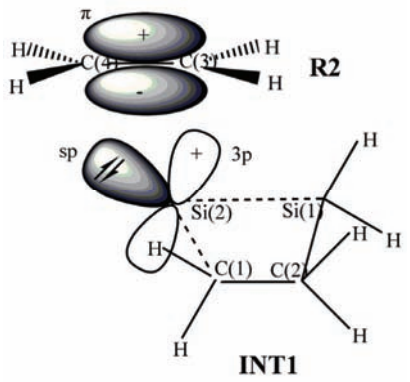

Fig. 5. A schematic interaction diagram for the frontier orbitals of INT1 and H_2C= CH_2 (R2).

CONCLUSIONS

From the potential energy profile of the cycloaddition reaction between singlet silylenesilylene and ethene obtained by the CCSD(T)//MP2/6-31G* method, it can be predicted that the dominant channel of this reaction consists of two steps: I) the two reactants first form a four-membered ring silylene (INT1) through a barrier-free exothermic reaction of 509.6 kJ mol^{-1} and (II) INT1 further reacts with ethene (R2) to form a silicic bis-heterocyclic compound (P2), which is also a barrier-free exothermic reaction of 141.7 kJ mol^{-1}.

ИЗВОД

AB INICIO ПРОУЧАВАЊЕ МЕХАНИЗМА НАСТАЈАЊА БИС-ХЕТЕРОЦИКЛИЧНОГ ЈЕДИЊЕЊА РЕАКЦИЈОМ СИЛИЛЕНСИЛИЛЕНА (H_2Si=Si:) И ЕТЕНА

XIUHUI LU, LEYI SHI, YONGQING LI и ZHINA WANG

School of Chemistry and Chemical Engineering, University of Jinan, Jinan, Shandong, 250022, People's Republic of China

Механизам циклоадицијске реакције између синглетног силиленесилилена (H_2Si=Si:) и етена, у којој настаје једно бис-хетероциклично једињење, истраживан је методом CCSD(T)//MP2/6-31G*. На основу профила потенцијалне енергије, предвиђа се да реакција има један доминантни реакциони пут. То је [2+2] циклоадиција која доводи до формирања

силилена са четворочланим прстеном (INT1). Када четворочлани прстен силилена (INT1) интерагује са етеном, услед sp3 хибридизације Si: атома у прстену, овај прстен се комбинује са етеном градећи једно бис-хетероциклично силицијумово једињење (P2).

(Примљено 15. јануара, ревидирано 4. октобра 2011)

REFERENCES

1. a) M. Jones Jr., R. A. Moss, *Reactive Intermediates*, Vol. 1, Wiley Interscience, New York, 1978, p. 229; b) M. Jones Jr., R. A. Moss, *Reactive Intermediates*, Vol. 2, Wiley Interscience, New York, 1981, p. 335; c) M. Jones Jr., R. A. Moss, *Reactive Intermediates*, Vol. 3, Wiley Interscience, New York, 1985, p. 333
2. R. A. Abramovitch, *Reactive Intermediates*, Vol. 2, Plenum Press, New York, 1982, p. 297
3. D. S. Rogers, K. L. Walker, M. A. Ring, E. O'Neal, *Organometallics* **6** (1987) 2313
4. J. A. Boatz, S. Gordon, *J. Phys. Chem.* **93** (1989) 3025
5. D. A. Horner, R. S. Grev, F. Schaefer, *J. Am. Chem. Soc.* **114** (1992) 2093
6. G. Inoue, M. Suzuki, *Chem. Phys. Lett.* **122** (1985) 361
7. A. Al-Rubaiey, R. Walsh, *J. Phys. Chem.* **98** (1994) 5303
8. R. Becerra, J. P. Cannady, R. Walsh, *J. Phys. Chem., A* **103** (1999) 4457
9. R. Becerra, J. P. Cannady, R. Walsh, *Phys. Chem. Chem. Phys.* **3** (2001) 2343
10. X. H. Lu, Y. X. Wang, C. B. Liu, C. H. Deng, *Acta Chim. Sinica* **56** (1998) 1075
11. X. H. Lu, Y. X. Wang, C. B. Liu, *Chem. J. Chin. Univ.* **20** (1999) 612
12. X. H. Lu, Y. X. Wang, C. H. Deng, *Acta Phys. Chem. Sinica* **14** (1998) 309
13. X. H. Lu, Y. X. Wang, C. B. Liu, *Chin. J. Chem. Phys.* **12** (1999) 460
14. X. H. Lu, H. B. Yu, W. R. Wu, *New J. Chem.* **29** (2005) 332
15. X. H. Lu, H. B. Yu, Y. H. Xu, P. P. Xiang, Y. D. Liu, *J. Mol. Struct. (Theochem)* **770** (2006) 185
16. X. H. Lu, H. B. Yu, Y. H. Xu, P. P. Xiang, X. Che, *Mol. Phys.* **105** (2007) 1961
17. X. H. Lu, X. Che, H. B. Yu, P. P. Xiang, Y. H. Xu, *J. Mol. Struct. (Theochem)* **821** (2007) 53
18. X. H. Lu, H. B. Yu, X. Che, P. P. Xiang, *Int. J. Quant. Chem.* **108** (2008) 1114
19. X. H. Lu, P. P. Xiang, R. Wei, X. Che, *J. Mol. Struct. (Theochem)* **853** (2008) 82
20. X. H. Lu, Z. X. Lian, Y. Q. Li, *J. Serb. Chem. Soc.* **76** (2011) 743
21. X. H. Lu, J. F. Han; H. B. Yu; Z. X. Lian, *Chin. J. Chem. Phys.* **23** (2010) 533
22. X. H. Lu, Y. Hua Xu, H. B Yu, W. R. Wu, *J. Phys. Chem., A* 109 (2005) 6970
23. X. H. Lu, Y. H. Xu, H. B. Yu, H. Lin, *Chin. J. Chem,* **23** (2005) 1339
24. C. L. Tian, Y. H. Xu, X. H. Lu, *Int. J. Quantum Chem.* **110** (2010) 1675
25. X. H. Lu, J. F. Han, Z. X. Lian, Y. Q. Li, *J. Serb. Chem. Soc.* **76** (2011) 1395
26. L. A. Curtis, K. Raghavachari, J. A. Pople, *J. Chem. Phys.* **98** (1993) 1293
27. K. Fukui, *J. Phys. Chem.* **74** (1970) 4161
28. K. Ishida, K. Morokuma, A. Komornicki, *J. Chem. Phys.* **66** (1981) 2153.

Journal of the Serbian Chemical Society
JSCS-info@shd.org.rs • www.shd.org.rs/JSCS
J. Serb. Chem. Soc. 77 (1) 83–94 (2012)
JSCS–4251
UDC 665+664.2+54–148:546.33'26:
547.461.6–312:532.135.004.12
Original scientific paper

Influence of the sodium dodecyl sulphate (SDS) concentration on the disperse and rheological characteristics of oil-in-water emulsions stabilized by octenyl succinic anhydride modified starch–SDS mixtures

VELJKO KRSTONOŠIĆ[1]*, LJUBICA DOKIĆ[2], IVANA NIKOLIĆ[2], TAMARA DAPČEVIĆ[3] and MIROSLAV HADNAĐEV[3]

[1]*Faculty of Medicine, Department of Pharmacy, University of Novi Sad, Hajduk Veljkova 3, 21000 Novi Sad, Serbia,* [2]*Faculty of Technology, University of Novi Sad, Bul. cara Lazara 1, 21000 Novi Sad, Serbia and* [3]*Institute for Food Technology, Bul. cara Lazara 1, 21000 Novi Sad, Serbia*

(Received 30 June 2010, revised 7 February 2011)

Abstract: Stability of oil-in-water emulsions can be achieved by chemically modified starch, such as octenyl succinic anhydride (OSA) starch, as an emulsifier. In order to analyse the disperse and rheological characteristics of emulsions containing two kinds of emulsifiers, part of the OSA starch can be substituted with an adequate concentration of sodium dodecyl sulphate (SDS), which is a small surfactant with the same charge as OSA starch. The oil contents of the examined emulsions were 5, 20 and 50 %. The selected OSA starch concentration was 10 % and replacements of a part of the OSA starch were realized with SDS concentrations of 1, 3 and 5 %. Dispersed droplets of emulsions were defined by determination of the Sauter mean diameter d_{32} and particle size distribution. Flow curves were used to describe the rheological properties of the emulsions. In addition, the stability of the emulsion samples was observed and expressed by the creaming index. The obtained results indicated a decrease in the Sauter mean diameter of the droplets, the standard deviation and the apparent viscosity of the emulsions with increasing amounts of SDS within the emulsifier mixture OSA starch–SDS. According to creaming rate, the emulsions with OSA starch were more stable than the emulsions stabilized by the OSA starch and SDS combinations.

Keywords: oil/water emulsions; octenyl succinic anhydride starch; sodium dodecyl sulphate, rheology; disperse characteristics.

* Corresponding author. E-mail: veljkokrst@yahoo.co.uk
doi: 10.2298/JSC100630150K

INTRODUCTION

An emulsion is a dispersed system that contains at least two immiscible liquids and a third component that ensures system stability, known as an emulsifier. An emulsifier adsorbs at the oil–water interface, where it decreases the surface tension and coats the dispersed droplets, thereby protecting them from coalescence.

The classification of emulsifiers includes two groups of widely applied compounds for emulsion stability: small-molecule surfactants and macromolecular emulsifiers, known as biopolymers. Sodium dodecyl sulphate (SDS) belongs to the first group and octenyl succinic anhydride (OSA) starch to the second.

Modified starches are native starches that have been chemically or physically changed in order to improve their properties and to satisfy specific demands of industrial application.[1] Chemically modified starches are, generally, obtained by introducing a chemical group or molecule part that reacts with hydroxyl groups of the starch molecules. Accordingly, the properties of native starch are more or less changed.[2]

OSA starch is formed by the modification of native starch by octenyl succinic anhydrides. One of the three accessible carbon atoms of the glucose molecule, at position 2, 3 and 6, are substituted by octenyl succinic anhydride. The substitution largely occurs at branched amylopectin chains, and the degree of substitution (*DS* value) for food application is in the range 0.01–0.03.[3,4] The hydrophobic OSA group incorporated into the hydrophilic structure of native starch provides surface active properties to the macromolecule. In addition, the hydrophobic OSA substituent contains a carboxylic group that can be negatively charged, thus considering the low degree of substitution, this modified starch has properties of a weakly charged polyelectrolyte.[5]

In this manner, OSA starch has dual properties; the amphiphilic nature of the molecules provides stronger surface activity compared to native starch molecules,[6] and the macromolecule characteristic increases the viscosity of the continuous phase. These characteristics make it suitable for stabilisation of dispersed systems, especially oil-in-water emulsions. The macromolecules are brought to the oil–water interface by short, hydrophobic, octenyl succinic chains that are in the oil phase, while long amylopectin chains stay at the water phase and protect the droplets against flocculation by the steric stabilization mechanism.[7,8]

Synthetic surfactants, such as SDS, are widely used components for different industrial formulations. The specific molecular structure of SDS, represented by long aliphatic chains with a sulphate ester group, confers amphiphilic properties and significant surface activity to the molecule.[9] The dispersed droplets of an emulsion are stabilized by electrostatic repulsion, unlike OSA starch that accomplishes stabilization by the steric mechanism.[10] The adsorption of negatively charged SDS molecules to the surface of the oil droplets increases the electro-

static repulsion between droplets.[11] Dickinson and Ritzoulis[12] examined creaming and rheology of an oil-in-water emulsion containing SDS and sodium caseinate. They concluded that an excess of SDS promoted destabilization through fast creaming and explained that non-adsorbed surfactant micelles in the aqueous phase of the emulsions caused depletion flocculation.

The aim of this work was to examine the properties of emulsions stabilized by OSA starch and mixtures of OSA starch and SDS. SDS is chosen because of its same electric charge as OSA starch, but different chemical structure and different stabilizing mechanism. Knowledge about properties of the final emulsion product, such as droplet size, stability and rheology, when those two surfactants are used together, is important in order to improve quality and the range of their application. Due to that part of the OSA starch, which are used as emulsifier, will be substituted with adequate concentrations of SDS and the characteristics of emulsions will be analyzed.

EXPERIMENTAL

Material

Sunflower oil "Olivko", acquired from the local oil production plant "Banat" Nova Crnja, Serbia, has a high content of oleic acid as a monounsaturated acid and is highly resistant to oil hydrolysis and oxidation. Its physico–chemical characteristics at 25 °C were: density, $\rho = 0.9145$ g cm^{-3}, viscosity coefficient, $\eta = 56$ mPa s, and total acid number, $TAN = 0.353$ mg KOH g^{-1} oil. The fatty acid composition of the "Olivko" oil presented in Table I was determined by gas chromatography–mass spectrometry analysis.[13]

As an emulsion stabilizer, OSA starch with the trade name Purity Gum 2000, which is a waxy maize derivative produced by the National Starch and Chemicals GmbH, Germany, was used. It is recommended as good natural emulsifier for food and pharmaceutical applications. The SDS was obtained from Centrohem, Beograd, Serbia. Double-distilled water was used. All chemicals were of reagent grade and were used as such.

Preparation of the emulsions

The continuous phase was formed by dissolving an appropriate amount of OSA starch or OSA starch–SDS mixtures in water and heating at 50 °C. The selected OSA starch concentration was 10 %. Part of the OSA starch was replaced with adequate SDS concentrations (1, 3 and 5 %). Hence, emulsions stabilized with: 10 % OSA starch; 9 % OSA starch and 1 % SDS; 7 % OSA starch and 3 % SDS; and 5 % OSA starch and 5 % SDS. The chosen amount of oil, the dispersed phase, based on the mass of emulsion, was added to the continuous phase in order to form an emulsion. The dispersed phase concentrations were 5, 20 and 50 %. In order to avoid microbial contamination, 0.01% of sodium azide was added. Homogenization was performed in an Ultra–Turrax T25 basic homogenizer, equipped with an S 25 N–18 G dispersing tool, at a constant temperature of 25±0.1 °C at 9500 min^{-1}. The energy density for the preparation of the emulsions[14] was 6.0×10^6 W m^{-3}. The total homogenization time was 20 min. Prior to the measurements, the prepared emulsions were kept at room temperature for 24 h.

Determination of the particle size and particle size distribution

The size distribution of the droplets was determined using microphotography. The emulsion samples required pre-arrangements before taking the microphotographs.[15]

The microphotographs were taken at few optical fields using an optical microscope (TP-1001C TOPICA CCD CAMERA (Kruss)). They were adjusted by adequate software and expanded 1:1000; hence, a droplet with an actual size of 1 μm corresponded to 1 mm on the photograph. Due to the diameter frequency, the Sauter mean diameter d_{32}, μm, (Eq. (1)) was determined in order to define the droplet size distribution.

$$d_{32} = \frac{\Sigma n_i d_i^3}{\Sigma n_i d_i^2} \tag{1}$$

The standard deviation was calculated according to Eq. (2):

$$\sigma^2 = \frac{\sum n_i \left(d_i - d_n\right)^2}{\sum n_i} \tag{2}$$

where n_i is number of droplets in each size class, d_i is the droplet diameter, Σn_i is total number of droplets, and d_n is the average droplet diameter:

$$d_n = \frac{\sum n_i d_i}{\sum n_i} \tag{3}$$

Rheological measurement

The determination of rheological behaviour was performed using a HAAKE Rheostress RS600 rotational viscometer ("Thermo Electron Corporation", Karlsruhe, Germany) with a cone–plate C60/1Ti sensor (the cone and plate gap was 0.052 mm). The measurements were realized at a constant temperature of 25±0.1 °C. The rheological method included hysteresis loop tests. The samples were exposed for the first 180 s to an increasing shear rate from 0 to 500 s^{-1}, the shear rate was held constant at 500 s^{-1} for 120 s and finally, the shear rate was decreased to 0 s^{-1} in 180 s.

Creaming rate determination

Creaming of the emulsion samples was observed at room temperature. The volume of the transparent serum layer formed at the bottom of the cylinder was registered visually and expressed by H_S. The total volume of the emulsion sample was H_E. The extent of creaming was characterized by the creaming index H / % (Eq. (4)):

$$H = 100\frac{H_S}{H_E} \tag{4}$$

Statistical analysis

Statistical analysis of the data and significant differences at the significant level 0.05 for several variables, based on three individual measurements, were determined by the ANOVA procedure and Duncan multiple range tests. The calculations were performed using the statistical software SPSS 15.0 (SPSS Inc, Chicago, Illinois, USA).

RESULTS AND DISCUSSION

Disperse characteristics

A comparison of the Sauter mean diameter d_{32} of the emulsions stabilized with OSA starch and suitable concentrations of SDS is given in Fig. 1A.

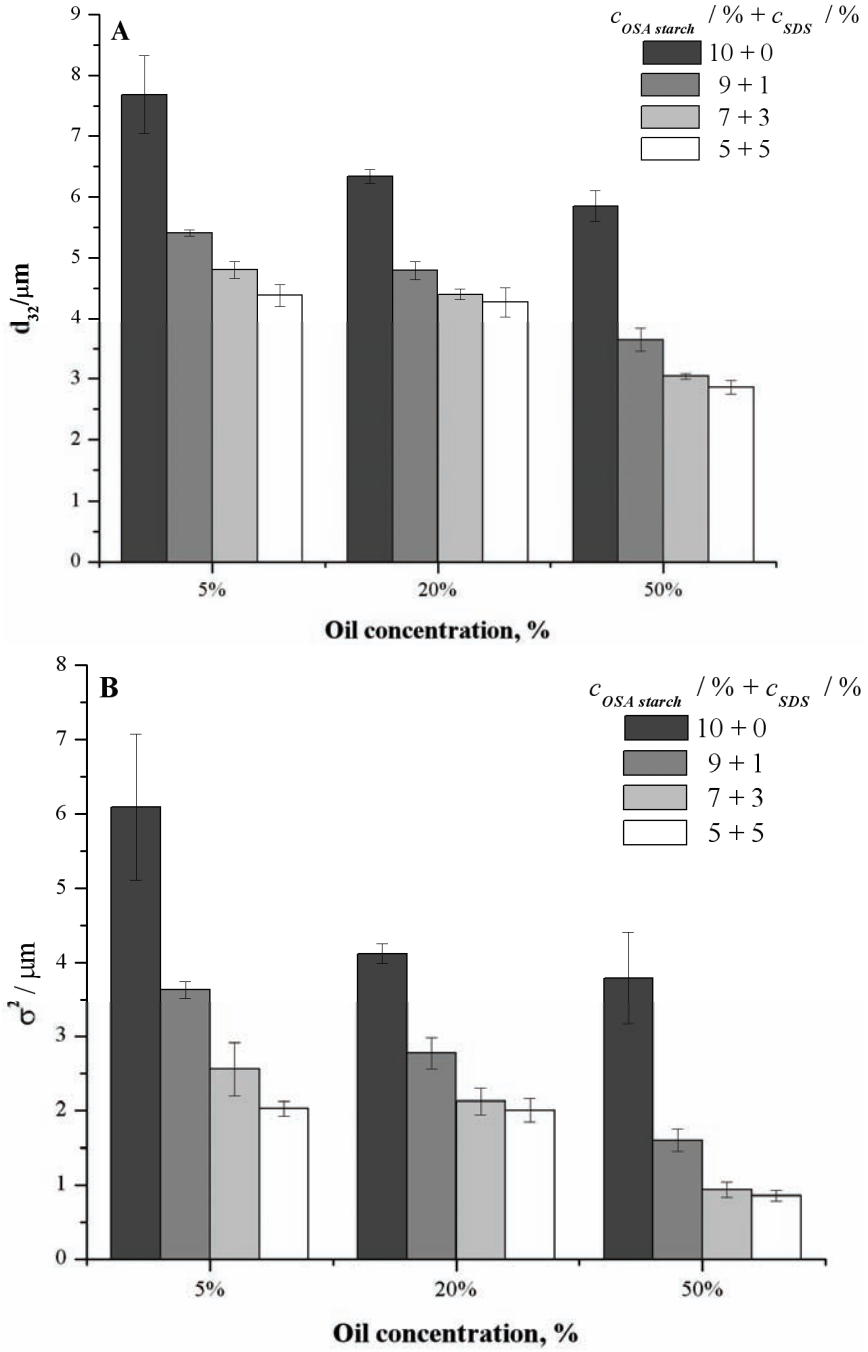

Fig. 1. The influences of OSA starch–SDS ratio on A) the Sauter mean diameter d_{32} of the dispersed droplets and B) the standard deviations of the investigated emulsions.

Increasing the amount of SDS in the OSA starch–SDS mixtures led to a decrease in the average droplet diameter of the examined emulsions. The same effect occurred for all the examined oil concentrations.

SDS molecules are able to adsorb at the oil–water interface more rapidly than biopolymers, such as OSA starch.[18,22] The slow adsorption of OSA starch is caused by the crowding of its hydrophobic and hydrophilic groups that slows down the diffusion process and delays adsorption.[16–18,22] Several biopolymer molecules can be adsorbed at a newly created interface at the early stage of the emulsification process, but presence of adsorbed small surfactant molecules cause biopolymer substitution from interface.[17,19,20]

The standard deviation is a value of the width of the size distribution of the droplets in a polydisperse emulsion.[21] The changes in the standard deviation (Fig. 1B) were similar to those for d_{32}. It is obvious that emulsions without SDS had the largest standard deviation values, irrespective of the oil content, which means that they were highly polydisperse.

Jafari *et al.*[18] announced that addition of Tween 20 to oil-in-water emulsions stabilized with OSA starch caused a considerable reduction of the average droplet diameter. This occurrence is a repercussion of the ability of the small Tween 20 molecules to adsorb at the interface before the OSA starch and to disable coalescence during the emulsification process. SDS is also a small molecule like Tween 20 and they have similar mobility and adsorption properties in comparison to OSA starch; hence, the premise by Jafari *et al.* could also be valid for the composite emulsifiers analyzed in this work. The results presented in Fig 1A were confirmed by Tesch *et al.*,[22] who reported that the average droplets diameters of emulsions stabilized by OSA starch were higher than those for emulsions stabilized by SDS. This was caused by the faster adsorption of small SDS molecules at the oil–water interface.

The observation is also in accordance to the results presented by Tangsuphoom *et al.*[23] They added SDS to coconut milk before the homogenization step and noticed a reduction in the average diameter of the droplets.

Rheological characteristics

To determine flow parameters of the emulsions, a power law equation (Eq. (5)) was suitable because the systems did not show yield stress:

$$\tau = K\dot{\gamma}^n \tag{5}$$

where τ is the shear stress, $\dot{\gamma}$ is the shear rate, K is a consistency index and n is the flow behaviour index.

The consistency index K is a measure of the system consistency and it is related to the apparent viscosity. The flow behaviour index n determines the degree of non-Newtonian behaviour and varies in the range between 0 and 1. The

non-Newtonian character of an inves tigated system is more pronounced for smaller values of constant *n*.

The values of *K* and *n* for the sa me concentration of oil phase, which are located in the same row, are presented in Table I. The values are presented at the confidence interval 95 % and the val ues of the in dividual measurements are given as mean value ± error of determination.

TABLE I. Flow curves parameters *K* and *n* of the emulsions stabilized with OSA starch and OSA starch–SDS mixtures; the values are presented at the confidence level 95 % and the values of the individual measurement are given as the mean value ± the error of determination; the mean values do not differ significantly ($p > 0.05$) if they are followed by the same letter in the superscript

Oil content, %	($c_{\text{OSA starch}} + c_{\text{SDS}}$), %	*K* / Pa s	*n*
5	10 + 0	0.0088990 ± 0.00016$^{(cd)}$	0.9463667 ± 0.00588$^{(d)}$
	9 + 1	0.0088623 ± 0.00041$^{(cd)}$	0.9772000 ± 0.00578$^{(c)}$
	7 + 3	0.0070097 ± 0.00032$^{(b)}$	0.9533667 ± 0.00745$^{(b)}$
	5 + 5	0.0042753 ± 0.00005$^{(a)}$	0.9634333 ± 0.00225$^{(a)}$
20	10 + 0	0.0216700 ± 0.00342$^{(cd)}$	0.9314000 ± 0.00375$^{(cd)}$
	9 + 1	0.0209600 ± 0.00038$^{(cd)}$	0.9300667 ± 0.00428$^{(cd)}$
	7 + 3	0.0190533 ± 0.00076$^{(b)}$	0.8834333 ± 0.00373$^{(b)}$
	5 + 5	0.0103467 ± 0.00048$^{(a)}$	0.9095333 ± 0.00621$^{(a)}$
50	10 + 0	0.2717333 ± 0.01986$^{(d)}$	0.7781333 ± 0.01249$^{(ad)}$
	9 + 1	0.2010000 ± 0.01288$^{(c)}$	0.7586000 ± 0.01102$^{(c)}$
	7 + 3	0.1697000 ± 0.00366$^{(b)}$	0.7423000 ± 0.01032$^{(b)}$
	5 + 5	0.1094000 ± 0.02085$^{(a)}$	0.7815333 ± 0.02315$^{(ad)}$

The conclusion of the re sults presented in Table I is that increasing the amount of SDS in the emulsifier mixtures of OSA starch and SDS, used to stabilize emulsions, led to a decrease in consistency index *K*, meaning a reduction in the apparent viscosity of the emulsions. The reason for such beha viour lies in the fact that OSA starch is macro molecular emulsifier, which has a significan t influence on the viscosity of continuous phase due to its macromolecular nature. A characteristic of polymers is their capability of modifying the viscosity of water. OSA starch replacement with a low-m olecular mass emulsifier, such as SDS, which has a negligible effect on the vi scosity, still resulted in a decrease in the viscosity of the continuous phase. The decrease in aqueous phase viscosity reflected on the consistency index of the emulsions. Changes in the SDS concentration did not show a specific dependence on the flow behaviour index *n*.

Increasing the oil concent ration in the e mulsions led to an incre ase in consistency index *K* due to the increase in the packing density of oil droplets, as well as a decrease in flow behaviour index *n*, indicating a pronounced shear thinning behaviour of the systems at higher oil contents. This phenomenon is related to the fact that the droplets are closer to one another at h igher oil concentrations a nd they tend to flocculate. Small hydrodynamic forces at low shear rates are not able

to disrupt the flocs, but at higher shear rates, the flocs became deformed and eventually disrupted, causing a reduction in the emulsion viscosity.[21,24,25]

Emulsion stability

Emulsions with only OSA starch were more stable in terms of their creaming appearance compared to emulsions stabilized by the OSA starch–SDS mixtures.

Particularly, on comparing the occurrence of creaming of emulsions stabilized by OSA starch–SDS mixtures with those that were stabilized only by OSA starch, it was noticed that the addition of SDS enhanced the separation of the droplets. The influence of different amount of SDS in the OSA starch–SDS mixtures on the creaming rate of the examined emulsions is shown in Fig. 2.

In the presence of SDS, rapid creaming was noticed. In the emulsions that contained 5 % and 20 % of dispersed phase, for all OSA starch and SDS ratios, the creaming index reached maximal values after an hour. In addition, increasing the amount of SDS in the mixture led to an increase of the maximum values of creaming index for the emulsions with 20 and 50 % of the oil phase, while this effect was less pronounced in the emulsions with an oil content of 5 % (Fig. 2).

The emulsions stabilized only by OSA starch showed a slower creaming behaviour and the maximum value of the creaming index was achieved after two days. Increasing the SDS concentration in the OSA starch–SDS mixtures led to a decrease in the creaming time. Emulsions that contained 50 % oil showed a delay time of creaming. For the emulsions with an OSA starch–SDS ratio of 9:1, as well as for the emulsions stabilized only by OSA starch, the delay period was 72 h. The delay time decreased with increasing amount of SDS, and it was 24 h for an emulsifier ratio of 1:1.

A significant difference in the turbidity of the transparent serum layer was noticed between the emulsions that contained SDS and those that were stabilized only by OSA starch. Namely, the serum layer of the emulsion that did not contain SDS, after the appearance of creaming, was turbid, and the border of the two layers was not sharp. The serum layer became clearer during storage while the border between the two layers became more noticeable. This is typical behaviour for highly polydisperse systems, and is in accordance with the Stocks Law. The larger droplets move faster, while the smaller ones remain longer in the serum layer thereby making it turbid.

Thus, emulsions stabilized with OSA starch and SDS mixtures after the creaming had a clear serum layer without remaining oil droplets. According to Dickinson[26] and McClements,[21] surfactants micelles and non-adsorbed biopolymers can lead to destabilization of an emulsion system by the depletion flocculation mechanism, which occurred in these examined systems. The oil droplets moved faster during the creaming process because of flocculation and the clear serum layer evidenced that all droplets were in the top layer.

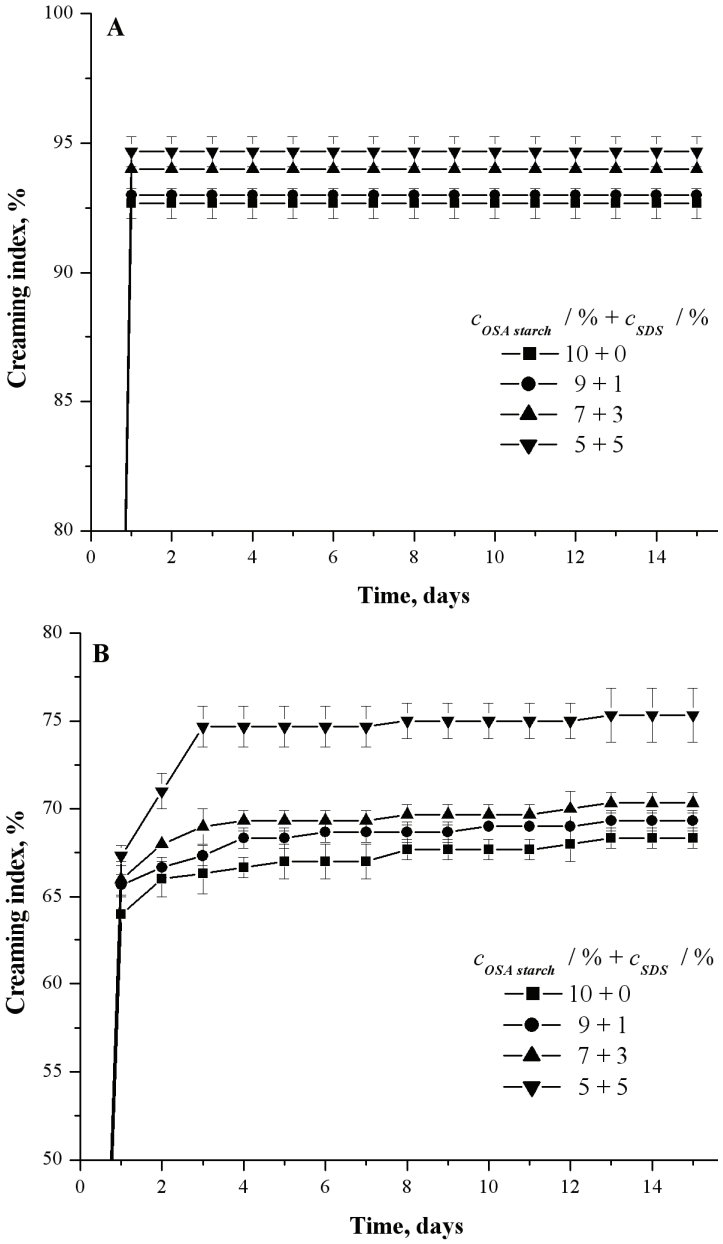

Fig. 2. The influence of OSA starch–SDS ratio on the creaming rate of the emulsions with different oil contents A) 5 and B) 20 %.

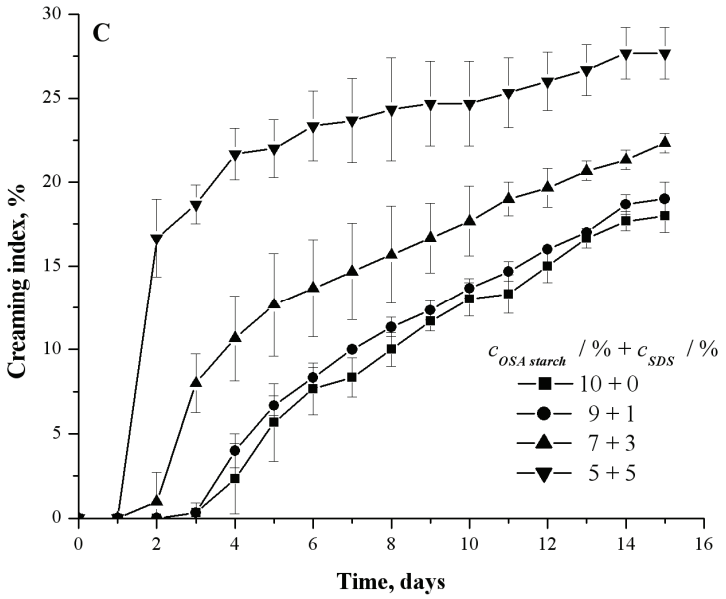

Fig. 2. (Continued) The influence of OSA starch–SDS ratio on the creaming rate of the emulsions with oil content 50 %.

CONCLUSIONS

From the presented results, it can be concluded that increasing the amount of SDS in OSA starch–SDS mixtures decreased the apparent emulsion viscosity and the mean diameter of the dispersed droplets. However, despite the slow adsorption, OSA starch molecules provide a better stability to the emulsion than a combination of OSA starch and SDS. This is be cause surfactant micelles and non-adsorbed biopolymers destabilize the emulsions by the depletion flocculation of the droplets when OSA starch and SDS are employed together.

Acknowledgements. This research was realized within the National Project No. 31014: "Development of new functional confectionery products based on oil crops", financed by the Ministry of Education and Science of the Republic of Serbia.

И З В О Д

УТИЦАЈ КОНЦЕНТРАЦИЈЕ НАТРИЈУМ ДОДЕЦИЛ СУЛФАТА НА ДИСПЕРЗИОНЕ И РЕОЛОШКЕ КАРАКТЕРИСТИКЕ ЕМУЛЗИЈА ТИПА УЉА У ВОДИ СТАБИЛИЗОВАНИХ СМЕШАМА ОСА СКРОБА И НАТРИЈУМ ДОДЕЦИЛ СУЛФАТА

ВЕЉКО КРСТОНОШИЋ[1], ЉУБИЦА ДОКИЋ[2], ИВАНА НИКОЛИЋ[2], ТАМАРА ДАПЧЕВИЋ[3] и МИРОСЛАВ ХАДНАЂЕВ[3]

[1]Катедра за фармацију, Медицински факултет,Универзитет у Новом Саду, Хајдук Вељкова 3, 21000 Нови Сад, [2]Технолошки факултет, Универзитет у Новом Саду, Бул. цара Лазара 1, 21000 Нови Сад и [3]Институт за прехрамбене технологије, Бул. цара Лазара 1, 21000 Нови Сад

Стабилизација емулзија типа уља у води може се остварити хемијски модификованим скробом, октенил сукцинат анхидридом скроба – OCA скробом, као емулгатором. У циљу испитивања дисперзионих и реолошких особина емулзија које садрже две врсте емулгатора део OCA скроба може да буде замењен адекватном концентрацијом натријум-додецил-сулфата, који је сурфактант истог наелектрисања као и OCA скроб. Садржај уља испитиваних емулзија износио је 5, 20 и 50 %. Поред одабране концентрације OCA скроба од 10 %, натријум-додецил-сулфат је уведен у концентрацијама 1, 3 и 5 % заменом адекватног дела OCA скроба. Методом одређивања величине и расподеле величине капи дефинисан је средњи пречник диспергованих капи – Саутеров пречник, d_{32}. Испитивањем кривих протицања утврђена су реолошка својства емулзија. Такође је праћена стабилност емулзија која је изражена преко криминг индекса. Добијени резултати указали су на смањење Саутеровог средњег пречника капи дисперговане уља и стандардне девијације и смањење вредности привидних вискозитета емулзија са повећањем удела натријум додецил сулфата у смеши емулгатора. Емулзије које су садржале само OCA скроб, на основу праћења појаве криминга, показале су већу стабилност од емулзија стабилизованих комбинацијом OCA скроба и натријум-додецил-сулфата.

(Примљено 30. јуна 2010, ревидирано 7. фебруара 2011)

REFERENCES

1. F. E. Ortega-Ojeda, H. Larsson, A. Eliasson, *Carbohydr. Polym.* **59** (2005) 313
2. J. Bao, J. Xing, L. D. Phillips, H. Corke, *J. Agric. Food Chem.* **51** (2003) 2283
3. R. Shorgen, G. Biresaw, *Colloids Surf., A* **298** (2007) 170
4. L. Nilsson, B. Bergenstahl, *Langmuir* **22** (2006) 8770
5. L. Nilsson, B. Bergenstahl, *J. Colloid Interface Sci.* **308** (2007) 508
6. K. Prochaska, P. Kedziora, L. J. Thanh, G. Lewandowicz, *Colloids Surf., B* **60** (2007) 187
7. E. Dickinson, *Food Hydrocoll.* **23** (2009) 1473
8. R. Bhosale, R. Singhal, *Carbohydr. Polym.* **66** (2006) 521
9. B. Jovčić, J. Begović, J. Lozo, L. Topisirović, M. Kojić, *Arch. Biol. Sci.* **61** (2009) 159
10. R. Pons, P. Taylor, F. T. Tadros, *Colloid Polym. Sci.* **275** (1997) 769
11. D. Kelley, D. J. McClements, *Food Hydrocoll.* **17** (2003) 87
12. E. Dickinson, C. Ritzoulis, *J. Colloid Interface Sci.* **224** (2000) 148
13. S. Ž. Kravić, Z. J. Suturović, J. V. Švarc-Gajić, Z. S. Stojanović, M. M. Pucarević, I. R. Nikolić, *Hem. Ind.* **65** (2011) 139
14. P. Walstra, in *Encyclopedia of emulsion technology*, Vol. I, P. Becher, Ed., Dekker, New York, 1983, p. 57
15. V. Krstonošić, Lj. Dokić, P. Dokić, T. Dapčević, *Food Hydrocoll.* **23** (2009) 2212
16. J. C. Arboleya, P. J. Wilde, *Food Hydrocoll.* **19** (2005) 485
17. L. A. Pungaloni, E. Dickinson, R. Ettelaie, A. R. Mackie, P. J. Wilde, *Adv. Colloid Interface Sci.* **107** (2004) 27
18. S. M. Jafari, Y. He, B. Bhandari, *Food Res. Int.* **40** (2007) 862
19. A. R. Mackie, A. P. Gunning, P. J. Wilde., V. J. Morris, *Langmuir* **16** (2000) 2242
20. S. Kerstens, B. S. Murray, E. Dickinson, *J. Colloid Interface Sci.* **296** (2006) 332
21. D. J. McClements, *Food emulsions: Principles, practice and techniques*, CRC Press, Boca Raton, FL, USA, 2005
22. S. Tesch, C. Gerhards, H. Schubert, *J. Food Eng.* **54** (2002) 167
23. N. Tangsuphoom, N. J. Coupland, *Food Hydrocoll.* **22** (2008) 1233

24. R. A. Taherian, P. Fustier, S. H. Ramaswamy, *J. Food Eng*. **77** (2006) 687
25. I. Nor Hayati, Y. B. Che Man, C. Ping Tan, I. Nor Aini, *Food Res. Int*. **40** (2007) 1051
26. E. Dickinson, *Food Hydrocoll*. **17** (2003) 25.

Journal of the Serbian Chemical Society
JSCS-info@shd.org.rs • www.shd.org.rs/JSCS
J. Serb. Chem. Soc. *77* (1) 95–104 (2012)
JSCS–4252
UDC 547.99:541.121:536.7:537.322:543
Original scientific paper

Determination of epinephrine by a Briggs–Rauscher oscillating system using a non-equilibrium stationary state

JINZHANG GAO*, YANJUN LIU, JIE REN, XIAOLI ZHANG, MING LI and WU YANG

Chemistry & Chemical Engineering College, Northwest Normal University, Lanzhou 730070, P. R. China

(Received 21 August 2010, revised 9 July 2011)

Abstract: A highly sensitive method for the determination of epinephrine is proposed, which is based on the perturbation of epinephrine to a Briggs–Rauscher oscillating system involving malonic acid, Mn^{2+}, H^+, IO_3^- and H_2O_2 at a non-equilibrium stationary state. The concentration of KIO_3 was chosen as a control parameter to find the bifurcation point in this study. The results showed that a good linear relationship between the difference in the potential and the negative logarithm of the concentrations of epinephrine existed in the range 1.1×10^{-7}–5.2×10^{-9} mol L^{-1} with a lower detection limit of 6.8×10^{-10} mol L^{-1} and a correlation coefficient of 0.9974. Compared to the classical oscillating reaction, this method has a lower detection limit and a wider linear range. The effects of some foreign species, which may possibly exist with epinephrine, on determination were also investigated. The proposed method was successfully used to determine epinephrine both in serum and adrenaline hydrochloride injection.

Keywords: Briggs–Rauscher oscillating system; epinephrine; determination; non-equilibrium stationary state.

INTRODUCTION

The application of classical oscillating chemical reactions in analytical chemistry has made significant progress since a continuously stirred tank reactor (CSTR)[1] was combined with the analyte pulse perturbation technique (APP).[2] The simple equipment used, the large linear range (*ca.* 10^{-7}–10^{-4} mol L^{-1}) and low detection limit (*ca.* 10^{-6}–10^{-8} mol L^{-1}) are its unique advantages, in general, which could satisfy the need of common determinations in many fields. In recent years, for improving further the sensitivity, the Perez-Bendito group[3,4] and the Strizhak group[5,6] investigated theoretically the largest Lyapunov exponent in the transient chaotic regime with the BZ (Belousov–Zhabotinsky) oscillating system and developed a new analytical method with a very high sensitivity (detection li-

* Corresponding author. E-mail: jzgao@nwnu.edu.cn
doi: 10.2298/JSC100821151G

mit ≤ 10^{-12} mol L^{-1}). Gao *et al.*[7,8] reported that a sulfide- modified BZ oscillating chemical system is very sensitive to trace amounts of some metal ions. Vukojevic and Pejic *et al.*[9–11] studied the characteristics of a non-equilibrium stationary state close to the bifurcation point between the non-oscillatory and oscillatory state, and proposed successfully a novel kinetic method for the determination of organic compounds and inorganic ions. The above methods are basically a BZ oscillating chemical system, *i.e.*, a cerium ion catalyzed oxidation reaction of malonic acid by BrO_3^- in sulfuric acid. In addition to the BZ oscillating reaction, the BR (Briggs–Rauscher) oscillating reaction is also very interesting in analytical chemistry.

The classical BR reaction[12] is the Mn^{2+} catalyzed oxidation of malonic acid by iodate and hydrogen peroxide in sulfuric or perchloric acid medium, which was reported by Briggs and Rauscher in 1973. Although the sustained oscillating time of the BR is shorter than that of the BZ oscillating reaction, it has been successfully used to analyze some antioxidant-type substances with one or more phenolic hydroxyl groups, such as polyphenolic compounds,[13] virgin olive oil[14] and red wine.[15] It is meaningful to determine food and drugs using the BR oscillating system because the pH employed is similar to the acidity of the fluids in the stomach[13] and the stomach is part of the digestive system. In the process of disease treatments, drugs are involved in some non-linear oscillation such as the human blood circulation and metabolism; hence exploring therapeutic mechanisms through studying oscillating reactions could more truly reflect the nature of the drugs.

As a natural catecholamine in the human body, epinephrine (the chemical structure of which is shown in Fig. 1) is an important compound for message transfer in the mammalian central nervous system, and it can also excite the heart, contract blood vessels and relax bronchial smooth muscle contraction. Many life phenomena are related to its concentration, thus, it is meaningful to develop an efficient determination method to study its physiological function and diagnosis in some diseases in clinical medicine. In this paper, a new method for the determination of epinephrine is proposed and compared with other methods, such as fluorimetry,[16] chemiluminescence,[17] voltammetry,[18] and molecular imprinting.[19] The results indicated that the sensitivity of the proposed method is better than those of the others.

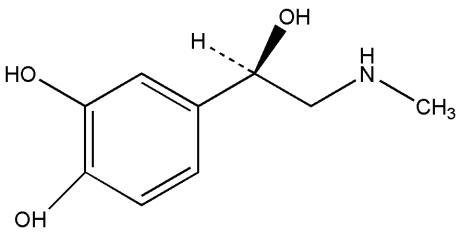

Fig. 1. Chemical structure of epinephrine.

EXPERIMENTAL

Apparatus

A SY-601 thermostat (Tianjin Ounuo Instrument Ltd. Co., China) with an accuracy±0.1 K and a Model ML-902 magnetic stirrer (Shanghai Pujiang Analytical Instrumental Factory, China) were used to maintain the temperature constant. A CHI-832 electrochemistry analyzer (Shanghai Chenhua Instrument Co., China) was directly connected to the reactor through two Pt-electrodes (Rex, 213, China), whereby, one served as the working electrode and the other as auxiliary electrode, and a Hg_2SO_4 reference electrode to record the potential changes. An injector was used to add the sample solutions.

Reagents

All the employed chemicals were of analytical-reagent grade and doubly distilled water was used throughout to prepare the working solutions, *i.e.*, malonic acid (0.25 mol L^{-1}), $MnSO_4$ (0.025 mol L^{-1}), H_2SO_4 (0.16 mol L^{-1}), H_2O_2 (4.8 mol L^{-1}) and KIO_3 (0.25 mol L^{-1}). The H_2O_2 solution was standardized by $KMnO_4$ solution before the use and preserved in a brown reagent-bottle. A stock solution of epinephrine was prepared with distilled water and stored in a refrigerator. Working solutions with lower concentrations were prepared by dilution immediately prior to use.

Procedure

The experiments were performed in a glass reactor (*ca.* 50 mL) coupled with a SY-601 thermostat and a Model ML-902 magnetic stirrer. A mixture containing malonic acid, $MnSO_4$, H_2SO_4, H_2O_2 and KIO_3 was placed in the reactor at 295±0.1 K. Then doubly distilled water was added to a final volume of 20 mL. Finally, the three electrodes were immersed into the reaction media under stirring, and the time–potential curve was recorded immediately.

RESULTS AND DISCUSSION

Finding bifurcation point

Generally, the initial concentration of reactants and the specific flow rate, as well as temperature, can be chosen as the control parameter to study a non-equilibrium stationary state. In this study, the initial concentration of KIO_3, which was varied from 5.75×10^{-2} to 4.0×10^{-3} mol L^{-1}, was chosen as the control parameter to define the bifurcation profile. With decreasing initial concentration of KIO_3, the amplitude of the system gradually decreased and eventually disappeared at a KIO_3 concentration 5.0×10^{-3} mol L^{-1} (Fig. 2A), *i.e.*, the system transformed from a steady oscillation state to a non- equilibrium stationary state. Then, the bifurcation profile (Fig. 2B) using the initial concentration of KIO_3 as the control parameter was made following Fig. 2A.

The theoretical bifurcation point of the system was also found at a concentration of 4.1×10^{-3} mol L^{-1} by linear extrapolation,[9] *i.e.*, a plot of the square of the amplitude of the oscillations *versus* the initial concentration of KIO_3 (Fig. 3).

In order to investigate the determination sensitivity in different non-equilibrium stationary states, the same amount of epinephrine was added into this system at different concentrations of KIO_3. Fig. 4 indicates that the closer to the

concentration of bifurcation point, the higher sensitivity is. Hence, a KIO_3 concentration of 5.0×10^{-3} mol L^{-1} was used in this study.

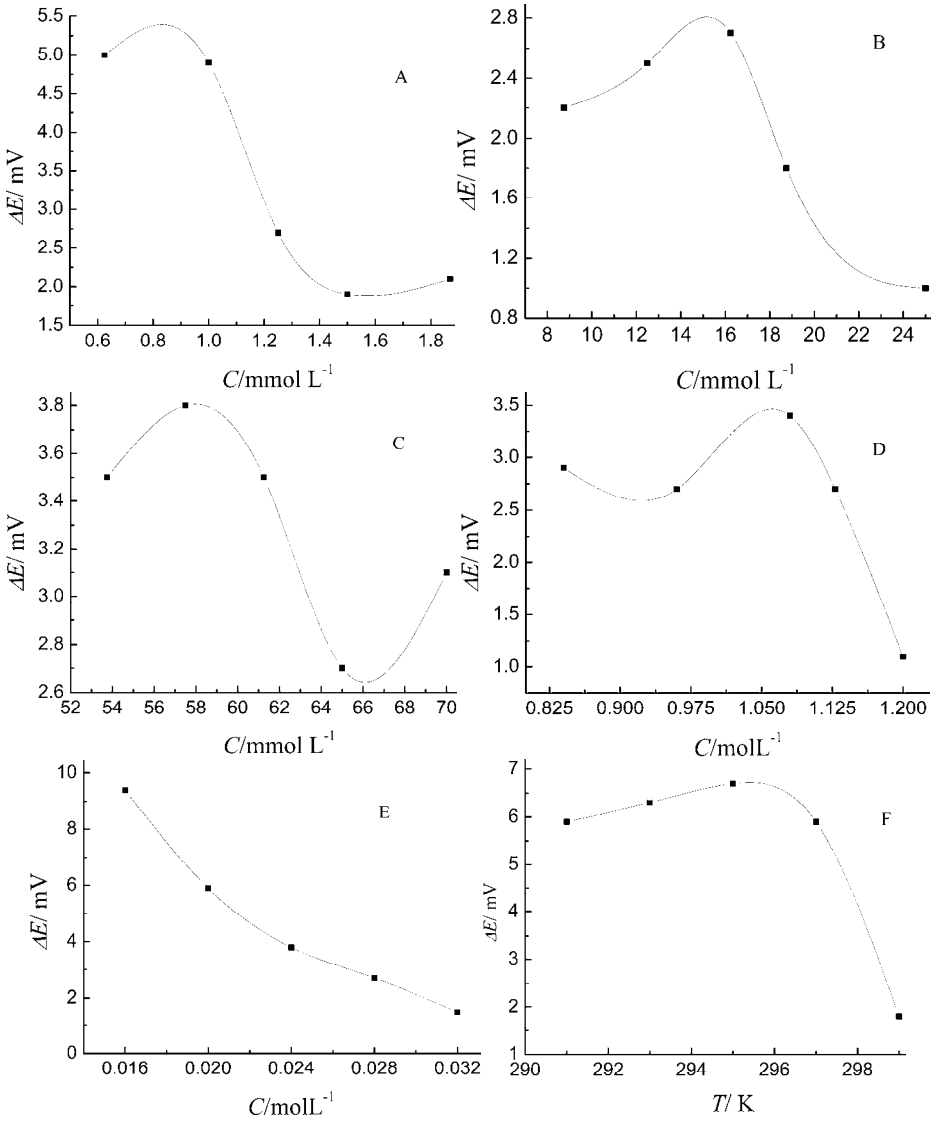

Fig. 2. A. Time series profiles at different initial concentration of KIO_3; A) 7.0×10^{-3}, B) 6.0×10^{-3}, C) 5.8×10^{-3}, D) 5.6×10^{-3} and E) 5.0×10^{-3} mol L^{-1}; F) bifurcation profile using the initial concentration of KIO_3 as the control parameter. Common conditions: [malonic acid] = 1.625×10^{-2} mol L^{-1}, [$MnSO_4$] = 1.0×10^{-3} mol L^{-1}, [H_2SO_4] = 0.02 mol L^{-1}, [H_2O_2] = 1.08 mol L^{-1}, T = 295 K.

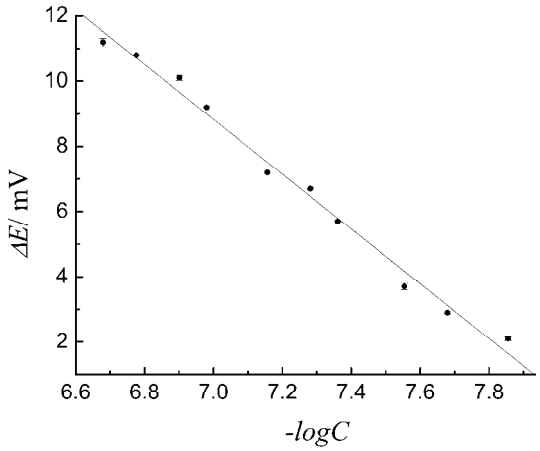

Fig. 3. The plot of the square of the amplitude *versus* the initial concentration of KIO_3 in mol m^{-3}.

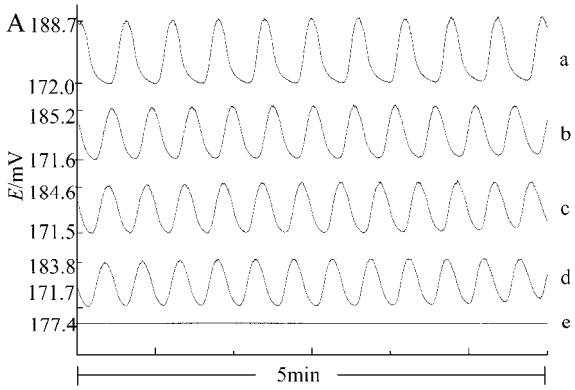

Fig. 4. The profiles of adding 2.1×10^{-8} mol L^{-1} epinephrine near to the point of bifurcation. [KIO_3]: a) 5.0×10^{-3}, b) 4.7×10^{-3}, c) 4.4×10^{-3}, d) 4.1×10^{-3} and e) 3.8×10^{-3} mol L^{-1}. The other conditions were the same as those given in the caption to Fig. 2.

Determination of epinephrine in non-equilibrium stationary state

In the vicinity of the bifurcation point, the system is extremely sensitive to surrounding change. When the epinephrine was injected into the system, the potential of system changed. In the range of 1.1×10^{-7} to 5.2×10^{-9} mol L^{-1}, the potential difference ΔE ($\Delta E = E - E_p$, where E and E_p are the potential of the system before and after addition of epinephrine, respectively) was linearly proportional to the negative logarithm of the epinephrine concentration (–log c), and the detection limit was 6.8×10^{-10} mol L^{-1} (Fig. 5). The linear relationship can be expressed by the following regression equation:

$$\Delta E \text{ (mV)} = 41.33–3.82 \text{ (–log } c \text{ / mol L}^{-1}\text{)} \quad (r = 0.9974, N = 11)$$

Moreover, a comparative study between the classical oscillating profile and the bifurcation point was performed for the same system.

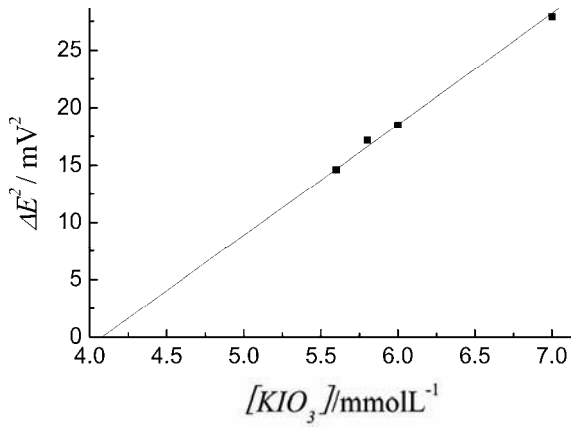

Fig. 5. Calibration curve for the determination of epinephrine using the non-equilibrium stationary state.

Determination of epinephrine in a regular oscillation system

In order to gain higher sensitivity, the effects of experimental variables on the determination were investigated. As shown in Fig. 6, 1.625×10^{-2} mol L^{-1} malonic acid, 5.75×10^{-2} mol L^{-1} KIO_3, 1.08 mol L^{-1} H_2O_2 and 295 K were chosen as the optimal conditions. In addition, the effects of the $MnSO_4$ concentration and solution acidity were studied over the range from 6.25×10^{-4} to 1.87×10^{-3} mol L^{-1} and from 0.016 to 0.032 mol L^{-1}, respectively. As the $MnSO_4$ and H_2SO_4 concentrations decreased, the perturbations of epinephrine increased. When the $MnSO_4$ concentration was lower than 6.25×10^{-4} mol L^{-1} and the H_2SO_4 concentration was lower than 0.016 mol L^{-1}, the oscillating profiles became irregular. In terms of stability and sensitivity, 1.0×10^{-3} mol L^{-1} $MnSO_4$ and 0.02 mol L^{-1} H_2SO_4 were finally adopted for further study.

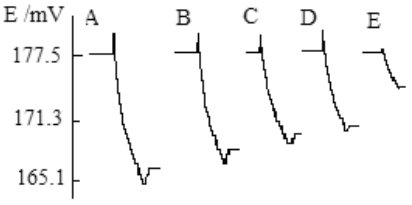

Fig. 6. Influence of the concentration of A) $MnSO_4$, B) malonic acid, C) KIO_3, D) H_2O_2, E) sulfuric acid and F) temperature on the determination of 5.24×10^{-8} mol L^{-1} epinephrine.

Under the optimal conditions mentioned above, a regular oscillating profile (*i.e.*, constantly oscillating amplitude and period) was obtained and then, the determination of was performed. The results showed that the difference in the oscillating amplitude ΔE ($\Delta E = E - E_0$, where E_0 and E are the amplitudes before and after injection of epinephrine, respectively) was linearly proportional to the negative logarithm of epinephrine concentration over the range of 1.4×10^{-8}–2.1×10^{-7} mol L^{-1} (Fig. 7), with a detection limit of 1.0×10^{-8} mol L^{-1}. The linear relationship can be expressed by the following regression equation:

$$\Delta E \text{ (mV)} = 67.65 - 8.40 \, (-\log c / \text{mol L}^{-1}) \; (r = 0.9950, N = 10)$$

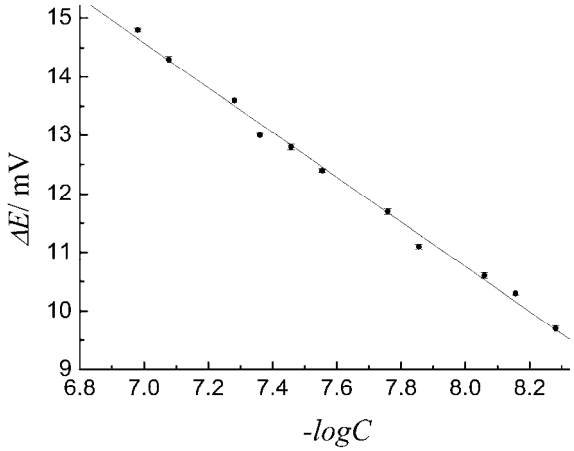

Fig. 7. Calibration curve for determination of epinephrine using the regular oscillating reaction.

Interferences

It is well known that a non-equilibrium stationary state is highly vulnerable to foreign species; hence, some potentially interfering species that may possibly be present in adrenaline hydrochloride injection or serum were investigated. The tolerable ratio (defined as the maximum amount of foreign species causing an error of less than ±5 % in the determination of 5.24×10^{-8} mol L^{-1} epinephrine) are listed in Table I. It can be seen that common inorganic ions, glucose and EDTA have no influence on the determination of epinephrine, while adenine affects the determination slightly.

TABLE I. Effects of foreign species on the determination of 5.24×10^{-8} mol L^{-1} epinephrine

Foreign species	Tolerable ratio (foreign/epinephrine)
K^+, Mg^{2+}, Na^+, Fe^{2+}	3000
Glucose, $EDTA^-$	2000
HPO_4^{2-}, HCO_3^-, Cl^-	500
Uric acid	100
Adenine	40

Comparison with other methods

In order to confirm the applicability and sensitivity of the non-equilibrium stationary state, the method developed in this study was compared with other methods employed for the determination of epinephrine, including regular oscillating reactions. From Table II, it can be seen that the detection limit of the proposed method was the lowest.

TABLE II. Comparison of the proposed method with others employed for the determination of epinephrine

Method	Linear range, mol L^{-1}	Detection limit, mol L^{-1}	Reference
Fluorescence	6.0×10^{-8}–1.0×10^{-5}	1.5×10^{-8}	16
Chemiluminescence	5.0×10^{-9}–1.0×10^{-7}	3.0×10^{-9}	17
Voltammetry	5.0×10^{-8}–5.5×10^{-4}	9.4×10^{-9}	18
Molecular imprinting	5.0×10^{-8}–2.0×10^{-5}	2.0×10^{-8}	19
Regular oscillating system	1.4×10^{-8}–2.1×10^{-7}	1.0×10^{-8}	This paper
Non-equilibrium, stationary state	5.2×10^{-9}–1.1×10^{-7}	6.8×10^{-10}	This paper

Sample analysis

Epinephrine in adrenaline hydrochloride injection (Tianjin Pharmaceutical Group, Xinzheng Ltd. Co., China) and serum were determined by the regular oscillator and bifurcation profile. Adrenaline hydrochloride injection and serum were directly used after dilution. The recovery was also examined by standard addition method using the non-equilibrium stationary state of the BR oscillating chemical reaction. Results in Tables III and IV indicated that this method could be used in routine analysis of epinephrine, benefiting from its reproducibility and accuracy.

TABLE III. The results of the determination of epinephrine in adrenaline hydrochloride injection

Sample No.	Original$\times10^8$, mol L^{-1}	Added$\times10^8$, mol L^{-1}	Found$\times10^8$, mol L^{-1}	Recovery, %
1	1.019	0	1.045	102.5
2	1.019	2.094	3.076	98.8
3	1.019	3.490	4.597	101.9
4	1.019	0.698	1.738	101.2

TABLE IV. The results of the determination and recovery analysis of epinephrine in serum

Sample No.	Original$\times10^9$, mol L^{-1}	Added$\times10^9$, mol L^{-1}	Found$\times10^9$, mol L^{-1}	Recovery, %
1	8.725	0	8.885	101.8
2	8.725	6.980	15.65	99.6
3	8.725	13.96	22.47	99.1
4	8.725	20.94	29.64	99.9

CONCLUSIONS

In this paper, epinephrine was successfully determined using a non-equilibrium stationary state in a BR oscillating chemical system. Moreover, larger linear range (*ca.* 10^{-9}–10^{-7} mol L^{-1}) and lower detection limit (*ca.* 10^{-10} mol L^{-1}) could satisfy the needs of routine determinations. It could be used for real sample due to its advantages compared with other instrumental analysis, such as ease of operation, inexpensive set-up, *etc.* In addition, the BR oscillating system is of

more interest for understanding the oscillators in biological system because the employed pH of about 1.7 is similar to the acidity of the fluids in the stomach.

Acknowledgements. This work was supported in part by the Project of International Cooperation between China and the Ukraine (043-05), the National Natural Science Foundation (20873101), and the Project of KJCXGC-01 of Northwest Normal University, China.

ИЗВОД

ОДРЕЂИВАЊЕ ЕПИНЕФРИНА ОСЦИЛАТОРНИМ СИСТЕМОМ BRIGGS–RAUSCHER ПРИ НЕРАВНОТЕЖНИМ СТАЦИОНАРНИМ СТАЊИМА

JINZHANG GAO, YANJUN LIU, JIE REN, XIAOLI ZHANG, MING LI и WU YANG

Chemistry & Chemical Engineering College, Northwest Normal University, Lanzhou 730070, P. R. China

Развијен је високо селективан метод за одредјивање епинефрина, базиран на пертурбацији Briggs–Rauscher осцилаторног система који укључује малонску киселину, Mn^{2+}, H^+, IO_3^- и H_2O_2 при неравнотежним стационарним стањима. У раду је изабрана концентрација KIO_3 као контролни параметер за утврђивање бифуркационе тачке Резултати су показали добро линерно слагање (корелациони коефицијент 0,9974) између разлике потенцијала и негативног логаритма концентрације епинефрина у опсегу $1{,}1\times10^{-7}$–$5{,}2\times10^{-9}$ mol L^{-1}, и детекциони лимит $6{,}8\times10^{-10}$ mol L^{-1}. У поређењу са класичном осцилаторном реакцијом, овај метод има нижи детекциони лимит и шири опсег линеарности. Утицаји других врста, које могу постојати поред епинефрина су такође испитани. Развијен метод се може користити за одређивање епинефрина у серуму и адреналинским инекцијама.

(Примљено 21. августа 2010, ревидирано 9. јула 2011)

REFERENCES

1. I. R. Epstein, *J. Phys. Chem.* **88** (1984) 187
2. R. J. Prieto, M. Silva, D. P. Bendito, *Anal. Chem*. **67** (1995) 729
3. R. Jimenez-Prieto, M. Silva, D. Perez-Bendito, *Analyst* **121** (1996) 563
4. R. Jimenez-Prieto, M. Silva, D. Perez-Bendito, *Analyst* **122** (1997) 287
5. O. Z. Didenko, P. E. Strizhak, *Chem. Phys. Lett*. **340** (2001) 55
6. P. E. Strizhak, O. Z. Didenko, T. S. Ivashchenko, *Anal. Chim. Acta* **428** (2001) 15
7. J. Z. Gao, H. Chen, H. X. Dai, D. Y. Lv, J. Ren, L. Wang, W. Yang, *Anal. Chim. Acta* **571** (2006) 150
8. H. Chen, W. Yang, H. X. Dai, X. X. Wei, J. Qu, J. Z. Gao, *Chin. Chem. Lett*. **17** (2006) 1221
9. V. B. Vukojević, N. D. Pejić, D. R. Stanisavljev, S. R. Anić, L. Z. Kolar-Anić, *Analyst* **124** (1999) 147
10. N. D. Pejić, L. Z. Kolar-Anić, S. R. Anić, D. R. Stanisavljev, *J. Pharmaceut. Biomed. Anal.* **41** (2006) 610
11. N. D. Pejić, S. M. Blagojević, S. R. Anić, V. B. Vukojević, M. D. Mijatović, J. S. Ćirić, Z. S. Marković, S. D. Marković, L. Z. Kolar-Anić, *Anal. Chim. Acta* **582** (2007) 367
12. T. S. Briggs, W. C. Rauscher, *J. Chem. Edu*. **50** (1973) 496
13. R. Cervellati, C. Renzulli, M. C. Guerra, E. Speroni, *J. Agric. Food Chem*. **50** (2002) 7504
14. T. Cecchi, P. Passamonti, P. Cecchi, *Food Anal. Methods* **3** (2010) 1

15. E. Prenesti, S. Toso, S. Berto, *J. Agric. Food Chem.* **53** (2005) 4220
16. J. H. Yang, G. L. Zhang, X. H. Cao, L. M. Sun, Y. J. Ding, *Spectrochim. Acta, A* **53** (1997) 1671
17. J. X. Du, L. H. Shen, J. R. Lu, *Anal. Chim. Acta* **489** (2003) 183
18. H. Beitollahi, H. K. Maleh, H. N. Khabazzadeh, *Anal. Chem.* **80** (2008) 9848
19. C. D. Liang, H. Peng, A. H. Zhou, L. H. Nie, S. Z. Yao, *Anal. Chim. Acta* **415** (2000) 135.

Journal of the Serbian Chemical Society
JSCS-info@shd.org.rs • www.shd.org.rs/JSCS
J. Serb. Chem. Soc. 77 (1) 105–117 (2012)
JSCS–4253
UDC 546.47/.49+546.56+546.815+551.463/.464:597(497.16)
Original scientific paper

Accumulation of trace metals in marine organisms of the southeastern Adriatic coast, Montenegro

DANIJELA JOKSIMOVIĆ[1]* and SLAVKA STANKOVIĆ[2]

[1]*Institute of Marine Biology, University of Montenegro, Dobrota bb, 85330 Kotor, Montenegro and* [2]*Faculty of Technology and Metallurgy, University of Belgrade, Karnegijeva 4, 11000 Belgrade, Serbia*

(Received 23 March, revised 13 April 2011)

Abstract: The concentration and accumulation of trace metals (Co, Ni, As, Cd, Pb and Hg) were measured in seawater, sediments and marine organisms on the coastline of Montenegro. The obtained results of trace metals in sea grass and mussels were compared with those found in the water column and sediment. Sampling was performed in the fall of 2005 at five locations on the Montenegrin coastline, Sveta Stasija, Herceg Novi, Zanjice, Budva and Bar, which present different levels and sources of human impact. The heavy metals analyses of seawater, sediment, *Posidonia oceanica* and *Mytilus galloprovincialis* identified the harbor of Bar as the most Hg-contaminated site, Zanjice as the most As-contaminated and Sveta Stasija as the most Pb-contaminated areas of the Montenegrin coastal area. This study showed that *P. oceanica* may have a greater bioaccumulation capacity than *M. galloprovincialis* for the considered metals, except for As and Hg, and both organisms may reflect contamination in the water column and in the sediment. For the first time, the sea grass *P. oceanica* and *M. galloprovincialis* were employed as metal bioindicators for the southeastern Adriatic. The results of this study could serve as a baseline for future assessments of anthropogenic effects in this marine ecosystem.

Keywords: heavy metals; seawater; sediment; marine organisms; biomonitoring; Montenegro.

INTRODUCTION

The Adriatic Sea is situated between the northeastern Italian coast and the southwestern coasts of Slovenia, Croatia, Montenegro and Albania. It is especially subject to pollution due to its enclosed character. The coastal parts of this Adriatic area receive large amounts of contaminants introduced by domestic, industrial and agricultural activities, directly, *via* rivers, or through atmospheric deposition. The pollution of the Adriatic Sea is more marked along the Italian

* Corresponding author. E-mail: djoksimovic@ibmk.org
doi: 10.2298/JSC110323159J

coast, especially of the northern basin, than along the eastern coast.[1] Most of the previous studies considered trace metal concentrations in sediments and mussels from selected coastal areas of the Adriatic, mainly of northern part of the Italian Adriatic coast.[2] Along the eastern Adriatic coast, the effects of coastal pollution were investigated mainly in the Slovenian[3] and Croatian coastal areas[4–7] and some initial investigations in the Montenegrin coastal area.[8,9] Investigation of sediments also included a number of sites in the Albanian coastal area.[10,11]

The chemical analysis of waters does not provide sufficient information on the bioavailability of the metals present in a marine environment.[12] Currently, there is great interest in the use of living organisms as pollution bioindicators in aquatic ecosystems in order to evaluate the quality of a marine environment. A comparison of metal contamination in different aquatic environments is possible by analysis of water,[13] sediment[14] and biota,[15–17] but in most cases, the impact and synergistic effects of trace metals in marine ecosystem are poorly understood.

Sea grasses and mussels are increasingly used as indicators of chemical contamination of coastal regions. The endemic sea grass *Posidonia oceanica* (L.) Delile has been used as a metal bioindicator[17] for the last two decades in the Mediterranean Sea, but in the area of the southeastern Adriatic coast, there is no published data concerning *P. oceanica* as a metal bioindicator. The mussel *Mytilus galloprovincialis* has the ability to accumulate metals from the environment in which lives[18] and their usefulness as sentinel organisms in metal biomonitoring studies is widely recognized. Bivalves are filter feeders and thus obtain elements not only from food and water but also from particulate materials.[19,20] In both organisms, the concentration of heavy metals is largely governed by the biological, chemical, and physical characteristics of the surrounding environment. For example, light and nitrogen availability positively affected the rate of Cd uptake in sea grass, which increased with increasing concentration of nitrate in the growth medium.[21] However, in environments with high nutrient levels, Ni uptake by plants can be inhibited due to complex formation between the nutrients and metal ions.[22]

For the first time, the concentrations of Co, Ni, As, Cd, Pb and Hg have been determined and compared in different marine environmental compartments in the area of the southeastern Adriatic Sea, Montenegro: seawater, sediment, the mussel *M. galloprovincialis* (L) Lamarck, 1819 and the sea grass *P. oceanica* (L) Delile. As there is no quantitative data available on the concentration of these metals in seawater, sediment, mussels and sea grass in this coastal part of the southeastern Adriatic Sea, the results of this study could serve as a baseline for future assessments of anthropogenic effects in this part of the Adriatic Sea.

EXPERIMENTAL

Chemicals and instrumentation

Ultra pure water (18.2 MΩ cm) from a Milli-Q system (Millipore, Bedford, MA, USA) was used to prepare all the aqueous solutions. All the employed mineral acids and oxidants (HNO_3, H_2O_2 and HCl) were of the highest quality (Suprapure, Merck, Germany). The mineralized samples were analyzed using a cold vapor atomic absorption spectrometer (CV–AAS and and F–AAS Perkin–Elmer, AAnalyst 200) and graphite furnace atomic absorption spectrometer (GF–AAS, Perkin–Elmer, 4100ZL, with Zeeman background correction).

Sampling locations

Samples were collected at five selected locations from this Adriatic coastal area: Sveta Stasija and Herceg Novi in the semi-enclosed Boka Kotorska Bay, which is on the UNESCO's World Heritage List, and on the open coastline at Zanjice, Budva and Bar, Fig. 1, situated in the proximity of different geochemical, hydrological and human impacts.

Fig. 1. Sampling locations in the southeastern Adriatic Sea, Montenegro: 1. Sveta Stasija, 2. Herceg Novi, 3. Zanjice, 4. Budva and 5. Bar.

Boka Kotorska Bay is on the northern coast of Montenegro with a mouth 2.95 km in width and an in-land length of 28.13 km, surrounded by mountains, with 75000 inhabitants living on its coast. Sveta Stasija is located in a small Kotor bay near Kotor, a city where a previous galvanization plant discharged used galvanization baths directly into the sea between 1965 and 1991. Herceg Novi was/is a favored tourist city with marine, shipyard and food industries. The beach Zanjice with hotels and cottages is situated close to the entrance of the Bay. Budva is an urban, tourist and industrial city located in the middle of the Montenegrin coastline with 18000 inhabitants. The Harbor Bar is in the south of the Montenegrin coastal area with 15000 inhabitants. Bar was an important industrial harbor in former Yugoslavia, the largest on the eastern side of the Adriatic, especially for crude oil and oil products traffic, and still is. The problem of pollution in the vicinity of these sites increases in the fall periods because of the summer tourist seasons and increased discharge of wastewater directly into the sea. For this reason, the samples of seawater and sediment, and mussels and sea grass were collected in the fall, at the same time. No mussels were found at the location Budva.

Sampling method, sample preparation and trace metal analyses

All the seawater samples, from the surface and the bottom, were collected at the same time as the sediment and the biota samples at all the studied locations. The water samples were analyzed after filtration and acidification with nitric acid (pH ≤ 2) for the determination of metals, immediately in the days following sampling. The pre-concentration technique was applied for the analysis of the seawater samples following a solvent extraction technique[23] prior to analysis by GF–AAS (Ni, Co, Cd and Pb), while Hg and As were measured following a CV–AAS procedure[17] using a Perkin–Elmer Hydride System coupled to an atomic absorption spectrometry (AAS). The accuracy of the methods was checked with three calibration standards laboratory prepared from standard solutions of 1000 mg L^{-1} (Merck) and a seawater matrix was used for the preparation of the Ni, Co, Cd and Pb standards. These standards were analyzed directly after solvent extraction as mentioned above.

Surface sediments (500 g) were collected in the vicinity of *P. oceanica* meadows. Only the top 5 cm was used for the purpose of this study. The fraction of the sediment smaller than 2 mm was frozen, lyophilized and analyzed by AAS. At the same time and place, about 350 g of fresh *P. oceanica* samples and two liters of seawater from the bottom were collected at a depth of 7±1 m. The *P. oceanica* samples were washed very thoroughly, rinsed with ultra pure water, frozen, lyophilized and reduced to powder, dissolved and analyzed.

The mussels and the seawater samples from the surface were collected in the vicinity of the *P. oceanica* meadows. 25–30 mussels of similar shell length were collected, placed in plastic bags and transported to the laboratory. The mussels were washed and cleaned out, opened raw and the flesh scraped out of the shells, which was then frozen, lyophilized, reduced to powder, dissolved and analyzed.

Preparation of dissolved biota samples (approximately 0.5 g) for trace metal analysis was performed as follows: the powder was digested with a mixture of 7 mL concentrated HNO_3 (65 % Merck, Suprapur) and 2 mL H_2O_2 (30 % Merck, Suprapur). The sediment samples (0.5 g), were digested with 2 mL of HNO_3 (65 %) and 6 mL HC1 (37 %) in a high microwave digestion system (CEM. Corporation, MDS-2100) for 30 min at 200 °C. The digested samples were diluted with ultra pure water in 25 mL volumetric flasks and then transferred to 100 mL polypropylene bottles until analysis.

To ensure the quality control and accuracy of the applied analytical procedure for the determination of heavy metals in the sediments, mussels and sea grass, certified reference materials, IAEA 158 (Marine sediment), NIST 2976 (Mussel homogenate) and IAEA 140 (Fucus sample), were also digested and analyzed.

All the results of the investigated elements in sediment, sea grass and mussel are expressed in dry weight (dw). To check for contamination, procedural blanks were analyzed after every five samples. The recovery of metals in the standard reference materials was in the range of 82–115 % of the certified total concentrations. This was indicated by results of triplicate measurements for the all samples. No correction was applied to the obtained data.

To evaluate the efficiency of metal bioaccumulation by *M. galloprovincialis* and *P. oceanica*, the bioconcentration factor (*BCF*) and the biosediment factor (*BSAF*), defined as the ratio between the metal concentration in the organism and that in the seawater[24] and sediment,[16] respectively, were calculated.

Statistical analysis

The certified values and analysis results of the reference materials are given in Table I. The analytical precision, measured as the relative standard deviations for Ni, Co and Hg, were routinely under or around 10 %, but were higher than 10 % for Cd, Pb and As. The average

analytical standard errors observed with the reported certified materials were below 10 % for all investigated elements, except for Ni and As in the sediment samples, and Cd and As in the mussel tissue and *Fucus* samples.

TABLE I. Analysis of certified reference materials: certified values and found values (mean ± ± S.D., mg kg^{-1} dw.)

Element	IAEA 158 (marine sediment)		NIST 2976 (mussel tissue)		IAEA 140 (*Fucus* sample)	
	Certified	Found	Certified	Found	Certified	Found
Ni	29.4±4.12	31.0±0.72	0.93±0.12	0.91±0.20	3.79±0.41	4.10±0.31
Co	9.0±1.35	10.1±1.5	0.61±0.02	0.70±0.05	0.83±0.13	0.95±0.09
Pb	38.0±7.7	35.0±3.9	1.19±0.18	0.98±0.23	2.19±0.28	1.87±0.11
As	11.4±1.71	12.6±0.91	13.3±1.8	14.7±2.10	44.3±2.1	47.10±3.4
Cd	0.37±0.09	0.45±0.05	0.82±0.16	0.84±0.18	0.54±0.04	0.65±0.03
Hg	0.132±0.017	0.12±0.018	0.061±0.0036	0.053±0.006	0.038±0.006	0.037±0.009

For the metal concentrations in the sediment, differences between the sampling locations were evaluated by the Kruskal–Wallis test. For the metal concentrations in *M. galloprovincialis* and *P. oceanica*, the differences between the organisms and between locations were determined by a two-way analysis of the variance (ANOVA). Correlations between the metal concentrations in *P. oceanica* and *M. galloprovincialis* and in the sediment and water samples were performed by analysis of the Pearson's correlations.

RESULTS AND DISCUSSION

Marine water

The measured trace element concentrations are listed in Table II. The Co, Ni, As, Cd, Hg and Pb mean levels are relatively high (up to 10.4. μg L^{-1} Co, 7.8 μg L^{-1} Ni, 3.1 μg L^{-1} As, 8.1 μg L^{-1} Cd, 1.56 μg L^{-1} Hg and 27.8 μg L^{-1} Pb). In the Venice lagoon and southern Adriatic of Italy such a high levels of elements in sea water were also found.[2,3] The concentration of Cd was below the detection limit at the location Budva. The relative standard deviation of replicate analyses of each sample was within 10–30 %.

Following recommended marine water quality criteria for the protection of aquatic life and human health, *i.e.*, the *MAC* values[25] of the investigated metals in surface waters, the Hg concentrations were below the *MAC* value for Hg and the Pb concentrations were above the *MAC* value for Pb in seawater at three locations (Table II). Considering the Montenegrin regulations for the maximum permissible concentrations of hazardous and harmful substances in waste water that may be discharged into surface waters,[26] the concentrations of the investigated elements that may be discharged into the seawater of Montenegro are much higher than the *MAC* values and the values measured in this study. The EU Directive 2008/56/EC in the field of marine environmental policy establishes common principles based on which Member States must draw up their own strategies, in

cooperation with other Member States and third countries, to achieve a good ecological status in the marine waters for which they are responsible.[27]

TABLE II. Total metal concentrations in seawater in μg L^{-1} (*MAC* – maximum allowable concentration; nv – no value)

Sampling place	Co	Ni	As	Cd	Hg	Pb
		Surface				
Sv. Stasija	4.4	5.7	1.4	2.5	1.38	18.0
H. Novi	4.3	3.4	2.5	6.2	1.36	3.9
Zanjice	3.5	4.9	3.1	1.9	1.56	2.09
Budva	–	4.3	2.7	–	0.70	5.75
Bar	4.7	6.9	2.4	7.0	1.01	27.8
		Bottom				
Sv. Stasija	3.9	6.4	2.5	2.5	0.92	5.7
H. Novi	10.4	5.9	2.6	6.2	0.98	3.9
Zanjice	4.5	5.0	2.9	3.3	0.40	2.6
Budva	3.9	3.9	2.5	–	0.62	2.9
Bar	4.3	4.3	2.7	8.1	1.28	26.4
MAC[25]	nv	8.2	36.0	8.8	0.94	8.1
Montenegrin Regulation[26]	100	1250	100	10	5.0	500

Sediment

The highest As and Cd concentrations were recorded in Zanjice, the highest Hg and Co levels in the Harbor Bar, whereas the concentrations of Ni and Pb were the highest in H. Novi and Sveta Stasija ($p < 0.05$; Table III). In Table III, the Interim Marine Sediment Quality Guidelines (*ISQG*) and Probable Effect Level (*PEL*) values are given in dry weight. The *ISQG* and *PEL* values for marine organisms have been adopted by Environment Canada for a range of toxic substances.[28] These guidelines may not be validated for use everywhere; there may be fundamental differences in sediment geochemistry.[28] However, in the absence of any standards, these guidelines can be used as a first approximation in assessing whether organisms are at risk from sediment concentrations of toxic substances. The concentrations of the investigated elements measured in this study were below the PEL values in the all sediment samples.

TABLE III. Trace metal concentrations in surface sediment (mean ± S.D. in mg kg^{-1} dw, for Hg μg kg^{-1} dw; nv – no value)

Sampling place	Co	Ni	As	Cd	Hg	Pb
Sv. Stasija	3.9±0.35	18.2±1.7	4.9±0.55	0.75±0.10	24.2±2.2	7.0±1.2
H. Novi	9.0±0.80	32.3±3.3	3.7±0.4	0.77±0.11	28.4±2.3	3.7±0.4
Zanjice	6.6±0.72	16.3±1.5	19.7±2.6	0.87±0.13	9.20±1.0	3.9±0.5
Budva	5.2±0.5	2.7±0.2	2.6±0.37	0.063±0.01	14.0±1.1	2.6±0.3
Bar	11.4±1.1	15.8±1.2	3.1±0.4	0.068±0.01	154.7±9	5.2±0.7
ISQG[28]	nv	15.9	7.24	0.7	130	30.2
PEL[28]	nv	42.8	41.6	4.2	700.0	112.0

Biota

The metal concentrations found in the marine organisms *M. galloprovincialis* and *P. oceanica* from the different locations are presented in Table IV. The maximum allowable concentrations or *MAC*s[8] for Ni, As, Hg and Pb in mussels are shown in Table IV. In the all investigated mussel samples, the Cd concentrations were lower than the *MAC* value for Cd and the Hg concentrations were higher than the MAC value for Hg. Recommended *MLC* values for the sea grass do not exist in the literature.

TABLE IV. Trace metal concentrations in *M. galloprovincialis* (*Mg*) and *P. oceanica* (*Po*); mean ± SD in mg kg^{-1} dw; *MAC* – maximum allowable concentration; nv – no value

Sampling place	Co	Ni	As	Cd	Hg	Pb
			Mg			
Sv. Stasija	3.92±0.4	3.35±0.3	7.35±1.0	2.15±0.3	0.95±0.12	9.10±1.1
H. Novi	1.10±0.10	4.7±0.46	17.8±2.3	1.50±0.19	0.35±0.031	3.50±0.4
Zanjice	8.98±0.76	18.9±1.8	40.8±5.6	1.70±0.24	0.59±0.062	1.77±0.23
Bar	6.07±0.6	12.3±1.2	7.54±1.1	3.53±0.47	1.06±0.130	8.50±0.9
MAC[8]	nv	3.40	16.0	3.70	0.23	3.20
			Po			
Sv. Stasija	4.15±0.4	24.8±2.3	3.82±0.53	2.20±0.25	0. 26±0.03	10.1±1.5
H. Novi	3.75±0.38	22.8±2.1	2.71± 0.41	2.90±0.39	0.35±0.04	8.2±0.9
Zanjice	4.30±0.41	31.0±3.2	7.96± 1.34	2.80±0.46	0.57±0.06	3.4±0.28
Bar	6.50±0.60	36.7±3.6	2.50±0. 29	3.50±0.52	1.37±0.12	5.1±0.60
Budva	3.80±0.39	24.7±2.5	2.68±0. 38	2.70±0.44	0.46±0.04	4.5±0.5

The *M. galloprovincialis* and *P. oceanica* samples from Zanjice presented the highest As concentrations ($p < 0.05$), whereas from the Harbor Bar, they had the highest Cd and Hg concentrations ($p < 0.05$) and from Sveta Stasija, the highest Pb concentrations ($p < 0.05$; Table IV). The Cd and Hg concentrations in the biota samples from Bar and the Pb concentrations in the Sveta Stasija samles were very similar. The concentrations of Ni were significantly higher in *P. oceanica* than in *M. galloprovincialis*, whereas the As concentrations were significantly higher in *M. galloprovincialis* ($p < 0.05$; Table IV).

Bioconcentration and sediment accumulation factors

The bioconcentration and sedim ent accumulation factors (*BCF* and *BSAF*) are shown for both species from the same sampling points, Figs. 2 and 3, respectively. The mean values the *BCF* should be multiplied by 10^3 in Fig. 2. The metal which presents the highest mean *BCF* is As and Hg is the metal with the lowest one (Fig. 2), while Cd is the metal which presents the highest mean *BSAF* and Hg is the metal with the lowest one (Fig. 3). *P. oceanica* exhibited higher mean *BCF* and *BSAF* values compared to *M. galloprovincialis*, except for As and Hg (Figs. 2. and 3).

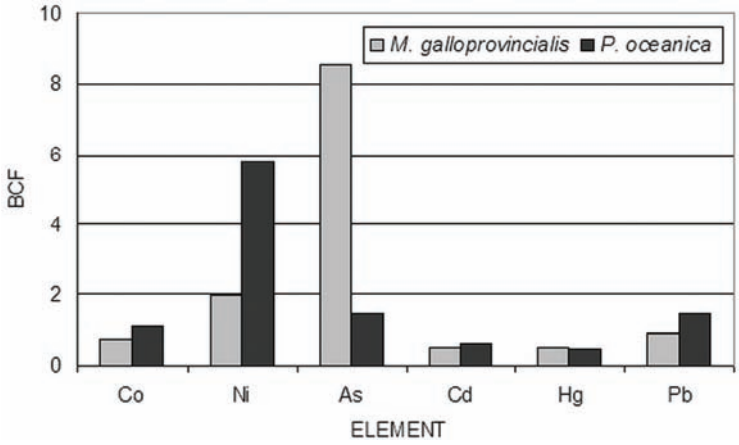

Fig. 2. Mean bioconcentration factor (*BCF*) values in *M. galloprovincialis* and *P. oceanica* (multiplied by 10^3).

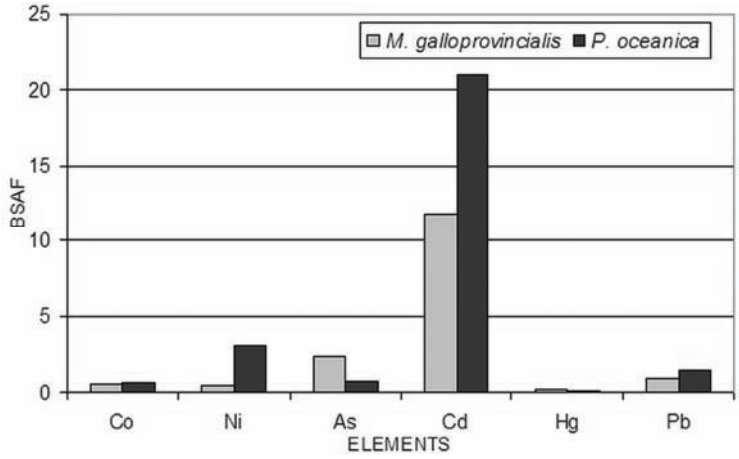

Fig. 3. Mean biosediment accumulation factor (BSAF) values in *M. galloprovincialis* and *P. oceanica.*

Relation between the metal concentrations in P. oceanica *and* M. galloprovincialis *with the metal concentrations in seawater*

There were significant positive correlations for the Cd and Pb concentrations in *M. galloprovincialis* and *P. oceanica,* relative to their concentrations in seawater ($r_{Cd} = 0.95$; $r_{Pb} = 0.92$; $p < 0.05$, and $r_{Cd} = 0.95$; $r_{Pb} = 0.95$; $p < 0.05$, respectively) and positive relations for the As and Co concentrations ($r_{As} = 0.62$; $r_{Co} = 0.73$; $p < 0.05$ and $r_{As} = 0.78$; $r_{Co} = 0.66$; $p < 0.05$, respectively). Significant relations were found in the case of Ni ($r_{Ni} = 0.61$; $r_{Ni} = 0.49$).

Relation between the metals concentrations in P. oceanica *and* M. galloprovincialis *with the metal concentrations in the sediments*

There were positive correlations for the As in *P. oceanica* and the Hg concentrations in *M. galloprovincialis* relative to their concentrations in the sediments ($r_{As} = 0.52$; $r_{Hg} = 0.65$; $p < 0.05$) and positive relations for the Pb concentrations in *P. oceanica* and *M. galloprovincialis* relative to their concentrations in sediments ($r_{Pb} = 0.65$; $r_{Pb} = 0.52$; $p < 0.05$), but non-significant relations were found in the case of the Cd concentrations for both organisms ($r_{Cd} = -0.70$; $r_{Cd} = -0.64$; $p < 0.05$), respectively.

The Harbor Bar was previously identified as the most Hg- and Cd-contaminated location based on previous mussels studies[29] and by the investigated compartments, except for Cd in the sediment analysis, for which a maximum value was revealed for Zanjice. The fact that no correlations were found between the Cd concentrations in *M. galloprovincialis* and *P. oceanica* and in the sediment, but very high correlations were found between the Cd concentrations in the investigated biota and seawater indicate that the Cd in *P. oceanica*[5,15,30] and *M. galloprovincialis*[6,31] tissues reflect the Cd in the water column. Cd accumulation in *M. galloprovincialis* and *P. oceanica* seems to be a function of the Cd concentration in seawater, which was also found in the present study.

The Harbor Bar was identified as the most Hg-contaminated location according to the results obtained for all the investigated compartments, especially the surface sediment. This result is probably related to the effluents from the storage of crude oil and oil products, transoceanic ships and tankers traffic, as well as untreated urban and industrial effluents. In this study, a positive correlation was found between the Hg concentrations ($r_{Hg} = 0.65$) in *M. galloprovincialis* and in the sediment but a non-significant relation with the concentration in seawater ($r_{Hg} = 0.01$). This result could be related to the presence of a high level of Hg from sediment in the suspended particulate matter and of high levels of the particulate matter in the water column.[19] Metals in mussels can correlate with metal levels in sediments, although mussels are not in direct contact with the sediment, which is resuspended and wafted to them by wave action.[32]

Sveta Stasija was identified as the most Pb-contaminated location according to the results obtained for all the investigated compartments, except the bottom seawater. Seawater had maximum Pb values in the Harbor Bar. The extreme Pb contamination in the vicinity of Sveta Stasija could be associated with an anthropogenic impact due to the proximity of Kotor, a city with a harbor, chemical industry, food industry and the geographical location of Sveta Stasija, *i.e.*, there is a low hydrological influx to the small Kotor Bay.

The identification of Sveta Stasija as the most Pb-contaminated site was previously explained by the fact that the bed of the small Kotor bay is clay[33] and a trace element such as Pb is preferentially associated with clay mineral particles,[34]

which form more or less soluble organic matter particles, indicating that the evidenced Pb originated primarily from human activities.[7] Significant correlations between the concentrations Pb in the organisms and Pb in the surrounding water were obtained. The positive correlations found between the Pb concentrations in *P. oceanica* and *M. galloprovincialis* and in the water would suggest that Pb in the tissues of the organisms primarily reflects the Pb in the water.[16,17] Therefore, in the case of *P. oceanica*, this leads to the hypothesis of preferential Pb uptake from the water column.[16] However, the positive correlation found for Pb related to the sediment, and previously in this study for Hg related to the water in this sea grass suggests that there could be some other uptakes and distributions routes for these two elements, not only by leaves and for Pb also by the root system,[5] and *vice versa*, leaves for Hg.[35] The maximum Pb level in sediment found in Sv. Stasija is related to the highest Pb level in *M. galloprovincialis* at this location. Pb in *M. galloprovincialis* is absorbed bound to particulate material and in a water-soluble form.[36]

Zanjice was identified as the most As-contaminated location by the results of all the investigated compartments. Arsenic was homogeneously distributed along the Montenegrin coast in the sediment except at the location Zanjice. This could be due to natural leaching of terrestrial soils and sediments or increases in the As concentration when the sediment content changed,[37] which in Zanjice could be attributable to the transport of metals by waves from the open sea and by the branch of the Mediterranean current coming from the southeastern side of the Adriatic[38] entering into the Bay, or on leaving, carrying wastes from the Bay. For the other locations, the low As concentrations in the sediment may be explained by the lack of low contaminant inputs and the low leaching of natural arsenic. In this study, the concentrations of As in *M. galloprovincialis* were higher than those in the sediment were, but slightly less in *P. oceanica* than in the sediment (Tables III and IV). Positive correlations were found between the As levels in these organisms and the As levels in the sediment and water. Generally, the arsenic levels in these organisms generally reflect the total arsenic in the sediment.[39] Langston[39] supports the view that particulate arsenic is the most important source of the metal accumulated in bivalves, although some absorption from solution cannot be disregarded, which is in agreement with the results obtained in the present study. The lower relationship between As in *P. oceanica* and in water/sediment, compared to mussels, may be explained by other factors such as phosphate competition related to As[39] or that As is mostly immobilized as a form not available to plants.[40]

The *M. galloprovincialis* from Zanjice, located at the entrance of the Bay, had greater contents of As, Ni and Co than *M. galloprovincialis* from the Bay. This could be attributable to the hydrological influence mentioned above in the case of this location.[19,20]

The Ni concentrations in the bio monitored organisms in this study were similar to those reported in the literature.[2,15,17] Positive correlations between the Ni concentrations in the organisms and those in seawater/sediment were not evidenced. This is possibly due to the background Ni levels[15] in the organisms. In the case of the Co concentrations, the positive correlations found between the Co concentrations in *P. oceanica* and *M. galloprovincialis* with those in seawater indicate that Co in these organisms mainly came from the water, which is contrary to the assertions of Lafabrie.[16,17]

CONCLUSIONS

The data obtained in the present investigation showed that the sea grass *P. oceanica* and the mussel *M. galloprovincialis* could be used as organisms for the biomonitoring of heavy metals pollution in the marine environment of the southeastern Adriatic Sea. These data showed that the accumulation ratios of the six studied metals in the sea grass and in the mussel differed. From the determined *BCF* and *BSAF* values calculated for the two different marine species investigated in this study, *P. oceanica* was found to be a stronger accumulator for Cd, Pb, Ni and Co, and *M. galloprovincialis* for As and Hg. *P. oceanica* was a stronger Cd accumulator from the surrounding water and *M. galloprovincialis* had a higher capacity to accumulate As, mostly from particles. The Hg accumulation by both the investigated organisms was the lowest of the investigated metals.

However, it must be born in mind that the actual uptake mechanisms of heavy metals by the studied organisms are probably rather complex because their exposure to trace elements is not limited to soluble metals in the aquatic medium. Metal uptake from sediment particles and food, in the case of the mussels, and from sediments (through the roots), in the case of the sea grass, cannot be ignored.

The results of this first study provide a valuable baseline for further monitoring of the marine ecosystem of the southeastern Adriatic Sea.

Acknowledgments. This research was financed by the Ministry of Education and Science of the Republic of Serbia, Contract No. III43009 and EAR, Contract No. 04SER02/05/007.

ИЗВОД

АКУМУЛАЦИЈА ТРАГОВА МЕТАЛА У МОРСКИМ ОРГАНИЗМИМА ЈУГОИСТОЧНЕ ЈАДРАНСКЕ ОБАЛЕ

ДАНИЈЕЛА ЈОКСИМОВИЋ[1] и СЛАВКА СТАНКОВИЋ[2]

[1]*Институт за биологију мора, Универзитет Црне Горе, Доброта бб, 85330 Котор, Црна Гора и* [2]*Технолошко–металуршки факултет, Универзитет у Београду, Карнегијева 4, 11000 Београд*

Концентрација и акумулација трагова метала (Co, Ni, As, Cd, Pb и Hg) одређивана је у седименту, морским организмима и морској води дуж Црногорске обале. Добијени резултати трагова метала у морској трави *Posidonia oceanica* и шкољкама *Mytilus galloprovincialis* били су анализирани у односу на исте елементе добијене у морској води и седиментима.

Узорковање је вршено у јесен 2005. године на пет локација, Света Стасија, Херцег Нови, Жањице, Будва и Бар, које су под утицајем различитих загађивача изазваних човековом активношћу. Анализом трагова метала у морској води, седиментима и испитиваним морским организмима у приобалном делу Црногорског приморја утврђено је да је лука Бар првенствено загађена живом, Жањице арсеном, а Света Стасија оловом. Такође је утврђено да морска трава *P. oceanica* има већи капацитет биоакумулације у односу на шкољку *M. galloprovincialis* за Co, Ni, Cd и Pb, али не и за As и Hg. Први пут у овом раду морска трава *P. oceanica* и шкољка *M. galloprovincialis* коришћене су као биоиндикатори трагова метала у морској води и седименту Црногорског приморја. Такође резултати овог рада могу бити коришћени као основа за процену будућих антропогених утицаја на испитивани екосистем.

(Примљено 23. марта, ревидирано 13. априла 2011)

REFERENCES

1. UNEP, *MAP technical report Series* **86** (1994) 91
2. L. Giusti, H. Zhang, *Environ. Geochem. Health* **24** (2002) 47
3. L. Manfra, A. Accornero, *Mar. Pollut. Bull*. **50** (2005) 686
4. J. Scancar, T. Zuliani, T. Turk, R. Milačić, *Environ. Monit. Assess.* **127** (2007) 271
5. Z. Kljaković-Gašpić, B. Antolić, T. Zvonarić, A. Barić, *Fresenius Environ. Bull*. **13** (2004) 1210
6. Z. Kljaković-Gašpić, N. Ozak, I. Ujević, T. Zvonarić, A. Barić, *Fresenius Environ. Bull*. **15** (2006) 1041
7. Z. Kljaković-Gašpić, D. Bogner, I. Ujević, *Environ. Geol.* **58** (2009) 751
8. M. Jović, R. A. Stanković, L. Slavković Beskoski, I. Tomić, S. Degetto, S. Stanković, *J. Serb. Chem. Soc*. **76** (2011) 933
9. D. Joksimović, I. Tomić, R. A. Stanković, M. Jović, S. Stanković, *Food Chem*. **127** (2011) 637
10. D. Babi, V. Çelo, A. Çullaj, N. Pano, *Fresenius Environ. Bull*. **7** (1998) 577
11. V. Çelo, D. Babi, B. Baraj, A. Çullaj, *Water Air Soil Pollut.* **111** (1999) 235
12. J. Morillo, J. Usero, I. Gracia, *Chemosphere* **58** (2005) 1421
13. L. Manfra, A. Accornero, *Mar. Pollut. Bull.* **50** (2005) 686
14. D. Acevedo-Figueroa, B. D. Jimenez, C. J. Rodriguez-Sierra, *Environ. Pollut.* **141** (2005) 336
15. L. Campanella, M. E. Conti, F. Cubadda, C. Sucapane, *Environ. Pollut*. **111** (2001) 117
16. C. Lafabrie, G. Pergent, R. Kantin, C. Pergent-Martini, J. L. Gonzalez, *Chemosphere* **68** (2007) 2033
17. C. Lafabrie, C. Pergent-Martini, G. Pergent, *Environ. Poll*. **151** (2008) 262
18. M. Romeo, C. Frasila, M. Gnassia-Barelli, G. Damiens, D. Micu, G. Mustata, *Water Res*. **39** (2005) 596
19. D. Cossa, J. M. Martin, K. Takayanagi, J. Sanjuan, *Deep-Sea Res*. **44** (1997) 721
20. K. M. El-Moselhy, M. N. Gabal, *J. Mar. Syst*. **46** (2004) 39
21. Y. W. Lee, W. X. Wang, *Sci. Total Environ*. **213** (2001) 273
22. B. M. Žarković, S. D. Blagojević, *J. Serb. Chem. Soc.* **74** (2009) 1009
23. M. Murakami, T. Takada, *Talanta* **39** (1992) 1293
24. R. Serrano, F. J. López, F. Hernández, J. B. Peña, *Bull. Environ. Contam. Toxicol*. **59** (1997) 968

25. US EPA (United States Environmental Protection Agency), 2009, *National Recommended Water Quality Criteria*, United States Environmental Protection Agency. http://water.epa.gov/scitech/swguidance/standards/current/upload/nrwqc-2009.pdf (last accessed: April, 2011)
26. Montenegrin regulation, 2008, *The quality of wastewater discharged into the recipient, No. 45/08 of 31.07.2008, 09/10 of 19.02.2010*, Ministry of Agriculture, Forestry and Water Management, with the prior opinion of the Ministry of Tourism and Environment and the Ministry of Health, Labour and Social Welfare
27. EU (2008), *Strategy for the marine environment*, http://europa.eu/legislation_summaries/maritime_affairs_and_fisheries/fisheries_resources_and_environment/l28164_en.htm (last accessed: April, 2011)
28. CCME (Canadian Council of Ministers of the Environment), 2002, *Canadian Sediment Quality Guidelines for the Protection of Aquatic Life*, Canadian Council of Ministers of the Environment. http://www.ccme.ca/assets/pdf/sedqg_summary_table.pdf (last accessed: April, 2011)
29. S. Stankovic, M. Jovic, R. Milanov, D. Joksimovic, *J. Serb. Chem. Soc.* **76** (2011) 1725
30. M. E. Conti, B. Bocca, M. Iacobucci, G. Finoia, M. Mecozzi, A. Pino, A. Alimonti, *Arch. Environ. Contam. Toxicol.* **58** (2010) 79
31. G. Adami, P. Barbieri, M. Fabiani, S. Piselli, S. Predonzani, E. Reisenhofer, *Chemosphere* **48** (2002) 671
32. J. Burger, M. Gochfeld, *Sci. Total Environ.* **368** (2006) 937
33. S. Degetto, C. Cantaluppi, D. Desideri, M. Schinitu, S. Stankovi ć, Z. Kljajić, in *Proceeding of 7th Int. Conf. Methods and Applications of Radioanalytical Chemistry-MARC VII*, (2006), Kailua-Kona, Hawaii, USA, 2006, p. 83
34. P. G. Glasby, P. Szefer, J. Geldon, J. Warzocha, *Sci. Total Environ.* **330** (2004) 249
35. M. A. Schlacher-Hoenlinger, T. A. Schlacher, *Mar. Biol.* **131** (1998) 401
36. P. Irato, G. Santovito, A. Cassini, E. Piccinni, V. Albergoni, *Arch. Environ. Contam. Toxicol.* **44** (2003) 476
37. F. Galgani, J. F. Chiffoleau, V. Orsoni, L. Costantini, P. Boissery, S. Calendin, B. Andral, *Chem. Ecol.* **22** (2006) 299
38. B. Cushman-Roisin, E. C. Naimie, *J. Mar. Syst.* **37** (2002) 279
39. W. J. Langston, *J. Mar. Biol. Ass. U.K.* **60** (1980) 869
40. P. Richtera, R. Seguel, I. Ahmuda, R. Verdugo, J. Narvaez, Y. Shibatac, *J. Chil. Chem. Soc.* **49** (2004) 333.

Journal of the Serbian Chemical Society
JSCS-info@shd.org.rs • www.shd.org.rs/JSCS
J. Serb. Chem. Soc. *77* (1) 119–129 (2012)
JSCS–4254
UDC 504.53.054+546.76:66.061.34:550.4+550.8.013
Original scientific paper

Leaching of chromium from chromium contaminated soil – a speciation study and geochemical modelling

DARKO H. ANDJELKOVIĆ[1]*, TATJANA D. ANDJELKOVIĆ[2#], RUŽICA S. NIKOLIĆ[2], MILOVAN M. PURENOVIĆ[2], SRDJAN D. BLAGOJEVIĆ[3#], ALEKSANDAR LJ. BOJIĆ[2#] and MILICA M. RISTIĆ[1]

[1]*Water Works Association "Naissus", Kneginje Ljubice 1/I, 18000 Niš, Serbia,* [2]*Faculty of Sciences and Mathematics, University of Niš, Višegradska 33, 18000 Niš, Serbia and* [3]*Faculty of Agriculture, University of Belgrade, Nemanjina 16, 11081 Belgrade, Serbia*

(Received 16 December 2010, revised 20 February 2011)

Abstract: The distribution of chromium between soil and leachate was monitored. The natural process of percolation of rainwater through soil was simulated under laboratory conditions and studied by column leaching extraction. Migration of chromium in soil is conditioned by the level of chromium soil contamination, the organic matter content in the soil and rainwater acidity. Chromium(III) and chromium(VI) were determined by a spectrophotometric method with diphenylcarbazide in acidic media. Comparing the results of chromium speciation in the leachate obtained by experimental model systems and geochemical modelling calculations using the Visual MINTEQ model, a correlation was observed regarding the influence of the tested parameters. Leachate solutions showed that the concentration of Cr depended on the organic matter content. The influences of pH and soil organic matter content were in compliance after their experimental and theoretical definition. The Stockholm humic model used to evaluate the leaching results corresponded rather well with the measured values.

Keywords: chromium; speciation; leaching; rainwater; soil organic content.

INTRODUCTION

Speciation analysis is a measurement process giving quantitative and qualitative data about the chemical forms of an element in a sample. It usually involves two phases: separation of the target element from the sample matrix and its determination. Differentiation of the forms of the element is realized between oxidation states, simple and coordinated ions, cationic, neutral and anionic forms, protonated and unprotonated, and monomeric and polymeric species.[1]

* Corresponding author. E-mail: darko.andjel@gmail.com
# Serbian Chemical Society member.
doi: 10.2298/JSC101216154A

Chromium speciation is important due to its wide usage in the metallurgic and chemical industries. Improper disposal, poor storage and leakage of chromium from waste discharge through soil can release chromium to the environment, causing contamination of groundwater and adverse biological and ecological effects.[2] Cr(VI) is a strong oxidizing agent and shows chronic toxic effects including carcinogenic property and it induces dermatitis. Occupational exposure to Cr(VI) compounds leads to a variety of clinical problems. A significant concentration of Cr(III) can cause adverse effects because its strong capability to coordinate various organic compounds results in inhibition of some metallo–enzyme systems.[3,4]

Chromium is present in the environment in the form of Cr(III) and Cr(VI). These two forms show different chemical, physico-chemical and biochemical properties. Cr(VI) species are more soluble, mobile and bioavailable than Cr(III) species. The presence of these two forms and their relative ratio is dependent on chemical and photochemical redox transformation, precipitation/dissolution and adsorption/desorption reactions.[5] Due of these differences in chemistry, biochemistry and physico–chemistry of Cr(III) and Cr(VI) species, the determination of the total Cr concentration in a variety of samples does not give the necessary information to evaluate the effects of the different species. The potential risk of chromium from soils is determined by its solid–solution partitioning rather than its content. The release of chromium to the aqueous phase depends on its affinity to bind to reactive surfaces in the soil matrix. Quantifying adsorption/desorption and precipitation/dissolution reactions is a critical aspect of predicting the chemical behaviour of chromium in soil. Many factors can influence the migration process, such as pH, dissolved and solid organic matter and soil characteristics,[6,7] *e.g.*, cation exchange capacity, clay content, and competition from other metal ions. In addition, the presence of soluble natural organic ligands in soil, such as fulvic acid (FA), may significantly influence metal adsorption through the formation of stable complexes.

The objectives of this investigation were to study the distribution of chromium between soil and soil leachate. The natural percolation of rainwater through the soil was simulated under laboratory conditions and studied by column leaching extraction. Migration of chromium in the soil is conditioned by the level of chromium soil contamination, the organic matter content of the soil and the acidity of rainwater.

Comparing the results of speciation of chromium in soil and infiltration water obtained by experimental model systems and geochemical modelling calculations using the Visual MINTEQ model, a correlation was observed regarding the influence of the tested parameters.

Visual MINTEQ includes three different models for calculating cation binding to humics: *i*) the Gaussian dissolved organic matter (DOM) model,[8] *ii*) the

Stockholm humic model (SHM),[9] which can be used for both aqueous speciation and solid–solution partitioning, and *iii*) the non-ideal competitive adsorption-Donnan (NICA-Donnan) model,[10] which is available only for aqueous speciation. Each of these models show considerable complexity caused by the extreme heterogeneity of the humic binding sites, the variable stoichiometry of metal–humic binding reactions and the presence of electrostatic interactions.

This study focused on the Stockholm humic model (SHM),[9] which was created to provide a more realistic assessment of metal–humic complexation than had been possible using the Gaussian DOM model in MINTEQ. The SHM is related to more mechanistic models and the NICA-Donnan model, although it is also different in some respects, *i.e.*, in the electrostatic model.

EXPERIMENTAL

Soil sampling, properties and soil column set up

Two soil types were used in this study: *i*) grass-covered and well-drained urban green--field soil and *ii*) organic substrate for horticultural container growing. A 10-cm depth of park soil (situated within the city centre of Niš, Serbia) was collected immediately beneath the upper zone, in which plant remains were dominant. The soils were air dried and passed through a 60 mesh sieve. Selected physico-chemical soil properties, *i.e.*, pH, electrical conductivity (EC) and organic matter content, are given in Table I. The electric conductivity and pH were measured in water suspensions. The soil content of organic matter was determined on finely ground samples by the wet combustion method based on bichromate reduction.[11]

TABLE I. Characteristics of the employed soil and rainwater

Characteristic	Urban soil	Organic substrate	Rainwater	Acid rainwater
pH	8.6	8.3	5.7	3.2
Electrical conductivity, μS cm^{-1}	113.0	677.0	26.7	270.0
Organic matter, %	1.76	15.77	–	–

Glass columns, 20 cm in length with an internal diameter of 2 cm were used in this study. The bottom of each column contained a porous glass frit. Soil (30 g) was carefully packed with gently tapping on the sides of the column to ensure good contact between the materials without making air compartments.

Chromium leaching and determination

Four different treatments were included in the study. In all treatments, artificial rainwater was added to the columns. The chemical composition of the artificial rainwater was similar to that of average rainwater in urban areas (SO_4 – S 0.8 mg L^{-1}, Cl 0.5 mg L^{-1}, NO_3 – N 0.4 mg L^{-1}, NH_4 – N 0.3 mg L^{-1}, Na 0.2 mg L^{-1}, K 0.03 mg L^{-1}, Mg 0.03 mg L^{-1}, pH 5.0). The acid rainwater was obtained by acidification of rainwater with H_2SO_4 to pH 3.5. Before starting the leaching, de-ionized water was added to the columns to bring the soil to field water capacity. 40 mL of inflow solution was added slowly (2 h) as droplets to the top of the columns. The total volume of rainwater corresponded to 734 mm, the average total annual precipitation in the region of Serbia. The pH value and EC of the rainwaters are given in Table I.

The urban soil and organic substrates were polluted with potassium dichromate. Considering the fact that the average chromium content of urban soil is 40–80 mg Cr kg^{-1} soil,[12] the applied Cr amount was 2.4 mg Cr per 30 g of soil.

Leaching was monitored after treatment of soil and organic substrate (polluted and unpolluted) with rainwater and acid rainwater. All treatments were conducted in triplicate for both soils and both rainwater types in 3 columns.

The leachate was collected in 10 mL portions. After centrifugation of the leachate portions, the pH, EC and chromium contents were determined. pH and EC were determined using HACH SensIon 3 pH-meter and HACH SensIon 5 conductometer. The most common method for determining Cr(VI) in aqueous solutions is based on the reaction of diphenylcarbazide with Cr(VI) at a pH of 1.0±0.3. As stated by many researchers, diphenylcarbazide has a very sensitive colour reaction with Cr(VI) in acid solution.[13-15] Chromium(III) was analyzed spectrophotometrically with diphenylcarbazide after oxidation with persulphate using a Lovibond multidirect colorimeter.

Modelling of chromium solubility

Equilibrium modelling of the metal concentrations in the leachates was performed using the Stockholm humic model (SHM). The parameterisation of the model uses the total concentrations of each component and the stability constants of species formed at equilibrium to set up a series of simultaneous mole balance and mass law equations, which are solved to give the equilibrium concentration of each species. The SHM was implemented in Visual MINTEQ, ver. 3.0 (www.lwr. kth.se/english/ourSoftware/Vminteq/index.htm).[9,16,17]

RESULTS AND DISCUSSION

There are several soil characteristics, such as soil pH, electrical conductivity and organic matter content, which are important for defining processes in soil. The urban soil used in the present study was a highly alkaline soil[18] and, due to the organic matter content (1.76 %), is considered as a soil with a low organic matter content[19] (Table I). The organic substrate for horticultural container growing had a similar pH value but with a characteristically high organic matter content (15.77 %).

During leaching with rainwater and acid rainwater, there was a significant change in pH and EC of the leachate at the start of the treatment, while subsequently all the values converged to a similar pH and EC level (Fig. 1).

In the first 70 mL of the leachate, the amount chromium leached was less than 2 % of the total chromium added to the soil for the treatments with polluted soil (PS) and polluted organic substrate (POS) (Table II). The obtained results for PS indicate that more chromium was leached with acid rainwater (2.01 %) than with rainwater (1.44 %). Acid rainwater, which frequently precipitates in urban areas, can control chromium accumulation in the soil profile, enhance the downward movement of chromium to the groundwater and the bioavailability for plant uptake.

However, in the case of soil rich in organic matter (POS), the acidity of the rainwater decreased the amount of leached chromium. Only 0.29 % of the total chromium applied to the soil is leached by acid rainwater. This decrease is pro-

bably due to the retention of some of the chromium by the soil in the form of insoluble $Cr(OH)_3$, which is adsorbed on the surface of the soil.[12] The insoluble $Cr(OH)_3$ was formed by the reduction of Cr(VI) that was enhanced by the high content of organic matter and the increased acidity of system.[12] This was confirmed by the fact that only a minor quantity of chromium was detected in the leachate and that only Cr(VI) species were detected in the leachate. On the other hand, in the case of low acidity, more chromium was leached (0.63 %) than with acid rainwater, because in the acidic pH range, chromium appears only as soluble Cr(III) species, generated by reduction of Cr(VI). This was also confirmed by the fact that only Cr(III) species were detected in the leachate.

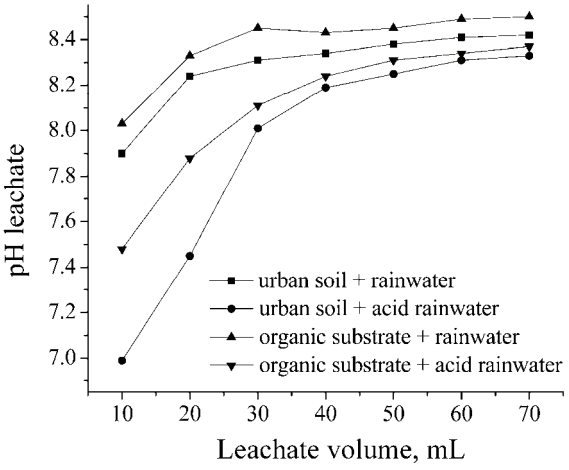

(a)

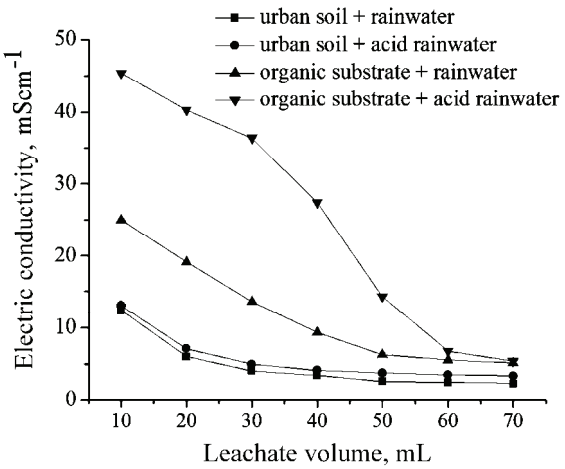

(b)

Fig. 1. a) pH and b) electrical conductivity of the leachate during the leaching of polluted soil and organic substrate.

TABLE II. Ratio of leached chromium to total added Cr in the soil column (%)

Sample	Rainwater	Acid rainwater
Polluted soil (PS)	1.44	2.01
Polluted organic substrate (POS)	0.63	0.29

Humic substances (HS), that mostly comprise soil organic matter, are very important components that control the adsorption of heavy metals by soil. Humic substances are heterogeneous in nature and are considered as polydisperse mixtures of natural organic polyelectrolytes containing a large number of different functional groups. The ability of HS to form stable complexes with polyvalent cations is attributed to their high content of oxygen-containing functional groups, including carboxyl, phenol, hydroxyl, enol and carbonyl structures of various types.[20,21]

If this highly complex natural ligand strongly complexes with Cr in solution, the presence of this ligand in the soluble form has the potential to reduce sorption to soil and increase leaching. The results presented in Table II show that the humic ligand mixture in POS sorbed to the soil and increased the amount of ternary soil–ligand–chromium complexes, facilitating the chromium retention in soil column, and leading to decreased mobility.[22–25] Thus, in the treatment set with POS and acid rainwater, the decrease of chromium in leachate was 10 times more compared to the soil with the low organic matter content – PS (0.29 comparing to 2.01 %). This confirms the influence of organic matter on the retention of chromium by soil.

The speciation diagram of Cr(III) as a function of pH, calculated by the speciation software MINT EQ, is shown in Fig. 2a. The dominant species of Cr(III) for pH < 4.5 are $Cr^{3+}_{(aq)}$ and $Cr(OH)^{2+}$. For pH > 4.5, mainly insoluble $Cr(OH)_3$ is formed. Soluble polyhydroxyl species, such as $Cr(OH)_4^-$, $Cr_2(OH)_2^{4+}$, $Cr_3O_4(OH)_4^{3-}$, $Cr_4(OH)_4^{5+}$, $Cr_2O_2(OH)_4^{2-}$ and others, appear at highly alkaline values.[26,27]

The speciation diagram of Cr(III) *vs.* pH in the presence of soil organic matter, as defined by the Stockholm humic model (SHM), is presented in Fig. 2b. The SHM was created to provide a more realistic assessment of metal–humic complexation than the Gaussian dissolved organic matter model in MINTEQ. The SHM allows metals binding to humic to be described either as monodentate or as bidentate ligand. As humic substances may occur both in the dissolved and solid phases, cation binding was considered both for dissolved and solid-phase humic substances. This model is based on the following: dissolved fulvic acid ($FA_{(aq)}$) and its value of 0.048 g L^{-1} represents the concentration of 'active' dissolved organic matter in the system. The humic substances in the solid phase are assumed to be a mixture of humic and fulvic acid and the relative proportions of these were set to $FA_{(s)}$ 0.845 g L^{-1} and $HA_{(s)}$ 1.457 g L^{-1}. To accelerate the cal-

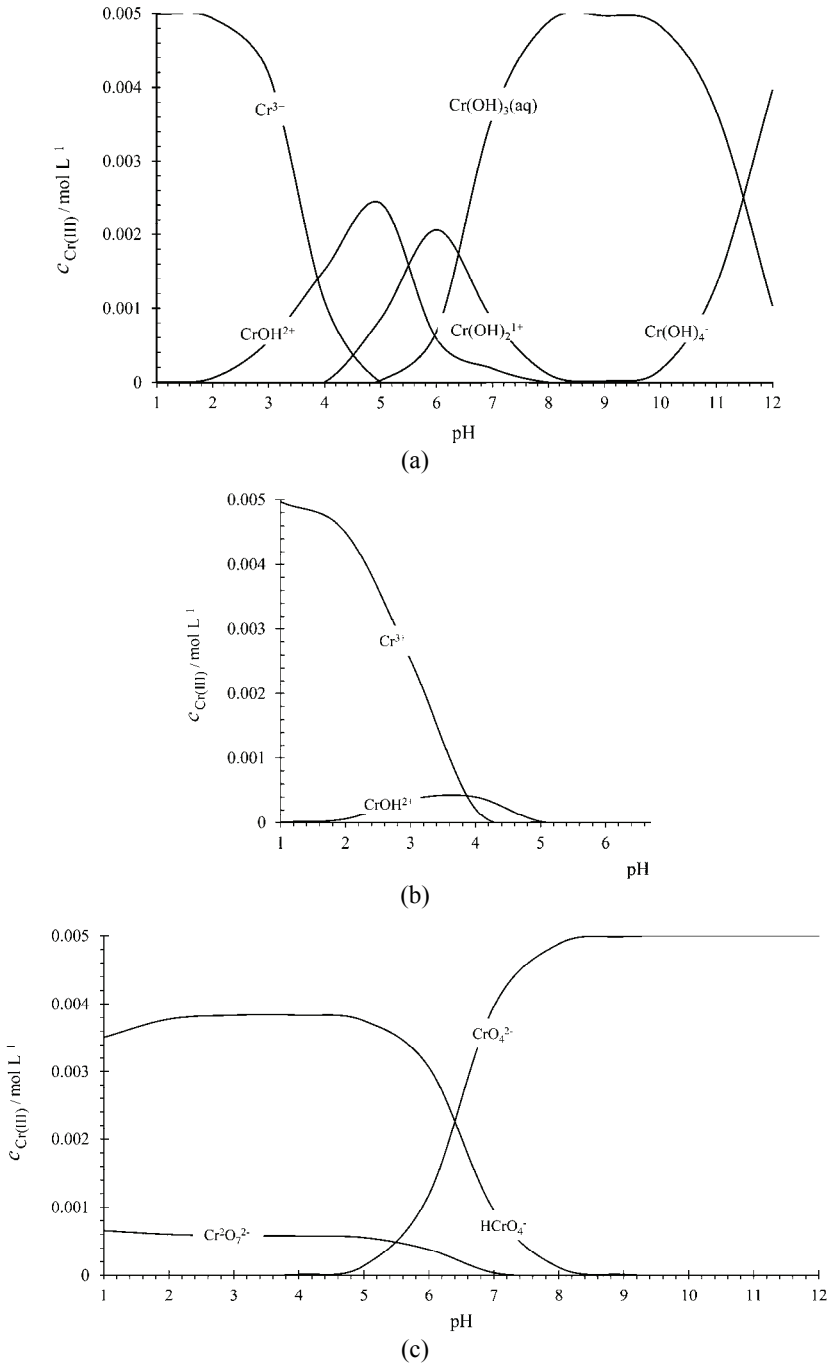

Fig. 2. Concentration of chromium species (mol L^{-1}) at different pH values, calculated by Visual MINTEQ in the presence of a) Cr(III), b) Cr(III) and organic matter and c) Cr(VI).

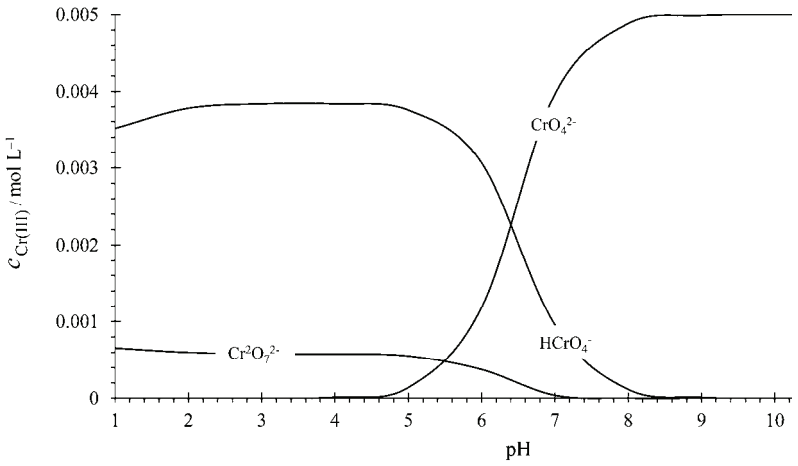

(d)

Fig. 2. (Continued) Concentration of chromium species (mol L^{-1}) at different pH values, calculated by Visual MINTEQ in the presence of d) Cr(VI) and organic matter.

culations, solid-phase HA (humic acid) and solid-phase FA are normally bulked together as one component. Using such a defined humic model, the equilibrium chemistry of a soil suspension with 2.5 g L^{-1} of active humic substances, of which 62 % is HA and 38 % FA, was simulated. 48 mg L^{-1} FA was dissolved (equivalent to 24 mg L^{-1} dissolved organic carbon (DOC) if the entire DOC is assumed to be FA). The soil was suspended with SO_4 – S 0.8 mg L^{-1}, Cl 0.5 mg L^{-1}, NO_3^- – N 0.4 mg L^{-1}, NH_4 – N 0.3 mg L^{-1}, Na 0.2 mg L^{-1}, K 0.03 mg L^{-1} and Mg 0.03 mg L^{-1}. In this problem, the total concentrations of K, Mg and Na constitute the sum of the dissolved + complexed ions. The equilibrium constants of the chromium species and the model parameters for soil FA and soil HA defined in Visual MINTEQ are given in Table III.

TABLE III. Model parameters and equilibrium constants defined in Visual MINTEQ for the system Cr(III), Cr(VI) and soil organic matter

Sample	Proton dissociating groups (mmol g^{-1})	Site density (sites nm^{-2})	ΔpK_A (strong acid groups)	ΔpK_B (weak acid groups)
Soil FA	7.02	1.2	3.48	2.49
Soil HA	5.33	1.2	3.03	3.03
Equilibrium constants				
$Cr(OH)_2^+ + 2H^+ \leftrightarrow Cr^{3+} + H_2O$			$\log K = 9.84$	
$2Cr(OH)_2^+ + 2H^+ \leftrightarrow Cr_2(OH)_2^{4+} + 2H_2O$			$\log K = 14.68$	
$3Cr(OH)_2^+ + 2H^+ \leftrightarrow Cr_3(OH)_4^{5+} + 2H_2O$			$\log K = 18.77$	

TABLE III. Continued

Equilibrium constants	
$CrO_4^{2-} + 2H^+ \leftrightarrow H_2CrO_4$	log K = 6.31
$CrO_4^- + H^+ \leftrightarrow HCrO_4^-$	log K = 6.51
$2CrO_4^{2-} + 2H^+ \leftrightarrow Cr_2O_7^{2-} + H_2O$	log K = 14.56
$Cr(OH)_2^+ + H^+ \leftrightarrow CrOH^{2+} + H_2O$	log K = 6.27

The distribution of chromium between dissolved, sorbed and precipitated phases for Cr(III) and organic matter and Cr(VI) and organic matter, calculated by Visual MINTEQ, are presented in Table IV. Under the leaching conditions, 99 % of Cr(III) is sorbed (Table IV), which confirms the experimentally observed trend. Chromium(III) was not detected in the leachate of the organic substrate when acid rainwater was used, due to its sorption on organic matter (Fig. 2b).

TABLE IV. Equilibrium mass distribution of chromium between dissolved, sorbed and precipitated phases calculated by Visual MINTEQ for systems: Cr(III) and organic matter and Cr(VI) and organic matter

Sample	Dominant species	Dissolved, %	Sorbed, %	Precipitated, %
Cr(III) + organic matter	$Cr(OH)_2^{1+}$	0.966	99.034	0.0
Cr(VI) + organic matter	CrO_4^{2-}	100	0	0.0

The chromium speciation when the soil has a low organic matter content is shown in Fig. 2c. The dominate chromium(VI) ionic species are $HCrO_4^-$ and $Cr_2O_7^{2-}$ for pH < 6.5. On increasing the pH, the concentration of $HCrO_4^-$ decreases rapidly and at pH 8 approaches zero. For pH > 6.5, CrO_4^{2-} is preferably observed. Under highly alkaline conditions, Cr(VI) exists only in the form of CrO_4^{2-}.

It is apparent comparing to Fig 2d that the presence of organic matter does not affect the Cr(VI) concentration in infiltration water. Leaching of soil with high or low organic matter content, the concentration of Cr(VI), in the form of $HCrO_4^-$, $Cr_2O_7^{2-}$ and CrO_4^{2-}, is the same. This is probably due to the fact that no interaction occurs between the negatively charged ionic species and the negatively charged active functional groups of the organic matter, which leads to leaching of chromium and its migration to the groundwater. The results in Table IV show also that no chromium is sorbed or precipitated, leading to its total dissolution and possible downward movement to the groundwater or plant uptake.

CONCLUSIONS

This study demonstrated that the extent of chromium transport in soil columns depends on the mobility of the organic matter–metal complexes and that this mobility is governed by a variety of factors: the extent of soil pollution by chromium, the chromium valence state, soil organic matter content and acidity of the rainwater.

Chromium leaching was monitored for urban soil and an organic substrate for horticultural container growing with and without chromium pollution by treating with rainwater. The leachate solutions from all treatments showed that the concentration of Cr was strongly influenced by the organic matter content. This is explained by the increased metal sorption onto the organic matter of soil. Increasing the rain acidity resulted in the presence of not only Cr(VI), but also Cr(III) in the leachate. Considering that the soil was artificially polluted with chromium(VI) by addition of $K_2Cr_2O_7^{2-}$ to the soil, the Cr(VI) was reduced to Cr(III) only when the acidity of the rain was increased, because dichromate reduction by electron donor soil components, such as soil organic matter (humic substances), is realised with the consumption of H^+.

The experimentally and theoretically determined influences of pH and soil organic matter content are in agreement. The Stockholm humic model was used to evaluate the leaching results, and the obtained theoretical values corresponded rather well with the measured ones

И З В О Д

ИЗЛУЖИВАЊЕ ХРОМА ИЗ ХРОМОМ ЗАГАЂЕНОГ ЗЕМЉИШТА – СПЕЦИЈАЦИОНА АНАЛИЗА И ГЕОХЕМИЈСКО МОДЕЛОВАЊЕ

ДАРКО Х. АНЂЕЛКОВИЋ[1], ТАТЈАНА Д. АНДЈЕЛКОВИЋ[2], РУЖИЦА С. НИКОЛИЋ[2], МИЛОВАН М. ПУРЕНОВИЋ[2], СРЂАН Д. БЛАГОЈЕВИЋ[3], АЛЕКСАНДАР Љ. БОЈИЋ[2] и МИЛИЦА М. РИСТИЋ[1]

[1]ЈКП „Naissus“, Кнегиње Љубице 1/I, 18000 Ниш, [2]Природно–математички факултет, Универзитет у Нишу,Вишеградска 33, 18000 Ниш и [3]Пољопривредни факултет, Универзитет у Београду, Немањина 16, 11081 Београд

У раду је праћена дистрибуција хрома између земљишта и инфилтрационих вода. Природни процес перколирања кишнице кроз земљиште је симулиран у лабораторијским условима помоћу екстракције и излуживања у колони. Миграција хрома у земљишту је праћена у зависности од нивоа загађења земљишта хромом, садржаја органске материје земљишта и киселости кишнице. Хром(III) и хром(VI) су одређени спектрофотометријски помоћу дифенилкарбазида у киселој средини. Специјација хрома у инфилтрационим водама добијена експерименталним модел системом је у сагласности са специјацијом добијеном прорачуном геохемијским моделом Visual MINTEQ. Концентрација хрома у инфилтрационим растворима показује значајну зависност од садржаја органске материје земљишта. Компјутерски геохемијски модел – Stockholm хуминski модел, који је коришћен за евалуацију експерименталних резултата може се применити у специјацији хрома у урбаном земљишту и органском супстрату, који су испитивани у раду.

(Примљено 16. децембра 2010, ревидирано 20. фебруара 2011)

REFERENCES

1. L. Campanella, in: *Element Speciation in Bioinorganic Chemistry*, S. Caroli, Ed., Wiley Interscience, New York, 1996, p. 419
2. J. Kotas, Z. Stasicka, *Environ. Pollut.* **107** (2000) 263
3. K. P. Lee, C. E. Ulrich, R. G. Geil, H. J. Trochimowicz, *Sci. Tot. Environ.* **86** (1989) 83
4. J. M. Pacyna, J. O. Nriagu, in *Chromium in Natural and Human Environments*, J. O. Nriagu, E. Nieboer, Eds., Wiley Interscience, New York, 1988, p. 105
5. D. C. Adriano, *Trace Elements in the Terrestrial Environment*, Springer, New York, 1986
6. L. X. Zhou, J. W. C. Wong, *J. Environ. Qual.* **30** (2001) 878
7. A. V. Zomeren, R. N. Comans, *Environ. Sci. Technol.* **38** (2004) 3927
8. E. M. Perdue, J. H. Reuter, R. S. Paerish, *Geochim. Cosmochim. Acta* **48** (1984) 1257
9. J. P. Gustafsson, *J. Colloid Interface Sci.* **244** (2001) 102
10. D. G. Kinniburgh, W. H. van Riemsdijk, L. K. Koopal, M. Borkovec, M. H. Benedetti, M. J. Avena, *Colloids Surf., A* **151** (1999) 147.
11. A. Walkley, L. A. Black, *Soil Sci.* **37** (1934) 29
12. M. Linde, *Trace Metals in Urban Soils – Stockholm as a Case Study*, PhD thesis, Swedish University of Agricultural Sciences, Uppsala, 2005
13. A. Tunceli, A. R. Turker, *Talanta*. **57** (2002) 1199
14. V. Gomez, M. P. Callao, *Trends Anal. Chem.* **25** (2006) 10
15. J. E. T. Andersen, *Anal. Chim. Acta* **361** (1998) 125
16. J. P. Gustafsson, J. W. J. van Schaik, *Eur. J. Soil Sci.* **54** (2003) 295
17. J. P. Gustafsson, D. B. Kleja, *Environ. Sci. Technol.* **39** (2005) 5372
18. M. Jakovljević, M. Pantović, *Chemistry of Solis and Waters*, Naučna knjiga, Beograd, 1991, p. 27 (in Serbian)
19. M. M. Kononova, *Soil Organic Matter*, 2nd ed., Pergamon Press, Oxford, 1966
20. T. Andjelkovic, R. Nikolic, A. Bojic, D. Andjelkovic, G. Nikolic, *Maced. J. Chem. Chem. Eng.* **29** (2010) 215
21. T. Andjelkovic, J. Perovic, M. Purenovic, S. Blagojevic, R. Nikolic, D. Andjelkovic, A. Bojic, *Anal. Sci.* **22** (2006) 1553
22. M. D. Jakovljević, N. M. Kostić, D. Stevanović, S. Blagojević, M. J. Wilson, Lj. Martinović, *Appl. Geochem.* **12** (1997) 637
23. B. R. James, R. J. Bartlett, *J. Environ. Qual.* **12** (1983) 173
24. B. R. James, R. J. Bartlett, *J. Environ. Qual.* **12** (1983) 177
25. B. R. James, R. J. Bartlett, in: *Chromium in Natural and Human Environments*, J. O. Nriagu, E. Nieboer, Eds., Wiley Interscience, New York, 1988, 265
26. A. R. Walsh, J. O'Halloran, *Water Res.* **30** (1996) 2393
27. F. C. Richard, A. C. M. Bourg, *Water Res.* **25** (1991) 807.

INSTRUCTIONS FOR AUTHORS (2010)

GENERAL

The ***Journal of the Serbian Chemical Society*** is an international journal publishing papers from all fields of chemistry and related disciplines. Twelve issues are published annually. The Editorial Board expects the editors, reviewers and authors to respect the well-known standard of professional ethics.

Types of Contributions

Original scientific papers	(about 10 typewritten pages) report original research which must not have been previously published.
Short communications	(about 5 pages) report unpublished preliminary results of sufficient importance to merit rapid publication.
Notes	(about 3 pages) report unpublished results of short, but complete, original research.
Authors' reviews	(about 30 pages) present an overview of the author's current research with comparison to data of other scientists working in the field.
Reviews	(about 30 pages) present a concise and critical survey of a specific research area. Generally, these are prepared at the invitation of the Editor.
Book and Web site reviews	(1–2 pages)
Extended abstracts	(about 3 pages) of Lectures given at meetings of the Serbian Chemical Society Divisions.

Submission of manuscripts

Manuscripts should be submitted using the **OnLine Submission Form**, available on the JSCS Web Site (www.shd.org.rs/JSCS/Form/). The manuscript must be uploaded as a Word.doc or .rtf file (tables and figures should follow the text, each on a separate page). Illustrations in TIF or EPS format (JPG format is acceptable for colour and greyscale photos, only), must be additionally uploaded as a separate archived (.zip, .rar or .arj) file. Figures and/or Schemes should be prepared according to the **Artwork Instructions**.

Manuscripts must be accompanied by a cover letter in which the type of the submitted manuscript and a warranty as given below are given. The Author warranties that the manuscript submitted to the *Journal* for review is original, has been written by the stated authors and has not been published elsewhere; is currently not being considered for publication by any other journal and will not be submitted for such a review while under review by the *Journal*; the manuscript contains no libellous or other unlawful statements and does not contain any materials that violate any personal or proprietary rights of any other person or entity. All manuscripts will be acknowledged on receipt (by e-mail) and given a reference number, which should be quoted in all subsequent correspondence. A password for "Article Tracking" (www.shd.org.rs/JSCS/) will also be supplied.

A MANUSCRIPT NOT PREPARED ACCORDING TO THESE INTRUCTIONS WILL BE RETURNED FOR RESUBMITION WITHOUT BEING ASSIGNED A REFERENCE NUMBER.

PROCEDURE

All contributions will be peer reviewed and only those deemed worthy will be accepted for publication. The Editor has the final decision. To facilitate the reviewing process, authors are encouraged to suggest up to three persons competent to review their manuscript. Such suggestions will be taken into consideration but not always accepted.

Manuscripts requiring revision should be returned according to the requirement of the Editor, within 60 days or the manuscript will be considered as having been withdrawn. Later, the manuscript would have to be resubmitted.

The *Journal* maintains its policy and takes the liberty of correcting the English of manuscripts scientifically accepted for publication.

When a manuscript is ready for printing, the corresponding author will receive a PDF-formatted manuscript for proof reading, which should be returned to the *Journal* within 2 days. Failure to do so will be taken as the authors are in agreement with any alteration which may have occurred during the preparation of the manuscript.

Accepted manuscripts of active members of the Serbian Chemical Society (all authors) have publishing priority.

The corresponding author will receive by e-mail a PDF-formatted version of the paper as published in the journal.

MANUSCRIPT PRESENTATION

Manuscripts should be typed in English (either standard British or American English, but consistent throughout) with 1.5 spacing (12 points Times New Roman; Greek letters in the character font Symbol) in A4 format leaving 2.5 cm for margins. For Regional specific, non-standard save documents with Embed fonts Word option: *Save as -> (Tools) -> Save Options… -> Embed fonts in the text.*

The authors are requested to seek the assistance of competent English language expert, if necessary, to ensure their English is of a reasonable standard. The Serbian Chemical Society can provide this service in advance of submission of the manuscript. If this service is required, please contact the office of the Society by e-mail (jscs-info@shd.org.rs).

Tables and figures and/or schemes should not be embedded in the manuscript but their position in the text indicated. In electronic version (Word.doc document) tables and figures and/or schemes should follow the text, each on a separate page. Please number all pages of the manuscript including separate lists of references, tables and figures and their captions.

IUPAC recommendations for the naming of compounds should be followed. SI units, or other permissible units, should be employed. The designation of physical quantities must be in italic throughout the text (including figures, tables and equations), whereas the units are in upright letters. They should be in Times New Roman font. In graphs and tables, a slash should be used to separate the designation of a physical quantity from the unit (example: p / kPa, t / °C, T / K, τ / h…). Designations such as: p (kPa), t [min]…, are not acceptable. However, if the full name of a physical quantity is unavoidable, it should be given in upright letters and separated from the unit by a comma (example: Pressure, kPa, Temperature, K…). Please do not use the axes of graphs for additional explanations; these should be mentioned in the figure captions and/or the manuscript (example: "pressure at the inlet of the system, kPa" should be avoided). The axis name should follow the direction of the axis (the name of *y*–axis should be rotated by 90°). Top and right axes should be avoided in diagrams, unless they are absolutely necessary.

Latin words, as well as the names of species, should be in *italic*, as for example: *i.e., e.g., in vivo, ibid, Calendula officinalis* L., *etc*. The branching of organic compound should also be indicated in *italic*, for example, *n*-butanol, *tert*-butanol, *etc*.

Decimal numbers must have decimal points and not commas in the text (except in the Serbian abstract), tables and axis labels in graphical presentations of results.

ARTICLE STRUCTURE

- TITLE PAGE
- MAIN TEXT
- TABLE CAPTIONS
- TABLES (each on a separate page)
- FIGURE and/or SCHEME CAPTIONS
- FIGURES and/or SCHEMES (each on a separate page)

Title page.

Title in bold letters, should be clear and concise, preferably 12 words or less. The use of non-standard abbreviations, symbols and formulae is discouraged.

AUTHORS' NAMES in capital letters with the full first name, initials of further names separated by a space and surname. Commas should separate the author's names except for the last two names when 'and' is to be used. In multi-affiliation manuscripts, the author's affiliation should be indicated by an Arabic number placed in superscript after the name and before the affiliation. Use * to denote the corresponding author(s).

Affiliations should be written in italic. The e-mail address of the corresponding author should be given after the affiliation(s).

Abstract: A one-paragraph abstract written of 150–200 words in an impersonal form indicating the aims of the work, the main results and conclusions should be given and clearly set off from the text. Domestic authors should also submit, on a separate page, an Abstract – Izvod, the author's name(s) and affiliation(s) in Serbian (Latin letters). For authors outside Serbia, the Editorial Board will provide a Serbian translation of their English abstract.

Keywords: Up to 6 keywords should be given. Do not use words appearing in the manuscript title

RUNNING TITLE: A one line (maximum five words) short title in capital letters should be provided.

Main text. The main text should have the form:

INTRODUCTION,
EXPERIMENTAL (RESULTS AND DISCUSSION),
RESULTS AND DISCUSSION (EXPERIMENTAL),
CONCLUSIONS,
NOMENCLATURE (optional),
Acknowledgements: If any,
REFERENCES (Citation of recent papers published in chemistry journals that highlight the significance of work to the general readership is encouraged.)

The sections should be arranged in a sequence generally accepted for publication in the respective fields. They subtitles should be in capital letters, centred and NOT numbered.

The INTRODUCTION should include the aim of the research and a concise description of background information and related studies directly connected to the paper.

The EXPERIMENTAL section should give the purity and source of all employed materials, as well as details of the instruments used. The employed methods should be described in sufficient detail to enable experienced persons to repeat them. Standard procedures should be referenced and only modifications described in detail. On no account should results be included in the experimental section.

The RESULTS AND DISCUSSION should include concisely presented results and there significance discussed and compared to relevant literature data. The results and discussion may be combined or kept separate.

The inclusion of a CONCLUSION section, which briefly summarizes the principal conclusions, is highly recommended. NOMENCLATURE is optional but, if the authors wish, a list of employed symbols may be included.

REFERENCES should be numbered sequentially as they appear in the text. When cited in the text, the reference number should be superscripted in Font 12, following any punctuation mark. In the reference list, they should be in normal position followed by a full stop. Reference entry must not be formatted using Carriage returns (enter key; ↵ key) or multiple space key. The formatting of references to published work should follow the *Journal's* style as follows:

Journals*:	1. A. B. Surname1, C. D. Surname2, *J. Serb. Chem. Soc.* **Vol.** (Year) first page Number
Books:	2. A. B. Surname1, C. D. Surname2, *Name of Book*, Publisher, City, Year, p. 100
Compilations:	3. A. B. Surname1, C. D. Surname2, in: *Name of Compilation*, A. B. Editor1, C. D. Editor2, Ed(s)., Publisher, City, Year, p. 100
Proceedings:	4. A. B. Surname1, C. D. Surname2, , in: *Proceeding of Name of the Conference or Symposium*, *Title of the Proceeding*, (Year of publishing), Place of the Conference, Country, Year, p. 100
Patents:	5. A. B. Inventor1, C. D. Inventor2, (Holder), Country Code and patent number (registration year)
Chemical Abstracts:	6. A. B. Surname1, C. D. Surname2, Chem. Abstr. CA 234 567a For non-readily available literature, the Chemical Abstracts reference should be given in square brackets: [C.A. 139/2003 357348t] after the reference
Standards:	7. EN ISO 250: *Name of the Standard* (Year)
Websites:	8. Title of the website, URL in full (date accessed)

* International Library Journal abbreviation is required. Please consult *e.g.* http://www.library.ubc.ca/scieng/coden.html

Only the last entry in the reference list should end with a full stop.

The names of all authors should be given in the list of references; the abbreviation *et al.* may only be used in the text. The original journal title is to be retained in the case of publications published in any language other than English (please denote the language in parenthesis after the reference). Titles of publications in non-Latin alphabets should be transliterated. Russian references are to be transliterated using the following transcriptions:

ж→zh, х→kh, ц→ts, ч→ch, ш→sh, щ→shch, ы→y, ю→yu, я→ya, э→e, й→i, ь→'.

Table Captions. A separate list of table captions, which makes the tables comprehensible without reference to the text, should be provided in numerical order on a separate page.

Tables. Tables are part of the text but must be given on separate pages. The tables should be numbered consequently in Roman numbers. Quantities should be separated from units by a slash (/). Footnotes to tables, in size 10 font, are to be indicated consequently (line-by-line) in superscript letters. Tables should be prepared with the aid of the WORD table function, without vertical lines. The minimum size of the font in the tables should be 10 pt. Table columns must not be formatted using multiple spaces. Table rows must not be formatted using Carriage returns (enter key; ↵ key). Tables should not be incorporated as graphical objects. In setting up tables, Authors should keep in mind the area of the Journal's page (12.5 cm × 19 cm) and should make tables conform to the limitations of these dimensions.

Figure and/or Scheme Captions. A separate list of figure and/or scheme captions, which makes the figures and/or schemes comprehensible without reference to the text, should be provided in numerical order on a separate page.

Figures and/or Schemes. Figures and/or Schemes (of moderate resolution) should follow the captions, each on a separate page of the manuscript. High resolution illustrations in TIF or EPS format (JPG format is acceptable for colour and greyscale photos, only) must be uploaded as a separate archived (.zip, .rar or .arj) file.

Figures and/or Schemes should be prepared according to the ARTWORK INSTRUCTIONS!

Mathematical and chemical equations must be numbered, Arabic numbers, consecutively in parenthesis at the end of the line. All equations should be embedded in the text except when they contain graphical elements (tables, figures, schemes and formulae). Complex equations (fractions, inegrals, matrix…) should be prepared with the aid of the WORD Equation editor.

Reporting analytic and spectral data

Adequate evidence to enable the identity and purity of all newly synthesized compounds should be provided.

The styles for the presentation of analytical and spectral data, which should be strictly adhered to (including the order), are as follows:

*Compound (**3a**)*. Yield: 60 %; m.p. 120 °C. Anal. Calcd. for $C_{30}H_{23}N_3O_5$: C, 71.27; H 4.58; N, 8.31. Found: C, 71.30, H, 4.54, N, 8.70. IR (KBr, cm^{-1}): 1535, 1469 (C=C– stretching of aromatic ring), 1680*s* (–C=O stretching of -COOH group), 3128 (–NH stretching of secondary amine). ^{1}H-NMR (200 MHz, DMSO-d_6, δ / ppm): 1.38–1.39 (3H, *t*, $–CH_2–CH_3$), 4.0–4.49 (2H, *q*, $–CH_2–CH_3$), 10.92 (1H, *s*, –NH, D_2O exchangeable), 7.75 (2H, *t*, aromatic, J = 7.8 Hz), 2.26–2.75 (2H, *m*, $–CH_2$). ^{13}C-NMR (100 MHz, $CDCl_3$, δ / ppm): 157.76 (C_1), 146.89 (C_2), 177.69 (–COO), 33.44 (–CH), 38.55 ($–CH_2$). MS (*m*/*z*, (relative abundance, %)): 252 (M+, 32.5) 225, 213, 211 (BP, 100). UV–Vis (EtOH) (λ_{max} / nm, eV or cm^{-1} (ε / L mol^{-1} cm^{-1})): 205 (2300), 243 (1800). Optical rotation values, α (589 nm, 20 °C, 10 g dm^{-3} in H_2O, 10 cm): +66.470°. Specific rotation $[\alpha]^{20}_{589}$ / deg dm^{-1} g^{-1} cm^3. Magnetic moment, μ_{eff} / μ_B: 3.1.

Deposition of crystallographic data

Prior to submission, the crystallographic data included in a manuscript presenting such data should be deposited at the appropriate database. Crystallographic data associated with organic and metal-organic structures should be deposited at the Cambridge Crystallographic Data Centre (CCDC) by e-mail to deposit@ccdc.cam.ac.uk

Crystallographic data associated with inorganic structures should be deposited with the Fachinformationszentrum Karlsruhe (FIZ) by e-mail to crysdata@fiz-karlsruhe.de. A deposition number will then be provided, which should be added to the reference section of the manuscript.

ARTWORK INSTRUCTIONS

JSCS accepts only **TIFF** or **EPS** formats, as well as **JPEG** format (only for colour and greyscale photographs) for electronic artwork and graphic files. **MS files** (Word, PowerPoint, Excel, Visio) **NOT acceptable**. Generally, scanned instrument data sheets should be avoided. Authors are responsible for the quality of their submitted artwork. Every single Figure or Scheme, as well as any part of the Figure (A, B, C…) should be prepared according to following instructions (every part of the figure, A, B, C…, must be submitted as an independent single graphic file).

TIFF

Virtually all common artwork and graphic creation software is capable of saving files in TIFF format. This "option" can normally be found under the "Save As..." or "Export..." commands in the "File" menu. TIFF (Tagged Image File Format) is the recommended file format for bitmap, greyscale and colour images. Colour images should be in the RGB mode. When supplying TIFF files, please ensure that the files are supplied at the correct resolution:

Line artwork: minimum of 1000 dpi

RGB image: minimum of 300 dpi

Greyscale image: minimum of 300 dpi

Combination artwork (line/greyscale/RGB): minimum of 500 dpi

Images should be tightly cropped.

If applicable, please re-label artwork with a font supported by JSCS (Arial, Helvetica, Times, Symbol) and ensure it is of an appropriate font size. Save an image in TIFF format with LZW compression applied. It is recommended to remove Alpha channels before submitting TIFF files. It is recommended to flatten layers before submitting TIFF files.

EPS

Virtually all common artwork creation software, such as Canvas, ChemDraw, CorelDraw, SigmaPlot, Origin Lab…, are capable of saving files in EPS format. This "option" can normally be found under the "Save As..." or "Export..." commands in the "File" menu. For vector graphics, EPS (Encapsulated PostScript) files are the preferred format as long as they are provided in accordance with the following conditions: when they contain bitmap images, the bitmaps should be of good resolution (see instructions for TIFF files).

JPEG

JPEG (Joint Photographic Experts Group) is the acceptable file format only for colour and greyscale photographs. JPEG can be created with respect to photo quality (low, medium, high; from 1 to 10), ensuring file sizes are kept to a minimum to aid easy file transfer. Images should have a minimum resolution of 300 dpi. Image width: minimum 8.0 cm; maximum 12.0 cm.

When colour is involved, it should be encoded as RGB. An 8-bit preview/header at a resolution of 72 dpi should always be included. Embed fonts should be always included and only the following fonts should be used in artwork: Arial, Helvetica, Times, Symbol. The vertical space between the parts of an illustration should be limited to the bare necessity for visual clarity. No data should be present outside the actual illustration area. Line weights should range from 1 pt to 2 pt. When using layers, they should be reduced to one layer before saving the image (Flatten Artwork).

Sizing of artwork

JSCS aspires to have a uniform look for all artwork contained in a single article. Hence, it is important to be aware of the style of the journal. Figures should be submitted in black and white or, if required, colour (charged). If coloured figures or photographs are required, this must be stated in the cover letter and arrangements made for payment through the office of the Serbian Chemical Society. As a general rule, the lettering on an artwork should have a finished, printed size of 11 pt for normal text and no smaller than 7 pt for subscript and superscript characters. Smaller lettering will yield a text that is barely legible. This is a rule-of-thumb rather than a strict rule. There are instances where other factors in the artwork, (for example, tints and shadings) dictate a finished size of perhaps 10 pt. Lines should be of at least 1 pt thickness. When deciding on the size of a line art graphic, in addition to the lettering, there are several other factors to address. These all have a bearing on the reproducibility/readability of the final artwork. Tints and shadings have to be printable at the finished size. All relevant detail in the illustration, the graph symbols (squares, triangles, circles, *etc*.) and a key to the diagram (to explain the explanation of the graph symbols used) must be discernible. The sizing of halftones (photographs, micrographs,...) normally causes more problems than line art. It is sometimes difficult to know what an author is trying to emphasize on a photograph, so you can help us by identifying the important parts of the image, perhaps by highlighting the relevant areas on a photocopy. The best advice that can be given to graphics suppliers is not to over-reduce halftones. Attention should also be paid to magnification factors or scale bars on the artwork and they should be compared with the details inside. If a set of artwork contains more than one halftone, again please ensure that there is consistency in size between similar diagrams.

General sizing of illustrations which can be used for the Journal of the Serbian Chemical Society:

Fig. size: Minimum 30 mm width; Small - 60 mm width; Large - 90 mm width; Maximum - 120 mm width

Pixel requirements (width) per print size and resolution for bitmap images:

	Image width	A	B	C
Minimal size	30 mm	354	591	1181
Small size	60 mm	709	1181	2362
Large size	90 mm	1063	1772	3543
Maximal size	120 mm	1417	2362	4724

A: 300 dpi > RGB or Greyscale image; B: 500 dpi > Combination artwork (line/greyscale/RGB); C: 1000 dpi> Line artwork